Proceedings of the
Thirty-Third
DOE Solar Photochemistry
Research Conference

Solar Photochemistry

Photosynthetic Systems
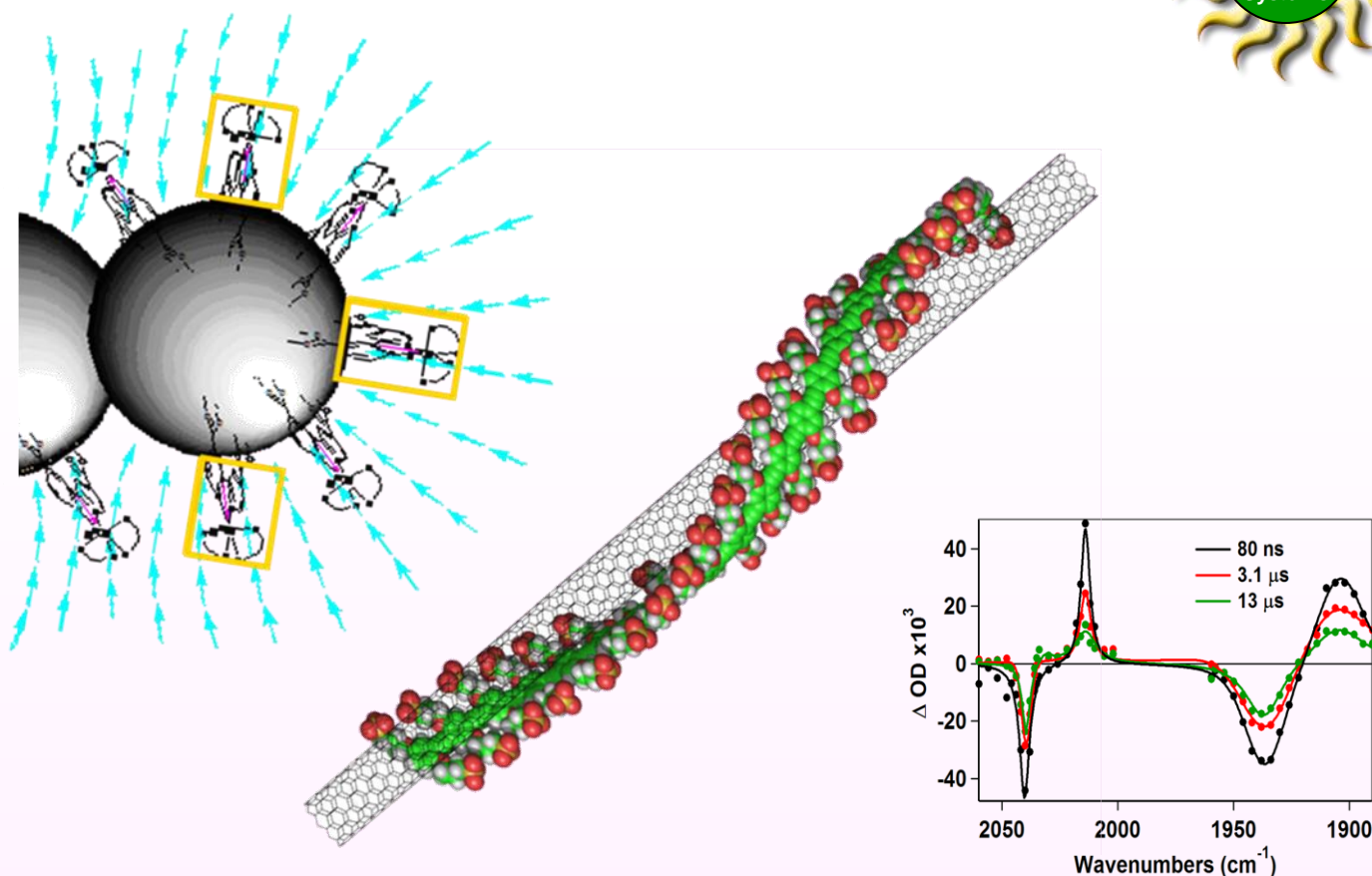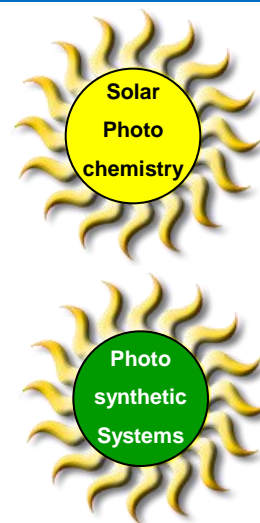
Wintergreen Conference Center, Wintergreen VA, June 5-8, 2011
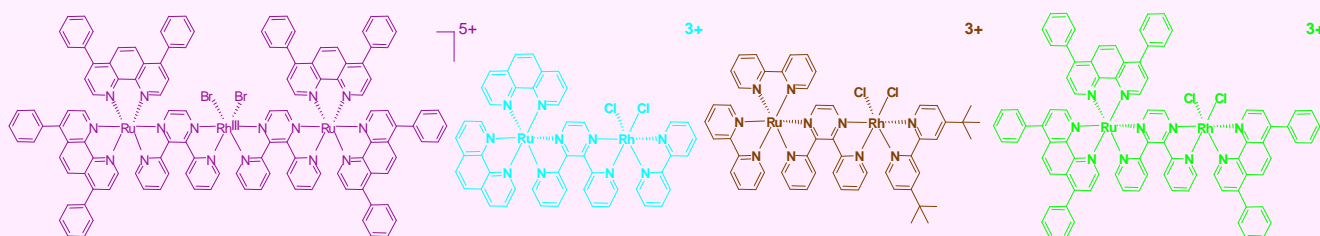
Cover Graphics

The cover figures are drawn from the abstracts of this meeting. Clockwise from upper left, the first figure represents the Stark effect at sensitized nanocrystalline TiO_2 (G. Meyer *et al.*, p. 79). The second depicts the single-chain helical wrapping of a polymer on a single-wall carbon nanotube designed for electron transport studies (Therien, p. 14). The third shows time resolved infra-red spectra of $[Re(bpy)(CO)_3(CH_3CN)]^+$ as the catalyst is reduced (Grills, p. 47), and the fourth shows the structures of mixed-metal supramolecular complexes developed as photocatalysts for H_2 production (Brewer *et al.*, p. 115).

Program and Abstracts

Solar Photochemistry Program
Research Meeting

Wintergreen Conference Center
Wintergreen, Virginia
June 5-8, 2011

Chemical Sciences, Geosciences, and Biosciences Division
Office of Basic Energy Sciences
Office of Science
U.S. Department of Energy

Foreword

The 33rd Department of Energy Solar Photochemistry Research Meeting, sponsored by the Chemical Sciences, Geosciences, and Biosciences Division of the Office of Basic Energy Sciences, is being held June 5-8, 2011, at the Wintergreen Conference Center in Wintergreen, Virginia. These proceedings include the meeting agenda, abstracts of the formal presentations and posters of the conference, and an address list for the participants.

This conference is composed of the grantees who do research in solar photochemical energy conversion with the support of the Chemical Sciences, Geosciences, and Biosciences Division. These program meetings provide unique fora for initiation of collaborations between researchers as well as exchanges of new concepts and ideas. This synergistic element of research within the program is one of its major strengths and promotes the excellence in research that has sustained this program over the years.

The Solar Photochemistry Research Conference will have as its guests this year a number of researchers from the Photosynthetic Systems Program, which is a sibling program in the newly formed Photo- and Biochemistry Team within the Division. They will present posters on their exploration of photochemistry in photosynthesis, which has long served as a model for energy transduction schemes in the Solar Photochemistry Program. One of their members will serve as the special guest lecturer for this conference, Professor Donald Ort of the University of Illinois, who will give a presentation on the limits to the efficiency of natural photosynthesis, a topic that was the subject of a Divisional workshop in 2009. The conference sessions that follow will feature presentations on photocatalysis, spectroscopy at nanoparticles, dye sensitized solids, novel molecular structures, and charge transfer in organic molecular systems.

This proceedings volume is dedicated to Professor Paul Barbara who passed away in December of last year. Paul was an active researcher in both the Solar Photochemistry and Radiation Chemistry aspects of this program for two decades, and his counsel and critique on its research projects during those years was much valued. He lived with a passion and a contagious enthusiasm for science that will be sorely missed.

I would like to express my appreciation to Dr. Amy Ryan of the Pacific Northwest National Laboratories, to Diane Marceau of the Division of Chemical Sciences, and to Tim Ledford and Connie Langston of the Oak Ridge Institute for Science and Education for their assistance with the preparation of this volume and the coordination of the logistics of this meeting. I must also thank all of the researchers whose dedication to scientific inquiry and enduring interest in research on solar energy transduction have enabled these advances in solar photoconversion and made this meeting possible.

Mark T. Spitler
Chemical Sciences, Geosciences,
    and Biosciences Division
Office of Basic Energy Sciences

i

Solar Photochemistry Research Conference Overview

Time	Sunday, June 5	Monday, June 6	Tuesday, June 7	Wednesday, June 8	Time
7:30 AM		**BREAKFAST**			7:30 AM
7:45 AM		**7:30 - 8:15**	**BREAKFAST**	**BREAKFAST**	7:45 AM
8:00 AM			**7:30 - 8:30**	**7:30 - 8:30**	8:00 AM
8:15 AM		**Opening Remarks**			8:15 AM
8:30 AM					8:30 AM
8:45 AM			**Photo-**	**Spectroscopy**	8:45 AM
9:00 AM		**Opening**	**Catalysis I**	**at Nanoparticles**	9:00 AM
9:15 AM		**Session**			9:15 AM
9:30 AM			*Session IV*	*Session VII*	9:30 AM
9:45 AM		*Session I*			9:45 AM
10:00 AM			**BREAK**	**BREAK**	10:00 AM
10:15 AM		**BREAK**	**10:00 - 10:30**	**10:00 - 10:30**	10:15 AM
10:30 AM		**10:15 - 10:45**			10:30 AM
10:45 AM		**Novel Molecular**	**Photo-**	**Dye-Sensitized**	10:45 AM
11:00 AM		**Structures**	**Catalysis II**	**Systems**	11:00 AM
11:15 AM		*Session II*			11:15 AM
11:30 AM			*Session V*	*Session VIII*	11:30 AM
11:45 AM		**Free time**			11:45 AM
12:00 PM					12:00 PM
12:15 PM		**LUNCH**	**LUNCH**	**LUNCH**	12:15 PM
12:30 PM		**12:00 - 1:00**	**12:00 - 1:00**	**12:00 - 1:00**	12:30 PM
12:45 PM					12:45 PM
1:00 PM				**Donors and**	1:00 PM
1:15 PM				**Acceptors**	1:15 PM
1:30 PM				*Session IX*	1:30 PM
1:45 PM					1:45 PM
2:00 PM					2:00 PM
2:15 PM		**Free time**		**Panel Discussion**	2:15 PM
2:30 PM		**1:00 - 4:30**	**Free time**	**2:00 - 2:45**	2:30 PM
2:45 PM			**1:00 - 5:30**	**Closing Remarks**	2:45 PM
3:00 PM					3:00 PM
3:15 PM					3:15 PM
3:30 PM					3:30 PM
3:45 PM	**Registration**				3:45 PM
4:00 PM	**3:00 - 6:00 PM**				4:00 PM
4:15 PM					4:15 PM
4:30 PM	**No-Host Reception**				4:30 PM
4:45 PM		**Charge Separation**			4:45 PM
5:00 PM		**in**			5:00 PM
5:15 PM		**Organic Systems**			5:15 PM
5:30 PM		*Session III*			5:30 PM
5:45 PM			**Catalysis**		5:45 PM
6:00 PM			**at Surfaces**		6:00 PM
6:15 PM		**Free time**	*Session VI*		6:15 PM
6:30 PM					6:30 PM
6:45 PM	**DINNER**	**DINNER**	**SOCIAL HOUR**		6:45 PM
7:00 PM	**6:00 - 8:00**	**6:30 - 7:30**	**6:30 - 7:30**		7:00 PM
7:15 PM					7:15 PM
7:30 PM					7:30 PM
7:45 PM			**DINNER**		7:45 PM
8:00 PM			**7:30 - 8:30**		8:00 PM
8:15 PM	**After Dinner Speaker**	**POSTERS**			8:15 PM
8:30 PM		**odd numbers**			8:30 PM
8:45 PM		**Refreshments**	**POSTERS**		8:45 PM
9:00 PM	**RECEPTION**		**even numbers**		9:00 PM
9:15 PM	**8:45 - 10:00**		**Refreshments**		9:15 PM
9:30 PM		**7:30 - 10:00**	**8:30 - 10:00**		9:30 PM
9:45 PM					9:45 PM

ii

Table of Contents

TABLE OF CONTENTS

Abstracts of Oral Presentations

Guest Speaker
Limits to the Efficiency of Natural Photosynthesis: Raising the Ceiling
on the Maximum Conversion Efficiency

Magnetic Resonance and DFT Study of Carotenoid Neutral Radicals: Dependence on
Conjugation Length and Substituents

Photophysics of Single and Multiple Excitons in Carbon Nanotubes
Lisa J. Carlson, Marat Khafizov, Andrea J. Lee, Julie A. Smyder, Shujing Wang,

Organic, Nanoscale, and Self-Assembled Structures Relevant to Solar Energy
Conversion

Transient Absorption Microscopy Studies of Carrier Dynamics in Graphene
and Polymer Blends
Libai Huang, Bo Gao, Christopher Wong, Fei Hua Li, Gregory Hartland, Michelle

Photo-Induced Electron Transfer in Conjugated Polymers with Colloidal Nanoparticles
Garry Rumbles, Nikos Kopidakis, Andrew Ferguson, Smita Dayal,

Poster Abstracts (by poster number)

Program

33rd DOE SOLAR PHOTOCHEMISTRY
RESEARCH MEETING

June 5-8, 2011

Wintergreen Conference Center
Wintergreen, Virginia

PROGRAM

Sunday, June 5

3:00 – 6:00 p.m.   Registration and Reception

6:00 – 8:00 p.m.   Dinner

8:00 – 8:45 p.m.   **After-Dinner Speaker**

Photoelectrochemical Production of Hydrogen: Real or Pathological Science?
John Turner, National Renewable Energy Laboratory

8:45 – 10:00 p.m.   Reception

Monday Morning, June 6

7:30 a.m.   Continental Breakfast

SESSION I
Opening Session
Mark T. Spitler, Chair

8:15 a.m.   Opening Remarks
Richard Greene and **Mark Spitler**, U. S. Department of Energy

8:45 a.m.   *Guest Speaker*

Limits to the Efficiency of Natural Photosynthesis: Raising the Ceiling
on the Maximum Conversion Efficiency
Donald R. Ort, University of Illinois

9:45 a.m.   Magnetic Resonance and DFT Study of Carotenoid Neutral Radicals: Dependence
on Conjugation Length and Substituents
Lowell D. Kispert, The University of Alabama

10:15 a.m.   Coffee Break

<div align="center">

SESSION II
Novel Molecular Structures
Louis Brus, Chair

</div>

10:45 a.m.   Photophysics of Single and Multiple Excitons in Carbon Nanotubes
Todd D. Krauss, The University of Rochester

11:15 a.m.   Organic, Nanoscale, and Self-Assembled Structures Relevant to Solar Energy Conversion
Michael J. Therien, Duke University

Monday Afternoon, June 6

12:00 p.m.   Lunch

Monday Evening, June 6

<div align="center">

SESSION III
Charge Separation in Organic Systems
Frederick Lewis, Chair

</div>

4:30 p.m.   Transient Absorption Microscopy Studies of Carrier Dynamics in Graphene and Polymer Blends
Libai Huang, University of Notre Dame

5:00 p.m.   Photo-Induced Electron Transfer in Conjugated Polymers with Colloidal Nanoparticles
Garry Rumbles, National Renewable Energy Laboratory

5:30 p.m.   A Farewell to Organic Semiconductors—and Some Recent Results
Brian A. Gregg, National Renewable Energy Laboratory

6:30 p.m.   Dinner

7:30 p.m.   Posters (odd numbers)
Refreshments

7:30 a.m.   Continental Breakfast

SESSION IV
Photocatalysis I
Karen Mulfort, Chair

8:30 a.m.   Membrane-Organized Chemical Photoredox Systems
                 James K. Hurst, Washington State University

9:00 a.m.   Water Oxidation Catalyzed by Mononuclear Ru(II) Complexes
                 Randolph P. Thummel, University of Houston

9:30 a.m.   Hydrogen and Oxygen Evolving Hangman Catalysts
                 Daniel G. Nocera, Massachusetts Institute of Technology

10:00 a.m.   Coffee Break

SESSION V
Photocatalysis II
Michael Hopkins, Chair

10:30 a.m.   Cobaloxime Catalyst for Biomimetic Hydrogen Production: EPR Investigation of
                 the Electronic Structure
                 Oleg G. Poluektov, Argonne National Laboratory

11:00 a.m.   Improving the Efficiency of Photocatalytic CO_2 Reduction Reactions
                 David C. Grills, Brookhaven National Laboratory

11:30 a.m.   All-Inorganic Polynuclear Assemblies for H_2O Oxidation and CO_2 Reduction on
                 Nanoporous Silica Surfaces
                 Heinz Frei, Lawrence Berkeley National Laboratory

Tuesday Afternoon, June 7

12:00 p.m.   Lunch

SESSION VI
Catalysis at Surfaces
Kara Bren, Chair

5:30 p.m.   Properties of Fe 'Doped' and (Fe, N) Co-doped Rutile $TiO_2(110)$
             Michael A. Henderson, Pacific Northwest National Laboratory

6:00 p.m.   Catalyzed Water Oxidation by Solar Irradiation of Band-Gap–Narrowed
             Semiconductors
             Etsuko Fujita, James T. Muckerman, Brookhaven National Laboratory

6:30 p.m.   Social Hour

7:30 p.m.   Dinner

8:30 p.m.   Posters (even numbers)
             Refreshments

Wednesday Morning, June 8

7:30 a.m.   Continental Breakfast

Session VII
Spectroscopy at Nanoparticles
Russell Schmehl, Chair

8:30 a.m.   Hot Carrier Interactions in Semiconductor Nanocrystals
             David M. Jonas, University of Colorado

9:00 a.m.   Exciton and Charge Carrier Dynamics at Interfaces between Quantum Dots and
             Metals and in Monodisperse Nanoclusters
             Piotr Piotrowiak, Rutgers University

9:30 a.m.   The Crystalline Nanocluster Ti-O Phase: Synthesis of New Clusters, Their
             Functionalization and Properties
             Philip Coppens and Jason B. Benedict, University at Buffalo, SUNY

10:00 a.m.   Coffee Break

<div align="center">

Session VIII
Dye Sensitized Systems
Wayne Gladfelter, Chair

</div>

10:30 a.m.	Electron Transfer Dynamics in Efficient Molecular Solar Cells **Gerald J. Meyer,** Johns Hopkins University
11:00 a.m.	Interfacial Photochemical Processes in Sensitized Nanostructured Electrodes **Arthur J. Frank**, National Renewable Energy Laboratory
11:30 a.m.	Metal-to-Ligand Charge Transfer Excited States on Surfaces and in Rigid Media. Application to Energy Conversion **Thomas J. Meyer**, University of North Carolina at Chapel Hill

Wednesday Afternoon, June 8

12:00 p.m.	Lunch

<div align="center">

Session IX
Donors and Acceptors
John Reynolds, Chair

</div>

1:00 p.m.	Structural Control of Excited State Properties: from Complexes to Dye Sensitizer Mimics **Lin X. Chen**, Argonne National Laboratory
1:30 p.m.	Metal-Linked Artificial Peptides as Photoinitiated Molecular Wires & Antennas **Mary Elizabeth Williams**, The Pennsylvania State University

<div align="center">

Session X
Panel Discussion

</div>

2:00 p.m.	**Future Directions of the Solar Photochemistry Program** With the advent of EFRCs and Solar Fuels Hub, selected members of the Program discuss its future directions
2:50 p.m.	Closing Remarks **Mark Spitler** and **Richard Greene**, U.S. Department of Energy

Session I

Opening Session

Limits to the Efficiency of Natural Photosynthesis:
Raising the Ceiling on the Maximum Conversion Efficiency

Donald R. Ort[1,2], Stephen P. Long[1], Xinguang Zhu[1]
Institute of Genomic Biology[1] & USDA/ARS[2]
University of Illinois
Urbana, IL 61801

The world population is projected to grow to ~10 billion before reaching a plateau in the later part of this century, and increasing economic prosperity of the developing world is forecast to soon place even greater demands on agricultural production than will population growth. With very few prospects to sustainably expand the 1.5 billion ha of cropland currently under cultivation, a doubling of productivity will be needed to meet the increasing demand before the end of this century. Current photosynthesis underlies the production of all of our food and fiber and biomass-based biofuel is increasingly being viewed as a source of renewable fuels. More solar energy reaches the Earth's surface every hour (4.3×10^{20} J) than is consumed on the planet in a year (4.1×10^{20} J). Despite its quantity, solar energy is diffuse, placing a premium on the overall efficiency of photosynthetic solar energy conversion. In this context it is not surprising that 'application of the revolutionary advances in biology and biotechnology to the design of plants and organisms that are more efficient energy conversion machines' was identified as a major solar energy research goal for the coming decades (Basic Research Needs for Solar Energy Utilization (http://www.sc.doe.gov/bes/). A key starting point for identifying and evaluating biotechnology targets for improving photosynthetic solar conversion efficiency is a critical re-examination of the maximum efficiency of photosynthetic solar energy conversion that could theoretically be achieved in managed ecosystems (Figure 1).
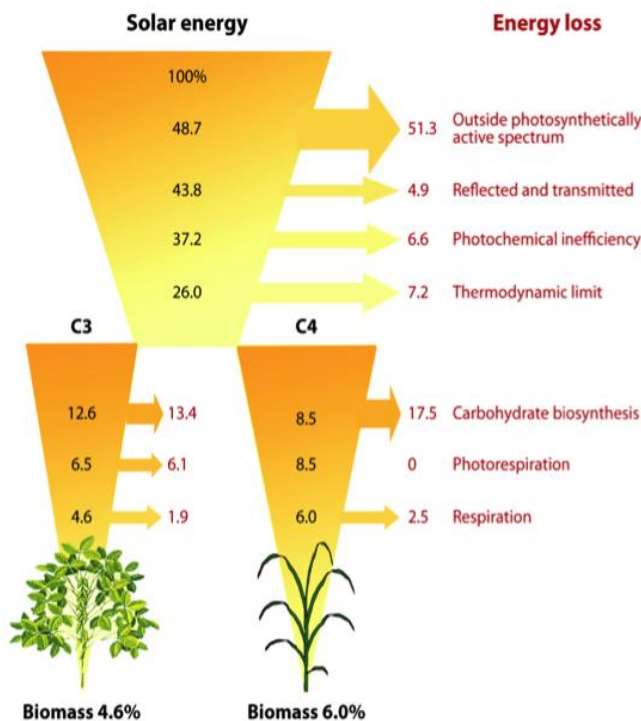
Figure 1. Minimum energy losses showing the percentage remaining (*inside arrows*) and percentage losses (*at right*) from an original 100% calculated for stage of photosynthetic energy transduction from sunlight incident on a leaf to plant biomass. Both C3 and C4 (NADP–malic enzyme type) photosynthesis are presented. Calculations assume a leaf temperature of 30 °C and an atmospheric [CO_2] of 387 ppm. The theoretical maximal photosynthetic energy conversion efficiency (ε_c) is 4.6% for C3 and 6% for C4 plants. These values are for total full-spectrum solar radiation. If the analysis is limited to photosynthetically active radiation (400–700 nm), then these values become 9.4% for C3 and 12.3% for C4.

The central challenge to improving photosynthetic efficiency is knowing how alterations made to the photosynthetic process at the level of the chloroplast will scale, because it is the impact on the integral of seasonal canopy photosynthesis, not the instantaneous rate of chloroplast or single leaf photosynthesis, that is related to biomass production and yield. Using experimental approaches to test the impacts of individual engineering options for different crops under different conditions on canopy photosynthesis is clearly unrealistic. Developing systems models of photosynthesis—and eventually plant primary metabolism and plant growth and development—that can be combined with optimization algorithms to evaluate impacts on photosynthetic efficiency of large numbers of virtual genetic and trangenic manipulations in multiple combinations holds the greatest promise for improving photosynthetic efficiency. Indeed, the emergent efforts to use this approach have already identified highly plausible targets for substantial improvements. The task of improving photosynthetic efficiency is not a distant challenge but is already upon us, given that even when these improvements are achieved it may take an additional 10–20 years to bring such innovations to farms in commercial cultivars at adequate scale. In this context, it seems valuable to group the various alterations that emerged from mechanistic modeling and proof-of-concept experiments by our best estimate of their relative time horizon and to identify the most important technical and/or scientific hurdles that must be overcome in order to be realized (Table 1).

Time horizon	Change to be made	[a]Increase in ε_c (%)	Major obstacle(s) to implementation
Long-term[b]	Rubisco with dramatically decreased oxygenase activity	30	Determining which molecular features of Rubisco control specificity
	Increase mesophyll conductance	20	Determining which physiological factors control mesophyll conductance
	Conversion of C3 to C4	30	Identifying suite of genes that control morphological and biochemical conversion
Mid-term[c]	Increased rate of recovery from photoprotective state	15	Determining combination of components in PSII photoprotective pathway to be altered
	Introduction of Rubisco with increased carboxylation rate	25	Developing efficient transformation technologies
Near-term[d]	Photorespiration bypass	13	Maximizing bypass flux; introducing into crop plants
	Improved canopy structure	30	Identifying genetic variability
	Rebalancing of RuBP regeneration rate with increased carboxylation	30	Demonstrating proof of concept experiments in crop plants; developing efficient transformation technologies
	Optimize canopy chlorophyll content	30	Developing optimization models; determining metabolically most efficient mode of reducing chlorophyll content

[a] Percent increase in the daily integral of carbon uptake estimated for a sunny day at midlatitudes.
[b] Theoretical basis for what change to make to affect the increase is missing. Not enough is known to determine if answers can be bought.
[c] Important science regarding what components to change to affect the increase is missing. With substantial focused investment, possible in a 20-year time frame.
[d] The basic science about what needs to be done is in place and the hurdles for implementation are technical. With adequate investment, possible in 10-year time frame.

Implementation of the four alterations to the photosynthetic process in the Near-term category is limited primarily by the will to invest sufficiently to make it happen. This is perhaps also the case for the table's Mid-term goal of transferring C4 (high-k^c_c) Rubisco into the chloroplasts of C3 plants. The theory establishing the benefit of the alteration is well developed, but the technical obstacles to transforming both genomes, i.e., in ensuring proper import, posttranslational processing and assembly, silencing of native genes, and efficient interaction with regulatory partners need to be overcome. Nevertheless, the solutions to implementation hurdles seem very plausible in a 20-year or shorter timeframe with sufficient investment. The same may be true for accelerating the rate of relaxation of photoprotection to restore fully efficient photosynthesis. The Long-term category includes proposed changes about which there exists too little science to judge feasibility. The molecular features of the Rubisco holoenzyme that control discrimination between oxygen and carbon dioxide are unknown, and it may be that the reaction mechanism of Rubisco precludes the possibility of engineering any significant decrease in oxygenation activity. The goal of converting C3 crops to C4 photosynthetic metabolism belongs in this Long-term category. Important science needed to judge feasibility remains critical; namely, discovering the genetic basis for Kranz anatomy and developmental compartmentation of the processes of C4 photosynthesis, which is still largely unknown. Another goal that remains long term is the engineering necessary to increase mesophyll conductance to CO_2, since critical information about the physiological and physical factors affecting mesophyll conductance, required to judge feasibility, is missing. Even longer term would be a redesign of the two photosystems that currently compete for the same regions of the solar spectrum, cutting the energy efficiency nearly in half compared to what might be achieved if the bandgaps were different and optimized to use different regions of the spectrum.

References

Zhu, X-G., Long, S.P., and Ort, D.R. What is the maximum efficiency with which photosynthesis can convert solar energy into biomass? Currnet Opinion Biotechnology. 19:153-159. 2008

Zhu, X-G., Long, S.P., and Ort, D.R. Towards more efficient crop photosynthesis. Annual Reviews of Plant Biology. 61:235-261. 2010

Ort, D.R., Zhu, XG., and Melis, A. Optimizing antenna size to maximize photosynthetic efficiency. Plant Physiology 155:79-85. 2011

Magnetic Resonance and DFT Study of Carotenoid Neutral Radicals: Dependence on Conjugation Length and Substituents

Lowell D. Kispert,[1] A. Ligia Focsan,[1] Michael K. Bowman,[1]
Nikolay E. Polyakov,[2] and Peter Molnar[3]
[1]The University of Alabama, Department of Chemistry, Tuscaloosa, AL 35487-0336
[2]Institute of Chemical Kinetics and Combustion, Novosibirsk, Russia
[3]Department of Biochemistry and Medical Chemistry, University of Pécs, Hungary

Scope of the project: The excess energy of chlorophyll in photosynthetic light harvesting complex II (LHC II) is quenched when a charge transfer complex is formed between chlorophyll and the neighboring carotenoid. The resulting carotenoid radical cations formed are weak acids ($pK_a \sim$ 4-7) and deprotonate to form carotenoid neutral radicals. It has been previously shown that the presence of a radical in the vicinity (up 10 Å) of a species in an excited state quenches the excited state. This has prompted the need to examine the properties of carotenoid neutral radicals as a function of substituents like allene, epoxide, methoxy, carbonyl and conjugation length as a possible additional means of quenching the excited state of chlorophyll as a protective mechanism.

Recent results: The radical intermediates formed upon catalytic or photooxidation of the carotenoid 9'-*cis* neoxanthin inside MCM-41 molecular sieves were detected by pulsed Mims and Davies electron nuclear double resonance (ENDOR) spectroscopies and characterized by density functional theory (DFT) calculations. Mims ENDOR spectra (20 K) were simulated using the hyperfine coupling constants predicted by DFT, which showed that a mixture of carotenoid radical cations ($Car^{\bullet+}$) and neutral radicals ($\#Car^{\bullet}$) is formed. The DFT relative energies of the neutral radicals formed by proton loss from the C5, C5', C9, C9', C13, and C13'-methyl groups of $Car^{\bullet+}$ showed that $\#Car\bullet(9')$ is energetically most favorable, while $\#Car^{\bullet}(9)$, $\#Car^{\bullet}(13)$, $\#Car^{\bullet}(13')$, $\#Car^{\bullet}(5')$, and $\#Car^{\bullet}(5)$ are less favorable for formation by 2.6, 5.0, 5.1, 22.5, and 25.6 kcal/mol. No evidence for formation of $\#Car^{\bullet}(5)$ was observed in the EPR spectra, consistent with DFT calculations. The allene bond at the unprimed end and the epoxy group at the prime end prevent protons loss at the C5 and C5'-methyl groups by reducing the conjugation so crucial for the neutral radical stability. These examined properties and the known crystal structure of the light harvesting complex II (LHC II) suggest the neutral radicals of 9'-*cis* neoxanthin are not available for quenching the excited states of Chl, consistent with its observed lack of quenching properties.

This observation is in agreement with the non-quenching ability of violaxanthin where the presence of the epoxide groups on the terminal rings prevents proton loss on the terminal ring and reduces the conjugation length for the neutral radicals formed by proton loss at the C9 and C13 methyl groups. However, proton loss from the terminal rings of zeaxanthin or lutein give rise to neutral radicals with longer conjugation length.

This study of the properties of the carotenoid neutral radicals has been extended to linear open chain carotenoids as a function of conjugation length from n = 15 (bisdehydrolycopene) to 9 (neurosporene). For a conjugation length of n=15 and a symmetrical radical cation, proton loss requires the same energy within 1 kcal from any of the methyl groups. However upon adding protons to the ends to maintain or eliminate symmetry or by adding methoxy groups to one end

or both ends, the most stable radicals are formed by proton loss at either C2 (anhydrorhodovibrin, spirilloxanthin) or C4 (lycopene) at the unprimed end, and C8' (neurosporene, spheroidene, spheroidenone) at the primed end. A quenching role is reported for these. The relative energy of proton loss versus the conjugation length show a systematic behavior relative to the energy loss from the methyl group at C5.
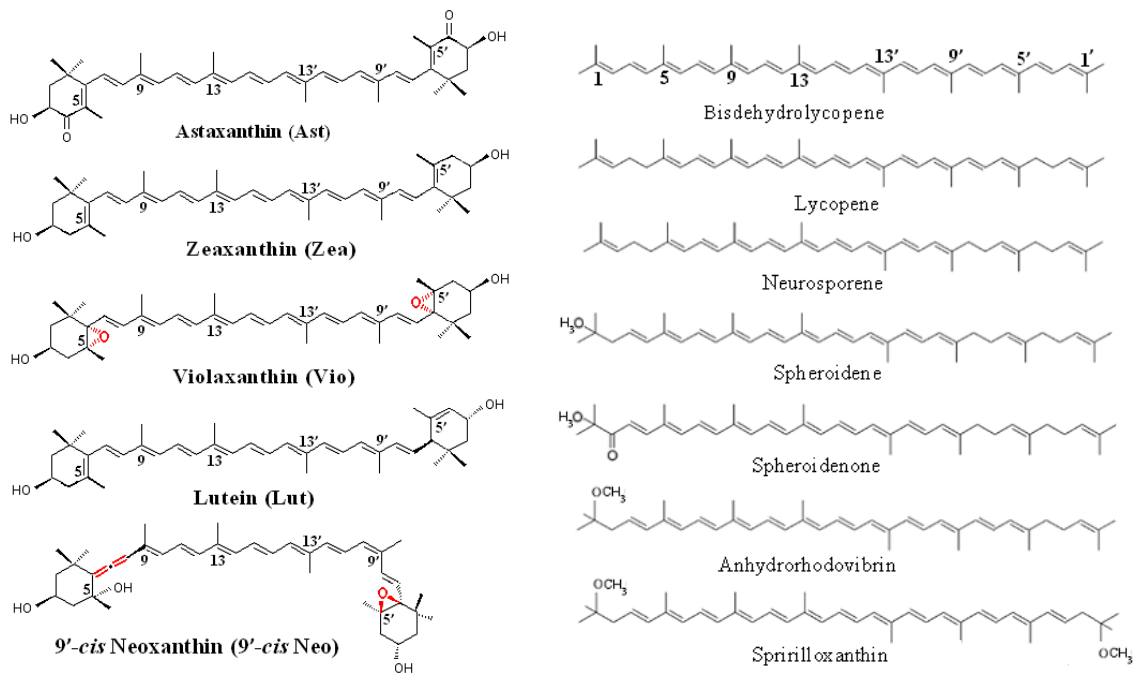
The carotenoid astaxanthin forms novel metal ion complexes with Ca^{2+}, Zn^{2+} and Fe^{2+}. MS and NMR measurements indicate that the two oxygen atoms on the terminal cyclohexene rings of astaxanthin adjacent to substituted hydroxyl group chelate the metal to form 1:1 complexes with Ca^{2+} and Zn^{2+} at low salt concentrations <0.2 mM. Pulsed EPR measurements were carried out on UV-produced radicals of astaxanthin supported on silica-alumina, MCM-41 or Ti-MCM-41. The pulsed EPR measurements detected the radical cation and neutral radicals formed by proton loss at 77 K from the C3, C5, C9, and C13 methyl groups and a radical anion formed by deprotonation of the neutral radical at C4. There was more than an order of magnitude increase in the concentration of radicals on Ti-MCM-41 relative to MCM-41, and the radical cation concentration exceeded that of the neutral radicals.

Water soluble complex of carotenoids were formed by complexing carotenoids with the natural polysaccharide arabinogalactan (PA). These complexes showed enhanced photostability by a factor of 10 in water solution, a decrease by a factor of 20 in the reactivity toward metal ions (Fe^{3+}) and reactive oxygen species in solution. Canthaxanthin radical cations formed in these complexes are stable for ~10 days at room temperature.

Photoirradiation of TiO_2 nanoparticles by visible light in the presence of the water-soluble polysaccharide (PA) complexes of carotenoid β-carotene leads to enhanced yield of the reactive hydroxyl (OH) radicals. The observed enhancement of the photocatalytic efficiency for carotenoid complexes, as measured by the quantum yield of the desired spin adducts, arises from the decrease in the rate constant for the back electron transfer to the carotenoid radical cation.

7

Future Plans: Electrochemical measurements of mono- and di-esters of astaxanthin and its salt complexes will be performed to establish the antioxidant activity and its relation to scavenging properties of peroxyl radicals.

Papers published in 2008 – 2011

1. A. L. Focsan, M. K. Bowman, T. A. Konovalova, P. Molnár, J. Deli, D. A. Dixon, and L. D. Kispert "Pulsed EPR and DFT Characterization of Radicals Produced by Photooxidation of Zeaxanthin and Violaxanthin on Silica Alumina", *J. Phys. Chem. B*, **112**, 1806-1819 (2008).

2. J. Lawrence, A. L. Focsan, T. A. Konovolova, P. Molnár, J. Deli, M. Bowman, and L. D. Kispert "Pulsed ENDOR Studies of Carotenoid Oxidation in Cu(II)-Substituted MCM-41 Molecular Sieves", *J. Phys. Chem. B*, **112**, 5449-5457 (2008).

3. L. D. Kispert, A. L. Focsan, P. Molnar, and J. Deli "Structure and Properties of 9'-cis Neoxanthin Carotenoid Radicals by EPR Measurements and DFT Calculations: Present in LHC II", *J. Phys. Chem. B*, **113**, 6087-6096 (2009).

4. Y. Gao, K. E. Shinopoulos, C. A. Tracewell, A. L. Focsan, G. W. Brudvig, and L. D. Kispert "Formation of Carotenoid Neutral Radicals in Photosystem II", *J. Phys. Chem. B,* **113***,* 9901-9908 (2009).

5. N.E. Polyakov, T.V. Leshina, E.S. Meteleva, A.V. Dushkin, T.A. Konovalova, and L.D. Kispert "Water Soluble Complexes of Carotenoids with Arabinogalactan", *J. Phys. Chem. B*, **113**, 275-282 (2009).

6. T. A. Konovalova, S. Li, N. E. Polyakov, A. L. Focsan, D.A. Dixon, and L. D. Kispert "Measuring Ti(III)-Carotenoid Radical Interspin Distances in Ti-MCM-41 by Pulsed EPR Relaxation Enhancement Method", *J. Phys. Chem. B*, **113**, 8704-8716 (2009).

7. N. E. Polyakov and L. D. Kispert "Water Soluble Supramolecular Complexes of β-Carotene and Other Carotenoids" in *Beta Carotene: Dietary Sources, Cancer and Cognition*. Eds. by L. Haugen and T. Bjornson, Nova Science Publishers, pp.191-230 (2009).

8. N. E. Polyakov, A. L. Focsan, M. K. Bowman, and L. D. Kispert "Free Radical Formation in Novel Carotenoid Metal Ion Complexes of Astaxanthin", *J. Phys. Chem. B*. **114**, 16968-16977 (2010).

9. L. D. Kispert and N. E. Polyakov "Carotenoid Radicals: Cryptochemistry of Natural Colorants", *Chem. Lett*. **39**, 148-155 (2010).

10. N. Polyakov, T. Leshina, E. Meteleva, A. Dushkin, T. Konovalova, and L. Kispert "Water Soluble Conjugates of Carotenoids and Drugs with Oligo- and Polysaccharides. Synergy of Drug Transport and Efficacy" in *Nanotech 2010 Proceedings*, CRC Press, Tailor & Francis Group, New York, Vol. 3, pp. 312-315 (2010).

11. N. E. Polyakov, T. V. Leshina, E. S. Meteleva, A. V. Dushkin, T. A. Konovalova, and L. D. Kispert "Enhancement of Photocatalytic Activity of TiO2 Nanoparticles by Water Soluble Complexes of Carotenoids" *J. Phys. Chem. B*, **114**, 14200-14204 (2010).

12. L. D. Kispert, L. Focsan and T. Konovalova "Applications of EPR Spectroscopy to Understanding Carotenoid Radicals", in *Carotenoids, Physical Chemical and Biological Functions and Properties*, J. T. Landrum, Editor, CRC Press, Boca Raton, FL, pp. 159-189 (2010).

13. A. L. Focsan, M. K. Bowman and L. D. Kispert "Carotenoid Radical Formation: Dependence on Conjugation Length", (In Preparation).

Session II

Novel Molecular Structures

Photophysics of Single and Multiple Excitons in Carbon Nanotubes

Lisa J. Carlson, Marat Khafizov, Andrea J. Lee, Julie A. Smyder,
Shujing Wang, Xiaoyong Wang, and Todd D. Krauss
Department of Chemistry
University of Rochester
Rochester, New York 14627-0216

Single-walled carbon nanotubes (SWNTs) are tubular graphitic molecules with high aspect ratios and exceptional electronic and optical properties. Single semiconducting SWNTs display remarkably stable and size-tunable photoluminescence at near-infrared (NIR) wavelengths, making them fundamentally interesting and technologically relevant materials [1]. However, individual SWNTs have a photoluminescence (PL) quantum yield (QY) of about 1%, much less than other NIR emitting nanomaterials such as semiconductor quantum dots (QDs) [1]. It is currently not understood whether the poor QY of SWNTs is an intrinsic property or the result of extrinsic quenching mechanisms indicative of non-optimal sample quality. With regards to applications in solar energy conversion, carbon nanotubes have been suggested as possible replacements for transparent semiconductor electrodes, as conductive materials for charge and ion transport in catalytic membranes, or even as photosensitizers. An understanding of photoinduced exciton dynamics in SWNTs, especially nonradiative decay mechanisms, directly impacts these future potential applications.
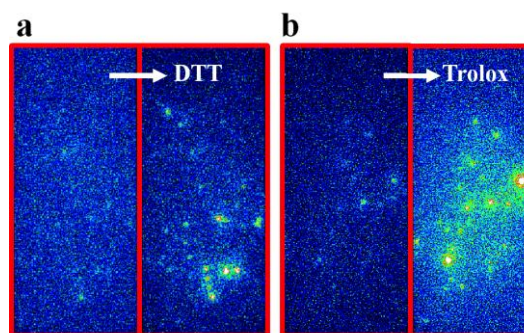
Figure 1. Fluorescence images of individual SWNTs before and after adding a) Dithiothreitol (DTT) and b) Trolox. The horizontal dimension for each fluorescence image is ~20 μm.

We will discuss our observation that the addition of mild reducing agents, such as dithiothreitol or trolox, to an aqueous solution of DNA-wrapped SWNTs results in an enormous enhancement of the QY for individual SWNTs by almost an order of magnitude (Figure 1). SWNT QY values ranged between 15 to 40%, making them as equally bright as highly fluorescent commercial CdTe/ZnS QDs. Brightening was reversible upon removal of the reducing molecules, suggesting that a transient reduction of defect sites on the SWNT sidewall causes the effect. These unexpectedly high QY values indicate that under the right conditions. SWNTs are intrinsically bright emitters, and that current understanding of the optical properties of SWNTs may have been obtained from defective SWNTs having their PL partially quenched [10].

In a related study, correlated measurements of fluorescence and topography were performed for individual SWNTs on quartz using epifluorescence confocal microscopy and atomic force microscopy (AFM) (Figure 2). This approach can not only quantify the average fraction of semiconducting SWNTs in a sample, but also makes it possible to elucidate the relationship between fluorescence intensity and SWNT structure, length, and orientation on the substrate. Surprisingly, only ~11% of all SWNTs as observed with AFM displayed fluorescence spectra at detectable levels in correlated measurements, despite high densities of SWNTs on the substrates.

In fact, given that the QY for each bright individual SWNT is ~3% [1] and that only ~11% of all semiconducting SWNTs were found to be emissive, the estimated QY for an ensemble of semiconducting SWNTs should equal the product of these two quantities. Indeed, we obtain a value of QY ~0.33%, which is in reasonable agreement with the ensemble QY for a similar (6,5)-enriched sample of DNA–SWNTs (QY ~ 0.14%). Therefore, our data suggest that the low ensemble QYs for carbon nanotubes can be largely attributed to a small percentage of relatively bright SWNTs in the ensemble, and not to a uniform population of SWNTs all with poor emission properties.
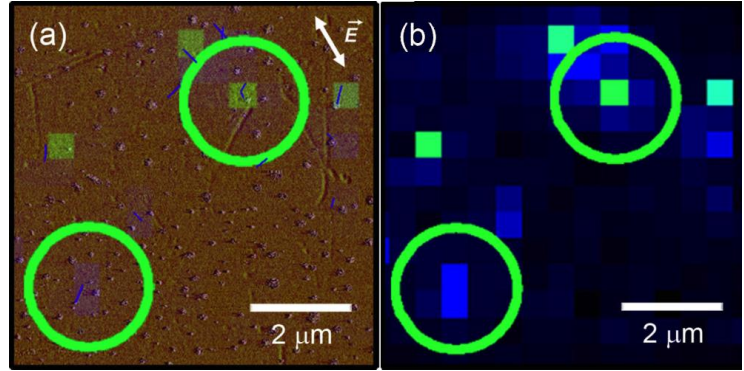
Figure 2. (a) Overlaid topography (tan) and fluorescence (blue) scans for SWNTs on patterned quartz. Blue lines represent the location of nanotubes and green circles indicate areas for which fluorescence spectra were observed. Long, straight features that are > 2 μm are etch pits in the quartz. (b) Fluorescence image for the same area in (a).

Absorption of a single high-energy photon in a semiconductor can potentially produce more than one charge carrier. Instead of creating heat, a highly energetic electron can lose excess energy by exciting a charge carrier across the energy gap, a process called multiple exciton generation (MEG). Nanoscale materials, such as QDs, may have efficient MEG (an idea pioneered by Nozik) leading to a possible inexpensive route to enhancing solar cell efficiency. We will present studies of MEG in isolated SWNTs using ultrafast transient absorption (TA) spectroscopy. Absorption of single photons with energies corresponding to three times the SWNT energy gap results in an electron-hole pair generation efficiency of 130% per photon [8]. Interestingly, MEG is observed despite extremely rapid exciton-exciton (i.e. Auger) annihilation (~ 1 ps). The fast Auger rate in SWNTs is in contrast to semiconductor QDs that have Auger annihilation times one to two orders of

Figure 3. (a) TA spectra measured under 800 nm (red) and 335 nm (black) excitation at low pump fluence where the average number of electron-hole pairs per SWNT $N_0 \approx 0.25$. Spectra are normalized at late decay times. Inset shows the difference between the two curves indicating the presence of MEG at 335 nm as measured through Auger annihilation.

magnitude longer than the SWNTs. Overall, the observation of more efficient MEG processes and faster Auger recombination in SWNTs relative to QDs is in agreement with the physical picture that electrons and holes in SWNTs experience stronger confinement and have enhanced many-body effects when compared to QDs. Our results also suggest that the MEG threshold in SWNTs can be close to the limit defined by energy conservation, which is highly relevant to the potential of MEG as a viable route to enhancing the efficiency of solar cells.

DOE Sponsored Solar Photochemistry Publications 2008-2011

1. L. J. Carlson and T. D. Krauss, "Photophysics of Individual Single-Walled Carbon Nanotubes," *Acc. Chem. Res.* **41,** 235–243 (2008).

2. R. Haggenmueller, S. S. Rahatekar, J. A. Fagan, J. Chun, M. L. Becker, R. R. Naik, T. Krauss, L. Carlson, J. Kadla, P. Trulove, D. Fox, Z. Fang, S. Kelley, J. W. Gilman, "A Comparison of Quality of Dispersion of Single Wall Carbon Nanotubes using Different Surfactants and Biomolecules," *Langmuir* **24**, 5070 (2008).

3. R. Priefer, K. E. Leach, T. D. Krauss, J. R. Drapo, M. L. Ingalsbe, M. A. van Dongen, J. C. Cadwalader, M. A. Baumler, and M. S. Pinto, "Multilayer Film Preparation of PVPh from Aqueous Media," *Surf. Coat. Technol.* **202**, 6109-6112 (2008).

4. K. E. Leach, H. N. Pedrosa, L. J. Carlson and T. D. Krauss, "Fluorescence from Isolated Carbon Nanotubes in Cross-linked Micelles," *Chem. Mater.* **21**, 436-438 (2009).

5. T. D. Krauss, "Biosensors: Nanotubes Light up Cells," *Nat. Nanotech.* **4**, 85-86 (2009).

6. R. Priefer, P. N. Grenga, A. Mandrino, D. M. Raymond, K. E. Leach, T. D. Krauss, "Multilayering of a very weak polyelectrolyte (PVPh) with a strong polyelectrolyte (PDMAC) from aqueous media, " *Surf. Sci.* **604**, 59-62 (2009).

7. H.-I. Peng, C. M. Strohsahl, K. E. Leach, T. D. Krauss, and B. L. Miller, "Label-Free DNA Detection on Nanostructured Ag Surfaces," *ACS Nano* **3,** 2265–2273 (2009).

8. S. Wang, M. Khafizov, X. Tu, M. Zheng, and T. D. Krauss, "Multiple exciton generation in single-walled carbon nanotubes," *Nano Lett.* **10**, 2381-2386 (2010).

9. H.-I Peng, T. D. Krauss, and B. L. Miller, "Aging Induced Ag Nanoparticle Rearrangement under Ambient Atmosphere and Consequences for Nanoparticle-Enhanced DNA Biosensing" *Anal. Chem.* **82**, 8664-8670 (2010).

10. A. J. Lee, X. Wang, L. J. Carlson, J. A. Smyder, X. Tu, M. Zheng, and T. D. Krauss, "Bright Fluorescence from Individual Single-Walled Carbon Nanotubes" *Nano Lett.* ASAP (2011).

Organic, Nanoscale, and Self-Assembled Structures Relevant to Solar Energy Conversion

Michael J. Therien
Department of Chemistry
French Family Science Center, 124 Science Drive
Duke University
Durham, NC 27708-0354

Understanding the molecular-level principles by which complex chemical systems carry out photochemical charge separation, transport, and storage will impact the design of practical solar energy conversion and storage devices. Towards this goal, this program focuses on: (i) delineating new compositions of matter relevant to solar energy conversion, (ii) elucidating factors that control charge transfer, charge migration, photoconductivity, and exciton diffusion dynamics in assemblies relevant to light-driven energy transduction, (iii) probing the extent of electronic coupling between conjugated organic materials and nanoscale structures in both ground and excited states, and (iv) engineering high quantum yield electron-hole pair production from initially prepared excitonic states in compositions that feature both molecular and nanoscale electrooptically active components. Projects carried out over the past three years include:

Single-Chain, Helical Wrapping of Individualized, Single-Walled Carbon Nanotubes by Ionic Poly(Aryleneethynylene)s: New Compositions for Photoinduced Charge Transfer Reactions and Photovoltaic Applications. Amphiphilic, linear, semi-conducting aryleneethynylene polymers such as poly[*p*-{2,5-bis(3-propoxysulfonicacid-sodiumsalt)}phenylene]ethynylene (PPES) and poly[2,6-{1,5-bis(3-propoxysulfonicacid-sodiumsalt)}napthylene]ethynylene (PNES) efficiently disperse single-walled carbon nanotubes (SWNTs) under ultra-sonication conditions into the aqueous phase. Vis-NIR absorption spectroscopy, atomic force microscopy (AFM), and transmission electron micro-scopy (TEM) demonstrate that these solubilized SWNTs are individualized, and feature a self-assembled superstructure in which a polymer monolayer helically wraps the nanotube surface; the observed PPES and PNES pitch lengths confirm structural predictions made via MD simulations. Appropriate metatheses reactions allow these self-assembled polymer-nanotube systems to be dissolved in organic solvents; electronic spectroscopy, transient absorption studies, and AFM and TEM data confirm that the helical wrapping structure observed for in aqueous solution persists in nonaqueous media.
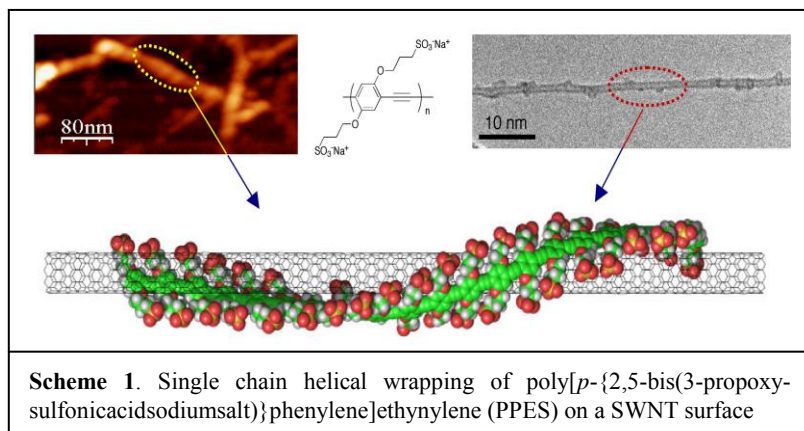
Scheme 1. Single chain helical wrapping of poly[*p*-{2,5-bis(3-propoxy-sulfonicacidsodiumsalt)}phenylene]ethynylene (PPES) on a SWNT surface

These well-defined nanotube-semi-conducting polymer hybrids can be further engineered to serve as electron transport elements in excitonic solar cells and function as electron acceptors in electron transfer reactions involving photoactivatable redox centers. These assemblies include
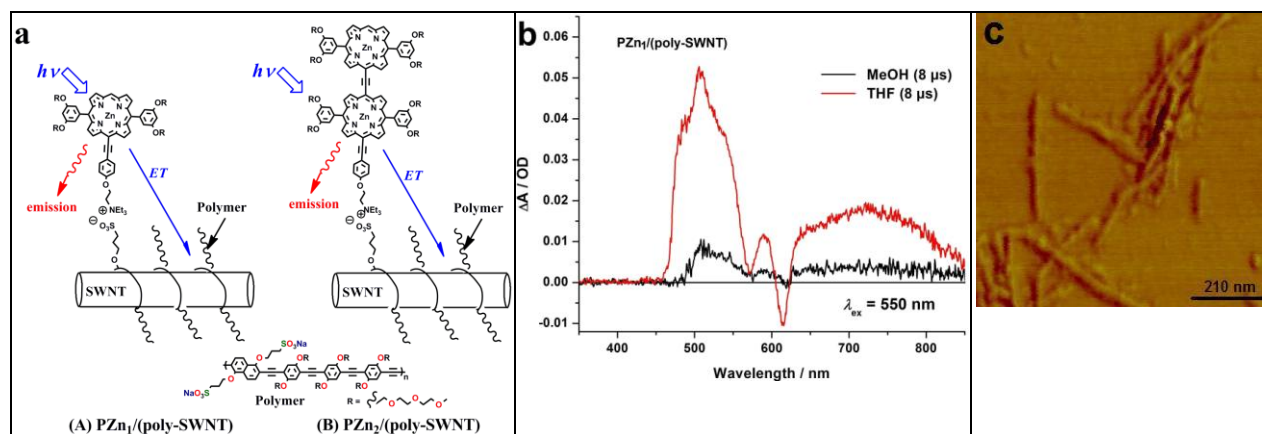
Figure 1. (a) Schematic representations of photoinduced electron transfer reactions in nanoscale assemblies based on **PZn$_1$** and **PZn$_2$** chromophores and ionic polymer-wrapped SWNTs. (b) TA-absorption spectra of **PZn$_1$/(poly-SWNT)** assemblies showing the porphyrin cation radical signature at t_{delay} = 8 μs [λ_{ex} =550 nm: solvent = methanol (black) and THF (red)]. (c) Topographic AFM images of the **PZn$_1$/(poly-SWNT)** assemblies underscoring their individualized nature.

(porphinato)zinc-based chromophores such as **PZn$_1$** and ethyne-bridged **PZn$_n$** motifs functionalized with ancillary cationic triethylammonium groups that have been anchored to anionic polymer-wrapped SWNTs via ion-metathesis reactions (Figure 1), and analogous **PZn$_1$** and **PZn$_n$** chromophores that have been incorporated into the backbones of polymers that helically wrap SWNTs (Figure 2). Electronic absorption data underscore that **BN-PZn$_2$** polymers have strong electronic interactions with SWNTs (Figure 2d). The large established charge mobilites of **PZn$_n$** species, their intense absorptivity over large windows of the UV, vis, and NIR, and the ease with which their frontier orbital energy levels can be manipulated underscore a broad range of opportunities to engineer function relevant to excitonic solar cells.
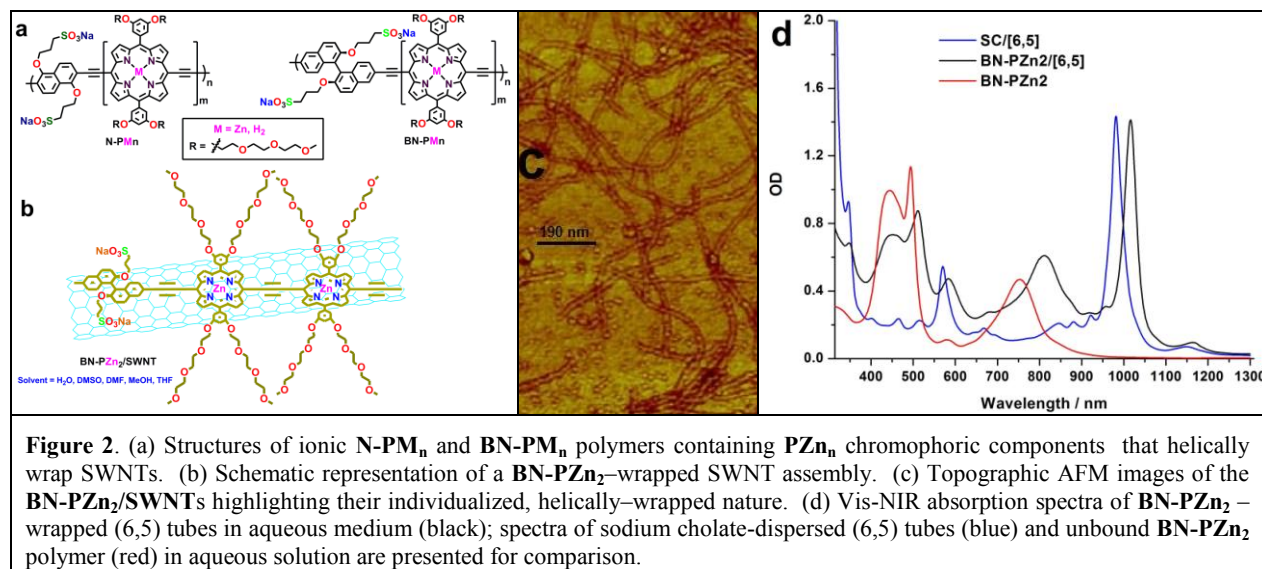
Figure 2. (a) Structures of ionic **N-PM$_n$** and **BN-PM$_n$** polymers containing **PZn$_n$** chromophoric components that helically wrap SWNTs. (b) Schematic representation of a **BN-PZn$_2$**–wrapped SWNT assembly. (c) Topographic AFM images of the **BN-PZn$_2$/SWNT**s highlighting their individualized, helically–wrapped nature. (d) Vis-NIR absorption spectra of **BN-PZn$_2$** –wrapped (6,5) tubes in aqueous medium (black); spectra of sodium cholate-dispersed (6,5) tubes (blue) and unbound **BN-PZn$_2$** polymer (red) in aqueous solution are presented for comparison.

Excited State Dynamics of Nanoscale, Chromophore-Containing Polymersomes. Polymersomes, self-assembled vesicles are comprised of amphiphilic diblock copolymers, demonstrate numerous properties in common with liposomes, their lipid counterparts, yet exhibit mechanical
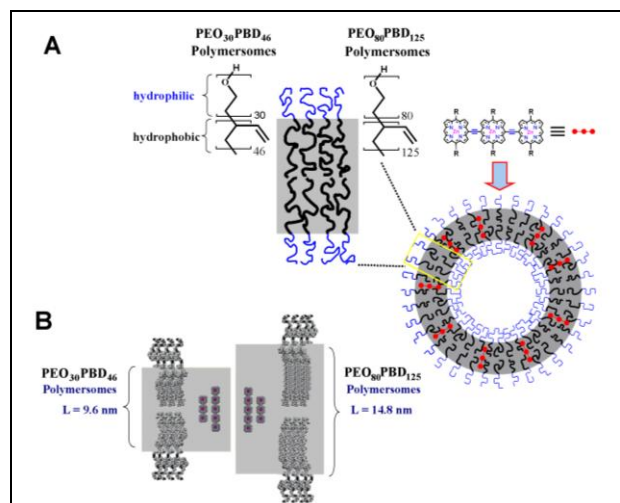
Scheme 2. (A) Depiction of **PZn₃** fluorophore dispersion within PEO-PBD NIR-emissive polymersome environments. (B) Hydrophobic bilayer thicknesses (L) of **PEO₃₀-PBD₄₆** and **PEO₈₀-PBD₁₂₅** polymersomes; generic **PZn₃** and **PZn₅** fluorophores are also shown, to scale, for comparison.

strengths 5-50 times greater. These features, coupled with the fact that the polymersome hydrophobic bilayer is 2-3 times thicker than that of classical liposomes suggest that polymersomes can incorporate, segregate, and disperse functional elements that are both larger and more morphologically diverse than that demonstrated to date in liposomes. Developing multi-component solar energy-transducing polymersomes requires fundamental studies of the electronic, optical, and photophysical properties of polymersomes that contain functional electrooptic elements. Polymersome membrane environments disperse ethyne-bridged oligo(porphinato)-zinc(II) based supermolecular fluorophores (**PZn$_n$** species) within the hydrophobic bilayer (Scheme 2). Ultrafast excited-state transient absorption and anisotropy dynamical studies of NIR-emissive polymersomes in which the **PZn$_n$** fluorophore loading per nanoscale vesicle is varied enable the exploration of concentration-dependent mechanisms for nonradiative excited-state decay. These experiments correlate fluorophore structure with its gross spatial arrangement within specific nanodomains of these nanoparticles, and reveal how compartmentalization of fluorophores within reduced effective dispersion volumes impacts bulk photophysical properties, and lay the groundwork for related assemblies that support complex energy, hole, and electron transfer functionality.

DOE Sponsored Solar Photochemistry Publications 2008-2011:

1. Synthesis of Water-Soluble Poly-(*p*-phenyleneethynylene) in Neat Water Under Aerobic Conditions via Suzuki-Miyaura Polycondensation using a Diborylethyne Synthon, Y. K. Kang, P. Deria, P. J. Carroll, and M. J. Therien, *Org. Lett.* **2008**, *10*, 1341-1344.

2. Ultrafast Excited State Dynamics of Nanoscale Near Infrared Emissive Polymersomes, T. V. Duncan, P. P. Ghoroghchian, I. V. Rubtsov, D. A. Hammer, and M. J. Therien, *J. Am. Chem. Soc.* **2008**, *130*, 9773-9784.

3. Plasmon Induced Electrical Conduction in Molecular Devices, P. Banerjee, D. Conklin, S. Nanayakkara, T.-H. Park, M. J. Therien, and D. A. Bonnell, *ACS Nano.* **2010**, *4*, 1019-1025.

4. Excitation of Highly Conjugated (Porphinato)palladium(II) and (Porphinato)platinum(II) Oligomers Produces Long-Lived, Triplet States at Unit Quantum Yield That Absorb Strongly over Broad Spectral Domains of the NIR, T. V. Duncan, P. R. Frail, I. M. Miloradovic, and M. J. Therien, *J. Phys. Chem. B.* **2010**, *114*, 14696–14702.

5. Electron Transfer Reactions of Rigid, Cofacially Compressed, π-Stacked Porphyrin-Bridge-Quinone Systems, Y. K. Kang, P. M. Iovine, and M. J. Therien, *Coord. Chem. Rev.* **2011**, *255*, 804-824.

6. Two-Photon Absorption Properties of Proquinoidal D-A-D and A-D-A Quadrupolar Chromophores, K. Susumu, J. A. N. Fisher, J. Zheng, D. N. Beratan, A. G. Yodh, and M. J. Therien. *J. Phys. Chem. A.* **2011**, *115*, In press.

Session III

Charge Separation in Organic Systems

Transient Absorption Microscopy Studies of Carrier Dynamics in Graphene and Polymer Blends

Libai Huang,[1]

Bo Gao,[1] Christopher Wong,[1] Fei Hua Li,[1] Gregory Hartland,[2] Michelle Kelley,[3] Grace Xing[3]

[1]Notre Dame Radiation Laboratory, University of Notre Dame, Notre Dame, IN 46556
[2]Department of Chemistry and Biochemistry, University of Notre Dame, Notre Dame, IN 46556
[3]Department of Electrical Engineering, University of Notre Dame, Notre Dame, IN 46556

Scope of the Project. A frontier in solar energy conversion research now lies in learning how to integrate functional entities across multiple length scales to create architectures that are optimized for solar energy conversion. The design and optimization of an effective solar energy conversion system requires experimental tools that provide understanding of these complex, multi-scale processes and their interplay at the system-wide level over a wide range of length and time scales. We are developing a research program to visualize in-situ charge carrier dynamics in solar energy conversion systems with simultaneous ultrafast time resolution and diffraction-limited spatial resolution. Transient absorption microscopy with simultaneous temporal (~ 200 fs) and spatial resolution (~ 200 nm) is achieved by coupling ultrafast pump-probe spectroscopy with confocal optical microscopy. This approach provides spatial maps of carrier dynamics in heterogeneous systems. In my talk, I will focus on our recent efforts in transient absorption imaging of carrier dynamics in graphene and photovoltaic polymer blends.

Recent Results. Transient absorption microscopy was employed to study charge carrier dynamics in epitaxial and chemical vapor deposition grown graphene on different substrates. Correlated transient absorption and atomic force microscopy (AFM) measurements have been performed for monolayer graphene, both free-standing and supported on a glass substrate (Fig.1). The transient absorption traces show a fast instrument response limited decay, followed by a slower intensity dependent decay of 1-2 ps. The fast decay is assigned to coupling between the excited charge carriers and the optical phonon modes, and the slow decay is due to the hot phonon effect. Interaction between graphene and the substrate was found to be critical
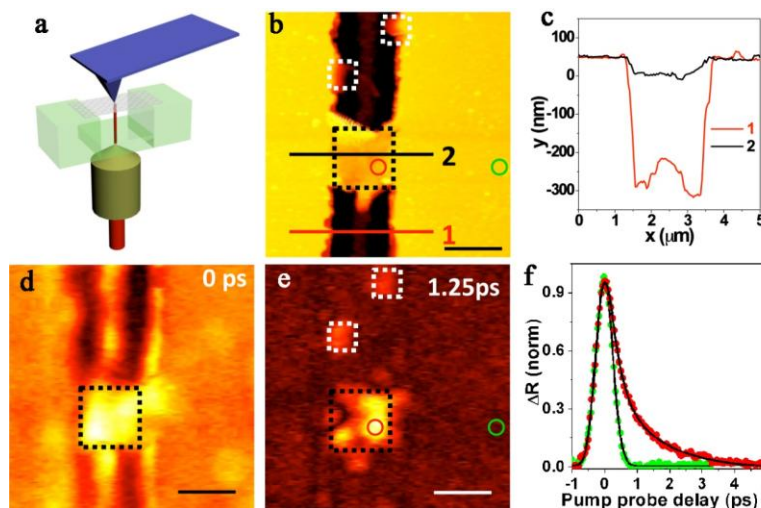
Fig.1 **a**: Schematic that shows the combined AFM-transient absorption microscopy measurements. **b**: AFM height image of the graphene sample. **c**: Line profile taken along the lines indicated in b. **d**: Transient absorption image of the same area at 0 ps delay. **e**: Transient absorption image at 1.25 ps delay. **f**: Transient absorption traces collected for suspended graphene (red filled circles) and substrate-supported graphene (green filled circles). The positions where the kinetic data are collected are indicate by the red and green circles in **b** and **e**. The scale bars in **b**, **d**, **e** are 2 μm. The pump fluence was 2 mJ/cm^2 for these measurements.

for charge carrier cooling. At a given pump laser fluence, the time constant for the slow decay is longer for suspended graphene compared to substrate-supported graphene (Fig.1). This is attributed to coupling between the excited charge carriers and the surface optical phonon modes of the substrate, which supplies an additional relaxation channel for supported graphene.

We have also examined charge carrier dynamics in bulk heterojunction film of poly(3-hexyl thiophene) (P3HT) and [6,6]-phenyl C61-butyric acid methyl ester (PCBM) by transient absorption microscopy. A pump wavelength of 410 nm and a probe wavelength of 820 nm were employed to probe the dynamics of photogenerated polarons in the blend. The effects of both annealing and morphology on charge transfer dynamics were explored. Significant spatial heterogeneity in charge carrier dynamics was observed in the bulk heterojunction film and morphology was found to play an important role in charge transfer dynamics. As shown in Fig.2, thermal annealing of the blend creates crystalline domains of P3HT and PCBM. We observed remarkably different dynamics corresponding to the local order and composition of the film. For instance, in the well mixed area of the film (area 3), a slow carrier dynamics was observed corresponding to the free mobile polarons created by charge separation at the interfaces of P3HT:PCBM. On the other hand, in the crystalline domain of P3HT where PCBM is depleted (area 1), the decay of charge carrier is much faster with a decay time of a few ps and this is attributed to the decay of singlet exciton in the crystalline P3HT phase. In summary, transient absorption microscopy allows us to directly visualize how charge transfer processes vary across these highly heterogeneous samples.
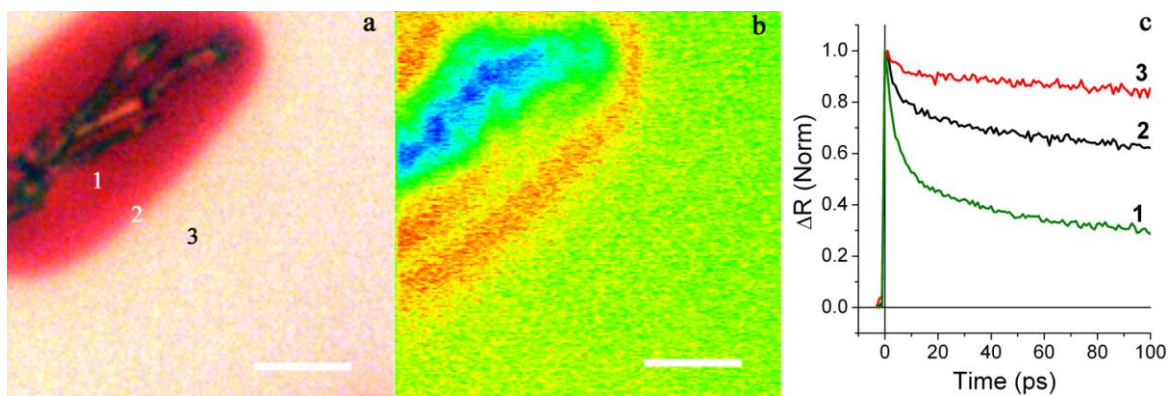
Fig.2 **a**: Optical micrograph of P3HT:PCBM blend (25%: 75% wt) after annealing at 140 °C for 30 mins. **b**: Transient absorption image of the same sample area at 0 ps delay **c**: Transient absorption traces collected at different locations of the film. The positions where the kinetics is collected are as indicated in **a.** The pump fluence was 0.1 mJ/cm^2 for these measurements.

Future Plans. The long term goal of our project is to resolve correlations between structural hierarchies and the fundamental mechanisms in solar energy harvesting architectures thus providing guidelines for designing more efficient solar harvesting devices. Current research efforts are underway to perform transient absorption imaging on working solar cells to directly correlate morphology-dependent device performance with charge carrier dynamics.

DOE Sponsored Solar Photochemistry Publications 2008-2011

1. Sean Murphy, Libai Huang, and Prashant V. Kamat, "Charge Transfer Complexation and Excited State Interactions in Porphyrin and Silver Nanoparticle Hybrid Nanostructures", *Manuscript in preparation*, 2011.

2. Libai Huang, Nina Ponomarenko, Gary P. Wiederrecht, David M. Tiede, "Resolution of Cofactor-Specific Delocalized Excited States and Charge Separation Pathways in Photosynthetic Reaction Centers by Single Crystal Spectroscopy", *Manuscript in preparation*, 2011.

3. Iltai Kim, Shana L. Bender, Jasmina Hranisavljevic, Lisa M. Utschig, Libai Huang, Gary P. Wiederrecht, and David M. Tiede, "Metal Nanoparticle Plasmon-Enhanced Light-Harvesting in a Photosystem I Thin Film", *Submitted*, 2011.

4. Bo Gao, Gregory Hartland, Tian Fang, Michelle Kelly, HuiLi Xing, Debdeep Jena, Libai Huang, "Studies of intrinsic hot phonon dynamics in suspended graphene by transient absorption microscopy", *Submitted* 2011.

5. Libai Huang, Bo Gao, Gregory Hartland, Michelle Kelly, HuiLi Xing, "Ultrafast relaxation of hot optical phonons in monolayer and multilayer graphene on different substrates", invited paper, *Surface Science*, in press 2011 (doi:10.1016/j.susc.2010.12.009).

6. Claire Deeb, Renaud Bachelot, Jrme Plain, Anne-Laure Baudrion, Safi Jradi, Alexandre Bouhelier, Olivier Soppera, Prashant K. Jain, Libai Huang, Carole Ecoffet, Lavinia Balan and Pascal Royer, "Quantitative Analysis of Localized Surface Plasmons Based on Molecular Probing", *ACS Nano* **4**, 4579 (2010).

7. Libai Huang, Gregory V. Hartland, Li-Qiang Chu, Luxmi, Randall M. Feenstra, Chuanxin Lian, Kristof Tahy and Huili Xing, "Ultrafast Transient Absorption Microscopy Studies of Carrier Dynamics in Epitaxial Graphene", *Nano Lett*. **10**, 1308 (2010).

8. Libai Huang, Gary P. Wiederrecht, Lisa M. Utschig, Sandra L. Schlesselman, Christina Xydis, Philip D. Laible, Deborah K. Hanson, and David M. Tiede, "Correlating Ultrafast Function with Structure in Single Crystals of the Photosynthetic Reaction Center", *Biochemistry* **47**, 11387 (2008).

Photo-Induced Electron Transfer in Conjugated Polymers with Colloidal Nanoparticles

Garry Rumbles, Nikos Kopidakis, Andrew Ferguson, Smita Dayal, and David Coffey
Chemical and Materials Science Center
National Renewable Energy Laboratory
Golden, Colorado, 80401-3393
and
Department of Chemistry and Biochemistry
University of Colorado
Boulder, Colorado 80309-0215

The fate of photogenerated excitons in conjugated polymers continues to be a topic of great fundamental interest. This is specifically important in the solid-state, where there are strong interactions between neighboring polymer chains that can lead to increased exciton mobility, as well as the formation of traps and dissociation sites that influence the exciton lifetime. The inclusion of additional species into the sample that have high electron affinities is of particular importance, as these provide a means of dissociating the excitons into separated, uncorrelated carriers that can be harvested by electrodes to produce, for example, a photovolatic solar cell. Species such as: fullerenes, single-walled carbon nanotubes (SWNTs), quantum-confined nanoparticles and nanoparticulate oxides; all have been shown to give a photovoltaic response, but with dramatically varying conversion efficiencies. However, our knowledge of the factors that encourage the dissociation process and, importantly, inhibit recombination remains poor, and this lack of basic fundamental knowledge impedes progress in this particular field solar photoconversion.

In order to focus studies on the important properties at interface formed between the conjugated polymer (donor) and an acceptor, we have established flash photolysis, time-resolved microwave conductivity (*fp*-TRMC, see Figure 1) as a tool for probing the generation of uncorrelated, separated electrons and holes from photoexcited excitons, and to follow their kinetic fate on time-scales from nanoseconds to milliseconds. The key assets of the system are its ability to detect the low-mobility carriers in organics, and to detect them in the absence of any electric fields associated with electrode materials. We have used this system to investigate a number of composite systems that includes: conjugated polymers with: fullerenes[2,16,18], SWNTs[3,4], colloidal quantum dots[5,8,20], as well as in donor-only systems[19]. Tracking the kinetics of carrier recombination and trapping provides insights into the photophysics that occurs at the interface formed by these nanoscale, donor-acceptor interfaces
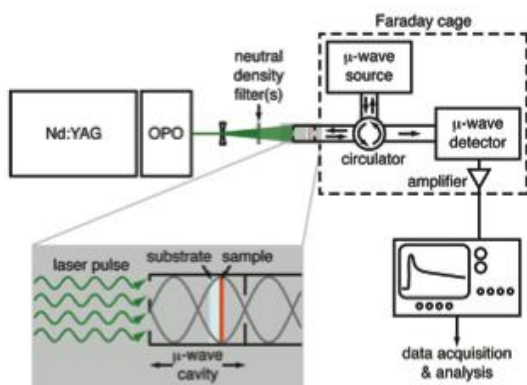
Figure 1 Schematic representation of the flash photolysis, time-resolved microwave conductivity system (*fp*-TRMC).

This presentation will focus on two specific systems: (i) conjugated polymers and dendrimers as the donor systems in composites with branched colloidal nanoparticles, where the charge-generating process is investigated, and (ii) thin films of weakly- and strongly-coupled colloidal quantum dots, where the strength of coupling on charge carrier is probed.
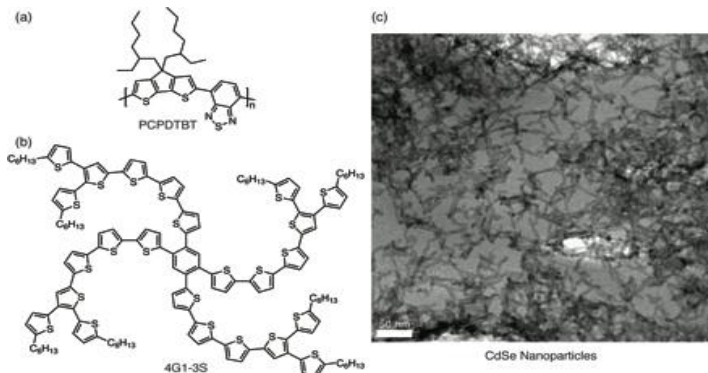
Figure 2   Molecular structures of (a) PCPDTBT, (b) 4G1-3S, and (c) a TEM image of the branched CdSe nanoparticles.

The first study investigates composites of branched (tetrapod) CdSe nanoparticles dispersed in either a low-bandgap polymer (PCPDTBT), or a phenyl-cored, thiophene-containing dendrimer (4G1-3S) [see Figure 2]. These two systems provide an opportunity to selectively excite the polymer to probe electron transfer to the nanoparticles, or to selectively excite the nanoparticle and probe hole transfer to the dendrimer. The time-resolved feature of the photoconductivity measurement has enabled us to demonstrate unequivocally, that photo-excitation of the nanoparticle leads to hole transfer to the dendrimer; a conclusion that cannot be drawn from device studies alone.

The second discussion will examine the role of coupling between colloidal CdSe quantum dots in layer-by-layer deposited thin films, where different-length alkane dithiols are used to control the separation of CdSe colloidal quantum dots. A series of fp-TRMC transients for this system are shown in Figure 3, where the linker between the quantum dots ranges from ethane through to octane to give average dot separations from 5Å to 20Å. With increasing separation the photoconductance transients can be seen to become longer, but decrease in magnitude (data not shown). This slightly unusual observation will be explained in terms of the influence of the yield of separated charge generation, although the mechanism of this process is unclear, and the respective carrier mobilities, both of which influence photoconductivity data from the fp-TRMC experiment.
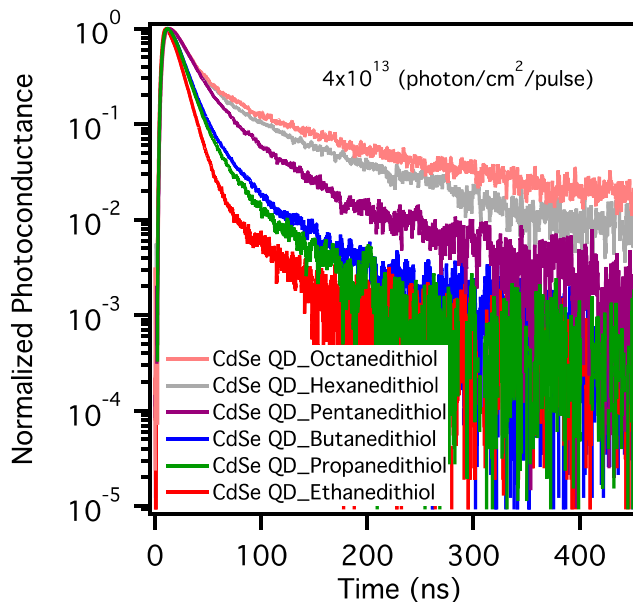
Figure 3   Normalized photoconductance transients of CdSe QDs capped with various alkyl dithiol molecules upon excitation at a wavelength of 500 nm wavelength, and a photon flux of 4×10^{13} photon/cm^2/pulse.

23

DOE Sponsored Solar Photochemistry Publications 2008-2011

1. Brown, K. A.; Dayal, S.; Ai, X.; Rumbles, G.; King, P. W. (2010). Controlled Assembly of Hydrogenase-CdTe Nanocrystal Hybrids for Solar Hydrogen Production. *Journal of the American Chemical Society*. 132(28), 2010; 9672-9680. doi:10.1021/ja101031r.

2. Coffey, D. C.; Ferguson, A. J.; Kopidakis, N.; Rumbles, G. (2010). Photovoltaic Charge Generation in Organic Semiconductors Based on Long-Range Energy Transfer. *ACS Nano*. 4(9), 2010; 5437-5445. doi:10.1021/nn101106b.

3. Holt, J. M.; Ferguson, A. J.; Kopidakis, N.; Larsen, B. A.; Bult, J.; Rumbles, G.; Blackburn, J. L. (2010). Prolonging Charge Separation in P3HT-SWNT Composites Using Highly Enriched Semiconducting Nanotubes. *Nano Letters*. 10(11), 2010; 4627-4633. doi:10.1021/nl102753z.

4. Ferguson, A. J.; Blackburn, J. L.; Holt, J. M.; Kopidakis, N.; Tenent, R. C.; Barnes, T. M.; Heben, M. J.; Rumbles, G. (2010). Photoinduced Energy and Charge Transfer in P3HT:SWNT Composites. *Journal of Physical Chemistry Letters*. 1(15), 2010; 2406-2411. doi:10.1021/jz100768f.

5. Dayal, S.; Reese, M. O.; Ferguson, A. J.; Ginley, D. S.; Rumbles, G.; Kopidakis, N. (2010). Effect of Nanoparticle Shape on the Photocarrier Dynamics and Photovoltaic Device Performance of Poly(3-hexylthiophene):CdSe Nanoparticle Bulk Heterojunction Solar Cells. *Advanced Functional Materials*. 20(16), 2010; 2629-2635. doi:10.1002/adfm.201000628.

6. Rance, W. L.; Rupert, B. L.; Mitchell, W. J.; Kose, M. E.; Ginley, D. S.; Shaheen, S. E.; Rumbles, G.; Kopidakis, N. (2010). Conjugated Thiophene Dendrimer with an Electron-Withdrawing Core and Electron-Rich Dendrons: How the Molecular Structure Affects the Morphology and Performance of Dendrimer:Fullerene Photovoltaic Devices. *Journal of Physical Chemistry C*. 114(50), 2010; 22269-22276. doi:10.1021/jp106850f.

7. Mitchell, W. J.; Ferguson, A. J.; Kose, M. E.; Rupert, B. L.; Ginley, D. S.; Rumbles, G.; Shaheen, S. E.; Kopidakis, N. (2009). Structure-Dependent Photophysics of First-Generation Phenyl-Cored Thiophene Dendrimers. Chemistry of Materials. 21(2), 2009; 287-297. doi:10.1021/cm802410d.

8. Dayal, S.; Kopidakis, N.; Olson, D.; Ginley, D.; Rumbles, G. Direct Synthesis of CdSe Nanoparticles in Poly(3-hexylthiophene). *Journal of the American Chemical Society*. 131(49), 2009; 17726-17727. doi:10.1021/ja9067673.

9. Rupert, B. L.; Mitchell, W. J.; Ferguson, A. J.; Kose, M. E.; Rance, W. L.; Rumbles, G.; Ginley, D. S.; Shaheen, S. E.; Kopidakis, N. (2009). Low-Bandgap Thiophene Dendrimers for Improved Light Harvesting. *Journal of Materials Chemistry*. 19(30), 2009; 5311-5324. doi:10.1039/b903427g.

10. Xu, Q.; Tucker, M. P.; Ahrenkiel, P.; Ai, X.; Rumbles, G.; Sugiyama, J.; Himmel, M. E.; Ding, S.-Y. (2009). Labeling the Planar Face of Crystalline Cellulose Using Quantum Dots Directed by Type-I Carbohydrate-Binding Modules. Cellulose. 16(1), 2009; 19-26. doi:10.1007/s10570-008-9234-4.

11. Xu,Q.; Song, Q.; Ai, X.; McDonald, T. J.; Long, H.; Ding. S. Y.; Himmel, M. E.; Rumbles,

G. (2009). Engineered Carbohydrate-Binding Module (CBM) Protein-Suspended Single-Walled Carbon Nanotubes in Water. Chemical Communications. (3), 2009; 337-339. doi:10.1039/b815597f.

12. Piris, J.; Ferguson, A. J.; Blackburn, J. L.; Norman, A. G.; Rumbles, G.; Selmarten, D. C.; Kopidakis, N. (2008). Efficient Photoinduced Charge Injection from Chemical-Bath Deposited CdS into Mesoporous TiO_2 Probed with Time-Resolved Microwave Conductivity. *Journal of Physical Chemistry C.* 112, 2008; 7742-7749. doi:10.1021/jp800527r.

13. Rumbles, G. (2008). Book Review: Photophysics of Molecular Materials, Guglielmo Lanzani (Ed.). *Advanced Materials*. 20(4), 2008; 843-845. doi:10.1002/adma.200702816.

14. Scholes, G. D.; Rumbles, G. (2008). Chapter 3: Excitons in Nanoscale Systems: Fundamentals and Applications. Cao, G.; Brinker, C. J., eds. *Annual Review of Nano Research*. Hackensack, NJ: World Scientific Vol. 2: 103-157.

15. Blackburn, J. L.; McDonald T. J.; Metzger, W. K.; Engtrakul, C.; Rumbles, G.; Heben, M. J. (2008). Protonation Effects on the Branching Ratio in Photoexcited Single-Walled Nanotube Dispersions. *Nano Letters*. 8(4), 2008; 1047-1054. doi:10.1021/nl072809g.

16. Ferguson, A. J .; Kopidakis, N.; Shaheen, S. E.; Rumbles, G. (2008). Quenching of Excitons by Holes in Poly(3-hexylthiophene) Films. *Journal of Physical Chemistry C*. 112(26), 2008; 9865-9871. doi:10.1021/jp7113412.

Submitted:

17. Photoinduced Carrier Generation and Decay Dynamics in Intercalated and Non-Intercalated Polymer:Fullerene Bulk Heterojunctions. William L. Rance, Andrew J. Ferguson, Martin Heeney, David S. Ginley, Dana C. Olson, Garry Rumbles and Nikos Kopidakis (*ACS Nano*).

18. Activation Control of Carrier Recombination in Neat P3HT and P3HT:PCBM Blends. Andrew J. Ferguson, Nikos Kopidakis, Sean E. Shaheen, and Garry Rumbles. (*JACS*)

19. The Influence of Solid-State Microstructure on the Origin and Yield of Long-Lived Photogenerated Charge in Neat Semiconducting Polymers. Obidiah Reid, Jennifer Nekuda-Malik, Nikos Kopidakis, Natalie Stingelin, Gianluca Latini, and Carlos Silva. (*Nature Materials*).

20. Selective Photoinduced Charge Carrier Generation in Composites of Branched Cadmium Selenide Nanoparticles with a Conjugated Polymer and Dendrimer. Smita Dayal, Nikos Kopidakis and Garry Rumbles (*Discussions of the Faraday Society*)

A Farewell to Organic Semiconductors — and Some Recent Results

Brian A. Gregg, Ziqi Liang, Alexander Hains, Alexandre Nardes, Jian V. Li, Jao van de Lagemaat and Russell A. Cormier
Chemical and Materials Science Center and National Center for Photovoltaics
National Renewable Energy Laboratory
Golden, Colorado 80401

After ~25 years in organic semiconductor (and dye-sensitized solar cell) research, the time has come to move on to greener pastures. These pastures will be described next year. This year we will touch on a few of the highlights from previous work to set the stage for our current efforts in studying defects, doping and transport in organic semiconductors and solar cells.
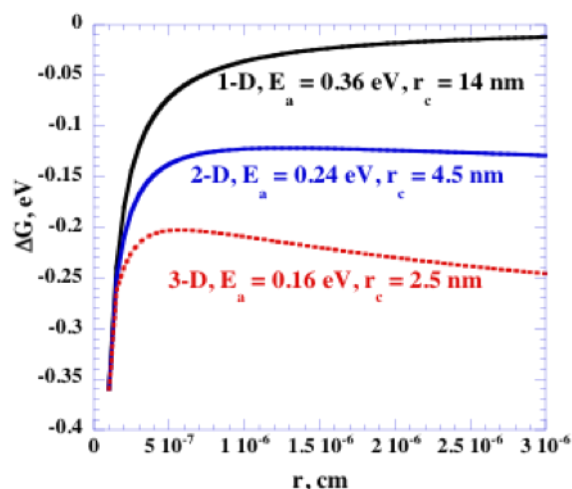
Figure 1. Estimate of the free energy of charge separation in a material of different dimensions having a dielectric constant of 4. Assumes a fixed positive charge at $r = 0$. E_a = activation energy, r_c = escape radius.

Our original efforts in doping liquid crystal perylene diimide derivatives showed that the doping efficiency (the number of free carriers produced per added dopant) is very small, only 10^{-2} to 10^{-3}. This was interpreted as resulting from two factors: 1) the Coulomb attraction between charges in low dielectric media, and 2) the relatively localized charges in organic semiconductors. As with inorganic semiconductors, the addition of dopants (electronic defects) causes a decrease in carrier mobility and exciton diffusion length while increasing the carrier recombination rate. When the doping efficiency is high, these negatives are outweighed by the lower resistance, the increased charge collection efficiency and the higher photovoltage caused by doping. Unfortunately when the doping efficiency is low, the negatives may outweigh the positives. This model applies to the crystalline materials with quasi-1-dimensional transport that we studied; now we include the effects of entropy in higher dimensional materials. Figure 1 shows a simple model for the free energy of charge separation versus distance in different dimensions. Clearly, a 3-dimensional material would have much lower binding energies and therefore higher doping efficiencies and greater ease of separating photogenerated charge pairs. Notably, there is only one known 3-dimensional organic semiconductor: C60. Some of its derivatives, such as the ubiquitous PCBM, are quasi-3-D. Not surprisingly perhaps, these are by far the best acceptors for organic bulk heterojunction solar cells. Such considerations do not bode well for the success of low-dimensional crystalline organic semiconductors, our main focus over the years.

Fixed charges above a certain concentration (10^{16} - 10^{17} cm^{-3}) are expected to limit carrier transport by introducing enough electrostatic hills and valleys that transport becomes Poole-Frenkel-like (ref. 4). Below this concentration, or at high fields, F, transport is expected to be

limited by the energetic disorder in the system. We measured the activation energies, E_a, of the dark currents of poly(3-hexylthiophene), P3HT, films on interdigitated electrodes, IDEs, for both as-purchased P3HT (free hole density $p_f = 5.3$ x 10^{16} cm^{-3}) and the same material treated with lithium aluminum hydride, LAH, to reduce the p-type defect density ($p_f = 3.9$ x 10^{15} cm^{-3}). Figure 2 shows the marked difference between the E_a vs. F in these two films. The untreated one shows a PF-like decay from zero field until a constant value of ~80 meV is reached by $F = 4$ x 10^4 V/cm. In contrast, the LAH-treated P3HT shows an almost field-independent $E_a \sim 70$ meV. These results support our previous prediction about transport mechanism as a function of charge density. Similar measurements on typical bulk heterojunction solar cells are shown in Figure 3
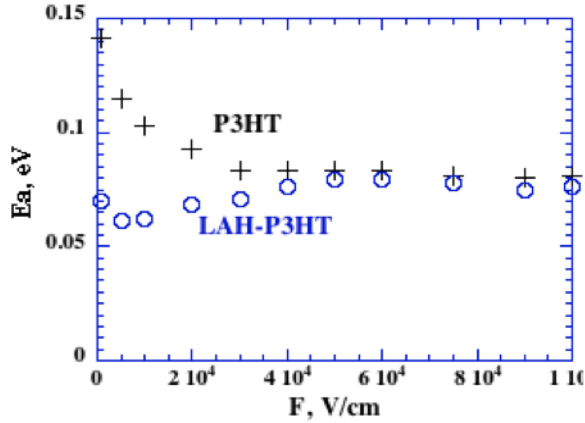
Figure 2. Activation energy for the dark current in P3HT and lithium aluminum hydride-treated P3HT with field, measured on IDEs. This system should be purely transport limited.
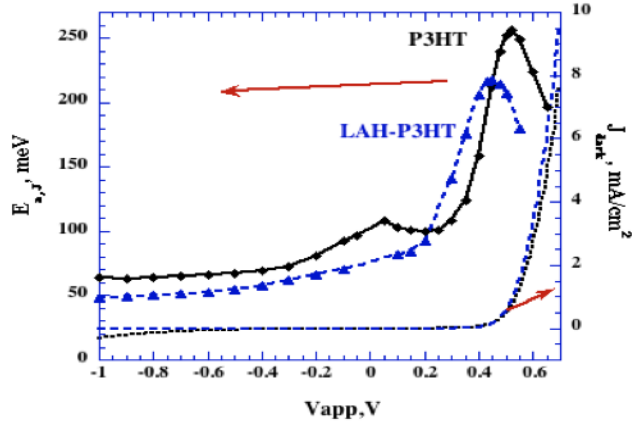
Figure 3. Activation energy for the dark currents in a bulk heterojunction cell (ITO/PedotPSS/P3HT+PCBM/Al). This system could be either transport or injection limited. The dark currents for the two devices are also shown.

showing a pronounced maximum near the zero-field potential, $0 = V_{app} - V_{bi}$ (the built-in potential). One explanation is that addition of PCBM to either kind of P3HT increases the charge density causing PF-like behavior near zero field in both cells. However, solar cells can also be limited by injection which can affect the results. Further experiments are in progress to distinguish between these two mechanisms. Regardless of mechanism, the increase in E_a near zero field (although smaller in the light) may be detrimental to the fill factor and the efficiency.

Commercial inorganic solar cells are mostly made from clean, crystalline materials that are precisely doped. Disordered or amorphous inorganic semiconductors have struggled to find a market niche. Organic PV is exactly backwards: the most successful cells are made from poorly ordered, relatively dirty materials in which the dopants are unknown and uncontrolled. It now appears that there may be some fundamental reasons for this curious state of affairs. Crystalline organic semiconductors (except C60, et al.) are low dimensional and it is therefore difficult to achieve charge separation. Disordered organics are effectively higher dimensional. This understanding may lead to new synthetic approaches for improved organic semiconductors.

DOE Sponsored Solar Photochemistry Publications 2008-2011

1. Gregg, B. A., Kose, M. E., "Reversible Switching Between Molecular and Charge Transfer Phases in a Liquid Crystalline Organic Semiconductor", *Chem. Mater.*, **2008**, *20*, 5235-5239.

2. Wang, D., Reese, M. O., Kopidakis, N., Gregg, B. A., "Do the Defects Make it Work? Defect Engineering in π-Conjugated Polymer Films and Their Solar Cells", *Proc. 33rd IEEE Photovoltaic Specialists Conference*, **2008**.

3. Wang, D., Kopidakis, N., Reese, M. O., Gregg, B. A., "Treating Poly(3-hexylthiophene) with Dimethylsulfate Improves Its Photoelectrical Properties", *Chem. Mater.,* **2008**, 20, 6307-6309.

4. Gregg, B. A., "Transport in Charged Defect-Rich π-Conjugated Polymers", *J. Phys. Chem. C.*, **2009**, *113*, 5899-5901.

5. Gregg, B. A., "Charged Defects in Soft Semiconductors and Their Influence on Organic Photovoltaics", *Soft Matter*, **2009**, 5, 2985-2989.

6. Liang, Z., Nardes, A., Wang, D., Berry, J. J., Gregg, B. A., "Defect Engineering in π-Conjugated Polymers, *Chem. Mater.* **2009**, *21*, 4914-4919.

7. Hains, A. W., Liang, Z., Woodhouse, M., Gregg, B. A., "Molecular Semiconductors in Organic Photovoltaic Cells", *Chem. Rev.* **2010**, *110*, 11, 6689-6735.

8. Rawls, M. T., Johnson, J. and Gregg, B. A., "Coupling One Electron Photoprocesses to Multielectron Catalysts: Towards a Photoelectrocatalytic System", *J. Electroanal. Chem.* **2010**, *650*, 10-15.

9. Woodhouse, M., Perkins, C. L., Rawls, M. T., Cormier, R. A., Liang, Z., Nardes, A., Gregg, B. A., "Non-Conjugated Polymers for Organic Photovoltaics: Physical and Optoelectronic Properties of Poly(Perylenediimides)," *J. Phys. Chem. C,* **2010**, 114, 6784-6790.

10. Liang, Z., Woodhouse, M., Cormier, R. A., Rawls, M. and Gregg, B. A., "Solution Processable n-type Perylene Diimide Copolymers for Organic Photovoltaics", *Synth. Met.* **2011**, in press.

Session IV

Photocatalysis I

Membrane-Organized Chemical Photoredox Systems

James K. Hurst
Department of Chemistry
Washington State University
Pullman, WA 99164-4630

Overview: This research project involves developing minimalist schemes for solar photoconversion that are based upon assembly on closed bilayer membranes. A generic scheme for a prototypical device that utilizes pseudo-base pyrylium ions as combined photosensitizers/transmembrane redox shuttles is shown below.

In this scheme, the photoexcited pyrylium cation undergoes one-electron reductive quenching by an electron donor (D) to the corresponding uncharged radical, which is then followed by electroneutral transmembrane diffusion, and reoxidation by an electron acceptor (A) occluded in the inner aqueous core of the vesicle. The regenerated pyrylium ion is membrane-impermeable but can add OH$^-$ to form a neutral 1,4-diketone that is capable of electroneutral transmembrane diffusion. Outward diffusion followed by reclosure of the ring completes the cycle, in which photoexcitation has led to net oxidation-reduction of the phase-separated donor and acceptor.
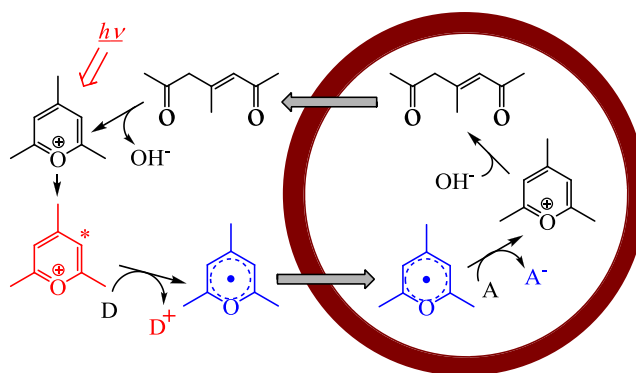
Ongoing research: In earlier DOE-sponsored research (e.g., Khairutdinov & Hurst, *Nature* **1999**, *402*, 509-11), we demonstrated that simple pyrylium ions are capable of efficiently carrying out photoredox cycles such as described in the scheme, although in these studies water-soluble zinc porphyrins were used as photosensitizers to generate the neutral pyrylium radical (thereby adding a second redox cycle). Quenching of the triplet lifetime of photoexcited pyrylium ions by H$_2$O and acetate ions was also observed, suggesting that the pyrylium ions might be capable of acting directly as photosensitizers in the overall redox process. This possibility has now been explored using a series of substituted pyrylium ions selected for their favorable properties (visible absorption, low fluorescence emission, low redox potential, appropriate pseudo-base equilibrium constant).[7] In ZnTPPS^{4-} photosensitized reactions, these ions mediate transmembrane charge transfer from sacrificial donors to occluded Co(bpy)$_3^{3+}$ ion through several types of bilayer membranes. Moreover, triphenylpyrylium and triphenylthiapyrylium ions, which absorb near-uv photons, can function as photosensitizers in the process, but the derivatized pyrylium ions that absorb visible photons apparently cannot. For these latter ions, overall quantum yields for transmembrane redox are low and their reducing capacity (as anticipated from homogeneous reduction potentials) does not appear to be fully realized in the vesicular systems. Estimates of these potentials made by substituting a series of viologens for Co(bpy)$_3^{3+}$ in the aqueous core suggested that the actual values were ~300 mV higher than expected. The reactivity patterns observed implicate strong solubilization of the dyes

within the membrane as the source of these effects, which may both impede electron transfer across the aqueous/organic interfaces and selectively stabilize the neutral reduced forms of the $Py^{+/o}$ couples.

Current investigations are directed at coupling the transmembrane redox step to catalyzed water oxidation, i.e., replacing the sacrificial donor (D) in the above scheme with WOCs. Catalysts being considered including the "blue dimer", recently described low-overpotential monomeric Ru catalysts, the Ru_4 POM cluster, and Co-doped nanoparticles. Adsorption to the membranes can be expected to promote reactivity in several ways, including perturbation of redox potentials and proximity/concentration effects. We are also completing studies designed to resolve mechanistic issues concerning water oxidation by the "blue dimer".[1-4,6,8] At present, we are characterizing reaction transients observed during catalytic turnover[2] by using: (1) advanced EPR techniques to characterized anomalous signals associated with the catalytically active oxidation state; (2) pulse-radiolytically generated $OH^{\bullet}$ to generate and dynamically characterize putative reaction transients; and (3) DFT-based simulations of designed to explore the plausibility of pathways involving "noninnocent" participation of the bipyridine ligands,[8] a possibility suggested by prior ^{18}O-isotope labeling studies.[1,2,4,6] Pertinent findings to date include the following: (1) ENDOR and HYSCORE spectra, and Ru and D_2O hyperfine coupling patterns suggest that the paramagnetic transient is a Ru-centered radical coordinated to a bpyOH π-cation; (2) $OH^{\bullet}$ has been shown to add to the bipridine ring in the $[(bpy)_2Ru^{III}(OH_2)]_2O^{4+}$ (**{3,3}**) dimer and reaction with the corresponding **{3,4}** ion leads to net *reduction* to **{3,3}**, consistent with a proposed catalytic pathway for water oxidation involving concerted addition of H_2O to **{5,5}** to give "covalent hydrates" containing bpy-OH bonds;[1,6] (3) DFT studies of "covalent hydration" in a model complex (shown below) indicate that water addition to the bipyridine ligand is energetically favorable for $Ru^{IV}=O$ and Ru^{IV}-OH species, but not $Ru^{IV}=O$ or lower oxidation states, and are also highly dependent upon the position of attack on the bipyridine ligand. The predicted lowest energy product is a bpy-OH π-cation (sbown below), with an unpaired spin density indicating net reduction of the Ru center, consistent with the EPR findings for the radical transient formed during catalytic turnover of the "blue dimer"

Ongoing computational efforts are directed at estimating reaction coordinates for formation and decay of the hypothetical "covalent hydrate".
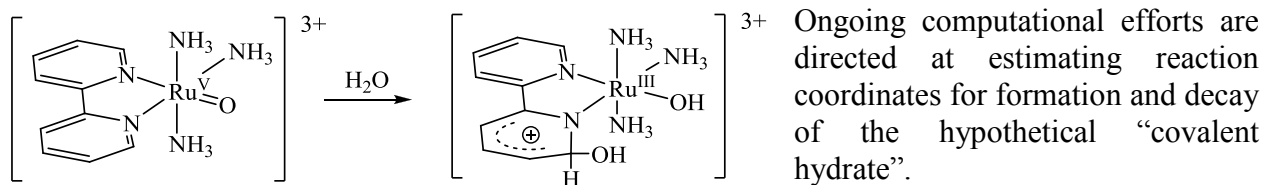
Future studies. In addition to completing the studies described above, in the coming year we will explore the potential of using more water-soluble naturally-derived pyrylium analogs, such as found among the anthocyanins and related flavinium ions, in these membrane-based assemblies. Increasing the extent of partitioning of the carrier in the aqueous microphases might remedy the problems described above that appear associated with strong dissolution of the dyes into the membrane interior. We will also explore the possibility of using more robust membrane films, notably block-copolymer "polymerosomes", as organizing matrices for these reactions. Because the bilayer width is relatively large in these constructs, designs that utilize mobile redox carriers are inherently more suitable than those based upon covalently-linked redox centers or molecular wires as electron transport chains.

DOE Sponsored Publications 2008-2011

1. J. K. Hurst, J. L. Cape, A. E. Clark, S. Das & C. Qin: "Mechanisms of Water Oxidation Catalyzed by Ruthenium Diimine Complexes". *Inorg. Chem.* **2008**, *47*, 1753-1764.

2. J. L. Cape & J. K. Hurst: "Detection and Mechanistic Relevance of Transient Ligand Radicals formed during $[Ru(bpy)_2(OH_2)]_2O^{4+}$-catalyzed Water Oxidation". *J. Am. Chem. Soc.* **2008**, *130*, 827-829.

3. Jonathan L. Cape, Sergei V. Lymar, Travis Lightbody, and James K. Hurst: "Characterization of Intermediary Redox States of the Water Oxidation Catalyst, $[Ru(bpy)_2(OH_2)]_2O^{4+}$", *Inorg. Chem.* **2009**, *48*, 4400-4410.

4. Jonathan L. Cape, William F. Siems, and James K. Hurst: "Pathways of Water Oxidation Catalyzed by Ruthenium "Blue Dimers" Characterized by ^{18}O-Isotopic Labeling", *Inorg. Chem.* **2009**, *48*, 8729-8735.

5. James K. Hurst: "A Water Oxidation Catalyst for the 21st Century?", *Science* **2010**, *328*, 315-316.

6. Aurora E. Clark and James K. Hurst: "Mechanisms of Water Oxidation Catalyzed by Ruthenium Coordination Complexes", *Prog. Inorg. Chem.* **2011**, *57*, in press.

7. Song Liang, Linyong Zhu, and James K. Hurst: "Cyclic Transmembrane Charge Transport Mediated by Substituted Pyrylium Ions", under review.

8. Abdullah Ozkanlar, Jonathan L. Cape, James K. Hurst, and Aurora E. Clark: "Covalent Hydration Reactions in Model Monomeric Ru 2,2'-bipyridine Complexes: Thermodynamic Favorability as a Function of Metal Oxidation and Overall Spin States", under review.

Water Oxidation Catalyzed by Mononuclear Ru(II) Complexes

Ruifa Zong, Nattawut Kaveevivitchai, Maya El Ojaimi,
Rubabe Haberdar, and <u>Randolph P. Thummel</u>
Department of Chemistry, 136 Fleming Building, University of Houston,
Houston, TX 77204-5003

Earlier work from our group and others has demonstrated that certain dinuclear Ru(II) complexes can serve as effective water oxidation catalysts. The initial motive for investigating dinuclear systems was the presumed necessity for having two proximal metal centers. It was expected that the oxidation of two closely positioned metal-aqua moieties to the corresponding metal oxo species would then lead to O-O coupling with the eventual release of dioxygen. The four electron oxidation required by this process might be more readily managed by two metal centers rather than one.

Somewhat surprisingly, we soon discovered that water oxidation could be accomplished even more effectively by mononuclear Ru(II) catalysts and thus far three fundamental classes of such catalyst have evolved from our studies. Using 4-*t*-butyl-2,6-di(1',8'-naphthyrid-2'-yl)pyridine as a tridentate ligand allowed a water molecule to be bound in the equatorial plane with two monodentate pyridines occupying the axial positions (**1**). This arrangement contrasts with the bpy-tpy complexes (**2**, bpy = 2,2'-bipyridine; tpy = 2,2';6,2"-terpyridine) where the water molecule would occupy an axial site. Complexes **3**, derived from tetradentate ligands related to 2,9-di(pyrid-2'-yl)-1,10-phenanthroline (dpp), are unique in that they do not have any site that can be readily substituted by water, yet they are among the most active catalysts.

1 (pynap-type ligand with H-bonded water) **2** (bpy-tpy-X complex: X = Cl, Br, I, H$_2$O) **3** (tetradentate dpp complex)
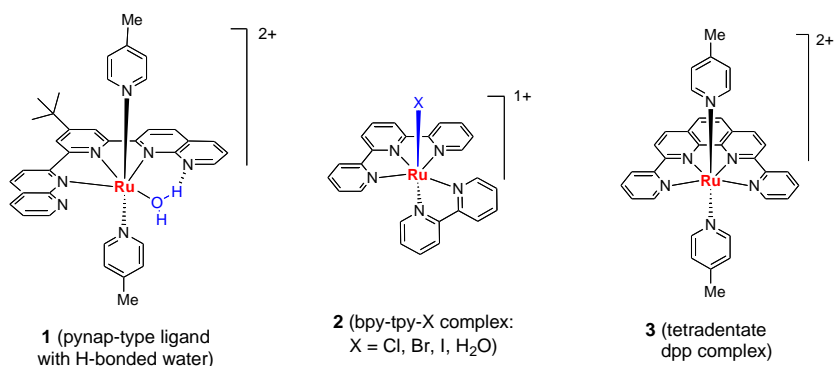
In the 2-pyridylnaphthyridine (pynap) complexes, we verified by an X-ray structure that the metal bound water molecule is H-bonded to an uncomplexed nitrogen on the naphthyridine. It is tempting to surmise that in a proton-coupled electron transfer (PCET) step the deprotonation of the bound water is assisted by this H-bonding. To investigate this possibility we examined a pair of model systems prepared in equal amounts by the reaction of pynap with [Ru(tpy)Cl$_3$]. Surprisingly, we found that the complex having a H-bonded water molecule (**5**) was considerably less active than one with a chloride bonded trans to the naphthyridine ring (**4a**). When iodide was substituted for chloride, the activity increased even further. This observation led us to study more carefully the series of potential catalysts **2**. The aqua complex reacted much more rapidly than the chloro or bromo complexes but was

comparable to the iodo complex although the iodo complex exchanged halogen for water considerably more slowly. A possible duality of mechanism may exist.

We have found that Ru(II) complexes of the tetradenate ligand dpp are consistently good water oxidation catalysts such that every system examined thus far has exhibited appreciable catalytic activity. We have prepared the reagent [Ru(dpp)Cl$_2$] as a versatile precursor to such

4a X = Cl (TN = 1170)
b X = I   (TN = 1540)

5 (TN = 1)

6 [Ru(dpp)Cl$_2$]

7
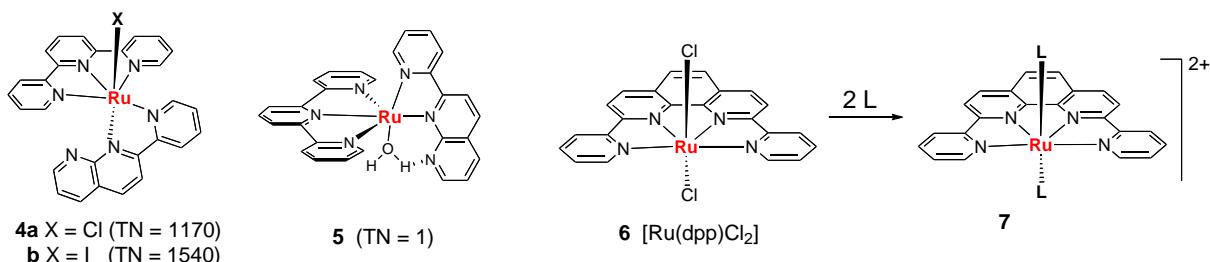
complexes involving a wide variety of axial ligands L. Furthermore we have utilized Friedländer methodology to prepare some interesting anionic tetradentate ligands leading to Ru complexes such as **8**-**10**. The anionic ligands stabilize higher oxidation states of the metal so that **10** is formed as a Ru(III) species. The complexes appear to be stable towards ligand replacement and most have an expanded N-Ru-N(O) angle in the equatorial plane which makes the 2-electron oxidized complex vunerable to attack by water leading to the proposal of a 7-coordinate reaction mechanism for water oxidation.

8

9

10
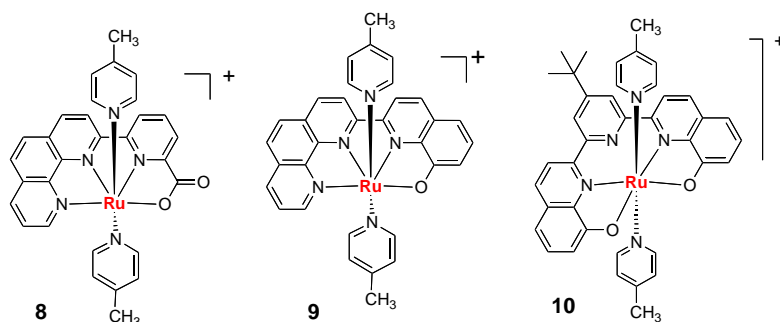
We prepared the ligand di-2-phenanthrolinyl-N-isoamylamine and its corresponding Ru(II) complex **11** as an example of an unstrained tetradentate system that might be less activated towards water addition. With the same motive we also examined the 8-quinolinyl phenanthroline complex **12**. While **11** somewhat surprisingly showed modest activity, complex **12** was completely inactive. Several other systems that further demonstrate steric, electronic, and conformational effects will be presented.

We have examined a wide variety of Ru(II) complexes as potential water oxidation catalysts. At this point no clear picture has yet emerged to explain the varying reactivity and stability of these species. We are moving forward in the direction of immobilizing the catalysts and incorporating them into photosensitized systems for eventual water decomposition.

11

12 **(**TN = 0**)**
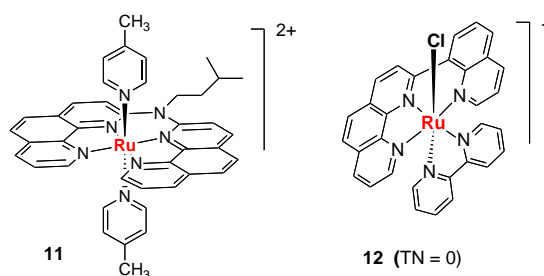
DOE Sponsored Publications

1. "A New Family of Ru Complexes for Water Oxidation," Zong, R.; Thummel, R. P. *J. Am. Chem. Soc.* **2005**, *127,* 12802-12803.

2. "Ruthenium(II) Complexes of 1,12-Diazaperylene and their Interactions with DNA," Chouai, A.; Wicke, S.; Turro, C.; Bacsa, J.; Dunbar, K.; Thummel, R. P. *Inorg. Chem.* **2005**, *44,* 5996-6003.

3. "Synthetic Approaches to Polypyridyl Bridging Ligands with Proximal Multidentate Binding Sites," Zong, R.; Wang, D.; Hammitt, R.; Thummel, R. P. *J. Org. Chem.* **2006**, *71,* 167-175.

4. "The Preparation and Study of a Family of Dinuclear Ru(II) Complexes which Catalyze the Decomposition of Water," Deng, Z.; Tseng, H.-W.; Zong, R.; Wang, D.; Thummel, R. *Inorg. Chem.* **2008**, *47,* 1835-1848 (invited Forum article).

5. "Ru(II) Complexes of Tetradentate Ligands Related to 2,9-Di(pyrid-2'-yl)-1,10-phenanthroline," Zhang, G.; Zong, R.; Tseng, H.-W.; Thummel, R. P. *Inorg. Chem.* **2008**, *47,* 990-998.

6. "Enhanced Metal Ion Selectivity of 2,9-Di-(pyrid-2-yl)-1,10-phenanthroline and Its Use as a Fluorescent Sensor for Cadmium(II)," Cockrell, G. M.; Zhang, G.; VanDerveer, D. G.; Thummel, R. P.; Hancock, R. D. *J. Am. Chem. Soc.* **2008**, *130,* 1420-1430.

7. "Mononuclear Ru(II) Complexes That Catalyze Water Oxidation," Tseng, H.-W.; Zong, R.; Muckerman, J. T.; Thummel, R. *Inorg. Chem.* **2008**, *47,* 11763-11773.

8. "Eu(III) Complexes of Tetradentate Ligands Related to 2,9-Di(pyrid-2'-yl)-1,10-phenanthroline and 2,2'-Bi-1,10-phenanthroline," Zong, R.; Zhang, G.; Eliseeva, S. V.; Bünzli, J.-C. G.; Thummel, R. P. *Inorg. Chem.* **2010**, *49,* 4657-4664.

9. "Differences of pH-Dependent Mechanisms on Generation of Hydride Donors using Ru(II) Complexes Containing Geometric Isomers of NAD$^+$ Model Ligands: NMR and Radiolysis Studies in Aqueous Solution," Cohen, B. W.; Polyansky, D. E.; Zong, R.; Zhou, H.; Ouk, T.; Cabelli, D.; Muckerman, J. T.; Thummel, R. P.; Fujita, E. *Inorg. Chem.* **2010**, *49,* 8034-8044.

10. "Water Oxidation by a Mononuclear Ruthenium Catalyst: Characterization of the Intermediates," Polyansky, D. E.; Muckerman, J. T.; Rochford, J.; Zong, R.; Thummel, R.P.; Fujita, E. *J. Am Chem. Soc.* (submitted).

11. "Effects of a Proximal Base on Water Oxidation and Proton Reduction Catalyzed by Geometric Isomers of [Ru(tpy)(pynap)(OH$_2$)]$^{2+}$," Boyer, J. L.; Polyansky, D. E.; Szalda, D. J.; Zong, R.; Thummel, R. P.; Fujita, E. *Angew. Chem. Int. Ed.* (submitted).

Hydrogen and Oxygen Evolving Hangman Catalysts

Dilek K. Dogutan, Robert C. McGuire Jr. and Daniel G. Nocera
Department of Chemistry
Massachusetts Institute of Technology
Cambridge, MA 02139-4307

A new class of catalysts—Hangman catalysts—are explored with an eye towards both half-reactions of water splitting. In Hangman constructs, an acid-base functionality is poised over a redox active metal platform. The acid-base functionality is used to form a secondary coordination sphere that can assist proton movement to and from substrates bound to the redox center. On a mechanistic front, the Hangman systems orthogonalize Proton Coupled Electron Transfer (PCET) and in doing so they permit control of proton transfer over short distances and electron transfer over long distances. Hangman catalysts comprising porphyrin and corrole will be presented as O_2 and H_2 evolving catalysts. The value of these catalysts is that they allow the OER and HER mechanisms to be disentangled. The mechanism will be discussed.

DOE Sponsored Solar Photochemistry Publications 2008-2011

1. "A ligand field chemistry of oxygen generation by the oxygen evolving complex and synthetic active sites." T. A. Betley, Y. Surendranath, M. V. Childress, G. E. Alliger, R. Fu, C. C. Cummins and D. G. Nocera, *Phil. Trans. Royal Soc. B* **2008**, *363*, 1293-303.

2. "Metal oxo complexes for oxygen-oxygen bond formation." T. A. Betley, Q. Wu, T. Van Voorhis and D. G. Nocera, *Inorg. Chem.* **2008**, *47*, 1849-61.

3. "Manganese amido-imine bisphenol hangman complexes." J. Y. Yang and D. G. Nocera, *Tetrahedron Lett.* **2008**, *49*, 4796-8.

4. "Hangman salen platforms containing two dibenzofuran scaffolds: Catalase activity and epoxidation of unfunctionalized olefins." J. Y. Yang and D. G. Nocera, *ChemSusChem.* **2008**, *1*, 941-9.

5. "Efficient synthesis of hangman porphyrins." D. K. Dogutan, D. K. Bediako, T. S. Teets, M. Schwalbe and D. G. Nocera, *Org. Lett.* **2010**, *12*, 1036-9.

6. "Oxygen reduction reactivity of cobalt(II) hangman porphyrins"; R. McGuire Jr., D. K. Dogutan, T. S. Teets, J. Suntivich, Y. Shao-Horn and D. G. Nocera, *Chem. Sci.* **2010**, *1*, 411-4.

7. "Hangman corroles: Efficient synthesis and oxygen reaction chemistry." D. K. Dogutan, S. Stoian, R. McGuire Jr., M. Schwalbe, T. S. Teets and D. G. Nocera, *J. Am. Chem. Soc.* **2011**, *133*, 131-40.

8. "Synthesis and characterization of iron xanthene corrole complexes and its application as catalysts for hydrogen peroxide dismutation." M. Schwalbe, D. K. Dogutan, S. Stoian and D. G. Nocera, *Inorg. Chem.* **2011**, *50*, ASAP.

9. "Xanthene-Modified and Hangman Iron Corroles"; Matthias Schwalbe, Dilek K. Dogutan, Sebastian A. Stoian, Thomas S. Teets, and Daniel G. Nocera, *Inorg. Chem.* **2011**, *50*, 1368-77.

10. "Oxygen Evolution Reaction Chemistry of Oxide-Based Electrodes"; Yogesh Surendranath and Daniel G. Nocera, *Prog. Inorg. Chem.* **2011**, in press.

11. "Electocatalytic Water Oxidation by Cobalt(III) Hangman Fully Fluorinated Corroles"; Dilek K. Dogutan, Robert McGuire Jr., Yang Shao-Horn and Daniel G. Nocera, *J. Am. Chem. Soc.* **2011**, *133*, in press.

12. "Hydrogen Generation by Hangman Metalloporphyrins"; Chang Hoon Lee, Dilek K. Dogutan and Daniel G. Nocera, *J. Am. Chem. Soc.* **2011**, *133*, in press.

13. "Hangman Effect on Hydrogen Production by Cobalt Macrocyclic Complexes"; Chang Hoon Lee, Dilek K. Dogutan, Dino Villagrán, Timothy R. Cook, Jonas C. Peters and Daniel G. Nocera, *Inorg. Chem.* **2011**, *50*, submitted for publication.

14. "Orthogonal proton-coupled metal-to-ligand charge transfer in a ruthenium aqua complex." R. F. Kelley, E. J. McLaurin, J. L. Yang and D. G. Nocera, *J. Phys. Chem.* **2011**, submitted for publication.

Reviews and Commentaries

15. "Living healthy on a dying planet." D. G. Nocera, *Chem. Soc. Rev.* **2009**, *38*, 13-5.

16. "Personalized energy: The home as a solar power station and solar gas station." Daniel G. Nocera, *ChemSusChem,* **2009**, *2*, 387-90.

17. "Chemistry of personalized solar energy." D. G. Nocera, *Inorg. Chem.* **2009**, 48, 10001-7.

18. "I just love seeing all those solar panels." D. G. Nocera, *Nach. Chem.* **2010**, *58*, 29-31.

19. "Footsteps on the sustainability trail." M. Beller, G. Centi, D. G. Nocera, G. M. Kemeling and P. Gölitz, *ChemSusChem* **2010**, *3*, 3-5.

20. "Fast food energy." D. G. Nocera, *Energy Environ. Sci.* **2010**, *3*, 993-5.

Patents

21. "Highly efficient synthesis of A3 corroles, trans-A2B hangman corroles, and A3B hangman porphyrins." D. K. Dogutan and D. G. Nocera, Invention Disclosure, MIT Case No. 13780, U.S. Prov. Pat. Appl. No. 61/286,196; 14 December 2009.

22. "Electrochemical water oxidation by beta-fluorinated cobalt-hangman-corrole-xanthene complex." D. K. Dogutan, R. C. McGuire and D. G. Nocera, MIT Case. No. 14460

Session V

Photocatalysis II

Cobaloxime Catalyst for Biomimetic Hydrogen Production:
EPR Investigation of the Electronic Structure

Oleg G. Poluektov, Lisa M. Utschig, Karen L. Mulfort, Jens Niklas, and David M. Tiede
Chemical Sciences and Engineering Division
Argonne National Laboratory
Argonne, IL 60439

The ultimate goal of our natural photosynthetic energy research is to resolve fundamental mechanisms of photochemical energy conversion in photosynthetic proteins and to use this information in the design of bio-inspired materials for solar fuels production. The initial photosynthetic energy conversion reactions occur in integral membrane reaction center (RC) proteins that efficiently couple light-harvesting to water-splitting catalysis and fuels production. Solar fuels research aims to mimic photosynthesis and devise integrated systems that can capture, convert, and store solar energy in high-energy molecular bonds. Currently, our group is designing both synthetic supramolecular photocatalytic systems as well as Photosystem I (PS I)-catalyst biohybrids that photochemically produce hydrogen. Further development and improvement of these systems relies on understanding the inherent, fundamental mechanisms for coupling captured photons to fuel generation. To this end, we are applying advanced spectroscopic techniques such as multifrequency pulsed electron paramagnetic resonance (EPR) to elucidate important structure-function relationships in our artificial and biochemical complexes.

The catalysts of choice for our research are cobaloxime derivatives. Cobaloximes (cobalt complexes with diglyoxime ligands) rank among the most promising first row transition metal complexes for the reduction of protons to molecular hydrogen. The catalytic properties of cobaloximes depend on the local surrounding and in particular on the direct ligands to the central metal ion. The knowledge of the electronic properties is essential for understanding the catalytic properties of the molecule. EPR is an excellent tool to achieve this goal. In case of PS I, the other essential component of our biohybrid system, EPR spectroscopy has contributed tremendously to the current understanding of its electronic structure and function.

Solvent and axial coordination effects. In this work, difluoroboryl cobaloxime $Co(dmgBF_2)_2$ in a variety of solvents has been investigated with multi-frequency EPR spectroscopy at X-band (9 GHz), Q-band (34 GHz), and D-band (130 GHz) microwave frequencies.[20] BF_2-capped cobaloxime $Co(dmgBF_2)_2$ was chosen for these studies because this complex has a higher resistivity toward acidic hydrolysis compared to H-capped cobaloximes. In addition, the lowered nucleophilicity of its hydride derivative limits undesired hydrogenation reactions. The multi-frequency approach along with simultaneous fitting of the EPR spectra at all microwave frequencies allows us to determine g-tensor anisotropy and hyperfine splitting due to the central metal (^{59}Co) and coordinating solvents molecules/ligands (L)
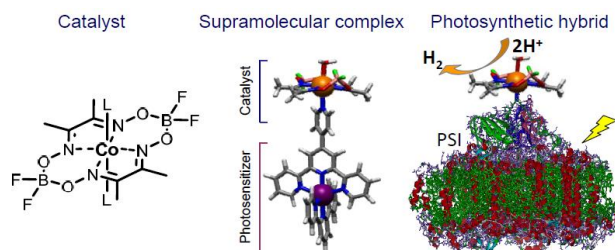
Figure 1. Structure of BF_2 "capped" cobaloxime (left) and schematic representation of the supramolecular, and photosynthetic hybrid complexes.

that have ^{14}N, ^{15}N, or ^{31}P magnetic nuclei (Fig.2). The ENDOR, ESEEM, and hyperfine sublevel correlation (HYSCORE) techniques revealed that the spin density distribution in the equatorial plane of the complex is negligible, which again emphasizes the importance of axial ligation for tuning the catalytical properties of cobaloximes by electronic structure modulation.

A variety of solvents were studied, including (i) polar and protic solvents, (ii) polar but non-protic solvents, (iii) non-polar solvents with different stochiometric amounts of potential ligands to the central cobalt. Those ligands include "small and simple" molecules like pyridine and several pyridine derivatives with different electron-donating/electron-withdrawing properties, as well as two rather bulky molecules, N-cyclohexyl-N'-4-pyridyl-1,7-dipyrrolidinylperylene-3,4:9,10-tetracarboxylic acid bisimide (PDI) and triphenylphosphine (PPh$_3$). Currently, the PDI scaffold is widely used in many light-harvesting applications because of its inherent high extinction coefficient, broad absorbance, redox tunability, and exceptional structural integrity. The nitrogen atom of PDI or pyridine ligates the central cobalt ion. The nuclear spin of nitrogen (I = 1) allows us to monitor the hyperfine interaction of the ligating atom with the unpaired electron of the cobaloxime. For PPh$_3$, the central phosphorous atom ligates to the metal ion and the ^{31}P nuclear spin of I = ½ probes the interaction between cobalt ion and ligand molecule. It was observed that PPh$_3$ forms a stable paramagnetic adduct with cobaloximes in the presence of molecular oxygen. Oxygenation dramatically changes the EPR spectrum of the cobalt complex, e.g. resulting in a pronounced reduction of g-tensor anisotropy. In addition, the proportional decrease in both the ^{31}P and ^{59}Co hyperfine interaction constants for the reversible LCo(dmgBF$_2$)$_2$ + O$_2$ ↔ LCo(dmgBF$_2$)$_2$OO$^\bullet$ transformation is consistent with a pronounced shift of electron spin density to oxygen.

These experimental results have been compared to DFT calculations of Co(dmgBF$_2$)$_2$ with different axial ligands and for oxygen adducts in the presence of PPh$_3$ (Fig.3). The modeling allows us to distinguish between different stable conformers and validate the structure of the axial ligand(s)-Co(dmgBF$_2$)$_2$ complexes.
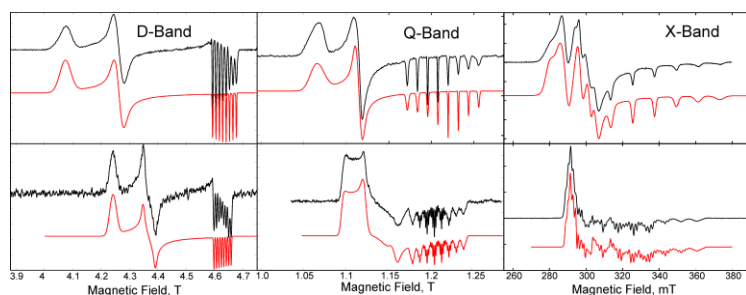
Figure 2. Experimental (black) and theoretically simulated (red) multi-frequency ERP spectra of cobaloxime in pure methanol (upper row) and methanol with pyridine (lower row).
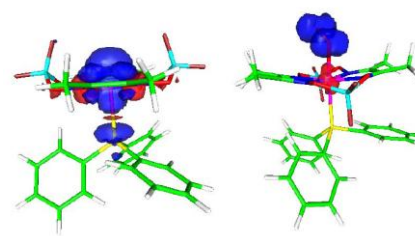
Figure 3. DFT geometry optimization and spin density distribution for PPh3:Co(dmgBF$_2$)$_2$ complex (left) and PPh3:Co(dmgBF$_2$)$_2$:O$_2$ complex (right).

Photosystem I-cobaloxime biohybrid. Recently, we have prepared a Photosystem I-cobaloxime biohybrid complex. PSI and the cobalt-containing catalyst self-assembles and the resultant complex rapidly produces hydrogen in aqueous solution upon exposure to visible light. EPR of this biohybrid will help determine where and how cobaloxime is binding to the protein, as well as identify important intermediates in the photo-catalytic cycle. This research will help us optimize this system and provide a benchmark for designing future RC-based biohybrids for solar fuel production.

DOE Sponsored Solar Photochemistry Publications 2008-2011

1. Kothe, G., Norris, J. R., Poluektov, O. G., and Thurnauer, M. C. (2008) High-Time Resolution Electron Paramagnetic Resonance - Study of Quantum Beat Oscillations Observed in Photosynthetic Reaction Center Proteins. In: Matysik J. and Aartsma T. J., (eds) *Biophysical Techniques on Photosynthesis II*, Vol. 26 pp. 305-323, Chapter 15, Springer, Dordrecht, The Netherlands.

2. Utschig, L. M., Chen, L. X., and Poluektov, O. G. Discovery of Native Metal Ion Sites Located on the Ferredoxin Docking Side of Photosystem I, Biochem., 2008, v. 47, 3671–3676.

3. Utschig, L. M., Chemerisov, S. D., Tiede, D. M., and Poluektov, O. G. Electron paramagnetic resonance study of radiation damage in photosynthetic reaction center crystals, *Biochem.,* 2008, v. 47, 9251-9257.

4. Moore, G. F., Hambourger, M., Gervaldo, M., Poluektov, O. G., Rajh, T., Gust, D., Moore, T. A., and Moore, A. L. A Bioinspired Construct That Mimics the Proton Coupled Electron Transfer between P680$^{\bullet+}$ and the Tyr$_Z$-His190 Pair of Photosystem II, *J. Am. Chem. Soc.*, 2008, v. 130, 10466–10467.

5. Poluektov, O. G. and Utschig, L. M. (2009) Protein Environments and Electron Transfer Processes Probed with High-Frequency ENDOR. In: Hunter CN, Daldal, F, Thurnauer MC, and Beatty JT (eds) The Purple Phototrophic Bacteria. Advances in Photosynthesis and Respiration, Vol. 28, pp. 155-179, Springer, Dordrecht, The Netherlands.

6. Poluektov, O. G., Paschenko, S. V., and Utschig, L. M. "Spin-Dynamics of the Spin-Correlated Radical Pair in Photosystem I. Pulsed Time-Resolved EPR at High Magnetic Field." *Phys. Chem. Chem. Phys.* 2009, v. 11, 6750-6756.

7. Schoessow, P., Antipov, S., Kanareykin, A., Jing, C., and Poluektov, O. (2009) Microwave PASER Experiment. In: Schroeder, C. B., Leemans, W., and Esarey, E., (eds) Advanced Accelerator Concepts, Vol. 1086**,** pp. 526-531**,** Amer. Inst. Physics, USA.

8. Utschig, L. M., Dalosto, S. D., Thurnauer, M. C., and Poluektov, O. G. "The Surface Metal Site in *Blc. Viridis* Photosynthetic Bacterial Reaction Centers: Cu^{2+} as a Probe of Structure, Location, and Flexibility" *Appl. Magn. Reson.*, 2010, v. 38, 1–17.

9. Antipov, S., Schoessow, P., Kanareykin, A., Jing, C., Poluektov, O., and Gai, W. (2010) Paramagnetic Materials for PASER and Tunable Absorption. In: Gold, S. H., and Nusinovich, G. S., (eds) Advanced Accelerator Concepts, Vol. 1299, pp. 653-657**,** Amer. Inst. Physics, USA.

10. Ponomarenko N.S., Poluektov O.G., Bylina E. J., Norris J.R. "Characterization of the Primary Donor of *Blastochloris viridis* Heterodimer Mutants by High Field EPR" *Biochimica et Biophysica Acta*, 2010, v. 1797, 1617–1626.

11. Ponomarenko N.S., Poluektov O.G., Bylina E. J., Norris J.R. "Electronic structure of the primary electron donor of Blastochloris viridis heterodimer mutants: High-field EPR study" *Biochimica et Biophysica Acta*, 2010, v. 1797 (9), 1838-1840.

12. Poluektov, O. G., Filippone, S., Martín, N., Sperlich, A., Deibel, C., and Dyakonov, V.

"Spin Signatures of Photogenerated Radical Anions in Polymer-[70]Fullerene Bulk-Heterojunctions: High-Frequency Pulsed EPR Spectroscopy", *J. Phys. Chem. B*, 2010, v. 114, 14426–14429.

13. Liedtke, M., Sperlich, A., Kraus, H., Deibel, C., Dyakonov, V.. Filipponec, J., Delgado, L., Martín, N., and Poluektov, O. G. "Spectroscopic Signatures of Photogenerated Radical Anions in Polymer-[C70]Fullerene Bulk Heterojunctions" *ECS Transactions*, 2010, v. 28(17), 3-10.

14. Baranov, P. G., Romanov, N. G., Poluektov O. G., and Schmidt, J. "Self-Trapped Excitons in Ionic-Covalent Silver-Halide Crystals and Nanostructures: High Frequency EPR, ESE, ENDOR and ODMR Studies" *Appl. Magn, Reson.*, 2010, v. 39 (4), 453–486.

15. Santabarbara, S.,Kuprov, I., Poluektov, O., Hore, P. J., Casal, A., Russell, C. A., Purton, S., and Evans, M. C.W. "Directionality of electron transfer reactions in Photosystem I of prokaryotes: universality of the bidirectional electron transfer model" J. Phys. Chem. B, 2010. v. 114 (46), 15158-15171.

16. Utschig, L. M., Tiede, D. M., and Poluektov, O. G. Light Induced Alteration of Low Temperature Interprotein Electron Transfer Between Photosystem I and Flavodoxin, Biochem. Communication, 2010, v. 49(45), 9682-9684.

17. Dimitrijevic, N., Vijayan, B., Poluektov, O., Rajh, T., Gray, K. A., He, H., and Zapol, P. "Role of Water and Carbonates in Photocatalytic Transformation of CO2 to CH4 on Titania" J. Amer. Chem. Soc., 2011, v. 133, 3964-3971.

18. Utschig, L. M., Dimitrijevich, N. M., Poluektov, O. G., Chemerisov, S. D., Mulfort, K. L., and Tiede, D. M. "Photocatalytic Hydrogen Production from Noncovalent Biohybrid Photosystem I/Pt Nanoparticle Complexes" *J. Phys. Chem. Lett.*, 2011, v. 2(3), 236-241.

19. Poluektov, O. G., Utschig, L. M., and Tiede, D. M. "Imaging Electron Transfer Pathways in Natural Photosynthesis Using Time-Resolved Hig-Frequency EPR/ENDOR Spectroscopy" *J. Amer. Chem. Soc.,* manuscript in preparation.

20. Niklas, J., Rakhimov, R. R, Mulfort, K. L., Mardis, K. L., Tiede, D. M., and Poluektov, O. G. "Electronic Structure of Difluoroboryl Cobaloxime (II) Complexes with Different Ligands: Multifrequency EPR and DFT Study" *J. Phys. Chem. B*, manuscript in preparation.

Improving the Efficiency of Photocatalytic CO_2 Reduction Reactions

David C. Grills

Chemistry Department, Brookhaven National Laboratory, Upton, NY 11973-5000

The goal of our research in this program is to gain a fundamental understanding of the processes involved in the capture and chemical conversion of solar energy using transition metal complexes as catalysts. In this project we have been focusing on the photoreduction of CO_2 because of its relevance to our future energy needs. In particular, we are developing methods to improve the efficiency of catalysis in order to increase turnover rates of desired product formation. In addition, gaining a detailed mechanistic knowledge of a catalytic process is crucial for understanding and developing more efficient photoconversion systems. To this end we develop new spectroscopic techniques, targeting improved characterization of catalytic intermediates. Here, we highlight our recent work in these areas, together with future directions.

Photocatalytic CO_2 Reduction in Supercritical CO_2 and Ionic Liquids. The photochemical reduction of CO_2 to CO using homogeneous catalysts such as $ReCl(bpy)(CO)_3$ (bpy = 2,2'-bipyridine), in the presence of sacrificial electron donors (*e.g.* triethanolamine, TEOA) is well known. This family of catalysts efficiently produces CO with quantum yields, ϕ_{CO} as high as 0.59. However, turnover frequencies are very low and catalyst lifetimes are limited due to the formation of non-productive side products. The goal of this project is to increase the efficiency of these catalytic reactions by (i) eliminating the use of conventional coordinating organic solvents, which can bind to vacant metal sites and slow down reactivity, and (ii) considerably increasing the concentration of available CO_2 by using high-pressure supercritical CO_2 ($scCO_2$) as a reaction medium. We synthesized a series of new CO_2-soluble homogeneous catalysts, $[Re(4,4'-(C_xF_{2x+1}CH_2CH_2CH_2)_2-2,2'-bpy)(CO)_3L]^n$ (x = 6 and 8; L = Cl^- (n = 0), $P(OCH_2CF_3)_3$ (n = 1+, x = 6 only), and CO (n = 1+, x = 6 only); bpy = bipyridine), employing the fluorinated $[B(Ar_F)_4]^-$ anion for the cationic complexes. Their photophysical properties in $scCO_2$ were found to be suitable for CO_2 reduction. However, photocatalysis in $scCO_2$ was hindered by the fact that efficient sacrificial electron donors such as TEOA are not soluble in $scCO_2$, and that the reactions are carried out in a single-phase environment, which can cause a build-up of CO around the active catalytic species resulting in catalyst poisoning. Room temperature ionic liquids (RTILs) offer the possibilty to carry out these photocatalytic reactions under high pressures, and thus high concentrations of CO_2, while maintaining two phases due to their unique biphasic phase behavior with $scCO_2$. Additional advantages of RTIL/$scCO_2$ biphasic systems include: (i) the RTIL can be weakly- or non-coordinating, leaving the active metal center free to react with CO_2; (ii) $scCO_2$ is generally very soluble in RTILs, meaning that the advantage of a high CO_2 concentration is maintained; (iii) the viscosity of an RTIL is reduced by $>10\times$ in the presence of $scCO_2$; (iv) efficient sacrificial electron donors, *e.g.* TEOA, are soluble in many RTILs; (v) polar or charged catalysts can easily dissolve in RTILs without the need for synthetic modifications; and (vi) the RTIL, catalyst and electron donor will not leech out into the $scCO_2$ phase, even at very high pressures (see schematic diagram above).
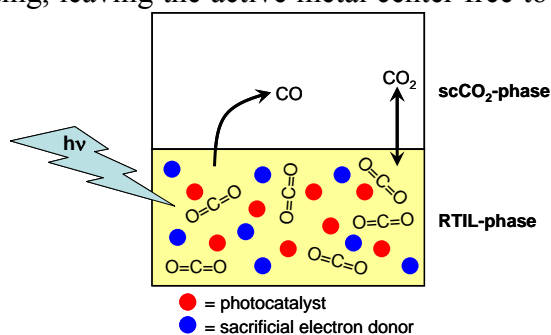
We are investigating the photophysical properties of $ReCl(bpy)(CO)_3$ and the efficiency of CO_2 reduction in a series of RTILs and biphasic RTIL/scCO$_2$ systems. In particular, we have focused initially on RTILs containing the tetracyanoborate anion; 1-butyl-1-methylpyrrolidinium tetracyanoborate ([bmpyrr][TCB]) and 1-ethyl-3-methylimidazolium tetracyanoborate ([emim][TCB]). The photophysical properties of $ReCl(bpy)(CO)_3$ in these RTILs are very similar to those in conventional solvents, such as MeCN. Interestingly though, Stern-Volmer emission lifetime quenching experiments (see right) reveal TEOA quenching rate constants in the RTILs that are only ~10× lower than in acetonitrile, despite the RTILs being ~100× more viscous (*e.g.* $k_q = 8 \times 10^6$ M^{-1} s^{-1} in [bmpyrr][TCB] *vs.* 8×10^7 M^{-1} s^{-1} in MeCN). In photocatalytic CO_2 reduction experiments in the presence of TEOA, relative turnover numbers (TONs) for the production of CO (moles of CO produced/moles of catalyst used) have been obtained by performing experiments under identical

photolysis conditions. The viscosity of the RTIL appears to play a crucial role in the efficiency of the photocatalytic CO_2 reduction. For example, in [bmpyrr][TCB] under 1 atm of CO_2, TON = 4 @ 15 °C, increasing to TON = 10 @ 35 °C, when the RTIL is less viscous. This is in contrast to the same reaction in DMF, where the TON *decreases* by 50% upon increasing the temperature from 15 to 35 °C. Furthermore, preliminary experiments indicate that the TON increases by a factor of ~7× when performed in a biphasic mixture with scCO$_2$. This demonstrates that the high $[CO_2]$ in a biphasic RTIL/scCO$_2$ system results in significant improvements in catalyst efficiency compared to under ambient pressures. We are currently in the process of obtaining ultrapure TCB RTILs, which should improve overall TONs. Other RTILs that we plan to investigate are those based on the tris(pentafluoroethyl)trifluorophosphate (FAP) anion, since this is a non-coordinating anion that will not bind to vacant sites at the metal center during catalysis.
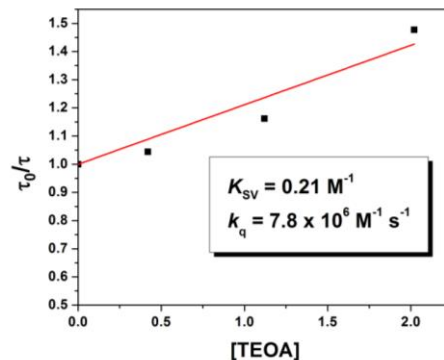
Infrared Detection for Pulse Radiolysis – A New Method for Gaining Mechanistic Knowledge of Radiation-Induced Processes. Understanding the mechanisms of redox processes, such as CO_2 reduction and other solar energy conversion reactions, is crucial for the development of more efficient systems. Pulse radiolysis, utilizing high-energy electrons from accelerators, is a powerful method for the rapid addition of single positive or negative charges to molecules and is therefore an ideal tool for such mechanistic investigations. However, the transient species formed are sometimes difficult to identify due to their broad and featureless UV/visible bands. Time-resolved infrared (TRIR) spectroscopy is a powerful structural probe of short-lived species, often allowing their definitive identification. However, due to several
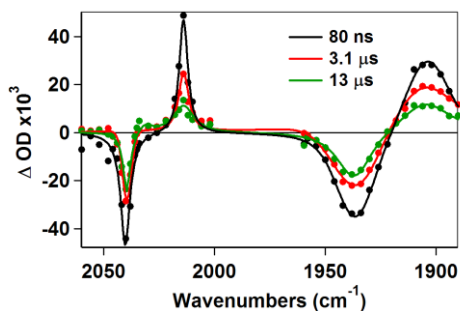
technical challenges, it has previously only been applied to a handful of gas-phase pulse radiolysis studies. Taking advantage of new mid-IR laser technology in the form of external-cavity quantum cascade lasers (EC-QCLs), which are tunable, compact, high-power mid-IR lasers, we have recently demonstrated, for the first time, the application of nanosecond TRIR detection to the pulse radiolysis of condensed-phase systems at our LEAF pulse radiolysis facility. Using two EC-QCLs, we monitored the

one-electron reduction of the CO_2 reduction catalysts, $[Re(bpy)(CO)_3(CH_3CN)]^+$ and $[Ru(bpy)_2(CO)(H)]^+$ in acetonitrile, probing their $\nu(CO)$ IR bands. The figure above shows a set of TRIR spectra for $[Re(bpy)(CO)_3(CH_3CN)]^+$, exhibiting a characteristic red-shift of the $\nu(CO)$ bands following reduction of the catalyst. Since these preliminary experiments, we have received DOE funding to expand the project with the construction of a new electron beamline dedicated to TRIR experiments, and the acquisition of a suite of 11 EC-QCLs with broad tunability throughout much of the mid-IR ($2300 - 1000$ cm^{-1}). Installation of the new instrumentation is scheduled to occur in June 2011, and this will open the door to a series of new pulse radiolysis investigations that were previously difficult or impossible to perform without TRIR detection. For example, we plan to (i) study the reactivity of key redox intermediates involved in solar energy conversion processes, including one-electron reduced metal hydride complexes, (ii) better understand charge propagation along conjugated "molecular wires", and (iii) investigate many other systems of relevance to energy-related chemistry.

Other Projects. We are particularly interested in understanding the factors that control the bond formation rates between photoproduced metal-based intermediates and substrates in the early stages of photoreduction processes. To this end, we have studied the mechanism and kinetics of small molecule binding to photogenerated pincer (PCP)Rh(I) complexes. An investigation of unusual solvato- / thermochromic behavior of the $[Re(dnb)(CO)_3]_2$ dimer is also underway.

Acknowledgements

DOE Sponsored Solar Photochemistry Publications of D. C. Grills 2008-2011

1. Huang, K.-W.; Grills, D. C.; Han, J. H.; Szalda, D. J.; Fujita, E. "Selective Decarbonylation by a Pincer PCP-Rhodium(I) Complex" *Inorg. Chim. Acta* **2008**, *361*, 3327-3331.

2. Doherty, M. D.; Grills, D. C.; Fujita, E. "Synthesis of Fluorinated ReCl(4,4′-R$_2$-2,2′-bipyridine)(CO)$_3$ Complexes and Their Photophysical Characterization in CH$_3$CN and scCO$_2$" *Inorg. Chem.* **2009**, *48*, 1796-1798.

3. Doherty, M. D.; Grills, D. C.; Muckerman, J. T.; Polyansky, D. E.; Fujita, E. "Toward More Efficient Photochemical CO$_2$ Reduction: Use of scCO$_2$ or Photogenerated Hydrides" *Coord. Chem. Rev.*, **2010**, *254,* 2472-2482.

4. Grills, D. C.; Cook. A. R.; Fujita, E.; George, M. W.; Preses, J. M.; Wishart, J. F. "Application of External-Cavity Quantum Cascade Infrared Lasers to Nanosecond Time-Resolved Infrared Spectroscopy of Condensed-Phase Samples Following Pulse Radiolysis" *Appl. Spectrosc.* **2010**, *64*, 563-570 (cover article).

5. Grills, D. C; Fujita, E. "New Directions for the Photocatalytic Reduction of CO$_2$: Supramolecular, scCO$_2$ or Biphasic Ionic Liquid-scCO$_2$ Systems" *J. Phys. Chem. Lett.* **2010**, *1*, 2709-2718.

6. Grills, D. C.; Doherty, M. D.; Fujita, E. "New Catalysts for the Photochemical Reduction of CO$_2$ in Supercritical CO$_2$" *Prep. Pap.-Am. Chem. Soc., Div. Fuel Chem.* **2010**, *55*, 55-56.

7. Doherty, M. D.; Grills, D. C.; Huang, K.-W.; Muckerman, J. T.; Polyansky, D. E.; van Eldik, R.; Fujita, E. "Mechanisms of Small Molecule Binding to Pincer-PCP Rhodium(I) Complexes" *J. Am. Chem. Soc.* **2011**, submitted.

All-Inorganic Polynuclear Assemblies for H_2O Oxidation and CO_2 Reduction on Nanoporous Silica Surfaces

Heinz Frei

Physical Biosciences Division, Lawrence Berkeley National Laboratory
Berkeley, CA 94720

The long term goal of our work is to directly convert carbon dioxide and water with sunlight to a liquid fuel using robust inorganic assemblies. Focusing on molecularly defined all-inorganic hetero-polynuclear structures anchored in a nanoporous silica membrane, we are exploring photocatalytic units consisting of an oxo-bridged metal-to-metal charge-transfer chromophore coupled to a nanocluster catalyst. In this way, the light absorption/charge separation function is separated from the multi-electron catalysis. Flexible synthetic methods have been developed for the assembly of a range of heterobinuclear charge transfer chromophores made of first row transition metals that absorb across the visible spectrum. Free selection of metal centers enables matching of the redox potential of the donor or acceptor center with the driving force requirement for water oxidation or carbon dioxide reduction, a prerequisite for high thermodynamic efficiency of photon to chemical energy conversion. An example is a $Ti^{IV}OCr^{III}$ unit coupled to an Ir oxide nanocluster catalyst that evolved oxygen from water under visible light with 14 percent quantum efficiency (pH 6). In some cases, the charge-transfer chromophore itself can serve as photocatalytic site. Recent effort has focused on the elucidation of structure and mechanism of these polynuclear units using mainly transient vibrational, time-resolved optical, and EXAFS spectroscopy. The results provide insights that are critical for the design of units with improved photocatalytic efficiency.

Direct observation of surface hydroperoxide intermediate upon visible light-driven water oxidation at Ir oxide nanocluster catalyst

Following observation of efficient oxygen evolution from liquid water at Ir oxide nanocluster catalysts driven by a binuclear chromophore, we have initiated a study of the reaction mechanism by the detection of reaction intermediates using rapid-scan FT-IR absorption spectroscopy in the attenuated total reflection mode. When driving IrO_2 nanocluster catalysts by visible light excitation of a sensitizer for the duration of 1 second, a band was detected at 830 cm^{-1} in H_2O and at 800 cm^{-1} in D_2O that vanished at the end of the pulse (610 vs. 1830 ms time slice in adjacent figure). Given a turnover frequency per Ir surface site of around 10 O_2 molecules s^{-1}, this behavior indicates that the observed species is a kinetically relevant intermediate of water oxidation. The use of $D_2{}^{18}O$ revealed $^{16}O^{18}O$ and $^{18}O^{18}O$ bands at 776 and 750 cm^{-1} with ^{18}O shifts characteristic for an OO stretch mode. The observed D isotope shift implies a surface hydroperoxide (IrOOH) species. This is the first observation of a reaction intermediate upon water oxidation at an Ir oxide nanocluster catalyst. The proposed mechanism involves sequential two electron oxidation of an $Ir^{III}OH$ surface site to an $Ir^{V}=O$ group followed by nucleophilic attack of a water molecule (or insertion of a neighboring surface OH) on the electrophilic O to form the
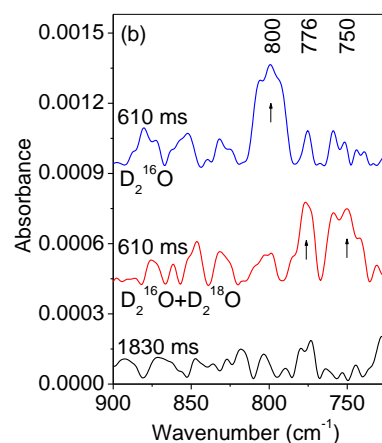
hydroperoxide intermediate. Sequential two electron oxidation of the $Ir^{III}OOH$ releases O_2 while restoring the surface Ir^{III} site. FT-IR experiments on faster time scales are in progress for detecting the shorter-lived intermediates of the 4-electron transfer reaction. Knowledge of the reaction intermediates of this efficient noble metal oxide catalyst will allow us to design second sphere interactions, e.g. by catalyst core/oxide shell constructs that may lower energy barriers for reaction steps of less active oxide nanocluster catalysts of abundant first row transition metals.

EXAFS structure of visible light $TiOMn^{II}$ charge-transfer chromphore
Curve fitting analysis of Ti and Mn K-edge EXAFS measurements of $TiOMn^{II}$ binuclear sites in silica mesopores (SBA-15) revealed structural details of the oxo-bridged unit. First shell analysis confirmed the tetrahedral coordination of the Ti center, while the Mn edge data revealed pseudo-octahedral O coordination in agreement with our previous measurements of Ti and Mn L-edge spectra. Most importantly, curve fitting showed two second shell scatterers, Si and a second transition metal. We find a common TiMn distance of 3.3 $\pm$ 0.1 Angstrom from the Ti and Mn data analysis, which implies a TiOMn angle of 114 degrees.
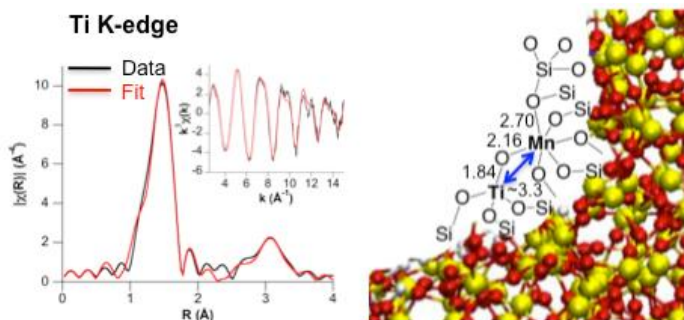
EXAFS analysis of a TiMn-SBA-15 sample treated by heating at high temperature (300 C) in the presence of oxygen demonstrated the chemical robustness of the oxo-bridged unit: While the oxidation state of Mn was increased to III or higher, curve fitting confirmed that the oxo bridge remained intact although it shortened to 3.0 Angstrom. Structural details of other binuclear chromophores of particular interest for photosynthetic applications, especially the $TiOCo^{II}$ and $ZrOMn^{II}$ were derived from similar EXAFS studies.

Light-driven CO_2 reduction at $ZrOCo^{II}$ binuclear charge transfer site
Using isotopically labeled $^{13}CO_2$ and $C^{18}O_2$ gas (1 atm) loaded into SBA-15 mesoporous silica with anchored $ZrOCo^{II}$ sites, we have discovered the splitting of carbon dioxide to carbon monoxide upon excitation of the $Zr^{IV}OCo^{II} \rightarrow Zr^{III}OCo^{III}$ charge-transfer transition. While the continuous MMCT optical absorption extends from the UV to 550 nm, photolysis experiments were conducted with 355 nm light to facilitate product analysis. In contrast to CO_2 splitting by photo-excitation of $ZrOCu^{I}$ units which we reported previously, no trapping of the CO product at the donor center was observed for the ZrOCo unit; carbon monoxide escaped instantly from the silica nanopores into the gas phase. In addition to CO, carbon dioxide reduction results in a carboxy product tentatively assigned to formate.

Taking advantage of optically transparent mesoporous silica films which we obtained recently by the spin coating technique, we are currently expanding our time-resolved optical studies of the mechanism of excited state electron transfer of the binuclear chromophores and coupled multi-electron transfer catalysts. In parallel, future effort will focus on the mechanistic understanding of H_2O oxidation at Co_3O_4 and Mn oxide nanocluster catalysts in mesoporous silica by the transient ATR-FT-IR method. New carbon dioxide reduction photocatalysts will be explored by spatially directed synthesis of metal cluster catalysts at the acceptor site of the binuclear chromophores in the silica nanopore.

DOE Sponsored Solar Photochemistry Publications 2008-2010:
Field Work Proposal "Chemistry with Near Infrared Photons"

1. H. Han and H. Frei. Controlled Assembly of Hetero-binuclear Sites on Mesoporous Silica: Visible Light Charge-Transfer Units with Selectable Redox Properties. *J. Phys. Chem. C* **112**, 8391-8399 (2008).

2. W. Weare, Y. Pushkar, V. Yachandra, and H. Frei. Visible Light-Induced Electron Transfer from Di-u-oxo Bridged Dinuclear Mn Complexes to Cr Centers in Silica Nanopore. *J. Am. Chem. Soc.* **130**, 11355-11363 (2008).

3. H. Han and H. Frei. In-Situ Spectroscopy of Water Oxidation at Ir Oxide Nanocluster Driven by Visible TiOCr Charge-Transfer Chromophore in Mesoporous Silica. *J. Phys. Chem. C* **112**, 16156-16159 (2008)

4. G. Mul, W.A. Wasylenko, and H. Frei. Cyclohexene Photooxidation over Vanadia Catalyst Analyzed by Time-Resolved ATR-FT-IR Spectroscopy. *Phys. Chem. Chem. Phys.* **10**, 3131-3137 (2008).

5. W. Weare and H. Frei. Artificial Photosynthesis, In: *Yearbook of Science and Technology;* Weil, J., Ed.; McGraw Hill: New York (2009); pp.28-31.

6. X. Wu, W.W. Weare, and H. Frei. Binuclear TiOMn Charge-Transfer Chromophore in Mesoporous Silica. *Dalton Trans.*, 10114-10121 (2009) (Hot Article).

7. H. Frei. Polynuclear Photocatalysts in Nanoporous Silica for Artificial Photosynthesis. *Chimia* **63**, 721-730 (2009).

8. T. Cuk, W.W. Weare, and H. Frei. Unusually Long Lifetime of Excited Charge-Transfer State of Binuclear TiOMn[II] Unit Anchored on Silica Nanopore Surface. *J. Phys. Chem. C* **114**, 9167-9172 (2010).

9. N. Sivasankar, W.W. Weare, and H. Frei. Direct Observation of Hydroperoxide Surface Intermediate upon Visible Light-Driven Water Oxidation at Ir Oxide Nanocluster Catalyst by Rapid-Scan FT-IR Spectroscopy. *J. Am. Chem. Soc.,* submitted.

10. H.S. Soo, W.W. Weare, J. Yano, and H. Frei. EXAFS Spectroscopic Analysis of Heterobinuclear TiOMn Charge-Transfer Chromophore in Mesoporous Silica. *J. Phys. Chem. C*, submitted.

Publications sponsored through SERC:

1. F. Jiao and H. Frei. Nanostructured Cobalt Oxide Clusters in Mesoporous Silica as Efficient Oxygen-Evolving Catalysts. *Angew. Chem. Int. Ed.* **48**, 1841-1844 (2009).

2. F. Jiao and H. Frei. Nanostructured Manganese Oxide Clusters Supported on Mesoporous Silica as Efficient Oxygen-Evolving Catalysts. *Chem. Commun.* **46**, 2920-2922 (2010).

3. F. Jiao and H. Frei. Nanostructured Cobalt and Manganese Oxide Clusters as Efficient Water Oxidation Catalysts. *Energy Environ. Sci.* **3**, 1018-1027 (2010).

4. F. Jiao and H. Frei. Nanostructured Cobalt Oxide and Manganese Oxide Clusters Supported on Mesoporous Silica as Efficient Water Oxidation Catalysts. *U.S. Patent Appl. Ser. No. 61/298,876,* filed Jan 27, 2010.

Session VI

Catalysis at Surfaces

Properties of Fe 'Doped' and (Fe,N) Co-doped Rutile TiO$_2$(110)

M.A. Henderson, A.N. Mangham, A.G. Joly, N. Govind and S.A. Chambers
Chemical and Materials Sciences Division
Pacific Northwest National Laboratory
Richland, WA 99352

Introduction

TiO$_2$-based materials are promising photocatalysts that show activity in the UV and stability over a wide range of conditions. However, TiO$_2$ absorbs little of the solar spectrum. Doping offers the possibility of incorporating donor and/or acceptor states into the TiO$_2$ band gap that lower the threshold energy for photon absorption without significantly compromising photoactivity. While much applied work exists involving doping of TiO$_2$, there has been little effort aimed at understanding the fundamental properties of doped TiO$_2$. In this project, we examine the controlled doping of single crystal films of anatase and rutile TiO$_2$ with both anion and cation dopants using plasma-assisted molecular beam epitaxy (MBE).

Characterization of doped films

We have grown and characterized homoepitaxial rutile TiO$_2$(110) films „doped' with Fe and co-doped with Fe and N.[1-3] Recent studies have yielded new insights into the relationship between the structural environment of a dopant in TiO$_2$ and its effect on photocatalytic activity.[4,5] For example, it has been shown that the solubility limit of N within the anion sublattice for rutile and anatase is only ~1 at.%.[5] In both rutile and anatase polymorphs, this concentration was sufficient to shift the absorption edge into the visible region. However, in the case of rutile, N doping reduced the photocatalytic activity, presumably due to hole trapping at N sites.[5] Our recent work has focused on methods for increasing the N-dopant concentration in TiO$_2$. Co-doping has been examined as one such method. In a combined experimental and theoretical study, Zhu et al.[6] presented evidence for mutually enhanced solubility of Cr and N via co-doping, with enhanced dopant concentrations attributed to the formation of dopant pairs stabilized by Coulombic interactions.

Several theoretical studies[7] predict that partially filled Fe 3d states arising from Fe doping should cause a redshift in the TiO$_2$ bandgap leading to visible light photocatalytic activity.[8] Cited dopant concentrations in this system range from as little as 0.001 mol%[9] to as much as 28 mol%,[8b] with the possibility of segregated Fe.[8f,9-11] By preparing homoepitaxial single-crystal thin films of Fe doped rutile TiO$_2$, we are able to employ a range of characterization techniques and explore the structural properties of this system at a deeper level than previously
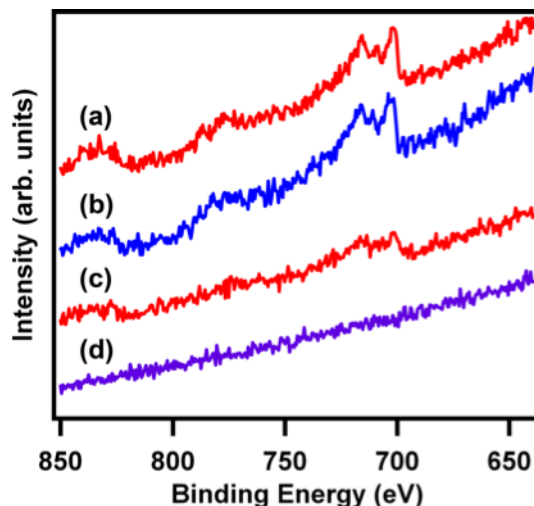
Fig. 1: Fe 2p XPS spectra for Fe doped TiO$_2$(110) before (a) and after (b) growth of a 10 nm pure TiO$_2$(110) epitaxial cap layer, as well as for (Fe,N) co-doped TiO$_2$(110) before (c) and after (d) growth of a 10 nm pure TiO$_2$(110) epitaxial cap layer.

achieved. We find that Fe, by itself, does not incorporate as an electronic dopant in the rutile lattice, but rather segregates to the film surface. XPS was used to probe the oxidation state and stability of Fe in $TiO_2(110)$. Fig. 1a shows the Fe 2p XPS spectrum from a 10 nm $TiO_2(110)$ film grown (on $TiO_2(110)$) with a nominal 2 at.% Fe dopant concentration. The Fe lineshape and binding energies matched those of Fe_2O_3, leading to a Fe^{3+} assignment. However, the surface concentration of Fe, determined with detection angle-dependent measurements, was ~10.2 at.% instead of the ~2% expected based on the growth conditions (i.e., from the impinging Ti and Fe fluxes). This indicates that the Fe dopant segregated to the $TiO_2(110)$ surface, possibly as a separate phase with a Fe_2O_3 composition. Subsequent deposition of an additional 10 nm of *undoped* epitaxial TiO_2 as a 'capping' layer did not bury this surface phase of Fe_2O_3 (Fig. 1b), which appeared to 'float' on the TiO_2 film as it was grown. In contrast, XPS results in Fig. 1c show that co-deposition of Fe and N during growth of rutile $TiO_2(110)$ enhanced the solubility of Fe and N in lattice. For the same nominal Fe dopant concentration, with the additional of N_2 in the oxygen plasma source, the (Fe,N) co-doped film showed significantly less Fe segregation. The Fe concentrations were much closer to the target doping level (~2 cation at.%) both at the surface (glancing angle detection) and in the bulk (normal angle detection). The N concentration, as gauged by the N 1s line, was also ~2 at.%, indicating an enhancement of N in the lattice due to Fe. Fig. 1d shows that Fe did not 'float' on top of the co-doped film when an additional 10 nm of TiO_2 was grown as a capping layer. DFT calculations (not shown) suggest that formation of a co-dopant complex is the driving force behind the enhanced solubilities of Fe and N in the rutile $TiO_2(110)$ lattice.
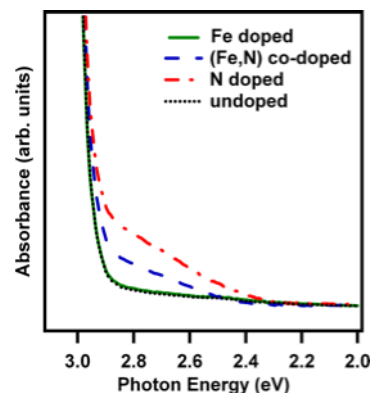
Fig. 2: Absorption spectra for Fe doped, (Fe,N) co-doped, N-doped and undoped rutile $TiO_2(110)$.

Photochemical properties

Both the N-doped and (Fe,N) co-doped films extended the optical absorptivity of rutile TiO_2 into the visible, but no significant change to the optical spectrum of TiO_2 was seen for Fe-doping (Fig. 2). Data in Fig. 3 shows CO_2 photodesorption spectra from the photodecomposition of adsorbed trimethyl acetate (TMA) on undoped, Fe-doped, N-doped and (Fe,N) co-doped $TiO_2(110)$ surfaces. The N-doped and (Fe,N) co-doped films were photochemically inert with respect to hole-mediated decomposition of adsorbed TMA. Only the Fe 'doped' and undoped films showed any photochemical response, and only when illuminated with UV light (data for visible light irradiation not shown). The N-doped film was inactive in the UV and visible, presumably because of hole trapping on N sites.[5] The (Fe,N) co-doped film was also photoinactive for the hole-mediated
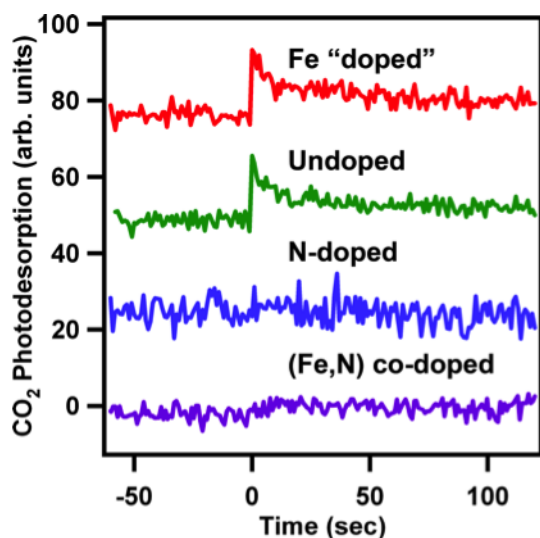
Fig. 3: Photodesorption data for Fe doped, (Fe,N) co-doped, undoped and N-doped TiO_2 under UV + visible irradiation.

decomposition of TMA. While this material could also be exhibiting hole-trapping on N sites, disorder in the lattice may contribute as a possible reason for photoinactivity. These results indicate that enhanced visible light absorptivity in TiO_2 due to doping does not necessarily translate into visible light initiated surface photochemistry.

Acknowledgements

References

1. Chambers, S.A.; Cheung, S.H.; Shutthanandan, V.; Thevuthasan, S.; Bowman, M.K.; Joly, A.G. Chem. Phys. 339 (2007) 27.

2. (a) Cheung, S.H.; Nachimuthu, P.; Engelhard, M.H.; Wang, C.M.; Chambers, S.A. Surf. Sci. 602 (2008) 133; (b) Cheung, S.H.; Nachimuthu, P.; Joly, A.G.; Engelhard, M.H.; Bowman, M.K.; Chambers, S. A. Surf. Sci. 601 (2007) 1754.

3. Mangham, A.N.; Govind, N.; Bowden, M.E.; Shutthanandan, V.; Joly, A.G.; Henderson, M.A.; Chambers, S.A. J. Phys. Chem. C., submitted.

4. Ohsawa, T.; Henderson, M.A.; Chambers, S.A. J. Phys. Chem. C 2010, 114, 6595.

5. Ohsawa, T.; Lyubinetsky, I.; Du, Y.; Henderson, M.A.; Shutthanandan, V.; Chambers, S.A. Phys. Rev. B 79 (2009) 085401.

6. Zhu, W.G.; Qiu, X.F.; Iancu, V.; Chen, X.Q.; Pan, H.; Wang, W.; Dimitrijevic, N.M.; Rajh, T.; Meyer, H.M.; Paranthaman, M.P.; Stocks, G.M.; Weitering, H.H.; Gu, B.H.; Eres, G.; Zhang, Z.Y. Phys. Rev. Lett. 103 (2009) 226401.

7. (a) Shao, G.S. J. Phys. Chem. C 113 (2009) 6800; (b) Thimsen, E.; Biswas, S.; Lo, C.S.; Biswas, P. J. Phys. Chem. C 113 (2009) 2014; (c) Umebayashi, T.; Yamaki, T.; Itoh, H.; Asai, K. J. Physics Chem. Solids 63 (2002) 1909.

8. (a) Naeem, K.; Feng, O.Y. Physica B 405 (2010) 221; (b) Zhang, Y.H.; Ebbinghaus, S.G.; Weidenkaff, A.; Kurz, T.; von Nidda, H.A.K.; Klar, P.J.; Gungerich, M.; Reller, A. Chem. Mater. 15 (2003) 4028; (c) Zhu, S.Y.; Li, Y. Z.; Fan, C.Z.; Zhang, D.Y.; Liu, W.H.; Sun, Z.H.; Wei, S.Q. Physica B 364 (2005) 199; (d) Egerton, T.A.; Kosa, S.A.M.; Christensen, P.A. Phys. Chem. Chem. Phys. 8 (2006) 398; (e) Zhu, S.Y.; Shi, T.F.; Liu, W.H.; Wei, S.L.; Xie, Y.I.; Fan, C.Z.; Lie, Y. Physica B 396 (2007) 177; (f) Tong, T.Z.; Zhang, J.L.; Tian, B.Z.; Chen, F.; He, D.N.J. Haz. Mater. 155 (2008) 572.

9. Hung, W.C.; Chen, Y.C.; Chu, H.; Tseng, T.K. Appl. Surf. Sci. 255 (2008) 2205.

10. Ambrus, Z.; Balazs, N.; Alapi, T.; Wittmann, G.; Sipos, P.; Dombi, A.; Mogyorosi, K. Appl. Catal. B 81 (2008) 27.

11. Choi, J.; Park, H.; Hoffmann, M.R. J. Phys. Chem. C 114 (2010) 783.

DOE Sponsored Solar Photochemistry Publications 2008-2011

1. Chambers, S.A. "Molecular Beam Epitaxial Growth of Doped Oxide Semiconductors." J. Phys.: Condens. Matter 20 (2008) 264004.

2. Cheung, S.H., P. Nachimuthu, M.H. Engelhard, C.M. Wang and S.A. Chambers. "N Incorporation, Composition and Electronic Structure in N-doped $TiO_2(001)$ Anatase Epitaxial Films Grown on $LaAlO_3(001)$." Surf. Sci. 602 (2008) 133.

3. Du, Y.G., Z. Dohnálek and I. Lyubinetsky. "Transient Mobility of Oxygen Adatoms upon O_2 Dissociation on Reduced $TiO_2(110)$." J. Phys. Chem. C 112 (2008) 2649. *(Featured on the journal's cover.)*

4. Kimmel, G.A. and N.G. Petrik. "Tetraoxygen on Reduced $TiO_2(110)$: Oxygen Adsorption and Reactions with

Bridging Oxygen Vacancies." Phys. Rev. Lett. 100 (2008) 196102.

5. Groves, J.F., Y. Du, I. Lyubinetsky and D.R. Baer. "Focused Ion Beam Directed Self-Assembly (Cu_2O on $SrTiO_3$): FIB Pit and Cu_2O Quantum Dot Evolution." Superlatt. Microstruct. 44 (2008) 677.

6. Li, S.-C., Z. Zhang, D. Sheppard, B.D. Kay, J.M. White, Y. Du, I. Lyubinetsky, G. Henkelman and Z. Dohnálek. "Intrinsic Diffusion of Hydrogen on Rutile $TiO_2(110)$." J. Am. Chem. Soc. 130 (2008) 9080.

7. Ohsawa, T., I.V. Lyubinetsky, M.A. Henderson and S.A. Chambers. "Hole-Mediated Photodecomposition of Trimethyl Acetate on a $TiO_2(001)$ Anatase Epitaxial Thin Film Surface." J. Phys. Chem. C 112 (2008) 20050.

8. Yu, Z.Q., C.M. Wang, Y. Du, S. Thevuthasan and I. Lyubinetsky. "Reproducible Tip Fabrication and Cleaning for UHVSTM." Ultramicroscopy 108 (2008) 873.

9. Chambers, S.A., T. Ohsawa, C.M. Wang, I. Lyubinetsky and J.E. Jaffe. "Band Offsets at the Epitaxial Anatase TiO_2/n-$SrTiO_3(001)$ Interface." Surf. Sci. 603 (2009) 771.

10. Du, Y., N.A. Deskins, Z. Zhang, Z. Dohnálek, M. Dupuis and I. Lyubinetsky. "Two Pathways for Water Interaction with Oxygen Adatoms on $TiO_2(110)$." Phys. Rev. Lett. 102 (2009) 096102.

11. Du, Y.G., N.A. Deskins, Z.R. Zhang, Z. Dohnálek, M. Dupuis and I. Lyubinetsky. "Imaging Consecutive Steps of O_2 Reaction with Hydroxylated $TiO_2(110)$: Identification of HO_2 and Terminal OH Intermediates." J. Phys. Chem. C 113 (2009) 666.

12. Ohsawa, T., I. Lyubinetsky, Y. Du, M.A. Henderson, V. Shutthanandan and S.A. Chambers. "Crystallographic Dependence of Visible-light Photoactivity in Epitaxial $TiO_{2-x}N_x$ Anatase and Rutile." Phys. Rev. B 79 (2009) 085401.

13. Petrik, N.G. and G.A. Kimmel (2009). "Nonthermal Water Splitting on Rutile TiO_2: Electron-Stimulated Production of H_2 and O_2 in Amorphous Solid Water Films on $TiO_2(110)$." J. Phys. Chem. C 113(11): 4451.

14. Petrik, N.G., Z.R. Zhang, Y.G. Du, Z. Dohnálek, I. Lyubinetsky and G.A. Kimmel. "Chemical Reactivity of Reduced $TiO_2(110)$: The Dominant Role of Surface Defects in Oxygen Chemisorption." J. Phys. Chem. C 113 (2009) 12407.

15. Zhang, Z., Y. Du, N.G. Petrik, G.A. Kimmel, I. Lyubinetsky and Z. Dohnálek. "Water as a Catalyst: Imaging Reactions of O_2 with Partially and Fully Hydroxylated $TiO_2(110)$ Surfaces." J. Phys. Chem. C 113 (2009) 1908.

16. Chambers, S.A. "Epitaxial Growth and Properties of Doped Transition Metal and Complex Oxide Films." Adv. Mater. 22 (2010) 219.

17. Dohnálek, Z., I. Lyubinetsky and R. Rousseau. "Thermally-Driven Processes on Rutile $TiO_2(110)$-(1x1): A Direct View at the Atomic Scale." Prog. Surf. Sci. 85 (2010) 161.

18. Du, Y.G., N.A. Deskins, Z.R. Zhang, Z. Dohnálek, M. Dupuis and I. Lyubinetsky. "Formation of O adatom pairs and charge transfer upon O_2 dissociation on reduced $TiO_2(110)$." Phys. Chem. Chem. Phys. 12 (2010) 6337.

19. Du, Y., N.A. Deskins, Z. Zhang, Z. Dohnálek, M. Dupuis and I. Lyubinetsky. "Water Interactions with Terminal Hydroxyls on $TiO_2(110)$." J. Phys. Chem. C 114 (2010) 17080.

20. Henderson, M.A., V. Shutthanandan, T. Ohsawa and S.A. Chambers. "Structural Environment of Nitrogen in N-doped Rutile $TiO_2(110)$." Proc. SPIE 7770 (2010) 777007.

21. Lyubinetsky, I., N.A. Deskins, Y.G. Du, E. K. Vestergaard, D.J. Kim and M. Dupuis. "Adsorption States and Mobility of Trimethylacetic Acid Molecules on Reduced $TiO_2(110)$ Surface." Phys. Chem. Chem. Phys. 12 (2010) 5986.

22. Ohsawa, T., M.A. Henderson and S.A. Chambers. "Epitaxial Growth and Orientational Dependence of Surface Photochemistry in Crystalline TiO_2 Rutile Films Doped with Nitrogen." J. Phys. Chem. C 114 (2010) 6595.

23. Petrik, N.G. and G.A. Kimmel. "Photoinduced Dissociation of O_2 on Rutile $TiO_2(110)$." J. Phys. Chem. Lett. 1 (2010) 1758.

24. Mangham, A.N., N. Govind, M.E. Bowden, V. Shutthanandan, A.G. Joly, M.A. Henderson and S.A. Chambers. "Photochemical Properties, Composition and Structure in MBE Grown Fe Doped and (Fe,N) Codoped Rutile $TiO_2(110)$," J. Phys. Chem. C, submitted.

25. Henderson. M.A. "A surface science perspective on TiO_2 photocatalysis," Surf. Sci. Rep., in press.

26. Henderson, M.A. and M.D. Robbins. "Methylene Bromide Chemistry and Photochemistry on Rutile $TiO_2(110)$," Surf. Sci., submitted.

Catalyzed Water Oxidation by Solar Irradiation of Band-Gap-Narrowed Semiconductors

Etsuko Fujita, James T. Muckerman, Dmitry E. Polyansky and J. A. Rodriguez
Chemistry Department
Brookhaven National Laboratory
Upton, NY 11973-5000

We are attacking four major issues hindering progress in solar-driven water splitting using an integrated experimental and theoretical approach that offers fundamental insights into the underlying photoelectrolysis processes occurring in band-gap-narrowed semiconductor (BGNSC) and catalyst components. Our research has resulted in a number of advances, especially in areas (1) and (2).

(1) Improve the light-harvesting and charge-separation abilities of stable oxide or oxide-derived *semiconductors for solar-driven water splitting* through a focused effort to achieve a better understanding of their structural and electronic properties, and a parallel broad effort to discover and characterize promising new candidate semiconductors.

(2) Investigate the *mechanism of water oxidation* by mononuclear metal aqua complexes and by dinuclear hydroxo metal complexes with quinonoid ligands in order to develop a better understanding of the critical four-electron water oxidation catalyst chemistry, and rationally search for improved catalysts.

(3) *Immobilize* the homogeneous water oxidation catalysts and (non-precious) metal oxide catalysts on conductive electrodes and/or metal oxide nanoparticles in order to determine the kinetics of *electrochemical water oxidation*, and identify the intermediates by spectroscopic techniques.

(4) Combine these elements to examine *photocatalytic water oxidation at BGNSC surfaces at the aqueous interface* and understand the core scientific challenges to the efficient coupling of the catalytic functions.

Photocatalytic Water Oxidation at the GaN (10$\bar{1}$0) – Water Interface. We constructed an atomistic model and proposed a sequence of intermediate steps for water oxidation at a pure GaN(10$\bar{1}$0)/water interface.[6,13] Ab initio molecular dynamics simulations examined the fully solvated aqueous interface at ambient temperature. An appropriate cluster model, that includes a polarizable continuum in addition to explicit solvent water molecules, was cut out from snapshots of these AIMD simulations for additional DFT-based calculations of the water oxidation mechanism. The reaction intermediates follow a sequence of four proton-coupled electron transfers. Four UV photons are consumed to generate the four photo-holes which drive the oxidation, producing $4H^+ + O_2$ from $2H_2O$. Calculated standard free energies show that the photogenerated holes in GaN have sufficient energy to drive the overall water oxidation reaction. Implications for the operation of GaN/ZnO alloy photocatalysts, which absorb in the visible wavelength range, are presented. The calculated potentials show a remarkable parallelism to the known potentials for the sequential one-electron oxidation of water in homogeneous
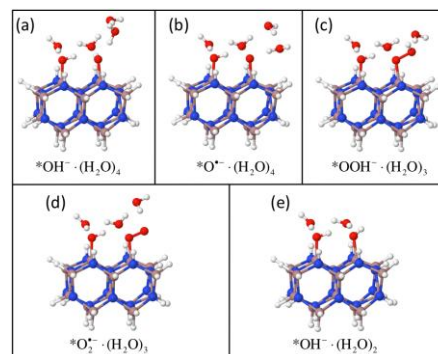
aqueous solution, suggesting that the proposed sequence may apply more generally than for the specific GaN (10$\bar{1}$0) surface catalyst.

Phase Diagram, Structure and Electronic Properties of (Ga$_{1-x}$Zn$_x$)(N$_{1-x}$O$_x$) from DFT-Based Simulations. We constructed an accurate cluster expansion (CE) for the (Ga$_{1-x}$Zn$_x$)(N$_{1-x}$O$_x$) solid solution based on density functional theory (DFT).[15] A subsequent Monte Carlo simulation revealed a phase diagram which has a wide miscibility gap and an x = 0.5 ordered compound. The disordered phase displays strong short-range order (SRO) at synthesis temperatures. To study the influences of SRO on the lattice and electronic properties, we conducted DFT calculations on snapshots from the MC simulation. Consistent with previous theoretical and experimental findings,[2,11] lattice parameters were found to deviate from Vegard's law with small upward bowing. Bond lengths depend strongly on local environment, with a variation much larger than the difference of bond length between ZnO and GaN. The downward band gap bowing deviates from parabolic by having a more rapid onset of bowing at low and high concentrations. An overall bowing parameter of 3.3 eV is predicted from a quadratic fit to the compositional dependence of the calculated band gap, all in agreement with our experimental data.[11] Our results indicate that SRO has significant influence over both structural and electronic properties.
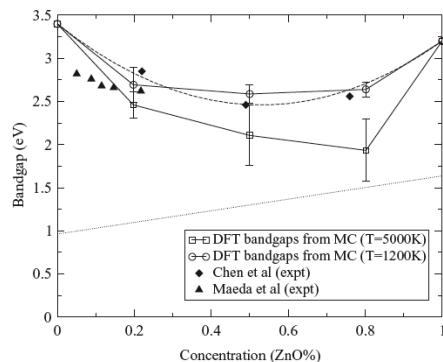
Characterization of the Intermediates Involved in Water Oxidation: A detailed characterization of intermediates in water oxidation catalyzed by a mononuclear Ru polypyridyl complex [**Ru**–OH$_2$]$^{2+}$ (**Ru** = Ru(NPM)(pic)$_2$) (figure at right) has been carried out using electrochemistry, UV-vis and resonance Raman spectroscopy, pulse radiolysis, stopped flow, and ESI-MS with H$_2$^{18}O labeling experiments, and theoretical calculations.[17] The results reveal a number of intriguing properties of intermediates such as [**Ru**=O]$^{2+}$ and [**Ru**–OO]$^{2+}$. Two consecutive one-electron steps take place at the potential of the [**Ru**–OH]$^{2+}$/[**Ru**–OH$_2$]$^{2+}$ couple, which is higher than or equal to the potential of the [**Ru**=O]$^{2+}$/[**Ru**–OH]$^{2+}$ couple. While pH-independent oxidation of [**Ru**=O]$^{2+}$ takes place at 1410 mV vs NHE, bulk electrolysis of [**Ru**–OH$_2$]$^{2+}$ at 1260 mV vs NHE at pH 1 (0.1 M triflic acid) and 1150 mV at pH 6 yielded a red colored solution with a Coulomb count corresponding to the *net four-electron oxidation.* ESI-MS with labeling experiments clearly indicate that this species has an O–O bond. This species required an additional oxidation to liberate an oxygen molecule, and, without any additional oxidant, it slowly decomposed to form [**Ru**–OOH]$^+$ over 2 weeks. We have assigned this species as ^{1}[**Ru**–η^2-OO]$^{2+}$ based on our electrochemical, spectroscopic, and theoretical data alongside a previously published conclusion by T. J. Meyer's group (*J. Am. Chem. Soc*. **2010**, *132*, 1545-1557).
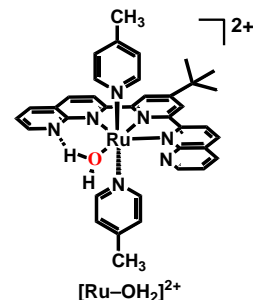
Effects of a Proximal Base on Water Oxidation and Proton Reduction Catalyzed by Geometric Isomers of [Ru(tpy)(pynap)(OH$_2$)]$^{2+}$: We have isolated the compounds p-[Ru(tpy)(pynap)(OH$_2$)]$^{2+}$ (p = proximal, tpy = 2,2';6',2"-terpyridine, pynap = 2-(pyrid-2'-yl)-1,8-naphthyridine), **1(OH$_2$)$^{2+}$**, and d-[Ru(tpy)(pynap)(OH$_2$)]$^{2+}$ (d = distal), **2(OH$_2$)$^{2+}$**, which differ in

the orientation of the asymmetric pynap ligand. The complex **1(OH₂)²⁺** has an uncoordinated naphthyridine nitrogen atom near the coordinated water molecule. Effects of a proximal base for water oxidation and proton reduction have been explored using electrochemistry and spectroscopy.[18] The catalytic activity for water oxidation was determined using $(NH_4)_2Ce(NO_3)_6$ as a sacrificial reagent. While **1(OH₂)²⁺** shows catalytic activity toward proton reduction, but not toward water oxidation, the geometric isomer, **2(OH₂)²⁺**, exhibits the opposite behavior. The compounds p-[Ru^{II}(tpy)(pynap)(OH₂)]Cl₂ and [Ru^{III}(tpy)(pynap)Cl](PF₆)₂ were also characterized crystallographically. Pourbaix diagrams of the two isomers are shown in the figure at left.
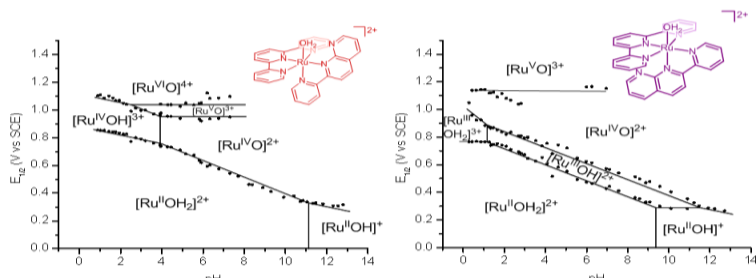
Pourbox diagram of geometric isomers **1(OH₂)²⁺** (left) and **2(OH₂)²⁺** (right).

The Tanaka Catalyst and Related Monomers: We discovered serious problems with the application of DFT methods in the accurate description of the bonding and energetics of the dimeric Tanaka catalyst and other ruthenium complexes with non-innocent ligands.[3,8,9,14] To circumvent the deficiencies of DFT methods, we resorted to very cpu-intensive CAS-MP2 calculations to clarify assignments of intermediates. In the pursuit of these studies on the Tanaka dimer, we made extensive use of insights gained from our theoretical/experimental studies of monomeric ruthenium complexes, including iminoquinone derivatives[10] of the original quinone ligands. Our revised mechanism is shown at left. Based on the construction of several key features of the Pourbaix diagram of the dimeric Tanaka catalyst, we believe the
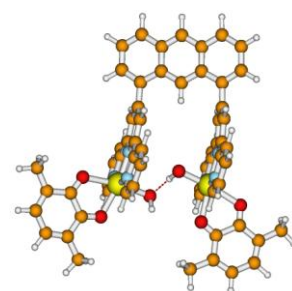
Calculated structure for the Tanaka catalyst with Me (instead of tBu) substituted quinone ligands.
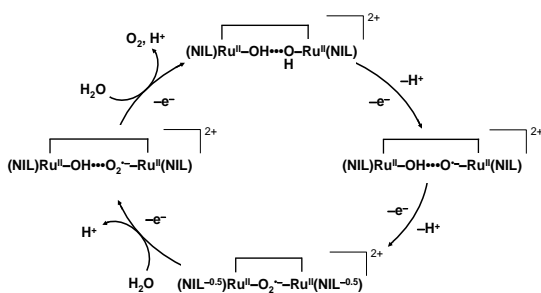
Proposed catalytic cycle for water oxidation in aq. solution at pH 4. NIL = non-innocent ligand, Q.

catalytic pathway to involve four sequential PCET oxidation steps in which the complex maintains a total charge of 2+ and (as before) the two metal centers maintain an oxidation state between 2+ and 3+. The O–O bond forms after the first two PCET steps as a peroxo or superoxo species bridging between the two metal centers, and it must undergo two more PCET steps in order for the O atom bound to each metal center to be replaced by a hydroxide ion to regenerate the resting state of the catalyst.

Acknowledgements

We thank our coworkers P. Khalifah, S. Lymar, C. Creutz, D. C. Grills, D. Cabelli and N. Sutin for fruitful discussions. We also thank our collaborators R. P. Thummel, K. Tanaka, T. Wada and D. J. Szalda. JTM gratefully acknowledges his collaboration with the SWaSSiT group (P. B. Allen, M. V. Fernandez-Serra, and M. S. Hybertsen).

DOE Sponsored Solar Photochemistry Publications 2008-2011

Hydrogen Fuel Initiative (PIs: Fujita, Khalifah, Muckerman, Polyansky, and Rodriguez)

1. Graciani, J.; Alvarez, L. J.; Rodriguez, J. A.; Fernandez-Sanz, J. "N Doping of Rutile TiO_2(110) Surface. A Theoretical DFT Study," *J. Phys. Chem. C* **2008**, *112,* 2624-2631.

2. Jensen, L.; Muckerman, J. T.; Newton, M. D. "First-Principles Studies of the Structural and Electronic Properties of the $(Ga_{1-x}Zn_x)(N_{1-x}O_x)$ Solid Solution Photocatalyst," *J. Phys. Chem. C* **2008**, *112*, 3439-3446.

3 Muckerman, J. T.; Polyansky, D. E.; Wada, T.; Tanaka, K.; Fujita, E. "Water Oxidation by a Ruthenium Complex with Non-Innocent Quinone Ligands: Possible Formation of an O–O Bond at a Low Oxidation State of the Metal. Forum „on Making Oxygen'," *Inorg. Chem.* **2008**, *47*, 1787-1802.

4 Tseng, H.-W.; Zong, R.; Muckerman, J. T.; Thummel, R. P. "Mononuclear Ru(II) Complexes That Catalyze Water Oxidation," *Inorg. Chem.* **2008**, *47*, 11763-11773.

5 Chen, H.; Wen, W.; Wang, Q.; Hanson, J. C.; Muckerman, J. T.; Fujita, E.; Frenkel, A.; Rodriguez, J. A. "Preparation of $(Ga_{1-x}Zn_x)(N_{1-x}O_x)$ Photocatalysts from the Reaction of NH_3 with Ga_2O_3/ZnO and $ZnGa_2O_4$: In situ Time-Resolved XRD and XAFS Studies," *J. Phys. Chem. C* **2009**, *113*, 3650-3659.

6 Shen, X.; Allen, P. B.; Hybertsen, M. S.; Muckerman, J. T. "Water Adsorption on the GaN $(10\bar{1}0)$ Non-polar Surface," *J. Phys. Chem. C* **2009,** *113*, 3365-3368.

7 Graciani, J.; Alvarez, L. J.; Rodriguez, J. A.; Sanz, J. F. "N Doping of Rutile TiO_2(110) Surface. A Theoretical DFT Study," *J. Phys. Chem. C* **2009**, *113*, 17464-17470.

8. Tsai, M.-K.; Rochford, J.; Polyansky, D. E.; Wada, T.; Tanaka, K.; Fujita, E.; Muckerman, J. T. "Characterization of Redox States of $Ru(OH_2)(Q)(terpy)^{2+}$ (Q = 3,5-di-tert-butyl-1,2-benzoquinone, terpy = 2,2′:6′,2″-terpyridine) and Related Species through Experimental and Theoretical Studies," *Inorg. Chem.* **2009**, 48, 4372-4383.

9. Boyer, J. L.; Rochford, J.; Tsai, M.-K.; Muckerman, J. T.; Fujita, E., "Ruthenium Complexes with Non-innocent Ligands: Electron Distribution and Implications for Catalysis," *Coord. Chem. Rev.* **2010**, *254*, 309-330.

10. Rochford, J.; Tsai, M.-K.; Szalda, D. J.; Boyer, J. L.; Muckerman, J. T.; Fujita, E., "Oxidation State Characterization of Ruthenium 2-Iminoquinone Complexes through Experimental and Theoretical Studies," *Inorg. Chem.,* **2010***, 49, 860-869.*

11. Chen, H.; Wang, L.; Bai, J.; Hanson, J. C.; Warren, J. B.; Muckerman, J. T.; Fujita, E.; Rodriguez, J. A. "*In Situ* XRD Studies of ZnO/GaN Mixtures at High Pressure and High Temperature: Synthesis of Zn-rich $(Ga_{1-x}Zn_x)(N_{1-x}O_x)$ Solid Solutions," *J. Phys. Chem. C.* **2010**, *114*, 1809-1814.

12. Concepcion, J. J.; Tsai, M.-K.; Muckerman, J. T.; Meyer, T. J. "Mechanism of Water

Oxidation by Single-Site Ruthenium Complex Catalysts," *J. Am. Chem. Soc.* **2010**, *132*, 1545-1557.

13. Shen, X.; Small, Y, A. Wang, J.; Allen, P. B.; Fernandez-Serra, M. V.; Hybertsen, M. S.; Muckerman, J. T. "Photocatalytic Water Oxidation Process at the GaN (10$\bar{1}$0) – Water Interface," *J. Phys. Chem. C*, **2010**, *114*, 13695-13704.

14. Wada, T.; Muckerman, J. T.; Fujita, E.; Tanaka, K. "Substituents Dependent Capability of Bis(ruthenium-dioxolene-terpyridine) Complexes Toward Water Oxidation," *Dalton Trans*., **2011**, *40*, 2225-2233.

15. Li, L.; Muckerman, J. T.; Hybertsen, M. S.; Allen, P. B. "Phase Diagram, Structure and Electronic Properties of $(Ga_{1-x}Zn_x)(N_{1-x}O_x)$ Solid Solution from DFT-Based Simulations," *Phys. Rev. B*, **2011**, *83*,134202.

16. Fujita, E.; Muckerman, J. T.; Domen, K. **"**A Current Perspective on Photocatalysis (Editorial)," *ChemSusChem*. **2011**, *4*, 155-157.

17. Polyansky, D. E.; Muckerman, J. T.; Rochford, J.; Zong, R.; Thummel. R. P.; Fujita, E. "Water Oxidation by a Mononuclear Ruthenium Catalyst: Characterization of the Intermediates," *J. Am. Chem. Soc*., submitted.

18. Boyer, J. L.; Polyansky, D. E.; Szalda, D. J.; Zong, R.; Thummel, R. P.; Fujita, E. "Effects of a Proximal Base on Water Oxidation and Proton Reduction Catalyzed by Geometric Isomers of $[Ru(tpy)(pynap)(OH_2)]^{2+}$," *Angew. Chem. Int. Ed*., submitted.

Solar Energy Utilization Initiative (PIs: Fujita, Muckerman, Creutz, Grills, and Cabelli)

S1. Fujita, E.; Muckerman, J. T. "Catalytic Reactions Using Transition-Metal-Complexes toward Solar Fuel Generation," (Invited Review Article) *Bull. Jpn. Soc. Coord. Chem.* **2008**, *51*, 41-54.

S2. Polyansky, D. E.; Cabelli, D.; Muckerman, J. T.; Fukushima, T.; Tanaka, K.; Fujita, E. "Mechanism of Hydride Donor Generation using a Ru(II) Complex Containing an NAD^+ Model Ligand: Pulse and Steady-State Radiolysis Studies," *Inorg. Chem.* **2008**, *47*, 3958-3968 (cover article).

S3. Creutz, C.; Chou, M. H. "Hydricities of d^6 Metal Hydride Complexes in Water" *J. Am. Chem. Soc.* **2009**, *113*, 3650-3659.

S4. Fukushima, T.; Fujita, E.; Muckerman, J. T.; Polyansky, D. E.; Wada, T.; Tanaka, K., "Photochemical Stereo-Specific Generation of a C-H hydride in a Ru Complex with an NAD^+/NADH-Type Ligand," *Inorg. Chem.*, **2009**, *48*, 11510-11512.

S5. Morris, A. J.; Meyer, G. J.; Fujita, E., "Molecular Approaches to the Photocatalytic Reduction of Carbon Dioxide for Solar Fuels," *Acc. Chem. Res.* **2009**, *42*, 1983-1994.

S6. Muckerman, J. T.; Fujita, E. "Artificial Photosynthesis" in *Chemical Evolution II: From Origins of Life to Modern Society. ACS Symposium Series*; Chapter 15, pp 283-312, Zaikowski, L.; Friedrich, J. M., Eds.; American Chemical Society: Washington, D.C., **2010**.

S7. Cohen, B. W.; Polyansky, D. E.; Zong, R.; Zhou, H.; Ouk, T.; Cabelli, D.; Thummel, R. P.; Fujita, E. "Differences of pH-Dependent Mechanisms on Generation of Hydride Donors using Ru(II) Complexes Containing Geometric Isomers of NAD^+ Model Ligands: NMR and Radiolysis Studies in Aqueous Solution," *Inorg. Chem.* **2010**, *49*, 8034-8044.

S8. Schneider J.; Fujita, E. "Carbon Dioxide Capture and Activation," *Comprehensive Inorganic*

Chemistry II, Vol. 8, Eds. Poeppelmeier K.; Reedijk, J. Elsevier, Oxford, England, submitted.

Core (CO-004) and Other DOE Sponsored Solar Photochemistry Projects

C1. Creutz, C.; Chou, M. H. "Binding of Catechols to Mononuclear Titanium(IV) and to 1- and 5-nm TiO_2 Nanoparticles" *Inorg. Chem.* **2008**, *47*, 3509-3514.

C2. Huang, K.-W.; Grills, D. C.; Han, J. H.; Szalda, D. J.; Fujita, E. "Selective Decarbonylation by a Pincer PCP-Rhodium(I) Complex," *Inorg. Chim. Acta* **2008**, *361*, 3327-3331.

C3. Cheng, T.-Y.; Szalda, D. J.; Hanson, J. C.; Muckerman, J. T.; Bullock, R. M. "Four-Electron-Donor Hemilabile η^3-PPh_3 Ligand that Binds through a C=C Bond Rather than an Agostic C−H Interaction, and Displacement of the C=C by Methyl Iodide or Water," *Organometallics* **2008**, *27*, 3785-3795.

C4. Petroski, J.; Chou, M. H.; Creutz, C. "The coordination chemistry of gold surfaces: formation and far-infrared spectra of alkanethiolate-capped gold nanoparticles" *J. Organomet. Chem.* **2009**, *694,* 1138-1143.

C5. Doherty, M. D.; Grills, D. C.; Fujita, E. "Synthesis and Photophysical Characterization of Fluorinated Re(4,4′-X_2-2,2′-bipyridine)$(CO)_3$Cl Complexes in CH_3CN and $scCO_2$," *Inorg. Chem.* **2009**, *48*, 1796-1798.

C6. Achord, P.; Fujita, E.; Muckerman, J. T.; Scott, B.; Fortman, G. C.; Temprado, M.; Xiaochen, C.; Captain, B.; Isrow, D.; Weir, J. J.; McDonough, J. E.; Hoff, C. D. "Experimental and Computational Studies of Binding of Dinitrogen, Nitriles, Azides, Diazoalkanes, Pyridine and Pyrazines to $M(PR_3)_2(CO)_3$ (M = Mo,W; R = Me, ^{i}Pr)," *Inorg. Chem.* **2009**, *48* 7891-7904

C7. Doherty, M. D.; Grills, D. C.; Muckerman, J. T.; Polyansky, D. E.; Fujita, E. "Toward More Efficient Photochemical CO_2 Reduction: Use of $scCO_2$ or Photogenerated Hydrides," *Coord. Chem. Rev.*, **2010**, *254,* 2472-2482.

C8. Grills, D.C.; Cook. A. R.; Fujita, E.; George, M. W.; Miller, J. R.; Preses, J. M.; Wishart, J. F. "Application of External-Cavity Quantum Cascade IR Lasers to Nanosecond Time-Resolved Infrared Spectroscopy of Condensed-Phase Samples Following Pulse Radiolysis," *Appl. Spec.* **2010**, *64*, 563-570 (cover article).

C9. Grills, D. C; Fujita, E. "New Directions for More Efficient Photocatalytic Reduction of CO_2: Supramolecular, $scCO_2$ or Biphasic Ionic Liquid-$scCO_2$ Systems," *J. Phys. Chem. Lett.* **2010**, *1*, 2709-2718.

C10. Chen, J.; Szalda, D. J.; Fujita, E.; Creutz, C. "Iron(II) and Ruthenium(II) Complexes Containing P, N, and H Ligands: Structure, Spectroscopy, Electrochemistry and Reactivity," *Inorg. Chem.* **2010**, *49*, 9380-9391.

C11. Creutz, C.; Chou, M. H.; Hou, H.; Muckerman, J. T. "Hydride Ion Transfer from Ruthenium(II) Complexes in Water: Kinetics and Mechanism," *Inorg. Chem.* **2010**, *49*, 9809-9822.

C12. Small, Y. A.; DuBois, D. L.; Fujita, E.; Muckerman, J. T. "Proton Management as a Design Principle for Hydrogenase-Inspired Catalysts," *Energy Environ. Sci.*, **2011**, accepted.

Session VII

Spectroscopy at Nanoparticles

Hot Carrier Interactions in Semiconductor Nanocrystals

Byungmoon Cho, Vivek Tiwari, William K. Peters, Trevor L. Courtney, Robert J. Hill, and
David M. Jonas
Department of Chemistry and Biochemistry
University of Colorado
Boulder, CO 80309-0215

Carrier multiplication is a potential route to more efficient photovoltaics, and has received considerable attention after kinetic signatures of Auger recombination were reported for single photon excitation of semiconductor quantum dots. At least three mechanisms have been proposed, and there are significant experimental disagreements for the Multiple Exciton Generation (MEG) yields. Our femtosecond experiments probing the relaxation of electronic excitation near 3 times the bandgap in lead sulfide (PbS) quantum dots show no initial bleach, in sharp contrast to quantum dot exciton states.[2,3] This suggests that the initial state prepared by a femtosecond pulse consists of fast (~1 nm/fs), spatially overlapping electron and hole wavepackets that rapidly separate into free carriers inside the nanocrystal; because the polaron radius is small for carriers with this energy in the bulk, it is likely that these free carriers scatter off phonons on a few fs timescale, as in the bulk. Efficient MEG must compete with this scattering, but no theory predicts MEG on this rapid timescale, which roughly corresponds to the rate of collisions with the nanocrystal surface.

In light of the above, it is perhaps surprising that our experiments sometimes show the signature conventionally taken to indicate MEG: for one sample, the maximum signal amplitude is twice the radiative recombination amplitude and decays with the bi-exciton lifetime (the conventional interpretation would be ~100% bi-exciton yield); for another sample, any MEG yield must be less than 10%. Parkinson has subsequently reported photocurrent carrier multiplication yields of ~85% at these energies in some PbS quantum dot samples. As there is no theoretical explanation of the observed size scaling for Auger recombination, which reverses the MEG process, something important seems to be missing from the theory.

To study new aspects of the interactions between carriers, we have carried out experiments that probe the timescale for annihilation processes among hot carriers. Sargent reported the apparent loss of carriers in excess of the maximum band edge occupancy on an unresolved time scale much faster than Auger recombination. In PbS quantum dots, the conduction and valence band edges (LUMO electrons and HOMO vacancies, respectively) are 8-fold degenerate. For a single nanocrystal that has absorbed 9 or more photons, filling of the band edge would force the excess carriers to remain in higher energy levels, which might have different Auger recombination rates. Our Auger recombination data and modeling support the hypothesis that excess carriers are rapidly annihilated.[4]

To characterize this annihilation, we have measured pump-probe signals (S) as a function of pump pulse energy (U_p) and quantified their saturation. By fitting the pump pulse energy dependence of the signal at each time delay (T) to a saturation curve,

$$S(T,U_P) = c(T)U_P \,/\, U_P + U_S(T) \ ,$$

and extrapolating the linear component,

$$L(T,U_P) = c(T)U_P / U_S(T),$$

we can extract the fraction of initially excited carriers remaining,

$$F(T,U_P) = S(T,U_P) / L(T,U_P).$$

This procedure isolates aspects of the signal that require interaction between multiple electron-hole pairs in a single quantum dot. The saturation (minimal when the probe just follows the pump) subsequently decreases the signal by ~40%.
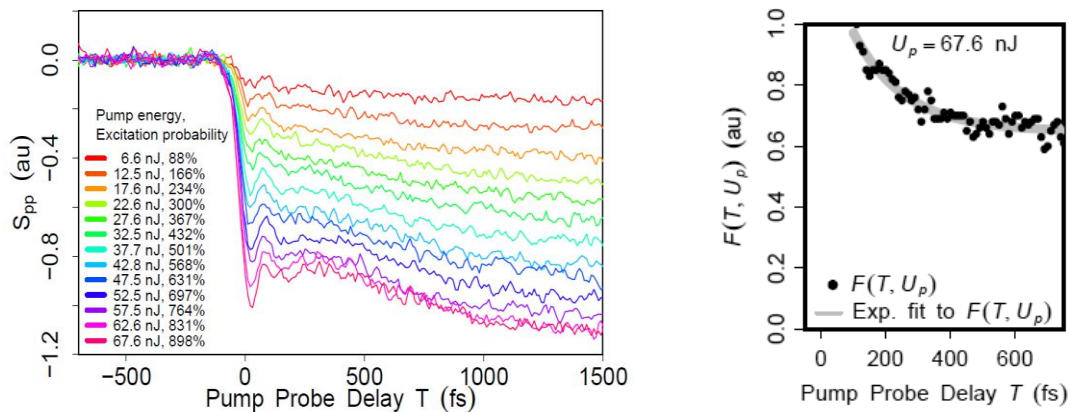
Figure 1 (left). The pump-probe signals as a function of pump energy (the excitation probability estimates are averaged over beam spatial profiles). The signals scale linearly with pump power while the pump and probe overlap in time, then saturation effects (most visible at the highest pulse energies) set in. The linear part of the signal has a risetime of 600 fs. Figure 2 (right). For about 9 excitations per dot, the fraction of photo-excited carriers decays in ~150 fs.

The hot carrier annihilation timescale of 150 fs is faster than the 600 fs timescale on which the linear component of the pump-probe signal reaches its maximum strength, which has been conventionally attributed to carrier cooling. This suggests that a very rapid Auger recombination process occurs during carrier cooling. Further, the estimated excitation probabilities suggest that hot carrier annihilation occurs within individual valleys of the band structure. This annihilation process may be the microscopic reversal of MEG (because MEG requires excess energy, it is not simply a microscopic reversal of conventional Auger recombination).

To better estimate the excitation probabilities, we are measuring the absolute strength of the pump probe signals.[5] Figure 3 compares a measurement on fluorescein in basic methanol to a calculation without any adjustable parameters. The agreement is within 5% (the discrepancy at early time arises because solvation dynamics are not included in the calculation) and indicates a shorter lifetime than literature data. Beyond accurate excitation probabilities needed for studies of hot carrier annihilation, such measurements will enable absolute tests for MEG.
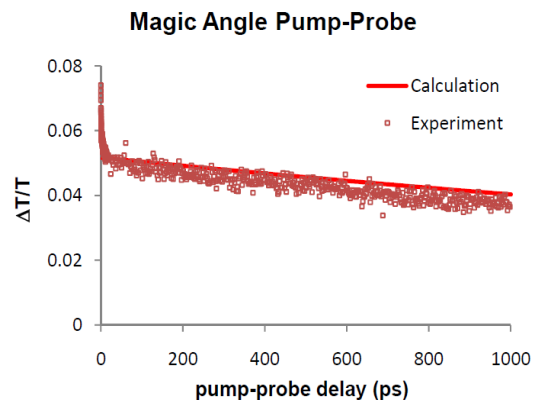
DOE Sponsored Solar Photochemistry Publications 2008-2011

1. "Spectral Restoration for Femtosecond Spectral Interferometry with Attosecond Accuracy" Michael K. Yetzbacher, Trevor L. Courtney, William K. Peters, Katherine K. Kitney, Eric Ryan Smith, and David M. Jonas, *Journal of the Optical Society of America B* **27**, 1104-1117 (2010) [DOI:10.1364/JOSAB.27.001104]. Article selected for the Virtual Journal of Ultrafast Science (June, 2010).

2. "Bulklike Hot Carrier Dynamics in Lead Sulfide Quantum Dots" Byungmoon Cho, William K. Peters, Robert J. Hill, Trevor L. Courtney, and David M. Jonas, *Nano Letters*, **10**, 2498–2505 (2010) [DOI: 10.1021/nl1010349].

3. "Hot Carrier Dynamics in Lead Sulfide Nanocrystals" Byungmoon Cho, William K. Peters, Robert J. Hill, Trevor L. Courtney, and David M. Jonas, in "*Ultrafast Phenomena XVII*" Edited by Majed Chergui, David M. Jonas, Eberhard Riedle, Robert W. Schoenlein, and Antoinette J. Taylor (Oxford University Press, 2011) pp. 266-268.

4. "Band Filling Dynamics and Auger Recombination in Lead Sulfide Nanocrystals" William K. Peters, Byungmoon Cho, Robert J. Hill, Trevor L. Courtney, and David M. Jonas, in "*Ultrafast Phenomena XVII*" Edited by Majed Chergui, David M. Jonas, Eberhard Riedle, Robert W. Schoenlein, and Antoinette J. Taylor (Oxford University Press, 2011) pp. 275-277.

5. "Absolute Measurement of Femtosecond Pump-Probe Signal Strengths" Byungmoon Cho, Vivek Tiwari, and David M. Jonas, *Applied Spectroscopy* (to be submitted).

Exciton and Charge Carrier Dynamics at Interfaces Between Quantum Dots and Metals and in Monodisperse Nanoclusters

Lars Gundlach,[1] Jianhua Bao,[1] Zhihao Yu,[1] Jason Benedict,[2] Philip Coppens,[2] Piotr Piotrowiak[1]

[1]Department of Chemistry, Rutgers University, Newark, New Jersey 07102
[2]Department of Chemistry, SUNY Buffalo, New York 14260

We employed femtosecond Kerr-gated fluorescence microscopy to investigate the mechanism of luminescence quenching and enhancement in individual CdSe/ZnS core/shell quantum dots on flat metal surfaces and in the vicinity of metal nanostructures. Hybrid quantum dot/metal nanoparticle/semiconductor substrate systems are of growing interest in solar energy conversion applications. It has been proposed, that through the coupling of the local transition dipole of a quantum dot or a molecular chromophore to the surface plasmon of a nanostructured metal, large enhancements of the absorption cross section can be achieved. Furthermore, the presence of metallic particles may facilitate charge collection and transport.

Despite this surge of interest and well-establised theories, little is known experimmntally about the ultrafast exciton dynamics at the interface between a chromophore and a metal. Efficient, essentially complete, photoluminescence quenching has been reported for quantum dots in the vicinity of metal surfaces. On the other hand, photoluminescence enhancement by as much as two orders of magnitude has been observed for quantum dots and molecular chromophores on rough metal surfaces. While the quenching process is attributed to resonant energy transfer, the mechanism for the enhancement is not yet fully understood, although it is certainly similar to the enhancement mechanism in SERS. Femtosecond photoluminescence microscopy measurements on single quantum dots are ideally suited for the study of these processes. Since the luminescence intensity can be monitored independently for individual quantum dots, the influence of the nano-environment on the enhancement vs. quenching can be probed in a highly heterogeneous environment, in which every emissive particle exhibit its own characteristic dynamics.
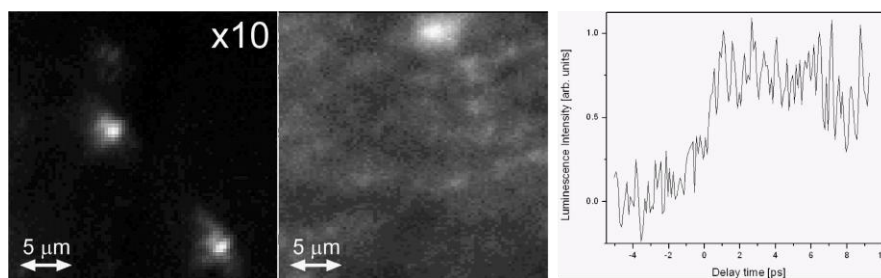
Figure 1. Luminescence images and femtosecond time-resolved luminescence of individual CdSe/ZnS core-shell quantum dots.

The first very promising results show the capabilities of our improved experimental setup which now utilizes a high repetition rate laser source (100 kHz) and individually adjustable Cassegrain objectives. Fig. 1 (left) shows a luminescence image of individual CdSe/ZnS quantum dots on flat and rough Au substrate. Fig. 1 (right) shows femtosecond time-resolved luminescence dynamics of several quantum dots on a flat Au surface. The ability to monitor femtosecond emission dynamics of individual Q-dots on metals is a significant breakthrough.

In a separate project we investigated the exciton relaxation and charge recombination dynamics in crystalline polyoxotitanate clusters Ti17Cat4 and Ti17. These materials offer a fascinating intermediate system that spans the gap between single center metal-ligand charge transfer complexes and dye-sensitized anatase nanopartcicle and mesoporous films. In contrast with colloidal anatase, they are perfectly monodisperse and form homogeneous solutions.

The Ti17 cluster, in which the surface is terminated with isopropoxy groups, is a model of a small anatase nanoparticle in which the correlated dynamics of the electron-hole pair can be investigated upon direct promotion of and electron to the conduction band. In Ti17Cat4 four surface catechol groups have been introduced. As a consequence of this modification, a charge transfer band corresponding to the injection of an electron from the HOMO orbital of the catechol moiety into the conduction band of the cluster appears in the spectrum of Ti17Cat4. We excited this band and monitored the subsequent dynamics over the entire visible range in several solvents of different polarity and viscosity.

The emerging picture suggests that the electron- hole pair in the clusters shows some behavior that is common molecular donor-acceptor systems and some characteristics more typical of dye sensitized anatase. Transient absorption depolarization data suggest that the tightly localized initial polaron undergoes rapid evolution into the fully charge-separated state. The long wavelength spectral component, which we tentatively assign to the injected, electron undergoes very fast depolarization within less than 100 fs. The short wavelength component, which is associated with the localized hole, undergoes much slower, picoseconds depolarization dynamics, suggesting thermally activated hopping between the four degenerate catechol sites. This behavior is typical of dye-sensitized colloidal anatase and dye-sensitized mesoporous films. On the other hand, it was found that the transient spectra and the depolarization dynamics of the Ti17Cat4 are solvent dependent. Such dependence on the polarity and viscosity of the medium is more characteristic of small molecule electron donor-acceptor systems in solution rather than charge injection and recombination at interfaces.

Figure 2. Tentative sequence of exciton and carrier relaxation events following photoexcitation of the charge transfer band of the Ti17Cat4 cluster.

Analogous transient absorption depolarization measurements on the unsubstituted Ti17 cluster are under way. In this case, our primary objective is to determine the degree of correlation between the electron and the hole in the small and perfectly monodisperse clusters. Indeed, it is not clear whether the exciton dissociation model applies to such small particles. It is also of interest, whether surface "trap states" in such a homogeneous system play a similar role as in the highly heterogeneous colloidal anatase.

DOE Sponsored Solar Photochemistry Publications 2008-2011

1. *Femtosecond Kerr-gated wide-field fluorescence microscopy*, L. Gundlach and P. Piotrowiak, *Opt. Lett.*, 2008, 33, 992.
   Paper subsequently selected by the editors for the June 2008 issue of the *Virtual Journal of Nanoscale Science & Technology* and the July 2008 issue of the *Virtual Journal of Ultrafast* of the APS and the AIP.

2. *Ultrafast wide-field fluorescence microscopy*, L. Gundlach and P. Piotrowiak, in *Ultrafast Phenomena XVI*, Springer Series in Chem. Physics 92, Eds. P. Corkum, S. De Silvestri, K.A. Nelson, E. Riedle, R.W. Schoenlein, Springer-Verlag, Berlin, 2009.

3. *Spatially resolved ultrafast luminescence dynamics of single nanobelts*, L. Gundlach and P. Piotrowiak, *Science in China G*, Femto IX Conference Focus Issue, Springer-Verlag, 2009.

4. *Ultrafast spatially-resolved carrier dynamics in single CdSSe nanobelts*, L. Gundlach and P. Piotrowiak, *J. Phys. Chem. C*, 2009, 113, 12162–12166, (cover page paper).

5. *Electrostatic docking of a supramolecular host-guest assembly to cytochrome-c probed by bidirectional photoinduced electron transfer,* K.I. Jankowska, C.V. Pagba, E.L. Piatnitski-Chekler, K. Deshayes and P. Piotrowiak, *J. Am. Chem. Soc.,* 2010, 132, 16423-16431.

6. *Efficiency and temporal response of crystalline Kerr media in collinear optical Kerr gating*, Z. Yu, L. Gundlach and P. Piotrowiak, submitted to *Opt. Lett.*

7. *Vibrational state dependence of electron injection at the molecule–semiconductor interface,* M. Myahkostupov, C.V. Pagba, L. Gundlach and P. Piotrowiak, submitted to *J. Am. Chem. Soc.*

8. *Fluorescence enhancement of a tolyl viologen by complexation in CB[7]*, M. Freitag, L. Gundlach, P. Piotrowiak and E. Galoppini, in preparation.

9. J. Bao, Z. Yu, J. Benedict, P. Coppens and P. Piotrowiak, in preparation.

The Crystalline Nanocluster Ti-O Phase: Synthesis of New Clusters, Their Functionalization and Properties

Philip Coppens and Jason B. Benedict
Department of Chemistry
University at Buffalo, State University of New York,
Buffalo, New York 14260-3000

In order to fill the gap in precise structural knowledge on the structure of polyoxotitanate nanoparticles as well as the mode of attachment of light-absorbing technologically relevant chromophores to the nanoparticles, a series of TiO clusters have been synthesized and functionalized. Since the products are monodisperse they can be condensed into crystalline periodic arrays suitable for atomic-resolution structure determination. Resulting knowledge of the detailed atomic arrangement allows theoretical calculations of electronic structure and dynamics and physical properties.

The complexes are synthesized by controlled hydrolysis of Ti-alkoxide precursors in suitable solvents using solution as well as solvatothermal techniques. The nature of the particles synthesized is dependent on several factors, including the Ti alkoxide precursor used, the relative concentrations of the reactants including that of oxygen supplying acetic acid, and the maximum temperature and cooling rate in the

Fig. 1. Top: Molecular structure of $Ti_{34}(DMBA)_6$ Right: Molecular packing in the crystal showing π-stacking of the ligands. Purple: Ti, red: O, blue: N, grey: C.
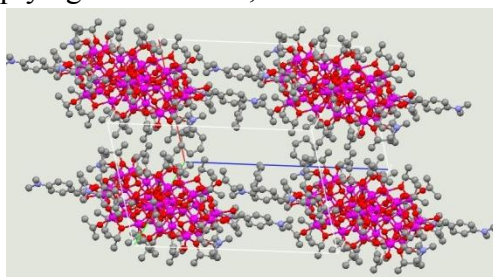
solvatothermal synthesis. Crystallization is achieved by slow evaporation, temperature reduction, and vapor diffusion. X-ray analyses show a wide variety of cluster shapes ranging from almost spherical to flattened assemblies. The largest monodisperse polyoxotitanate clusters obtained to date contain up to 34 titanium atoms. These Ti_{34} clusters are nearly 3.5 nm in diameter with a semi-conductor core of 2.2 nm.. Structures of TiO nanoparticles of this size have not been determined previously. The structure of the Ti_{34} cluster functionalized with dimethylamino benzoic acid (DMBA) is shown in Fig. 1. While the structures often exhibit features of the bulk TiO_2 polymorphs anatase, rutile and brookite, they also contain titanium under-coordination presumed to be present in and responsible for the reactivity of the surfaces of the pure phase nanoparticles. The chromophore-cluster binding modes in the structures determined so far show a dependence on the nature of the chromophore and the size of the cluster (Fig. 2). The diol catechol is found to be monodentate, bidentate and both combined bidentate and bridging (O,O, O') in the smaller clusters, but bidentate in Ti_{17}; carboxylic acid is bridging in all clusters up to Ti_{17}, both bridging (Ti_{17}-isonicotinate (INA) and -trans-cinnamate) and bidentate in Ti_{17}- and Ti_{34}-dimethylaminobenzoic acid; the acetylacetonate

linker group is bidentate in all complexes examined.
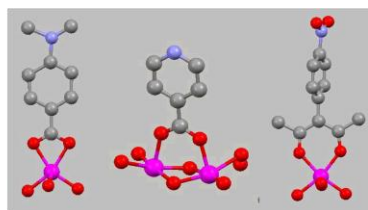
Fig. 2. Bidentate (left) and bridging (middle) binding of the carboxyl group and bidentate mode of acetyl acetonate (right).

With these results it is possible to base theoretical calculations on real structures rather than on model systems. DFT calculations on the band structure of a series of the INA and catechol functionalized nanoclusters were performed with the Gaussian03 package, the B3LYP functional and the LANL2DZ basis set. The results for INA functionalized nanoparticles are shown in Fig. 3. The HOMO-LUMO gap in the Ti_3-Ti_{17} series varies between 4.4 and 4.7 eV. It shows no clear correlation with cluster size in the clusters examined. However, increase of cluster size is accompanied by the formation of quasi-continuous conduction and valence bands (Fig. 3). Parallel spectroscopic measurements show bandgaps lower by ~10%, a difference attributed to approximations made in the DFT calculations. As a further extension of this work dynamic DFT calculations of electron injection are performed by the Yale group, initially on 4-amino- and 4-nitro- phenylacetylacetone functionalized Ti_{17}.[1] The dependence of electron injection and recombination dynamics on mode of attachment is as yet unknown.

Fig. 3 Density of state plots illustrating the band gap and evolution of quasi-valence and conduction bands with increasing cluster size.

Future work. Apart from further functionalization of the nanoparticles in collaboration with the Yale group[2] and a synthetic effort to increase TiO nanocluster size in our monodisperse samples by polymerization of the clusters already obtained, we will explore the dynamic properties by computational and time-resolved spectroscopic and crystallographic methods. Femtosecond visible transient absorption and luminescence measurements on samples of the synthesized nanoclusters are being made by Piotrowiak and coworkers.[3] Our time-resolved crystallographic methods developed at the 15-ID BIOCARS station at the Advanced Photon Source are now producing reliable atomic-resolution results with polychromatic radiation. The broader bandpass makes more efficient use of the available photons and allows collection of diffraction frames with a single synchrotron pulse, thus maximizing time resolution. Laser-pump/X-ray probe experiments on crystals of luminescent Cu(I) imines are currently underway and will be followed by experiments on TiO nanoclusters functionalized with Cu(I) chromophores. The time resolution that can be achieved at the synchrotron sources is limited to the ps range, which will in many cases be sufficient to observe structural changes due to charge separation before recombination occurs. Experiments on fs timescales are expected to become possible with methods currently being developed at LCLS, the Linac Coherent Light Source at SLAC.

---

[1] V. S. Batista, G. Brudvig, R. H. Crabtree, C. Schmuttenmaer, R. C. Snoeberger III, Chemistry Department, Yale University. This meeting.

[2] L. Allen and R. H. Crabtree, Chemistry Department, Yale University.

[3] P. Piotrowiak, Chemistry Department, Rutgers University, Newark.

DOE Sponsored Solar Photochemistry Publications 2008-2011

1. Vorontsov, I. I.; Graber, T.; Kovalevsky, A. Y.; Novozhiliva, I. V.; Gembicky, M.; Chen, Y.-S.; Coppens, P. Capturing and Analyzing the Excited-State Structure of a Cu(I. Phenanthroline Complex by Time-Resolved Diffraction and Theoretical Calculations *J. Am. Chem. Soc.* **2009**, *131*, 6566.

2. Coppens, P.; Pitak, M.; Gembicky, M.; Messerschmidt, M.; Scheins, S.; Benedict, J.; Adachi, S.-I.; Sato, T.; Nozawa, S.; Ichiyanagi, K.; Chollet, M.; Koshihara, S.-Y. The RATIO Method for Time-Resolved Laue Crystallography *J. Synchrotron Rad.* **2009**, *16*, 226.

3. Benedict, J. B.; Coppens, P. The crystalline nanocluster phase as a medium for structural and spectroscopic studies of light absorption of photosensitizer dyes on semiconductor surfaces *J. Am. Chem. Soc.* **2010**, *132*, 2938.

4. Benedict, J. B.; Freindorf, R.; Trzop, E.; Cogswell, J.; Coppens, P. Large Polyoxotitanate Clusters: Well-Defined Models for Pure-Phase TiO_2 Structures and Surfaces *J. Am. Chem. Soc.* **2010**, *132*, 13669.

5. Kaminski, R.; Graber, T.; Benedict, J. B.; Henning, R.; Chen, Y.-S.; Scheins, S.; Messerschmidt, M.; Coppens, P. Optimizing the accuracy and precision of the single-pulse Laue technique for synchrotron photo-crystallography *J. Synch. Rad.* **2010**, *17*, 479.

6. Coppens, P.; Benedict, J. B.; Messerschmidt, M.; Novozhilova, I.; Graber, T.; Chen, Y.-S.; Vorontsov, I.; Scheins, S.; Zheng, S.-L. Time-resolved synchrotron diffraction and theoretical studies of very short-lived photo-induced molecular species *Acta Cryst.* **2010**, *A 66*, 179-188.

7. Makal, A.; Trzop, E.; Sokolow, J. D.; Kalinowski, J.; Benedict, J.; Coppens, P. The development of Laue Techniques for single pulse diffraction of chemical complexes: time-resolved Laue diffraction on a binuclear-rhodium organometallic complex. *Acta Cryst.* **2011**, *in press*.

Session VIII

Dye Sensitized Systems

Electron Transfer Dynamics in Efficient Molecular Solar Cells

Shane Ardo, John Rowley, Byron Farnum, and <u>Gerald J. Meyer</u>
Departments of Chemistry and Materials Science & Engineering
Johns Hopkins University
Baltimore, MD 21210

A key objective of our Department of Energy supported research is to provide kinetic models for surface mediated photochemical processes relevant to solar energy conversion. Our emphasis has been on metal-to-ligand charge-transfer (MLCT) excited states in fluid solution and when anchored at nanocrystalline (anatase) TiO_2 and insulating ZrO_2 interfaces. Our current DOE supported work has focused on photo-induced iodide redox chemistry. This chemistry necessarily involves the utilization of light to break and form I-I bonds and is therefore of relevance to the generation of solar fuels. Iodide redox chemistry is also central to efficient electrical power generation in dye-sensitized solar cells. We have shown that I-I bonds are formed ion fluid solution by two discrete pathways and have quantified mechanistic details of this chemistry as well as I-I bond breaking chemistry. An unanticipated complication for our proposed studies of I-I bond formation at sensitized TiO_2 interfaces, was the observation that injected electrons influence the absorption spectra of surface anchored dyes though a Stark-like effect. The magnitude of the surface field has been quantified as well as the kinetics of interfacial charge „screening'.

1. Photogeneration of Iodine Atoms. Early attempts to sensitize iodide oxidation to visible light with the MLCT excited states of $Ru(bpy)_3^{2+}$ in aqueous solution revealed inefficient excited state electron transfer. This presumably resulted from the very positive $E^o(I^\bullet/I^-)$ reduction potential, $Ru(bpy)_3^{2+}*$ simply was not a strong enough oxidant. Ru(II) compounds based on 2,2'-bipyrazine (bpz), such as $Ru(bpz)_2(deeb)^{2+}$, where deeb is 4,4'-$(CO_2CH_2CH_3)_2$-2,2-
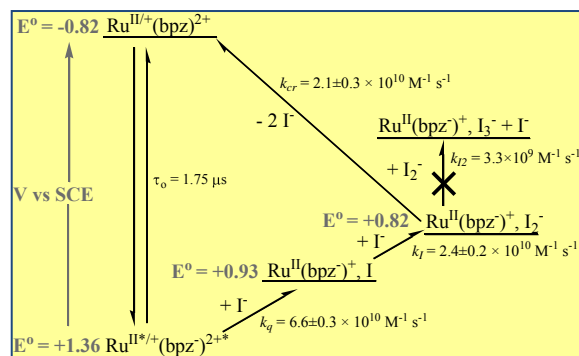
bipyridine, that are potent photo-oxidants, were found to oxidize iodide. A summary of the mechanistic details measured in CH_3CN is given in the accompanying Jablonski-type diagram. The growth of reduced ruthenium compound, $Ru(bpz^-)(bpz)(deeb)^+$, monitored by transient absorption was correlated with excited state decay indicating that it was a primary photoproduct. Diiodide appeared with a rate constant about three times slower, $k = 2.4 \times 10^{10}$ M^{-1} s^{-1}, indicating that it was not a primary photoproduct. This observation was in accord with the initial formation of an iodine atom that subsequently reacted with iodide to form the I-I bond of $I_2^{\bullet-}$. The back reaction of $Ru(bpz^-)(bpz)(deeb)^+$ with $I_2^{\bullet-}$ was significantly faster than $I_2^{\bullet-}$ disproportionation and was hence quantitative. We note also that the mechanism for I-I bond formation discovered here was distinctly different from that reported in our previous work where ion-pairs were present prior to light absorption.

2. The One-Electron Reduction of Tri-Iodide. Reactivity of I_3^- by the reduced ruthenium compound, $Ru(deeb^-)(deeb)_2^+$, revealed for the first time the product of the one-electron transfer

reduction. In a flash-quench experiment shown schematically, iodide oxidation of $Ru(deeb)_3^{2+*}$ generated $Ru(deeb^-)(deeb)_2^+$ whose reactivity with $I_2^{\bullet-}$ or I_3^- quantified on nanosecond and longer time scales. High concentrations of I_3^- allowed its reduction to be the predominate pathway. Transient absorption data confirmed that $I_2^{\bullet-}$ was a product of the one-electron reduction of triiodide. Kinetic analysis for the loss of $Ru(deeb^-)(deeb)_2^+$ and I_3^-, and the growth of $I_2^{\bullet-}$ revealed a linear dependence of the observed rate constant with triiodide concentration and yielded a self consistent second-order rate constant of 5.1×10^9 M^{-1} s^{-1} for the reduction of I_3^-. Marcus theory in the context of diffusional bimolecular reactions

allowed the reduction potential to be calculated, $E^o(I_3^-/(I_2^{\bullet-}, I^-)) = -0.34$ V vs. NHE. In calculating this reduction potential a reorganization energy ($\lambda = 1.0$ eV) and pre-exponential factor ($\nu_n \kappa_{el} = 10^{11}$ s^{-1}) were assumed. This data provided the first experimental estimate for the one-electron I_3^- reduction potential that was significantly less favored than the accepted reduction potential in water. This helps explain why I_3^- escapes the nanocrystalline TiO_2 thin films so efficiently: Reduction of I_3^- by electrons TiO_2 trap states is endothermic by over 100 mVs.
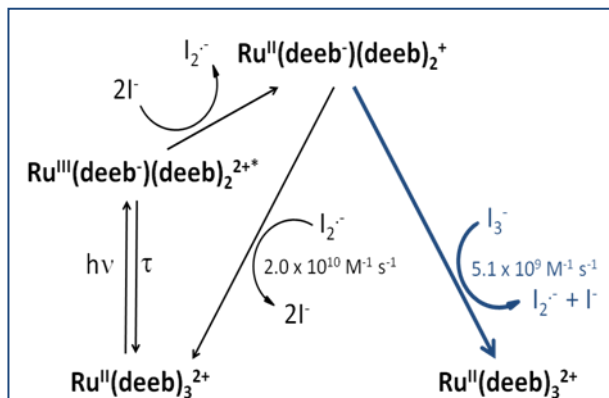
3. Stark Effects at Sensitized TiO$_2$ Interfaces. Photophysical studies of Ru(II) sensitizers anchored to mesoporous nanocrystalline TiO_2 thin films immersed in CH_3CN solutions revealed previously unrecognized behavior that accompanied excited state injection due to an underlying Stark effect. Electrons injected into TiO_2 from excited states or with a forward bias influence the absorption spectrum of dye molecules anchored to the surface. Spectral modeling as well as studies of films sensitized with two different Ru(II) compounds demonstrated that the electric field created by excited-state injection from one sensitizer influenced the absorption spectra of other sensitizers that had not undergone photo-induced electron injection. With some
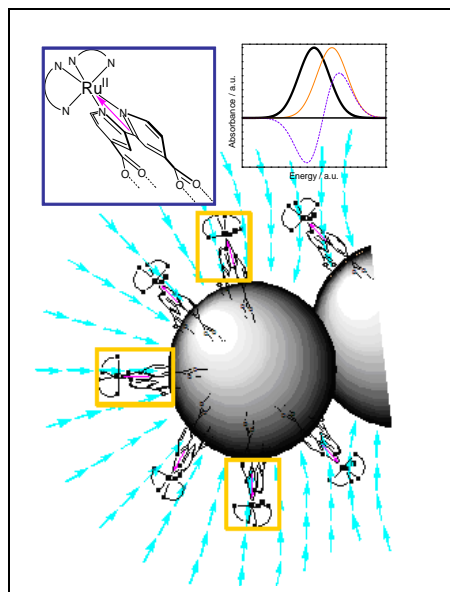
assumptions, the field strength was determined to be 2.7 MV/cm. The amplitude of the Stark effect decreased over time periods where charge recombination was absent, behavior attributed to "screening" of the electric field by interfacial ionic reorganization. The screening kinetics were non-exponential but were well described by the Kohlrausch–Williams–Watts model, from which a characteristic rate constant of 1.5×10^5 s^{-1} was abstracted. Due to the fixed orientation of the surface electric field relative to the sensitizer dipole, the influence on the absorption spectra were well modeled as a first-derivative of the dye absorption spectrum as is shown schematically. This differs significantly from the 2nd-derivative simulations of Stark spectra reported previously for Ru(II) diimine compounds randomly oriented with respect to the laboratory electric field.

DOE Sponsored Solar Photochemistry Publications 2008-2011

1. **Evidence for Iodine Atoms as Intermediates in the Dye Sensitized Formation of I-I Bonds.** Gardner, J.M.; Giaimuccio, J.M.; Meyer, G.J. *J. Am. Chem. Soc.* **2008**, *130*, 17252-17253.

2. **Slow Cation Transfer Follows Sensitizer Regeneration at TiO$_2$ Interfaces.** Staniszewski, A.; Ardo, S.; Sun, Y.; Castellano' F.N.; Meyer, G.J. *J. Am. Chem. Soc.* **2008**, *130*, 11586-11587.

3. **Halide Coordination to Zinc Porphyrin Sensitizers Anchored to Nanocrystalline TiO$_2$.** Morris, A.J.; Marton, A.; Meyer, G.J. *Inorg. Chem.* **2008**, *47*, 7681-7685.

4. **TiO$_2$ Surface Functionalization to Control the Density of States.** Morris, A.J.; Meyer, G.J. *J. Phys. Chem. C.* **2008**, *112*, 18224-18231.

5. **Photodriven Heterogeneous Charge Transfer with Transition-Metal Compounds Anchored to TiO$_2$ Semiconductor Surfaces**. Ardo, S.; Meyer, G.J. *Chem. Soc. Rev.* **2009**, *38*, 115-164.

6. **Large Footprint Pyrene Chromophores Anchored to Planar and Colloidal Metal Oxide Thin Films**. Thyagarajan, S.; Galoppini, E.; Persson, P.; Giaimuccio, J.M.; Meyer, G.J. *Langmuir* **2009**, *25*, 9219-9226.

7. **Meta-Substituted Ru^{II} Rigid Rods for Sensitization of TiO$_2$.** Abrahamsson, M.; Taratula, O.; Persson, P. Galoppini. E.; Meyer, G.J. *J. Photochem. & Photobiol, A:Chemistry* **2009**, *206*, 155-163.

8. **Visible Light Generation of Iodine Atoms and I-I Bonds: 1) Sensitized Iodide Oxidation, and 2) Tri-iodide Photodissociation.** Gardner, J.M.; Abrahamsson, M.; Farnum, B.; Meyer, G.J. *J. Am. Chem. Soc.* **2009**, *131*, 16206-16214.

9. **Reduction of I$_2$/I$_3^-$ by Titanium Dioxide.** Rowley, J.; Meyer, G.J. *J. Phys. Chem C* **2009**, *113*, 18444-18447.

10. **Molecular Approaches to the Photocatalytic Reduction of Carbon Dioxide for Solar Fuels.** Morris, A.J.; Meyer, G.J.; Fujita, E. *Acc. Chem. Res.* **2009**, *42*, 1983-1994.

11. **Stark-like Effects after Excited State Interfacial Electron Transfer at Sensitized TiO$_2$ Nanocrystallites.** Ardo, S.; Staniszewski, A.; Sun, Y.; Castellano' F.N.; Meyer, G.J. *J. Am. Chem. Soc.* **2010**, *132*, 6696-6709.

12. **Decreased Interfacial Charge Recombination Rate Constants with N3-type Sensitizers.** Abrahamsson, M.; Kopecky, A.; Johansson, P.G.; Galoppini. E.; Meyer, G.J. *J. Phys. Chem. Lett.* **2010**, *1*, 1725-1728.

13. **Direct Observation of Photo-Initiated Hole Transfer: Self-Exchange and Catalyst Oxidation Reactions Between Molecules Anchored to Metal-Oxide Nanocrystallites.** Ardo, S.A.; Meyer, G.J. *J. Am. Chem. Soc.* **2010**, *132*, 9283-9285.

14. **The Flash-Quench Technique Employed to Study the One Electron Reduction of Triiodide in Acetonitrile: Evidence for a Diiodide Reaction Product.** Farnum, B.H.; Gardner, J.M.; Meyer, G.J. *Inorg. Chem.* **2010**, *49*, 10223–10225.

15. **Iodide Chemistry in Dye-Sensitized Solar Cells: Making and Breaking I-I Bonds for Solar Energy Conversion.** Rowley, J.G.; Farnum, B.H.; Ardo, S.; Meyer, G.J. *J. Phys. Chem. Lett*. **2010**, *1*, 3132 - 3140.

16. **The 2010 Millenium Technology Grand Prize: Dye Sensitized Solar Cells.** Meyer, G.J. *ACS Nano* **2010**, *4*, 4337-4343.

17. **Excited-State Electron Transfer from Ruthenium Polypyridyl Compounds to Metal-Oxide Nanocrystallites: Evidence for a Stark Effect.** Ardo, S.; Staniszewski, A.; Sun, Y.; Castellano, F.N.; Meyer, G.J. *J. Phys. Chem. B* **2010**, *114*, 14596–14604. (Invited article for a special issue dedicated to Professor M. Wasielewski).

18. **Sensitization of TiO$_2$ by the MLCT Excited State of Co(I) Coordination Compounds.** Achey, D.; Ardo, S.A.; Xia, H.-L.; Siegler, M.A.; Meyer, G.J. *J. Phys. Chem. Lett*. **2011**, *2*, 305-308.

19. **Homoleptic Star-Shaped Ru(II) Complexes.** Zhang, Y.; Galoppini, E.; Johansson, P.G.; Meyer, G.J. *Pure & Appl. Chem.* **2011**, *83*,861-868.

20. **Di- and Tri- Iodide Reactivity at Illuminated Titanium Dioxide Interfaces.** Rowley, J.G.; Meyer, G.J. *J. Phys. Chem. C* **2011**, *in press.*

21. **Influence of Ion Pairing on the Oxidation of Iodide by MLCT Excited States.** Farnum, B. H.; Gardner, J. M.; Marton, A.; Narducci-Sarjeant, A. A.; Meyer, G. J. *Dalton Trans.* **2011**, *in press.*

22. **Slow Photoinduced Charge Transfer from Star-Shaped Ruthenium Polypyridyl Nanostructures Anchored to Mesoporous TiO$_2$ Thin Films.** Johansson, P.G.; Zhang, Y.; Abrahamsson, M.; Meyer, G.J.; Galoppini, E., *Chem. Comm.* **2011**, *in press.*

Interfacial Photochemical Processes in Sensitized Nanostructured Electrodes

Arthur J. Frank, Kai Zhu, Nathan R. Neale, Adam F. Halverson,
Jin Young Kim and Song-Rim Jang
Chemical and Materials Science Center
National Renewable Energy Laboratory
Golden, Colorado 80401

We are conducting basic studies to understand the primary factors that determine the charge-carrier dynamics and light-harvesting properties of sensitized nanostructured electrodes. Some recent issues addressed include determining photoelectrochemical (PEC) properties of nanotube (NT) arrays sensitized with a conformal semiconductor layer, the effects of thermally induced structural changes on charge-carrier dynamics and light harvesting, and the impact of charge-collection efficiencies and dark energy-loss processes on photoenergy conversion. These studies are summarized below.

Atomic Layer Deposition of a semiconductor as a sensitizer for TiO$_2$ NT Arrays. **(**Collaborators: S.M. George, CU-Boulder, C.M. Elliott, CSU) Covering the large surface area of nanoporous TiO$_2$ films with a conformal semiconducting layer is more difficult than covering the surface with discrete dye molecules. Simply soaking TiO$_2$ films in solutions containing the appropriate dye can lead to high dye coverage. ALD conditions for depositing a conformal film of In$_2$S$_3$ onto the surface of TiO$_2$ NTs and the PEC properties of the resulting films were investigated. SEM and energy dispersive X-ray analysis imaging revealed that In$_2$S$_3$ covered the full length of the NTs uniformly. PEC characterization of the In$_2$S$_3$ ALD-sensitized TiO$_2$ NT arrays with a Co^{2+}/Co^{3+} electrolyte showed only a small quantum efficiency (~10%), which was attributable to charge-injection and collection losses.

Effects of Annealing Temperature on the Morphology and Electron Dynamics in Oriented TiO$_2$ Nanotube Arrays. Modifying the nanostructure morphology (e.g., reducing disorder, changing the size and shape of the pores and crystallites) can significantly affect the light-harvesting,
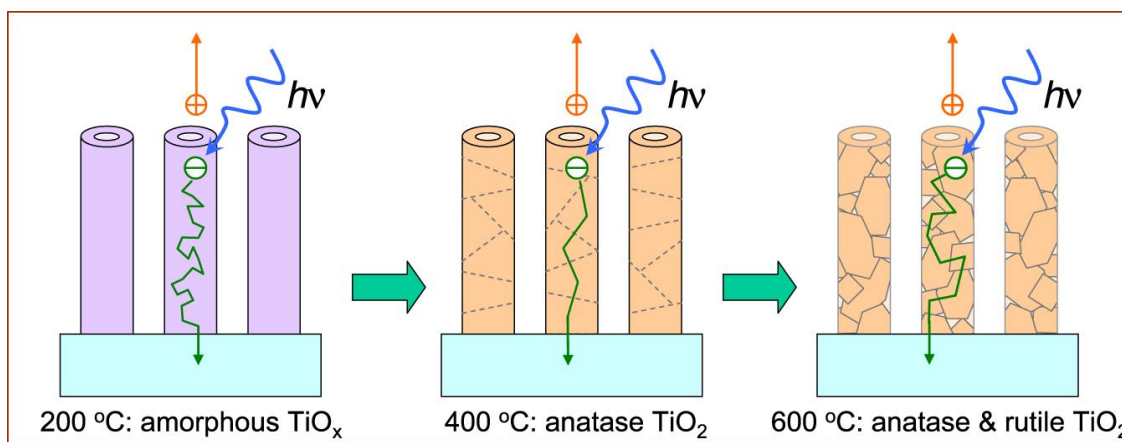
Fig. 1 Effects of thermally induced structural changes in TiO$_2$ nanotube arrays on electron transport properties

charge-injection, and charge-collection properties. A simple way to alter the morphology of titanium oxide NT arrays is to vary the annealing temperature T_a. We examined the influence of annealing temperature on the morphology of NT films and the consequences of those changes on the electron dynamics and PEC properties of dye-sensitized solar cells (DSSCs) (Fig. 1). Elevating T_a from 200 to 600 $^{\circ}$C alters the crystallinity, crystal phase, and structural integrity of the NTs while having relatively little effect on the overall film architecture. Changes in the NT structure strongly affect electron transport and recombination in distinct ways. These structural changes also affected the light-harvesting, charge-injection, and charge-collection properties. DSSCs with NT films having the highest morphological order displayed the highest light-to-energy conversion characteristics.

Transparent TiO$_2$ Nanotube photoelectrodes. High solar conversion efficiencies require that the incident light enters a DSSC from the photoelectrode side. However, it has been synthetically challenging to prepare transparent TiO$_2$ NT electrodes by directly anodizing Ti metal films on transparent conducting oxide (TCO) substrates because of the difficulties of controlling the synthetic conditions. We developed a general synthetic method for fabricating TiO$_2$ NT films on TCO substrates. With the aid of a conducting Nb-doped TiO$_2$ (NTO) layer between the Ti film and TCO substrate, the Ti film was anodized completely without degrading the TCO. The NTO layer was found to protect the TCO from degradation through a self-terminating mechanism by arresting the electric field-assisted dissolution process at the NT-NTO interface. The illumination geometry was found to strongly alter the transport times, incident photon-to-current conversion efficiency, and PEC properties of the DSSCs.

Charge-Collection Efficiencies and Dark Energy-Loss Processes in DSSCs. Electron transport through the TiO$_2$ network is incredibly slow, ranging from milliseconds to seconds, depending on the light intensity or photoelectron density. However, even with these long transit times, recombination of electrons with redox species in the electrolyte can be so slow that at short circuit essentially all of the photoinjected electrons reach the collecting electrode. We were interested in determining whether the charge-collection efficiency (η_{cc}) is still high from short circuit to open circuit, as suggested in the literature, and, more importantly, the impact of a high η_{cc} on the performance of DSSCs. Toward that end, we investigated the effect of the η_{cc} and dark energy-loss processes in determining the *J–V* characteristics of DSSCs. Both dark and light processes were found to be important in governing the *J–V* properties.

DOE/BES Sponsored Publications 2008-2011

1. "Impact of High Charge-Collection Efficiencies and Dark Energy-Loss Processes on Transport, Recombination, and Photovoltaic Properties of Dye-Sensitized Solar Cells" Zhu, K.; Jang, S.-R.; Frank, A.J. *J. Phys. Chem. Lett.* **2011**, ASAP (DOI: 10.1021/jz200290c).

2. "General Strategy for Fabricating Transparent TiO_2 Nanotube Arrays for Dye-Sensitized Photoelectrodes: Illumination Geometry and Transport Properties" Kim, J.Y.; Noh, J.H.; Zhu, K.; Halverson, A.D.; Neale, N.R.; Park, S Hong, K.S.; Frank, A.J. *ACS Nano*. **2011**, ASAP (DOI: 10.1021/nn200440u).

3. "Oriented nanotube-based dye- and semiconductor-sensitized solar cells: light harvesting, charge-carrier dynamics, and fabrication" Zhu, K.; Frank, A.J. *MRS Bulletin.* **2011**, accepted for publication.

4. "Recent Advances in Sensitized Solar Cells," Frank, A.J. In *WOLEDs and Organic Photovoltaics: Recent Advances and Application*; Yam, V.W.W., Ed; Spring-Verlag Berlin Heidelberg 2010, pp. 153–168.

5. "In_2S_3 Atomic Layer Deposition and Its Application as a Sensitizer on TiO_2 Nanotube Arrays for Solar Energy Conversion" Sarkar, S.K.; Kim, J.Y.; Goldstein, D.N.; Neale, N.R.; Zhu, K.; Elliott, C.M; Frank, A.J.; George, S.M. *J. Phys. Chem. C.* **2010,** *114,* 8032–8039.

6. "Effects of Annealing Temperature on the Charge-Collection and Light-Harvesting Properties of TiO_2 Nanotube-Based Dye-Sensitized Solar Cells" Zhu, K.; Neale, N.R.; Halverson, A.F.; Kim, J.Y.; Frank, A.J. *J. Phys. Chem. C.* **2010**, *114*, 13433–13441.

7. "Constructing Ordered Sensitized Heterojunctions: Bottom-up Electrochemical Synthesis of p-type Semiconductors in Oriented *n*-TiO_2 Nanotube Arrays" Wang, Q.; Zhu, K.; Neale, N.R.; Frank, A.J. *Nano Lett.* **2009**, *9*, 806–813.

8. "Synthesis of CdSe-TiO_2 Nanocomposites and Their Applications to TiO_2 Sensitized Solar Cells" Kim, J.Y.; Choi, S.B.; Noh, J.H.; Yoon, S.H.; Lee, S.; Noh, T.H.; Frank, A.J.; Hong, K.S. *Langmuir* **2009,** *25*, 5348–5351.

9. "Temporal Evolution of the Electron Diffusion Coefficient in Electrolyte-Filled Mesoporous Nanocrystalline TiO_2 Films" van de Lagemaat, J.; Zhu, K.; Benkstein, K. D.; Frank, A. J. *Inorg. Chim. Acta* **2008**, *361*, 620–626. (Invited paper, Michael Grätzel commemorative issue)

Metal-to-Ligand Charge Transfer Excited States on Surfaces and in Rigid Media. Application to Energy Conversion

Thomas J. Meyer and John M. Papanikolas
Department of Chemistry
University of North Carolina at Chapel Hill
Chapel Hill, N.C. 27599-3290

Photophysical Properties and Reactivity of MLCT Excited States in PEG-DMA Films

The photophysical properties of MLCT excited states of PF_6^- and other salts of $[Ru(NN)_3]^{2+}$ and $[Os(NN)_3]^{2+}$ (NN = 2,2'-bpy, 1,10-phenanthroline, 4,4'-divinyl-2,2'-bpy (vbpy), and others) have been investigated in the polymerizable fluid PEG-DMA550 (polyethylene glycol dimethacrylate; n = 7, see below) and in films following photo- or thermal polymerization. Spectroscopic measurements show that the vinyl groups in $Ru(vbpy)_3^{2+}$ are incorporated into the polymerized vinyl network.

PEG-DMA
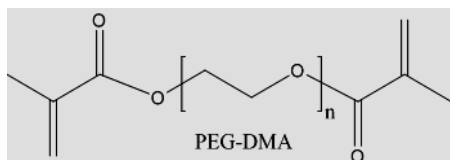
In the cross-linked films, emission maxima and lifetimes are enhanced due to a rigid medium effect. Considerable insight into film-complex interactions has been obtained by a combination of emission lifetime and emission spectral fitting studies. The results are consistent with a relatively rigid film environment with loss of medium dipole reorientation and, for $Ru(phen)_3^{2+}$, with specific interactions with the polar ester functional groups. Based on studies with a series of Os(II) polypyridyl complexes, it has been shown that nonradiative decay is dictated by energy gap law behavior over an extended energy range.

MLCT excited states retain their energy and electron transfer reactivity in the rigid PEG-DMA550 environment. Excited state quenching occurs with relatively high concentrations (10-100 mM) of added quenchers. With $Ru(bpy)_3^{2+}*$ as the excited state, reductive electron transfer quenching occurs with added tetramethyl benzidine (TMB), $Ru(bpy)_3^{2+}* + TMBD \rightarrow Ru(bpy)_3^+ + TMBD^+$, and oxidative quenching with added 2,5-di-tert-butyl-1,4-benzoquinone (Q), $Ru(bpy)_3^{2+}* + Q \rightarrow Ru(bpy)_3^{3+} + Q^-$, as shown by steady state emission, transient emission, and transient absorption measurements. Energy transfer occurs with high concentrations of added anthracene or diphenylanthracene, (An), $Ru(bpy)_3^{2+}* + An \rightarrow Ru(bpy)_3^{3+} + {}^3An$. Studies are currently under way exploring the distance dependence of electron and energy transfer quenching and of back electron transfer. We are also exploring long-range, long timescale redox storage with added traps.

Antenna and Catalytic Effects in Polymeric Films on TiO_2

Composite structures of $Ru(bpy)_2(4,4'-(PO_3H_2)_2bpy)^{2+}$ surface-bound to nanocrystalline TiO_2 with an overlayer of $Ru(bpy)_3^{2+}$ ion exchanged into Nafion, $FTO|nanoTiO_2$-$[Ru(bpy)_2 (4,4'-(PO_3H_2)_2bpy)]^{2+}$/Nafion,$Ru(bpy)_3^{2+}$ (FTO = fluorine-doped tin oxide), have been prepared and characterized. Steady-state emission and time-resolved lifetime measurements demonstrate that energy transfer occurs from Nafion,$Ru(bpy)_3^{2+}*$ to adsorbed $Ru(bpy)_2(4,4'-(PO_3H_2)_2bpy)^{2+}$ with

an efficiency of ~0.49, Figure 1. Energy transfer sensitizes photoinjection by the adsorbed MLCT excited state by an "antenna effect."
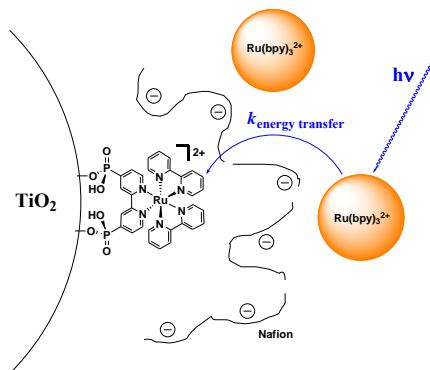
Figure 1. Antenna sensitized injection at FTO|nanoTiO$_2$-[Ru(bpy)$_2$(4,4′ (PO$_3$H$_2$)$_2$bpy)]$^{2+}$/Nafion,Ru(bpy)$_3^{2+}$ (FTO = fluorine-doped tin oxide)

Experiments are currently underway exploring the use of film overlayers to stabilize surface bonding and for the incorporation of catalysts for water oxidation and CO$_2$ reduction.

ATR-IR Analysis of Oxide Surfaces and Interfaces

We have designed an experiment to gain detailed structural information at photo- and/or electroactive oxide/molecule/solution interfaces based on attenuated total reflectance infrared spectroscopy (ATR-IR). The experiment is based on a Bruker Optics, model Vertex 80v IR spectrophotometer and an adapted multiple-pass ATR accessory (Pike Technologies, model HATR). With this instrument we are monitoring infrared spectral changes for ruthenium polypyridyl dyes bound to sintered nanocrystalline TiO$_2$ during surface binding and under a variety of conditions: under illumination, with applied potentials, and with pH and solvent changes. A clear understanding of how the dye-metal oxide interface changes structurally under redox change and with operating device conditions is an important prerequisite for further modification and optimization of DSSCs and DSPECs.
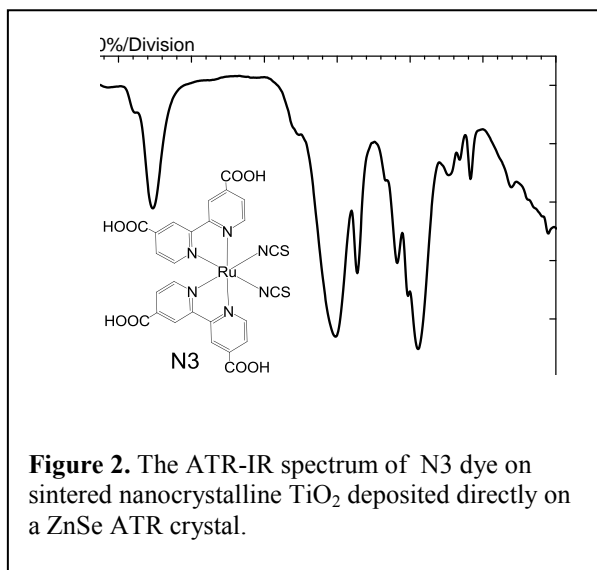
Figure 2. The ATR-IR spectrum of N3 dye on sintered nanocrystalline TiO$_2$ deposited directly on a ZnSe ATR crystal.

An ATR-IR spectrum of N$_3$ dye under nitrogen on a ZnSe crystal coated with TiO$_2$ loaded with N3 dye (inset Figure 2) is shown in Figure 2. The spectrum reveals intense (>40% transmittance) bands for the dye, thiocyano groups at ~2100 cm^{-1} and bpy ring modes at (~1300-1700 cm^{-1}) in agreement with previously published results for N3 on TiO$_2$.

DOE Sponsored Solar Photochemistry Publications 2008-2011

1. Interfacial Electron Transfer Dynamics Following Laser Flash Photolysis of $[Ru(bpy)_2((4,4'-PO_3H_2)_2bpy)]^{2+}$ in TiO_2 Nanoparticle Films in Aqueous Environments. Brennaman, M.K.; Patrocinio, A.O.T.; Song, W.; Jurss, J.W.; Concepcion, J.J.; Hoertz, P.G.; Traub, M.C.; Murakami Iha, N.Y.; Meyer, T.J.; *Chem Sus Chem*, **2011** (In Press - Available Online)

2. Structural and pH Dependence of Excited State PCET Reactions Involving Reductive Quenching of the MLCT Excited State of $[Ru^{II}(bpy)_2(bpz)]^{2+}$ by Hydroquinones. Forbes, M.; Stanton, I.; Concepcion, J.J.; Brennaman, M.K.; Therien, M.; Lebedeva, N.; Schmidt, R; Meyer, T.J. *J. Phys. Chem. A*. **2011** (In Press)

3. Influence of the Fluid-to-Film Transition on Photophysical Properties of MLCT Excited States in a Polymerizable Dimethacrylate Fluid. Knight, T.E.; Goldstein, A.P.; Brennaman, M.K.; Cardolaccia, T.; Pandya, A.; DeSimone, J.M.; Meyer, T.J.; *J Phys Chem B.* **2011**, *115*, 64-70.

4. Excited-State Dynamics in fac-$[Re(CO)_3(Me_4phen)(L)]^+$. Patrocinio, A.O.T.; Brennaman, M.K.; Meyer, T.J.; Murakami Iha, N.Y. *J. Phys. Chem. A* **2010**, *114*, 12129–12137.

5. Theory of Hydride-Proton Transfer (HPT) Carbonyl Reduction by $[Os^{III}(tpy)(Cl)(NH=CHCH_3)(NSAr)]$. Ess, D.H.; Schauer, C.K.; Meyer, T.J. *J. Am. Chem. Soc.* **2010**, *46*, 16318-16320

6. Application of High Surface Area Tin-Doped Indium Oxide Nanoparticle Films as Transparent Conducting Electrodes. Hoertz, P.G.; Chen, Z.; Kent, C.A.; Meyer, T.J.; *Inorg. Chem.* **2010** *49*, 8179–8181

7. Using the Voids. Evidence for an Antenna Effect in Dye-Sensitized Mesoporous TiO_2 Thin Films. Hoertz, P.G.; Goldstein, A.; Donley, C.; Meyer, T.J. *J. Phys. Chem. B*, **2010,** ASAP **DOI:** 10.1021/jp103867j

8. Integrating proton coupled electron transfer (PCET) and excited states. Gagliardi, C.J.; Westlake, B.C.; Kent, C.A.; Paul, J.J.; Papanikolas, J.M.; Meyer, T.J. *Coord. Chem. Rev.* **2010** *254*, 2459-2471,

9. Mechanism of Water Oxidation by Single-Site Ruthenium Complex Catalysts. Concepcion, J.J.; Tsai, M.-K.; Muckerman, J.T.; Meyer, T.J. *J. Am. Chem. Soc.,* **2010,** *132*, 1545–1557.

10. Oxidation by Single-Site Ruthenium Catalysts. Concepcion, J. J.; Jurss, J. W.; Norris, M.R.; Chen, Z.; Templeton, J.L.; Meyer, T.J. *Inorg. Chem.* **2010**, *49*, 1277–1279.

11. Concerted O Atom-Proton Transfer in the O---O Bond Forming Step of Water Oxidation. Chen, Z.; Concepcion, J.J.; Hu, X.; Yang, W.; Hoertz, P.G.; Meyer, T.J. *Proc. Nat. Acad. Sci.*, **2010**, *107*, 7225-7229.

12. Surface Catalysis of Water Oxidation by the Blue Ruthenium Dimer. Jurss, J.W.; Concepcion, J.J.; Norris, M.R.; Templeton, J.L.; Meyer,T.J. *Inorg. Chem.,* **2010**, *49, 3980-3982*

13. Making Oxygen with Ruthenium Complexes. Concepcion J.J.; Jurss,J.J.; Brennaman, M.K., Hoertz; P.G.; Patrocinio, A.O.T.; Murakami Iha, N.Y.; Templeton, J.L.; and Thomas J. Meyer. *Acc. Chem. Res.* **2009,** *42*, 1954-1965.

14. Catalytic Water Oxidation by Single-Site Ruthenium Catalysts. Concepcion,J.J.;Jurss,J.W.; Norris,M.R.; Chen,Z.; Templeton,J.L.; and Meyer,T.J. *Inorg. Chem.* **2010**, *49*, 1277-1279.

15. Single-Site, Catalytic Water Oxidation on Oxide Surfaces. Chen,Z; Concepcion,J.J.; Jurss,J.W.; Meyer,T.J. *J. Am. Chem. Soc.* **2009**, *131*, 15580-15581.

16. Catalytic and Surface-Electrocatalytic Water Oxidation by Redox Mediator–Catalyst Assemblies. Concepcion,J.J; Jurss,J.W.; Hoertz,P.G.;Meyer,T.J. *Angew. Chem. Int. Ed.* **2009**, *48*, 9473-9476.

17. Efficient, Long-Range Energy Migration in Ru^{II} Polypyridyl Derivatized Polystyrenes in Rigid Media. Antennae for Artificial Photosynthesis." Fleming,C.M.;Brennaman,M.K.; Papanikolas,J.M.; Meyer,T.J. *Dalton Trans*. **2009**, 3903-3910.

18. One Site is Enough. Catalytic Water Oxidation by $[Ru(tpy)(bpm)(OH_2)]^{2+}$ and $[Ru(tpy)(bpz)(OH_2)]^{2+}$. Concepcion, J. J.; Jurss, J. W.; Templeton, J. L.; Meyer, T. J. *J. Am. Chem. Soc.*, **2008**, *130*, 16462–16463.

19. Mediator-Assisted Water Oxidation by the Ruthenium "Blue Dimer" *cis,cis*-$[(bpy)_2(H_2O)RuORu(H_2O)(bpy)_2]_4$. Concepcion, J. J.; Jurss, J. W.; Templeton, J. L.; Meyer, T. J. *PNAS* **2008** *105*, 17632-17635.

Session IX

Donors and Acceptors

Structural Control of Excited State Properties:
from Complexes to Dye Sensitizer Mimics

Lin X. Chen,[1,3] Jenny V. Lockard,[1] Michael W. Mara,[1,3] Andrew B. Stickrath,[1] Xiaoyi Zhang,[2] Jier Huang,[1] Nosheen Gothard,[3] Karen Mulfort,[1] David M. Tiede[1]

[1]Chemical Sciences and Engineering Division, [2]X-ray Science Division,
Argonne National Laboratory, Argonne, Illinois 60439
[3]Department of Chemistry, Northwestern University, Evanston, Illinois 60208

Transition metal complexes play important roles and have even more important impact in current and future solar energy conversion and utilization when the first row transition metal complexes are utilized. A significant fraction of their functions in solar energy conversion are determined by their excited state properties that in turn can be controlled by the structures of the complexes. Because their importance as building blocks light sensitizers and molecular framework for solar energy conversion, we have been investigating excited state structures and properties of an array of Cu(I) diimine complexes with different coordination environments and structural constraints with transient optical and X-ray spectroscopies. The long term goal of these projects are aiming at understanding structural factors in controlling energy and electron flow in the excited states of these complexes for solar energy conversion processes. Specific research projects are outlined below:

1. Excited structural properties of Cu(I) diimine complexes modulated by structural constraints
The dihedral angle between the two aromatic ligands has been observed to change excited state properties significantly, including lifetimes and emission quantum yields. In our previous studies on $[Cu(I)(dmp)_2]^+$, three time constants of sub-ps, ~10 ps and ns were revealed for the excited state dynamics in coordinating and non-coordinating solvents. There has been controversy on the origins of the two fast components and whether a pseudo tetrahedral or flattened tetrahedral conformation will extend the excited state lifetime of singlet and triplet states due to the complication of multiple processes involved in the photoexcitation and decay pathways. A series of Cu(I) bis-phenanthroline complexes with different pheripheral groups at 2,9 positions has been investigated as shown in Figure 1a. In one serie on the left, the 2.9 positions attaches increasingly bulky groups intended to apply steric constraints to lock to the dihedral angle between the phenanthroline ligand planes into 90º. In another series on the right of Figure 1a, the dihedral angle is locked into a flattened geometry. These structural modifications result in the potential energy surface alterations shown in Figure 1b.
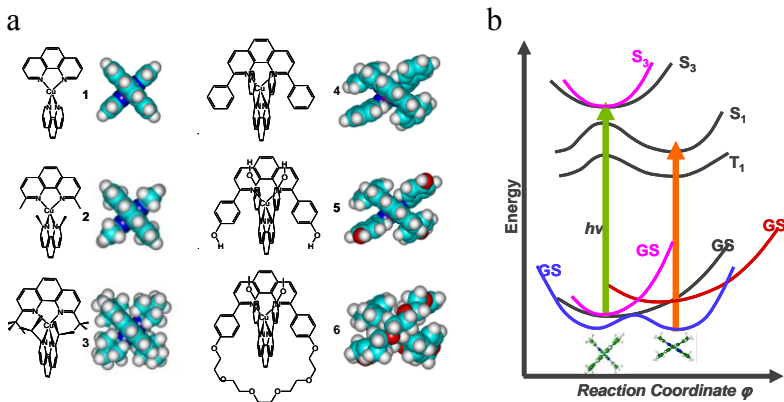

Figure 1. a) Structures of Cu(I) diimine complexes studied; 2) the potential surfaces of the ground and excited states as functions of the dihedral angle between the two phenanthroline ligands.

A systematic ultrafast transient optical spectroscopic studies have been carried out on these complexes, where we obsered that 1) the Jahn-Teller distortion that caused by the MLCT transition shiting electron density from the copper(I) center to the ligands is indeed the flattening of the dihedral angle because this component is absent when the orthogonal geometry is locked; 2) the intersystems crossing time constant is not significantly affected by the geometry as previsouly thought, and 3) the emission quantum yield can be significantly affected by slight change in steric hindrance even in non-coordinating solvents. These findings allow rational design for Cu(I) diimine complexes as dye-sensitizers for solar cells, the area that we are currently exploring.

2 Transient structural studies of Cu(I) diimine complexes in different solvents and with and without an electron acceptor Complementary to the dynamics studies, we carried out a series of transient structural studies on Cu(I)bis-2,9-diphenylphenanthroline, or $[Cu(I)(dpp)]^+$ and water soluble Cu(I)bis-2,9-dimethylphenanthrolinesulfonate, or $[Cu(I)(dmpS)_2]^+$ in different solvents and in presence of methylviologen, MV, as an electron acceptor. The results revealed that the initial MLCT state takes upto 400 ps to form the exciplex with coordinating solvent even though the flattening of the structure is present in both the ground and excited states almost immeiately after the formation of the MLCT state (Figure 2). X-ray transient absorption measurement with fs resolution has been proposed to be carried out in the LCLS in the fall after the initial commisioning experiments where fs XANES spectra of a testing molecule $[Fe(II)(bpy)_3]^{+2}$ has been observed at the LCLS.
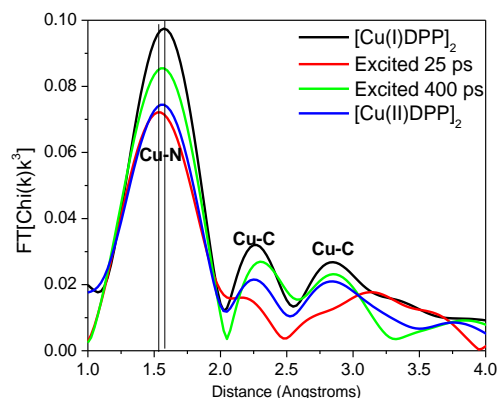
Figure 2. The structural evolution in the excited states of $[Cu(I)(dpp)_2]^+$, where distinct structural difference for the singlet/triplet state without the ligation at ~25 ps delay and with the ligation at ~400 ps delay are observed.

3. Transient structural studies of a dye sensitized solar cell mimic, RuN3 dye on TiO2 nanoparticle surfaces Transient RuN3 dye structures on TiO_2 nanoparticles as solar cell mimics have been carried out using X-ray transient absorption spectroscopy (XTA) (Figure 3). The transient structure after the charge injecting revealed an electron relay mechanism where the initially electron rich Ru-NCS moiety shifts electron density to dcbpy [bis(4,4'-dicarboxy-2,2'-bipyridine] that are directly linked to TiO_2 in the excited state, but the net electron density in Ru-dcbpy moiety is unchanged from that of the ground state. Hence the significant structural changes take place only in Ru-N(NCS) bonds not Ru-N(dcbpy) bonds. This is the first transient X-ray structure captured in the interfacial system.
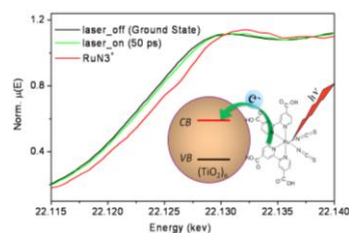
Figure 3. X-ray transient absorption of RuN3 dye on the surface of TiO_2 nanoparticles.

DOE Sponsored Publications 2008 – 2011

1. Local structure of photoexcited bimetallic complexes refined by quantitative XANES analysis, G. Smolentsev, S. E. Canton, J. V. Lockard, V. Sundstrom and L. X. Chen, Proceedings of the 37th International conference on Vacuum Ultraviolet and X-ray Physics, *Journal of Electron Spectroscopy and Related Phenomena*, in press (2011)

2. Current trends in the optimization of low bandgap polymers used in photovoltaic devices, Jodi M. Szarko and Lin X. Chen, Invited highlight article, *J. Mat. Chem.* in press (2011)

3. Coherence in Metal-Metal-to-Ligand-Charge-Transfer Transitions of a Dimetallic Complex Revealed by Ultrafast Transient Absorption Anisotropy, Sung Cho, Michael W. Mara, Xianghuai Wang, Jenny V. Lockard, Aaron A. Rachford, Felix N. Castellano, Lin X. Chen, *J. Phys. Chem. A.,* dx.doi.org/10.1021/jp109174f (2011)

4. Length-Dependent Self-Assembly of Oligothiophene Derivatives in Thin Films: Implications in Photovoltaic Material Fabrications, Brian S. Rolczynski1, Jodi M. Szarko1, Byeongdu Lee, Joe Strzalka, Jianchang Guo, Yongye Liang, Luping Yu and Lin X. Chen, *J. Mat. Chem.* **26**, 296-305 (2011).

5. Visualizing interfacial charger transfer in dye sensitized nanoparticles using X-ray transient absorption spectroscopy, Xiaoyi Zhang, Grigory Smolentsev, Jiancang Guo, Klaus Attenkofer, Chuck Kurtz, Guy Jennings, Jenny V. Lockard, Andrew B. Stickrath, and Lin X. Chen, *J. Phys. Chem. Lett.* dx.doi.org/10.1021/jz200122r (2011)

6. When Function Follows Form: Effects of Side-Chains in Conjugated Copolymers on Film Morphology and BHJ Solar Cell Performance, Jodi M. Szarko, Jianchang Guo, Yongye Liang, Byeongdu Lee, Brian S. Rolczynski, Joe Strzalka, Tao Xu, Stephen Loser, Tobin Marks, Luping Yu, Lin X. Chen, *Advanced Materials*, **22**, 5468–5472 (2010).

7. Triplet Excited State Distortions in a Pyrazolate Bridged Platinum Dimer Measured by X-ray Transient Absorption Spectroscopy, Jenny V. Lockard, Aaron Rachford, Xiaohuai Wang, Grigory Smolentsev, Xiaoyi Zhang, Klaus Attenkofer, Guy Jennings, Alexander V. Soldatov, Arnold L. Reinhard, Felix Castellano, Lin X. Chen, *J. Phys. Chem. A.,* **114***,* 12780–12787 (2010).

8. Metalloporphyrin Ligation Mechanisms Revealed by Transient X-ray Absorption Spectroscopy, Lin X. Chen, Xiaoyi Zhang, Erik C. Wasinger, Jenny V. Lockard, Klaus Attenkofer, and Guy Jennings, Grigory Smolentsev, Alexander Soldatov, *Chemical Sciences*, **1**, 642-650 (2010)

9. Room Temperature Light Emittion from the Low-Dimensional Semiconductors AZrPS6 (A = K, Rb, Cs), Santanu Banerjee, Jodi M. Szarko, Ben Yuhas, Christos D. Malliakas, Lin X. Chen, Mercouri G. Kanatzidis, *J. Am. Chem. Soc.,* **132**, 5348–5350 (2010).

10. Electronic Processes in Conjugated Diblock Oligomers Mimicking Low Band-gap Polymers: Experimental and Theoretical Spectral Analysis, Jodi M. Szarko, Brian S. Rolczynski, Jianchang Guo, Yongye Liang, Feng He, Michael W. Mara, Luping Yu, Lin X. Chen, *J. Phys. Chem. B*, **114**, 742–748 (2010).

11. Influence of Ligand Substitution on Excited State Structural Dynamics in Cu(I) bis-phenanthroline Complexes, Jenny V. Lockard, Sanaz Kabehie, Grigory Smolentsev, Alexander Soldato, Jeffrey I. Zink and Lin X. Chen, *J. Phys. Chem. B.* **114**, 14521–14527 (2010).

12. Structure, Dynamics, and Power Conversion Efficiency Correlations in a New Low Bandgap Polymer: PCBM Solar Cell, Jianchang Guo, Yongye Liang, Jodi Szarko, Byeongdu Lee, Hae Jung Son, Brian S. Rolczynski, Luping Yu, Lin X. Chen, *J. Phys. Chem. B* **114**, 742–748 (2010).

13. Dye-Sensitized Solar Cells: Sensitizer-Dependent Injection into ZnO Nanotube Electrodes, Rebecca A. Jensen, Hal Van Ryswyk, Chunxing She, Jodi M. Szarko, Lin X. Chen, Joseph T. Hupp, *Langmuir* **26**, 1401–1404 (2010).

14. Taking Molecular Snapshots in Disordered Media with X-ray Transient Absorption Spectroscopy: A Decade and Beyond, Lin X. Chen, Xiaoyi Zhang, Jenny V. Lockard, Andrew Stickrath, Klaus Attenkofer, Guy Jennings, Di-Jia Liu, *Acta Cryst.* **A66**, 240–251 (2010).

15. Picosecond Structural Dynamics at the Advanced Photon Source, A. Grigoriev; P. G. Evans; M. Trigo; D. Reis; L. Young; R. W. Dunford; E. P. Kanter; B. Krässig; R. Santra; S. H. Southworth; L. X. Chen; D. M. Tiede; K. Attenkofer; G. Jennings; X. Zhang; T. Graber; K. Moffat, *Synchrotron Radiation News*, **23**, 18 – 25 (2010).

16. Applications of X-ray Transient Absorption Spectroscopy in Photocatalysis for Hydrogen Generation, Lin X. Chen, in "Solar Hydrogen and Nanotechnology", Wiley, Chapter 7 (2010).

17. Highly Sensitive and Selective Gold(I) Recognition by a Metalloregulator in Ralstonia metallidurans Xing Jian, Erik C. Wasinger, Jenny V. Lockard, Lin X. Chen, and Chuan He, *J. Am. Chem. Soc.* **131**, 10869–10871 (2009).

18. Application of XANES spectroscopy to study local structure of photoexcited Cu complex Grigory Smolentsev, Galina Sukharina, Alexander V. Soldatov, Lin X. Chen, *Nuclear Instruments and Methods in Physics Research A* **603**, 122–124 (2009).

19. Revealing Structural Dynamics in Catalytic Reactions Using Ultrafast Transient X-ray Absorption Spectroscopy, Lin X. Chen and Dijia Liu, *Synchrotron Radiation News*, **22**, 17-21 (2009).

20. Effect of Regioregularity and Molecular Weights of Low Band Gap Polymers on the Bulk Hetero-junction Solar Cell Efficiency, Yongye Liang, Danqin Feng, Jiangchang Guo, Jodi M. Szarko, Claire Ray, Lin X. Chen and Luping Yu, *Macromolecules*, **42**, 1091–1098, (2009).

21. Photoinduced Electron Transfer of Conjugated Linear Donor-Acceptor Dyad in Solution and Films, Jianchang Guo, Yongye Liang, Shengqiang Xiao, Jodi Szarko, Michael Sprung, Mrinmay K. Mukhopadhyay, Jin Wang, Luping Yu, and Lin X. Chen. *New J. Chem.* **33** 1497-1507 (2009).

22. XANES analysis of structural changes in a transient photoexcited state of metalloporphyrin, S. Della-Longa, L. X. Chen, P. Frank, K. Hayakawa, K. Hatada, M. Benfatto, *Inorg. Chem.* **48,** 3934-3942 (2009).

23. An investigation of the electron and energy transfer between oligothiophenes and thieno[3,4-b]thiophene units, Jodi Szarko, Jianchang Guo, Yongye Liang, Shengqiang Xiao, Brian Rolczynski, Luping Yu and Lin X. Chen, PHYSICAL CHEMISTRY OF INTERFACES AND NANOMATERIALS VII, *SPIE Proceedings*, **7034,** 3403-3411 (2008)

24. Novel Zinc Phthalocyanine-Benzoquinone Rigid Dyad and Its Photoinduced Electron Transfer Properties, Chi-Hang Lee, Jianchang Guo, Lin X. Chen, Braja. K. Mandal, *J. Org. Chem.,***73,** 8219–8227 (2008)

25. Three-dimensional local structure of photoexcited Cu(I) diimine complex refined by quantitative XANES analysis, Grigory Smolentsev, Alexander V. Soldatov, Lin X. Chen, *J. Phys. Chem. A,* **112**, 5363–5367 (2008)

26. Discovery of Native Metal Ion Sites Located on the Ferredoxin Docking Side of Photosystem I, Lisa M. Utschig, Lin X. Chen, Oleg G. Poluektov, *Biochemistry* **47,** 3671–3676 (2008).

27. Selective Photocatalytic Decomposition of Nitrobenzene Using Surface Modified TiO_2 Nanoparticles, Donald Cropek, Patricia A. Kemme, Olga V. Markova, Lin X. Chen, Tijana Rajh, *J. Phys. Chem. C,* **112**, 8311–8318 (2008).

28. Aligned carbon nanotubes with built-in FeN_4 active sites for electrocatalytic reduction of oxygen, Junbing Yang, Di-Jia Liu, Nancy N. Kariuki and Lin X. Chen, *Chem. Comm.* 329-331(2008).

29. X-ray absorption spectroscopic characterization of the Compound II intermediate produced by reaction of a cytochrome P450 enzyme with peroxynitrite, J. Halgrimson, J. Horner, M. Newcomb, Erik C. Wasinger, Lin X, Chen, Sligar, *Proc. Natl. Acad. Sci. USA,* **105***, 8179-8184* (2008).

Metal-Linked Artificial Peptides as Photoinitiated Molecular Wires & Antennas

Carl P. Meyers, Joy A. Gallagher, Seth E. Ostheimer, Mary Elizabeth Williams
Department of Chemistry
The Pennsylvania State University
University Park, PA 16802

Self-assembly of biomacromolecules creates complex structures capable of performing the functions necessary for life. Synthetic supramolecular analogs of biological electron transfer cascades may ultimately lead to molecular photocatalysts, solar fuel production, etc. A challenge is to build large structures capable of long range, sequential electron transfers that are robust and versatile. To address the challenge of achieving the complexity needed to rival biological systems, we construct inorganic complexes with a mole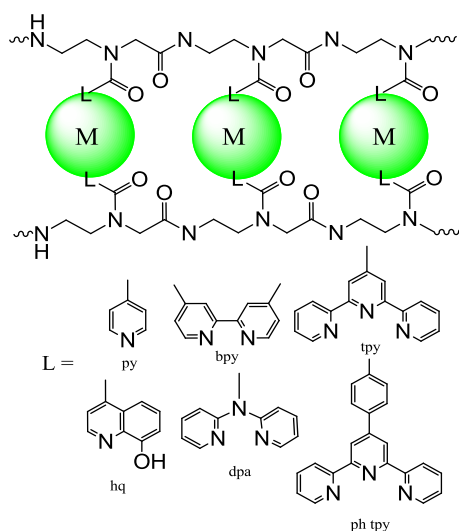cular design that mimics two of the prevalent strategies in nature: self-assembly by molecular recognition, and the use of modular amino acid units to form larger polyamide structures.

Figure 1. Top: schematic representation of coordinative crosslinks (ML$_2$) between two ligand-substituted polyamide strands. Bottom: structures the ligands that are installed on the aminoethylglycine backbone.

Our architectures are constructed using metal-coordination-based molecular recognition between chains built from easily interchangeable aminoethylglycine (aeg) units, such as shown in Figure 1. This molecular design provides a unique approach toward creating and varying model structures with which to study photo-induced charge separation and the structure-dependent function. In analogy to natural systems, our structures are distinctive because the oligopeptide provides a scaffold but not electronic coupling. Careful selection of metal complexes and optimization of the peptide-linked architecture provide the opportunity to create structures capable of multi-electron processes such as those required for artificial photosynthesis. Our long range aims are to use metal induced assembly of modular artificial peptides to build architectures with a high level of functionality that enables energy and electron transfer cascades leading to catalytic processes.

We have initially focused on using pyridine-based ligands, however any ligand bearing an acetic acid attachment point can be used in this motif. Extension to long, polyfunctional chains with straightforward and sequential amide coupling steps is a major advantage of this approach. This presentation describes our work during this initial project period, during which our goals were to develop strategies for using the modular units of
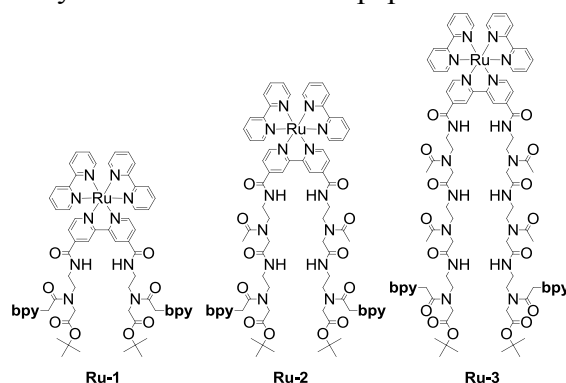

Figure 2. Structures of the Ru hairpin complexes with a single metal crosslinking site
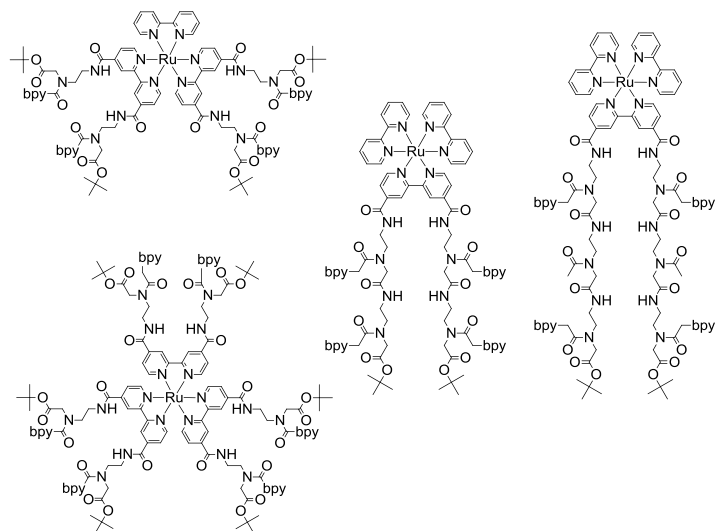
Figure 3. Ru complexes containing multiple pendant bpy sites for metal ion binding, made by either extension of the aeg backbone or heteroleptic substitution of the Ru complex.

ligand-substituted aeg amino acids to make heterometallic and heterofunctional assemblies linked by artificial oligopeptides, and to use spectroscopic methods to understand the mechanisms of energy and electron transfer in these model peptide duplexes.

A major aim of the project period was to develop methods by which heterometallic structures could be assembled. Figure 2 contains the structures of the first series of Ru complexes that were made: in each, two artificial oligopeptide strands substituted with free bpy ligands were attached via amides to one ligand of $[Ru(bpy)_3]^{2+}$. Ligand binding of the Cu^{2+} ions results in heterometallic structures with varying distance between the metal complexes. By comparison of the electrochemistry and time-dependent emission data, we observed only a shallow decrease in k_{nr} with increasing distance between the Ru and Cu complexes, and slightly higher rates in analogous trimetallic structures. The compiled data suggested an excited state electron transfer mechanism, and we have undertaken additional work to more fully understand this, including changing the bound metal ion, the solvent, and extensive NMR analysis of the solution structure. We also used the flexibility of the oligopeptide design to construct larger assemblies such as those shown in Figure 3 to investigate the photodynamics of tri- and tetrametallic architectures.

A second goal was to synthesize and investigate alternative aeg sequences that control the geometry of the assembled structure by preventing the formation of parallel and antiparallel isomers. To accomplish this we developed the structural motif in Figure 4, a polyamide backbone with two (ester protected) acid termini. The first tripeptide contained three pendant bpy ligands and with these we demonstrated that electronic interactions between adjacent $[Cu(bpy)_2]^{2+}$ crosslinks was determined by their anion-dependent geometries. Tripeptides 2 and 3 were made to investigate molecular recognition between two dissimilar strands; we have shown that these selectively form heteroduplexes (containing one of each strand) using either Cu^{2+} or Pt^{2+}.
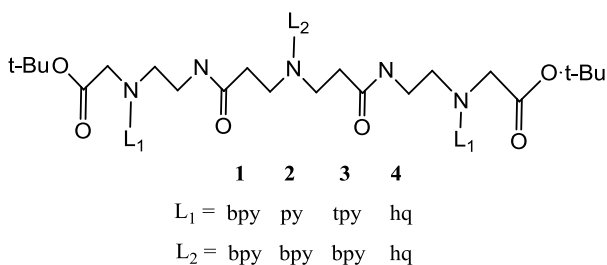
Figure 4. Series of four artificial tripeptides with "palindromic" structure

Using what we have learned, our ongoing investigations are focusing on modifications to the tunable polyamide structures to improve the distance and lifetime of charge separation. These structural variations aim to create redox cascades, optimize structural rigidity to enforce electron transfer distances and pathways, and insert redox sites that prevent back electron transfer.

DOE Sponsored Solar Photochemistry Publications 2008-2011

1. Myers, C.P.; Miller, J. R.; Williams, M. E. "$[Ru(bpy)_3]^{2+}$ with Pendant Oligo(aminoethyglycine): Variation of the Number of Chains to Form Multimetallic Structures with Cu(II) and Pd(II)", **2011** revision submitted

2. Myers, C.P.; Williams, M. E. "Directed Self-Assembly of Inorganic Redox Complexes with Artificial Peptide Scaffolds" *Coord. Chem. Rev.* **2010**, *254*, 2416 – 2428.

3. Myers, C. P.; Miller, J. R ; Williams, M. E. "Impacts of the Location and Number of $[Cu(bpy)_2]^{2+}$ Crosslinks on the Emission Photodynamics of $[Ru(bpy)_3]^{2+}$ with Pendant Oligo(aminoethylglycine) Chains" *J. Am. Chem. Soc.* **2009,** *42***,** 15291 – 15300.

4. Gallagher, J. A.; Levine, L.A.; Williams, M. E. "Anion-Dependent Electronic Coupling in Cu Crosslinked Palindromic Artificial Tripeptides with Pendant Bpy Ligands", **2011** submitted

5. Myers, C. P.; Showalter, S. A.; Lin, P.; Williams, M. E. "NMR and DFT Investigations of the Solution Structure of Ru-Zn Complexes Tethered by Oligo(aminoethylglycine) Chains" **2011** submitted

6. Ostheimer, S. E.; Myers, C. P.; Miller, J. R.; Williams, M. E. "Metal Bis(bpy) Complexes Tethered to $[Ru(bpy)_3]^{2+}$ with Pendant Oligo(aminoethyglycine) Control Excited State Relaxation" in preparation

Posters

"Electrochemically Wired" Semiconductor Nanoparticles: Toward Vectoral Electron Transport In Hybrid Materials

Neal R. Armstrong, S. Scott Saavedra, Jeffry Pyun
Department of Chemistry & Biochemistry
University of Arizona
Tucson, Arizona 85721

Our research has focused on three areas: A) photo-electrochemical processes of semiconductor nanocrystals (SC-NCs) capped with electroactive ligands, tethered to polymer hosts; B) potential modulated attenuated total reflectance (PM-ATR) on waveguide substrates probing the energetics and rates of electron transfer to/from sub-monolayer SC-NC films; C) development of oxide nanoparticle materials in which noble metals (Au, Pt) have been incorporated. Our focus is now progressing toward creation and characterization of aligned nanocrystal and nanorod arrays, modified to create compositional and energetic asymmetry, creating a "Type II heterojunction" format, capable of efficient photoelectrochemical fuel formation (Figure (A) at right).

i) We have shown that we can characterize the frontier orbital energies of CdSe and related NCs on conductive substrates, using both high vacuum photoemission spectroscopies, and waveguide-based spectroelectrochemical studies in solution. Recent studies suggest that the interactions between adjacent NCs on these substrates play an important role in determining the apparent E_{CB} and E_{VB} energies; *ii)* We have shown that we can form magnetically aligned oxide nanoparticles, and that these NPs can be further modified with Au or Pt nanoparticles to enhance their electrocatalytic activity; *iii)* We have demonstrated that we can create asymmetric CdSe nanorods, tipped at only one end with catalytic nanoparticles (either oxide or metal) – the next step is the creation of aligned arrays of these new materials.

We have recently focused on formation and characterization of LB films of CdSe NCs, probing their optical properties as we compress the array, and horizontally transfer monolayer to multilayer films. Figure (B) at right shows the blue-shift in the absorbance features for the LB film, suggesting that NC-NC interactions and NC-water interactions significantly impact on band energies for these materials. Figure (C) demonstrates that we can transfer compact NC monolayers to thin P3HT polymer films, while Figure (D) shows control of LB film thickness using on-trough absorbance to monitor film growth – Figure (E) (SEM and AFM images) shows that horizontal transfer of multilayer films leads to interesting textured NC multilayers, which exhibit the kind of pyramidal structures expected from incomplete, layer-by-layer growth of multilayer films.
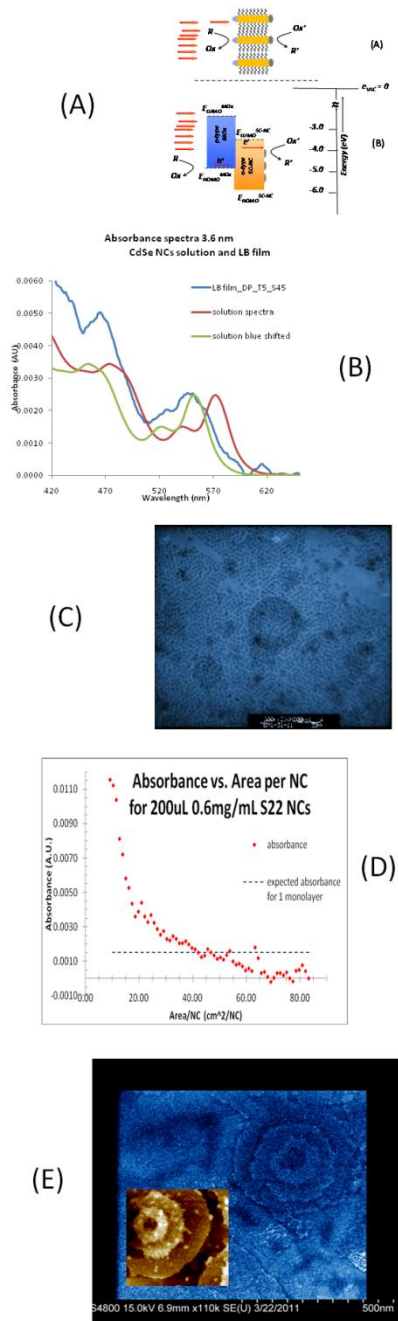
Electronic Structure of Ground and Charge Transfer Excited States
of Porphyrin-Fullerene Dyads

Rajendra R. Zope, Marco Olguin and <u>Tunna Baruah</u>
Department of Physics
University of Texas at El Paso
El Paso, TX 79912

The combination of porphyrins and fullerenes is one of the most extensively studied organic donor-acceptor pairs. The porphyrin system acts as a photosensitizer. Various factors which contribute to the electron-transfer efficiency and the lifetime of the charge-separated state are the donor-acceptor distance and relative orientation, electronic coupling, linker, and the nature of the bonding interaction between the fullerene and porphyrin systems. The fullerene is often linked to the porphyrin through a variety of linker molecules but the final structure often shows a pi-pi stacking between the flat porphyrin surface and the curved fullerene surface. There are also reports of systems in which the fullerene and porphyrins are deposited on surfaces through chemical vapor deposition but no covalent bond exists between these components. We have considered such four different non-bonded porphyrin-fullerene (P-F) dyads with Zn and base tetra-phenyl-porphyrin (ZnTPP/TPP) combined with C_{60} or C_{70} fullerenes. The purpose is to study the changes in ground and excited state electronic structure when the P or F component is changed. We have used our excited state method, previously shown to work well for charge transfer excited states, to calculate the charge transfer excitation energies for these systems. Some

Transition	C60/TPP	C70/TPP	C60/ZnTPP	C70/ZnTPP
H-2 → L+2	1.70*	1.81*	2.08	2.31
H-2 → L+1	1.67*	1.74*	2.09	2.38
H-2 → L	1.72*	1.75*	2.08	2.42
H-1 → L+2	2.01	2.38	2.12	2.23
H-1 → L+1	2.02	2.39	2.12	2.24
H-1 → L	1.97	2.46	2.12	2.28
H → L+2	1.75	2.08	1.69	1.98
H → L+1	1.76	2.05	1.68	1.95
H → L	1.75	2.13	1.69	1.99

Table 1: Energies of CT states of the P-F dyads in eV.

of the charge transfer states are depicted in Fig.1 and the calculated excited state energies for the four dyads are given in Table I. The ground state of the P-F dyads shows interfacial dipole moments. Figure 2 shows dipole moments as a function of P-F surface-to-surface distance.
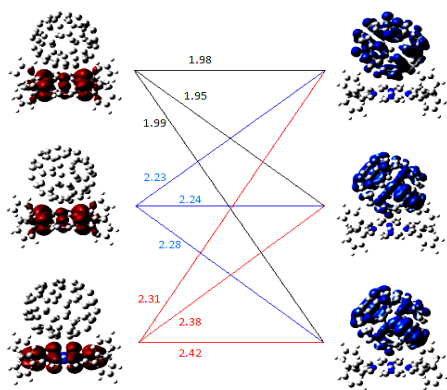

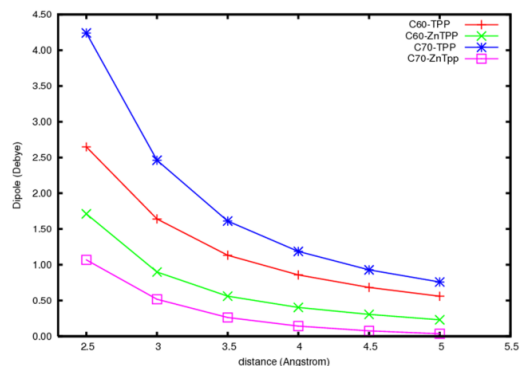Fig.1: Charge transfer states for C60/TPP dyads

Fig.2: Ground state dipoles as a function of P-F surface-to-surface separation.

Interfacial Electron Transfer in Sensitized TiO$_2$ Nanocrystals

Robert C. Snoeberger III[1], Laura J. Allen[1], Becky Millot[1], Jason Benedict[2], Philip Coppens[2], Gary W. Brudvig[1], Charles A. Schmuttenmaer[1], Robert H. Crabtree[1] and Victor S. Batista[1]

[1]Department of Chemistry, Yale University, New Haven, Connecticut, 06520-8107
[2]Department of Chemistry, University at Buffalo The State University of New York, Buffalo, NY 14260-3000

The development of inexpensive, robust, and efficient photocatalytic materials for water oxidation and CO$_2$ reduction would allow the sustainable production of fuel from renewable resources. We review our recent progress in the field, with emphasis on computational studies on characterization of catalytic surfaces based on sensitized TiO$_2$ nanocrystals. Theoretical work has been integrated with synthesis, electrochemistry and spectroscopy (X-ray, THz, EPR, UV-vis, NMR, ESM) in an interdisciplinary effort to advance our understanding of structure/function relations in well-characterized nanocrystals. The resulting insight is valuable for the design of novel photocatalytic materials for solar fuel production.
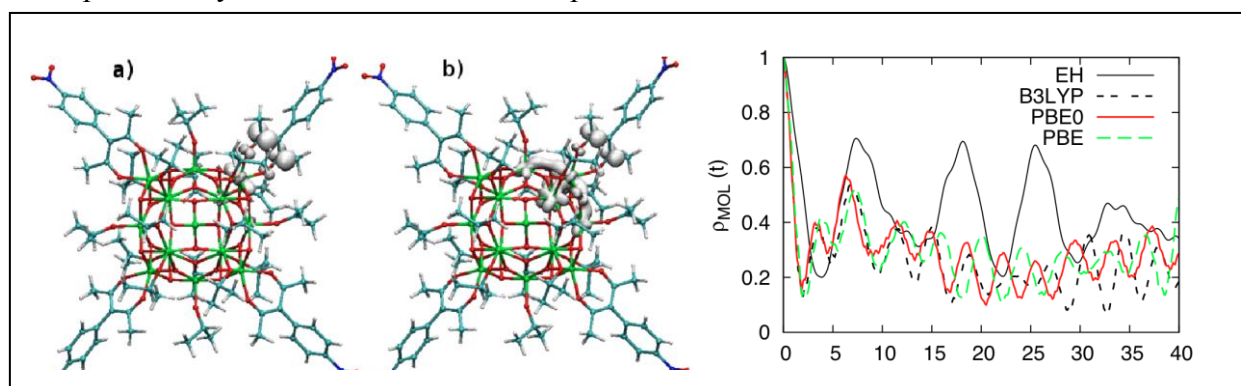
Figure 1. Left: Instantaneous snapsots of electronic densities at 0 fs (a) and 6 fs (b) after excitation of nitrophenylacac (NPA) adsorbed on a crystalline [Ti$_{17}$O$_{24}$(OPri)$_{20}$] nanocluster [Ti$_{17}$(μ_4-O)$_4$(μ_3-O)$_{16}$(μ_2-O)$_4$(NPA)$_4$(OPri)$_{16}$]. Right: Time-dependent adsorbate population as described by extended-Hüeckel (EH) and DFT wave packet propagtion, using B3LYP, PBE0 and PBE functionals.

References

1. R. C. Snoeberger III, L. J. Allen, J. Benedict, B. Millot, G. W. Brudvig, C. A. Schmuttenmaer, R. H. Crabtree, P. Coppens and V. S. Batista. In prep (2011), Interfacial Electron Injection in Sensitized TiO$_2$ Nanoclusters.

2. Chantelle L. Anfuso, R. C. Snoeberger, III, A. M. Ricks, W. Liu, D. Xiao, V. S. Batista, and T. Lian, *J. Am. Chem. Soc.* (2011) in press, Covalent Attachment of a Rhenium CO$_2$-Reduction Catalyst to Rutile TiO$_2$.

3. R. da Silva, L. G. C. Rego, J. A. Freire, J. Rodriguez, D. Laria and V. S. Batista. *J. Phys. Chem. C* (2010) 114:19433-19442. Study of Redox Species and Oxygen Vacancy Defects at TiO$_2$-Electrolyte Interfaces.

4. T. Wang, G. W. Brudvig and V. S. Batista. *J. Chem. Theory Comput.* (2010) 6:2395-2401. Study of proton coupled electron transfer in a biomimetic dimanganese water oxidation catalyst with terminal water ligands.

5. V. S. Batista, R. H. Crabtree (Ed), Wiley, Chichester. Inorganic Chemical Aspects (2010) pp. 191-198. Some Computational Challenges in Energy Research.

6. G. Li, E. M. Sproviero, W. R. McNamara, R. C. Snoeberger III, R. H. Crabtree, G. W. Brudvig, and V. S. Batista. J. Phys. Chem. B (2010) 114:14214-14222. Reversible Visible-Light Photooxidation of an Oxomanganese Water-Oxidation Catalyst Covalently Anchored to TiO$_2$ Nanoparticles.

7. L. G. C. Rego, R. da Silva, J. A. Freire, R. C. Snoeberger and V. S. Batista. *J. Phys Chem. C* (2010) 114:1317-1325. Visible light sensitization of TiO$_2$ surfaces with Alq3 complexes.

High-Potential Photoanodes for Light Induced Water Oxidation

Gary F. Moore, Rebecca L. Milot, Lauren Martini, James D. Blakemore, Lawrence Cai, Victor S. Batista, Charles A. Schmuttenmaer, Robert H. Crabtree, and <u>Gary W. Brudvig</u>
Department of Chemistry
Yale University
New Haven, CT 06520-8107

Artificial photosynthesis is a long-sought goal in solar energy research.[1] By splitting water into O_2 and a fuel such as H_2, two problems are addressed: energy storage and the production of a potential transport fuel.[2,3] We have recently reported a water splitting photocell that uses a specially designed photoanode to which are attached both a high potential porphyrin dye for light absorption and a Cp*-iridium catalyst for water oxidation in the presence of an applied bias voltage.[4] Recent efforts in our group have focused on improving the robustness and ease of assembly of our photochemical system. Modification of the anchoring groups used for surface attachment and perturbation of the electronic properties of the light-absorbing complex has been investigated. Preliminary results indicate that these modifications allow for operation of the system with zero bias voltage and no UV-light requirement. To the best of our knowledge, this is the first report of an integrated system capable of light induced water oxidation under such conditions. In future work, we aim to provide quantitative efficiency data on the basis of a better understanding of the loading of the components and the oxygen output of the cell.
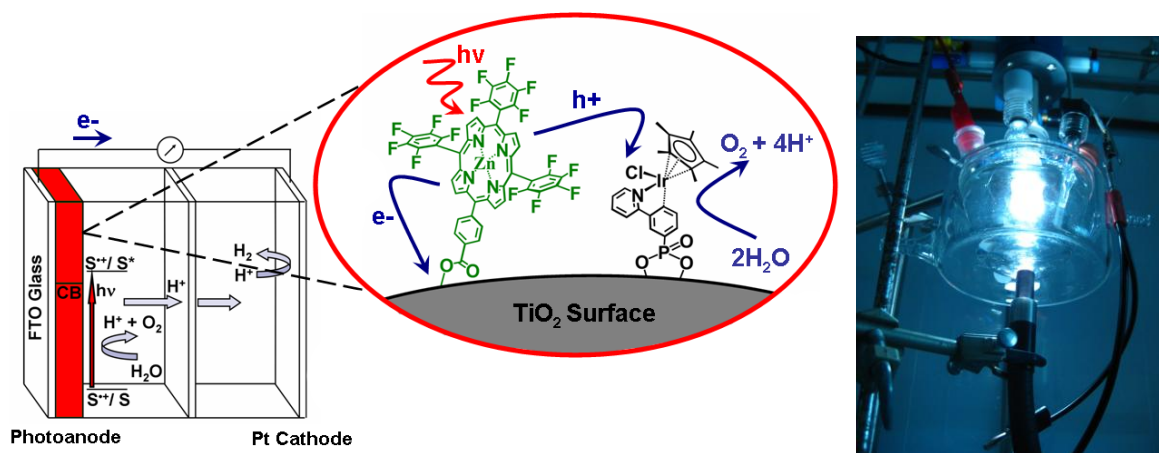

Figure 1. A schematic illustration of the photocatalytic anode (shown on the right) consisting of a TiO_2 nanoparticle surface (grey) sensitized with a high-potential porphyrin dye (green) and an Ir water oxidation catalyst (black) showing the proposed photo-initiated electron (e-)/hole transfers (h+) as well as the oxidative chemistry occurring at the surface.

References

1. G. F. Moore and G. W. Brudvig, Annu. Rev. Condens. Matter Phys., 2011, 2, 303-327.
2. *New Sciences for a Secure and Sustainable Energy Future*, U.S. Dep. of Energy, Washington, DC, December 2008.
3. *Basic Research Needs: Catalysis For Energy,* U.S. Dep. of Energy, Washington, DC, August 2007.
4. G. F. Moore, J. D. Blakemore, R. L. Milot, J. F. Hull, H. Song, L. Cai, C. A. Schmuttenmaer, R. H. Crabtree, and G. W. Brudvig, Energy Environ. Sci. (accepted)

Linkers and Catalysts for Light Induced Water Oxidation

Laura Allen, Lauren Martini, Nathan Schley, James D. Blakemore, Rebecca L. Milot, Julio L. Palma, Charles A. Schmuttenmaer, Victor S. Batista, Gary W. Brudvig, and Robert H. Crabtree
Department of Chemistry
Yale University
New Haven, CT 06520-8107

Artificial photosynthesis[1,2,3] requires water splitting catalysts as well as conducting linkers for attachment of the dyes and catalysts to the electrodes. One desirable feature of a linker is electronic rectification so successive electron transfers occur in the same desired direction. To try to incorporate this property, we have synthesized linkers that have amide bonds with opposite senses, as shown below, to see if directionality results. Computational data indeed suggest that our linkers do have this property, and we are currently collaborating with Stuart Lindsay at ASU to test this proposal experimentally from AFM data.

On the catalyst development side, the reactivity from our water oxidation catalyst series [Cp*Ir(L-L)Cl] (L-L = a variety of chelating ligands such as dipy, 2-hydroxypropyl-2-pyridyl) has been carefully characterized both with chemical oxidants and with electrochemical oxidation and O_2 evolution data collected.[4] One critical issue is the homogeneity of the catalyst, because just one catalyst precursor, $[Cp*Ir(OH_2)_3]SO_4$, does anodically deposit a catalytically active amorphous material, $IrO_{(2-x)}$.[5] Electrochemical nanobalance studies that measure the mass of any deposit formed on electrochemical oxidation, help distinguish the homogeneous cases from the single heterogeneous case, although our information so far only applies to short reaction times.
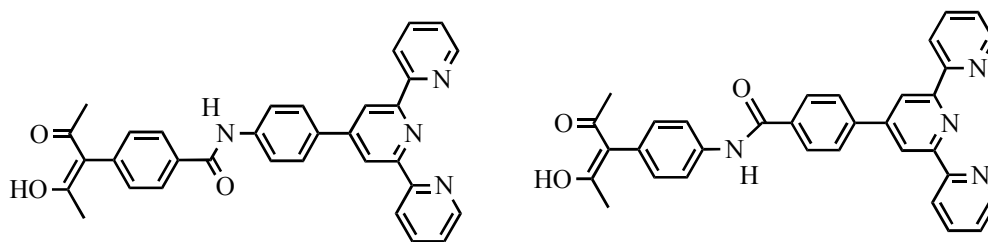

References

1. G. F. Moore and G. W. Brudvig, Annu. Rev. Condens. Matter Phys., 2011, 2, 303-327.

2. *New Sciences for a Secure and Sustainable Energy Future*, U.S. Dep. of Energy, Washington, DC, December 2008.

3. *Basic Research Needs: Catalysis For Energy,* U.S. Dep. of Energy, Washington, DC, August 2007.

4. Blakemore JD, Schley ND, Balcells D, Hull, JF, Olack G, Incarvito CD, Eisenstein O, Brudvig GW, Crabtree RH, J. Am. Chem. Soc., 2010, 132, 16017–16029 and unpublished data.

5. Blakemore JD, Schley ND, Olack G, Incarvito CD, Brudvig GW, Crabtree RH, Chem. Sci, 2011, 2, 94 – 98 and unpublished data.

Electron Injection Time Scales and Efficiencies in High-Potential Photoanodes, and Fluctuation-Induced Tunneling Conduction in Metal-Oxide Nanoparticles

Rebecca L. Milot, Gary F. Moore, Christiaan Richter, Diyar Talbayev, Steven J. Konezny, Robert C. Snoeberger III, Alexander R. Parent, Victor S. Batista, Robert H. Crabtree, Gary W. Brudvig, and <u>Charles A. Schmuttenmaer</u>
Department of Chemistry
Yale University
New Haven, CT 06520-8107

Two separate project updates will be presented. In the first one, we describe the charge injection time scale and efficiency for a selection of high-potential photoanodes (HPPAs) for photo-electrochemical cells.[1] The anodes consist of tris-pentafluorophenyl free-base and metallo-porphyrin sensitizers anchored to TiO_2 and SnO_2 nanoparticles. THz spectroscopic studies demonstrate the sensitizers used in these HPPAs are capable of injecting electrons into the conduction band of the metal-oxide materials in those cases where the energies of the donor (excited state dye) and acceptor (metal oxide conduction band minimum) components are appropriate. Importantly, the potentials photogenerated at the anode surface are high enough to permit the oxidation of high-potential electron sources.

In the second update, we report evidence of fluctuation-induced tunneling conduction (FITC) in nanoporous films made by sintering TiO_2 nanoparticles. Measured dark DC conductivities span over four orders of magnitude, exhibit a gradual transition from thermally activated behavior to temperature-independent tunneling with decreasing temperature, and are in quantitative agreement with a model describing interparticle FITC. Extracted tunnel junction parameters are consistent with a fully atomistic model of TiO_2 contact junctions and characterization of the films by diffraction and microscopy measurements.[2] We are in the process of extending these measurements and calculations to other metal oxides such as ZnO and SnO_2 nanoparticles, and expanding the DC measurements to AC frequencies from 0.1 Hz to 100 kHz.[3]

References

1. Rebecca L. Milot, Gary F. Moore, Robert H. Crabtree, Gary W. Brudvig, and Charles A. Schmuttenmaer, In preparation, April 2011.

2. Steven J. Konezny, Christiaan Richter, Robert C. Snoeberger III, Alexander R. Parent, Gary W. Brudvig, Charles Schmuttenmaer, and Victor S. Batista, Phys. Rev. B., Submitted, April 2011.

3. Steven J. Konezny, Diyar Talbayev, Robert C. Snoeberger III, Alexander R. Parent, Ismail Elbaggari, Victor S. Batista, and Charles A. Schmuttenmaer, In preparation, April 2011.

Size and Composition Dependent MEG in PbX Quantum Dots

Aaron Midgett, Barbara Hughes, Joseph Luther, Danielle Smith, Arthur J. Nozik,
Matthew C. Beard
Basic Sciences Center
National Renewable Energy Laboratory
Golden, CO 80401

Multiple exciton generation (MEG) in QDs is a very important process that if harnessed could lead to a new solar conversion efficiency limit. Here we report the MEG efficiencies for several different QD sizes representing bandgaps in the ranges of 0.6 to 1 eV for QD materials consisting of either PbSe, PbS, or a PbS_xSe_{1-x} alloy using ultrafast transient absorption spectroscopy. In previous MEG reports on PbSe QDs, no dependence on the QD size or bandgap were found. We find a clear size dependent MEG efficiency within the strong confinement region for both the PbS and PbS_xSe_{1-x} alloys that depends on the physical size of the quantum dot (QD), and its bandgap. The size-dependent MEG efficiency decreases for larger sizes and results from the decreased quantum confinement in PbS and PbS_xSe_{1-x} compared to PbSe. The decrease in MEG efficiency is correlated with a smaller Bohr exciton radius of PbS. Since MEG is more efficient in PbSe and PbS QDs than their bulk counterparts, a size-dependent MEG efficiency is expected. We extract the relative competition between a cooling channel and the MEG relaxation channel. We show that in small PbSe QDs the ratio between MEG and cooling~ 2 while in large PbS and bulk PbSe it is ~ 0.5. The Figure shown below (right) demonstrates how the competition between cooling and MEG changes as a function of the Bohr exciton radius divided by the radius of the QDs.
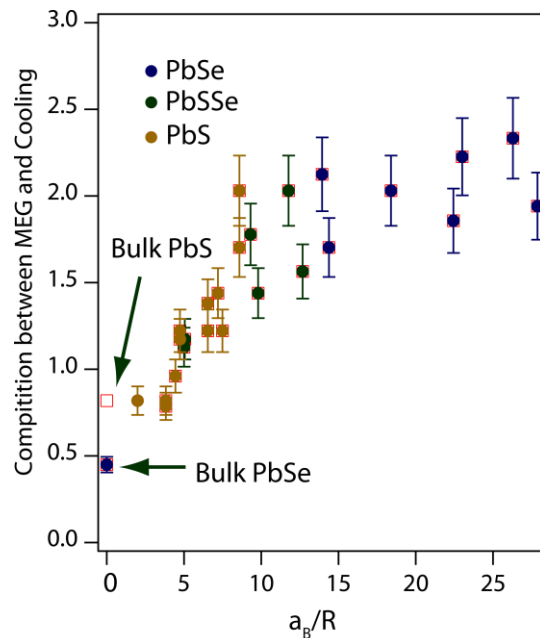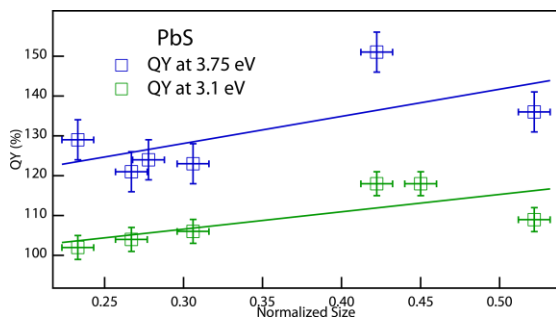
Charge Transfer in Single-walled Carbon Nanotube-Semiconducting Polymer Hybrids

Jeff Blackburn, Josh Holt, Andrew Ferguson, Nikos Kopidakis, Matt Beard, Garry Rumbles
National Renewable Energy Laboratory, Golden, CO

Single-walled carbon nanotubes (SWNTs) are two-dimensionally confined quantum wires that have the potential to impact a variety of solar photochemical applications. The ability to incorporate SWNTs into solar conversion schemes necessitates a deeper understanding of how SWNT diameter and electronic structure affects excited state charge transfer, as well as methods to control diameter and electronic structure for the rational formation of donor:acceptor blends.

This poster focuses on our recent studies aimed at rationally designed SWNT/polymer hybrids that promote long-lived photo-induced charge separation. A case study is presented for blends of SWNTs with the semiconducting polymer poly(3-hexylthiophene) (P3HT). We control the SWNT diameter and electronic structure through post-synthetic separation methods, and disperse SWNTs with controlled diameter populations and electronic structures into solutions, blends, and thin films with P3HT. Time-resolved microwave conductivity (TRMC) was used to study the dissociation of excitons at the interface between P3HT and SWNTs.
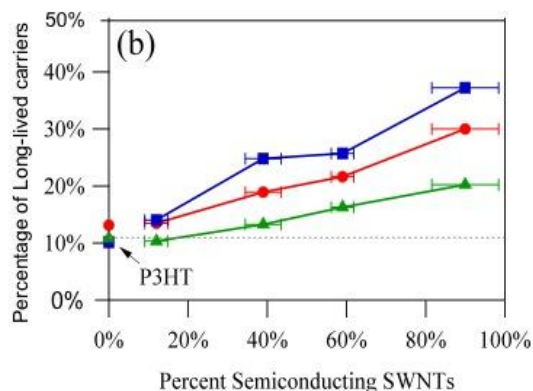

Figure 1. Relative measure of the percentage of long-lived carriers following photo-excitation of P3HT in a P3HT:SWNT blend, as a function of s-SWNT content. The three lines represent different photon fluences, ranging from low (squares) to high (triangles).

For large diameter SWNTs, we find that excitation of SWNTs at the second optical transition (S_{22}) does not result in appreciable hole transfer from SWNT to P3HT. In contrast, excitation of the polymer at 2.3 eV results in a dramatic increase in charge carrier generation relative to a film of P3HT with no SWNTs, along with a significant lengthening of the lifetime of free charges relative to charges created in isolated P3HT.[1] These observations indicate efficient electron transfer from the LUMO of the photo-excited P3HT to the LUMO of semiconducting SWNTs. In blends with smaller average diameter, we observe both electron transfer from P3HT to SWNT, as well as hole transfer from SWNT to P3HT. This diameter-dependent efficiency for the hole transfer step results from a diameter-dependent cutoff at which the charge transfer driving force exceeds the significant excitonic binding energy in SWNTs. We have also studied blends of P3HT with SWNTs separated by electronic structure into type-pure metallic and semiconducting SWNTs. We find that both the yield and lifetime of the photo-induced charge-separated state is dramatically increased as the percentage of semiconducting SWNTs within the blend is increased. This is the first experimental demonstration of the prevailing theoretical hypothesis that metallic SWNTs should act as efficient recombination centers in such polymer/SWNT systems.[2]

Finally, we will discuss our progress in the separation of bulk SWNTs into unique populations. These separations include isotope-enriched SWNTs for ^{13}C NMR, open versus end-capped SWNTs, and near-monochiral populations.

1. Ferguson, A. J.; Blackburn, J. L.; Holt, J. M.; Kopidakis, N.; Tenent, R. C.; Barnes, T. M.; Heben, M. J.; Rumbles, G., Photoinduced Energy and Charge Transfer in P3HT:SWNT Composites. *The Journal of Physical Chemistry Letters* **2010,** *1* (15), 2406-2411.
2. Holt, J. M.; Ferguson, A. J.; Kopidakis, N.; Larsen, B. A.; Bult, J.; Rumbles, G.; Blackburn, J. L., Prolonging Charge Separation in P3HT-SWNT Composites Using Highly Enriched Semiconducting Nanotubes. *Nano Lett.* **2010,** *10* (11), 4627-4633.

Probing the Rate of Hole Transfer in Oxidized Porphyrin Dyads Using Thallium Hyperfine Clocks
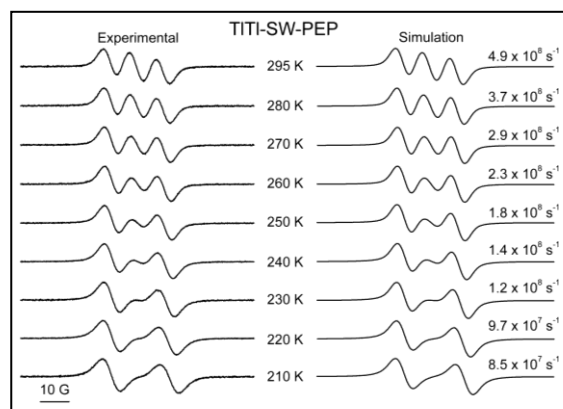
James R. Diers,[a] Masahiko Taniguchi,[b]
Dewey Holten,[c] Jonathan S. Lindsey,[b] and David F. Bocian[a]

[a]Department of Chemistry University of California, Riverside CA 92521-0403
[b]Department of Chemistry, North Carolina State University, Raleigh, NC 27695-8204
[c]Department of Chemistry, Washington University, St. Louis, MO 63130-4889

Efficient solar-energy conversion requires that holes generated after excited-state electron-injection can move efficiently away from the anode, thereby preventing charge-recombination. Thus, understanding hole mobility in prototypical light-harvesting and charge-separation systems is of fundamental interest. Understanding hole/electron-transfer processes among interacting constituents of multicomponent molecular architectures is central to the fields of artificial photosynthesis and molecular electronics. One strategy for examining ground-state hole/electron transfer in oxidized tetrapyrrolic arrays entails analysis of the hyperfine interactions observed in the EPR spectrum of the π-cation radical. We have found that ^{203}Tl/^{205}Tl hyperfine "clocks" are greatly superior to those provided by ^{1}H, ^{14}N, or ^{13}C owing to the fact that the ^{203}Tl/^{205}Tl hyperfine couplings are much larger (15-25 G) than those of the ^{1}H, ^{14}N, or ^{13}C nuclei (1-6 G). The large ^{203}Tl/^{205}Tl hyperfine interactions permit accurate simulations of the EPR spectra and the extraction of specific rates of hole/electron transfer. The ^{203}Tl/^{205}Tl hyperfine-clock strategy is applied to a series of seven porphyrin dyads. All of the dyads are joined at a meso position of the porphyrin macrocycle via linkers of a range of lengths and composition (diphenylethyne, diphenylbutadiyne and (p-phenylene)$_n$ where n = 1-4); substituents such as mesityl at the non-linking meso positions are employed to provide organic solubility. The

Variable-temperature EPR spectra of the monocation of **TlTl-SW-PEP** (left panel) and simulated spectra (right panel) with derived hole-transfer rates.

hole/electron-transfer time constants are in the hundreds of picosecond to sub-ten nanosecond regime, depending on the specific porphyrin and/or linker. Density functional theory calculations on the constituents of the dyads are consistent with the view that the relative energies of the porphyrin versus linker HOMOs strongly influence the hole/electron-transfer rates. Variable-temperature EPR studies further demonstrate that the hole/electron-transfer process is at best weakly activated (12-15 kJ mol^{-1}) at room temperature and somewhat below. At lower temperatures, the process is essentially activationless. The weak activation is attributed to restricted torsional motions of the phenyl rings of the linker. Collectively, the studies provide the physical basis for the rational design of multicomponent architectures for efficient hole/electron-transfer.

Synthetic Bacteriochlorins Bearing an Annulated Fifth Ring

Michael Krayer,[a] Eunkyung Yang,[b] James R. Diers,[c]
David F. Bocian,[c] Dewey Holten,[b] and <u>Jonathan S. Lindsey</u>[a]
[a]Department of Chemistry, North Carolina State University, Raleigh, NC 27695
[b]Department of Chemistry, Washington University, St. Louis, MO 63130
[c]Department of Chemistry, University of California Riverside, Riverside, CA 92521

The near-infrared spectral region has been comparatively underutilized for diverse applications owing to the lack of chromophores that afford stability, solubility, synthetic malleability, and tunable photophysical features. Bacteriochlorins are attractive candidates in this regard; however, preparation via modification of naturally occurring bacteriochlorophylls or reduction of porphyrins or chlorins has proved cumbersome.

Bacteriochlorophylls contain the bacteriochlorin chromophore and a fifth, five-membered oxopentano ring that encompasses positions 13–15 known as the "isocyclic" ring E. Such bacterio-13^1-oxophorbines have heretofore only been available in the naturally occurring compounds, and analogues bearing six-membered rings have only been available by derivatization of bacteriochlorophylls. A de novo route to synthetic bacteriochlorins, which bear a geminal dimethyl group in each pyrroline ring, has been extended to gain access to a bacterio-13^1-oxophorbine and bacteriochlorin-13,15-dicarboximides. The route relies on acid-catalyzed condensation of a dihydrodipyrrin–acetal to form the bacteriochlorin, which then is subjected to regioselective 15-bromination. Pd-mediated cyclization of the 15-bromobacteriochlorin bearing a 13-acetyl group (intramolecular α-arylation) or 13-ethoxycarbonyl group (carbamoylation and intramolecular imidation) gives the bacterio-13^1-oxophorbine or bacteriochlorin-13,15-dicarboximide, respectively.

The resulting macrocycles exhibit absorption in the near-infrared spectral region (733–818 nm), which extends the spectral coverage beyond that obtained previously with synthetic bacteriochlorins that lack a fifth ring. The macrocycles also exhibit excited singlet-state lifetimes (1.9–4.6 ns) comparable to or longer than those of natural photosynthetic pigments. Density functional theory calculations predict that the red-shifted absorption is primarily due to lowering of the energy of the lowest unoccupied molecular orbital. The new route complements existing semisynthetic routes and should enable fundamental spectroscopic studies and diverse photochemical applications.
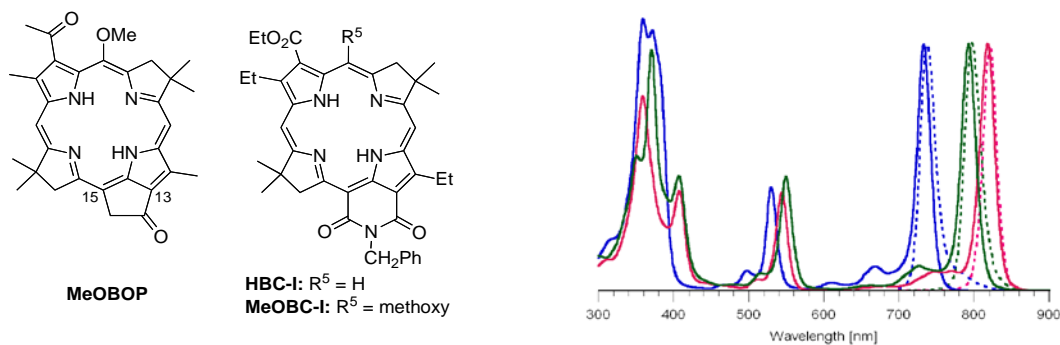

Figure. Absorption (— solid lines) and emission (--- dashed lines) spectra (normalized) in toluene at room temperature of **MeOBOP** (blue), **MeOBC-I** (green), and **HBC-I** (magenta).

Tuning the Light-Harvesting Characteristics of Perylene–Porphyrin Dyads via Perylene Substituents, Connection Motif, and 3-Dimensional Architecture

Christine Kirmaier,[a] Hee-eun Song,[a] Eunkyung Yang,[a] James R. Diers,[b]
Jonathan S. Lindsey,[c] David F. Bocian,[b] Dewey Holten[a]

[a]Department of Chemistry, Washington University, St. Louis, MO 63130
[b]Department of Chemistry, University of California Riverside, Riverside, CA 92521
[c]Department of Chemistry, North Carolina State University, Raleigh, NC 27695

Multipigment arrays that absorb visible light and funnel the resulting excited-state energy rapidly and efficiently to a designated site are of great interest for probing the mechanisms of electronic energy migration among pigments and may provide new types of molecular constructs for solar-energy applications. The ideal features of an accessory pigment for use with porphyrins appear to be largely satisfied by perylene-imide chromophores due to their complementary absorption characteristics, long excited-state lifetimes, stability, and synthetic malleability. Here we have investigated the photodynamics of seven perylene-porphyrin dyads that employ the most favorable design features identified in our prior studies.

The ideal dyad should undergo rapid and efficient excited-state energy transfer from perylene to porphyrin, and avoid electron-transfer quenching of the excited porphyrin by perylene in the medium of interest. Four dyads have different perylenes at the *p*-position of the meso-aryl group on the zinc porphyrin. In that set, ***p*-PMI(OR)-aep-Zn** is superior in providing rapid and essentially quantitative energy transfer from excited perylene to zinc porphyrin with minimal electron-transfer quenching in both toluene and benzonitrile. Analogs ***m*-PMI(OR)-aep-Zn** and ***o*-PMI(OR)-aep-Zn** exhibit similar results except for the *o*-linked dyad in benzonitrile, where significant excited-state quenching is observed. Such quenching does not occur with free base analog ***o*-PMI(OR)-aep-Fb** because electron transfer is thermodynamically unfavorable even in the polar medium. Strongly coupled dyad ***p*-PMI(OR)₂-ep-Zn** exhibits ultrafast and quantitative energy transfer in toluene; this dyad in benzonitrile exhibits ultrafast (<0.5 ps) perylene-to-porphyrin energy transfer, rapid (~5 ps) porphyrin-to-perylene electron transfer, and fast (~25 ps) charge recombination. Collectively, this study has identified suitable constructs for use in light-harvesting applications.
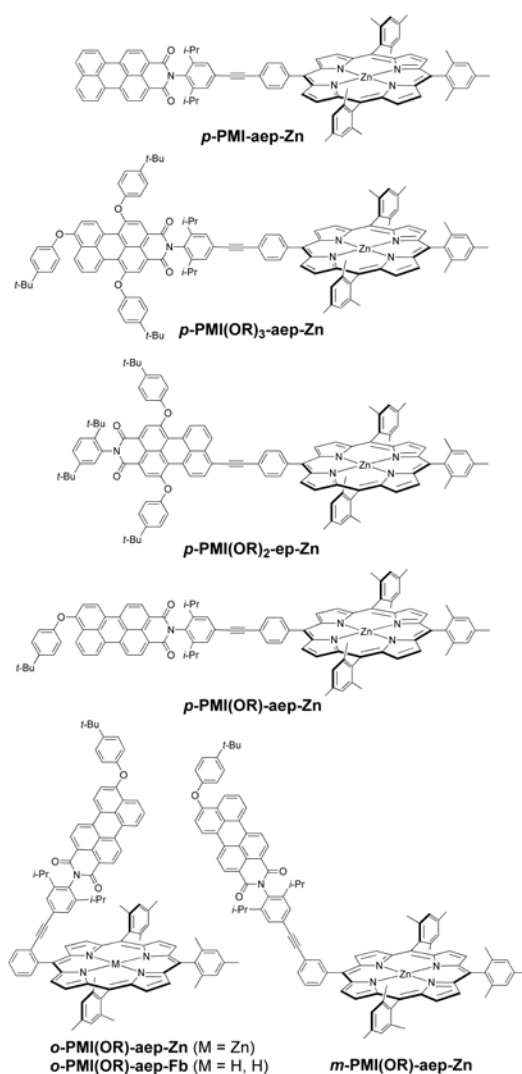
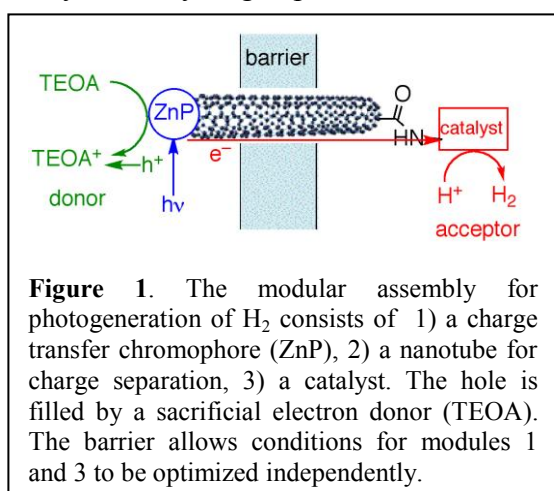# Modular Nanoscale and Biomimetic Assemblies for Photocatalytic Hydrogen Generation

Kara L. Bren, Richard Eisenberg, Patrick L. Holland, Todd D. Krauss
Department of Chemistry
University of Rochester
Rochester, NY 14627

The abundance and availability of solar energy makes it an attractive primary energy source for hydrogen (H_2) generation independent of fossil fuels. The objective of this project is to develop modular nanoscale assemblies for light-driven H_2 generation. The three modules are: (1) peptide-porphyrin-conjugate light-harvesting and charge-transfer chromophores, (2) carbon nanotubes (CNTs) for efficient long-range charge separation through an impermeable barrier, and (3) catalysts for hydrogen production from water based on earth-abundant metals (Fig. 1).

Figure 1. The modular assembly for photogeneration of H_2 consists of 1) a charge transfer chromophore (ZnP), 2) a nanotube for charge separation, 3) a catalyst. The hole is filled by a sacrificial electron donor (TEOA). The barrier allows conditions for modules 1 and 3 to be optimized independently.

For light harvesting and photoinduced charge separation (module 1), we have developed a new method for expression and purification of designed peptides with covalently attached metallo-porphyrins. This method uses a protease domain that undergoes autolysis in the presence of phytic acid to produce heme peptides and is a fundamental advance that is likely to be broadly applicable to artificial peptide synthesis. We have also found that zinc-substituted cytochrome c (ZnCyt c) can be bound to CNTs (module 2) as a key component of the assembly. This result also represents a new method for solubilizing CNTs.

With module 3, nickel complexes (Fig 2, left) that were previously known to electrocatalyze H_2 formation have been used for photocatalytic H_2 generation. We have also identified a series of cobalt-dithiolene catalysts (Fig 2, right) that were previously unrecognized for catalytic proton-reduction ability. Each of these catalysts gives a number of turnovers (>2000 per catalyst) that is higher than any values in the literature for solution photocatalytic systems. Rate studies have elucidated the dependence of the catalytic rates upon pH, solvent, and other factors. These molecules are also electrocatalysts with ~100% Faradaic efficiency. Future efforts will focus on incorporating these catalysts to integrated systems.

Figure 2. Earth-abundant catalysts in new photocatalytic systems for H_2 production from water.
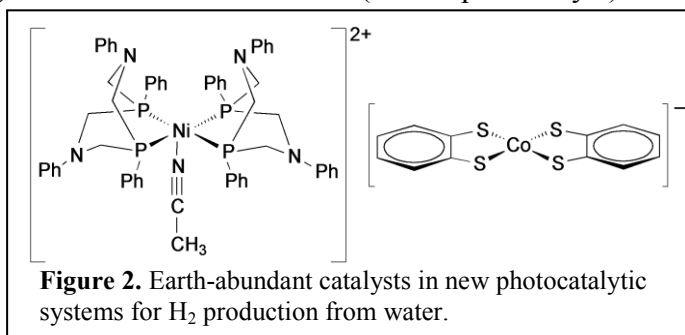
We have also begun evaluating CdSe nanocrystals (NCs) as sensitizers for photochemical H_2 production under aqueous conditions. Advantages of this strategy are the photostability of the NCs, the tunable band gap, and the ability to deliver multiple electrons to a catalyst. Initial experiments with a nickel catalyst and cysteamine-capped NCs have given 25 turnovers of H_2 per catalyst, showing that NCs can be used in multicomponent photocatalytic H_2 production.

Photoinitiated Electron Collection in Mixed-Metal Supramolecular Complexes: Development of Photocatalysts for Hydrogen Production

Shamindri Arachchige, Travis White, Jing Wang, Ryan Shaw, <u>Karen J. Brewer</u>
Department of Chemistry
Virginia Tech
Blacksburg, VA 24061-0212

This project is aimed at developing and studying a class of mixed-metal supramolecular complexes with promising redox and excited state properties. These systems couple charge transfer light absorbing metals to reactive metals such as rhodium(III) to undergo photoinitiated electron collection (PEC) at a reactive metal site capable of delivering collected electrons to a substrate such as H_2O to facilitate the production of H_2. The factors impacting multi-electron photochemistry and the reduction of water to produce H_2 have been explored providing a detailed understanding of the mechanism of action of these unique photocatalysts and the factors that impact functioning. The process of collecting electrons at a Rh^{III} center results in the production of a Rh^I center that is coordinatively unsaturated and thereby able to interact with substrates. Through studies of the photophysics of this motif we have designed catalysts with enhanced functioning, long term stability and good photocatalytic efficiencies. The study of Ru,Rh bimetallics has provided a new motif that undergoes photoinitiated electron collection at the Rh center but does not photocatalyze H_2 production. Our study of this motif has highlighted factors that are important to photocatalysis by Rh centered supramolecules. The careful tuning of sterics and electronics in the Ru,Rh motif has recently provided for active photocatalysts and insight into the energetically close $Rh(d\sigma^*)$ and $BL(\pi^*)$ orbitals in mixed-metal Ru, Rh archtectures.
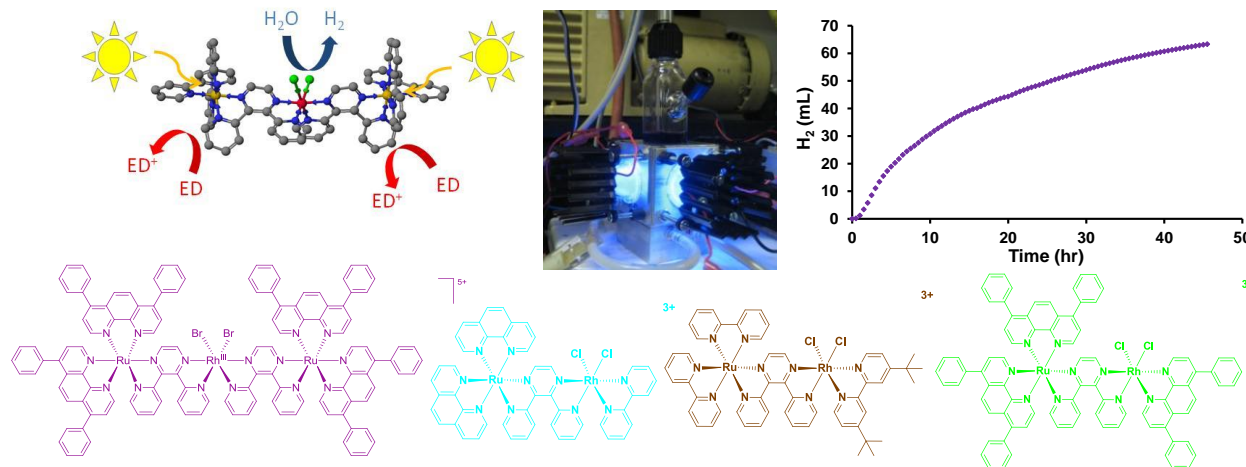
1. "A New Structural Motif for Photoinitiated Electron Collection: Ru, Rh Bimetallic Providing Insight into H_2 Production via Photocatalysis of Water Reduction by Ru,Rh,Ru Supramolecular, J. Wang, T. A. White, S. M. Arachchige, K. J. Brewer, *Chem. Comm.* **2011**, *47*, 4451-3.

2. "High Turnover in a Photocatalytic System for Water Reduction to Produce Hydrogen Using a Ru,Rh,Ru Photoinitiated Electron Collector," S. M. Arachchige, R. Shaw, T. A. White, V. Shenoy, H.-M. Tsui, and K. J. Brewer*, *ChemSusChem* **2011,** *4*, 514-8.

3. "Photocatalytic Hydrogen Production from Water," S. M. Arachchige, K. J. Brewer, *Energy Production and Storage-Inorganic Chemical Strategies for a Warming World, Encyclopedia of Inorganic Chemistry,* Robert Crabtree Editor, John Wiley and Sons, **2010**, in press.

Electron-Transfer in Ionic Liquids

C. S. Santos, H. Y. Lee, T. A. Fadeeva, N. S. Murthy and E. W. Castner, Jr.
Department of Chemistry and Chemical Biology
Rutgers, The State University of New Jersey
Piscataway, NJ   08854
H. Shirota
Department of Nanomaterials Science
Chiba University, Chiba 263-8522   Japan

Bimolecular electron-transfer reactions in ionic liquids display unusual properties, as illustrated by the two graphs below. The left graph shows the self-diffusion coefficients for an electron-donating ionic liquid anion (red) and its homologous neutral ester (blue) for a 0.1 M solution in the N-methyl-N-butylpyrrolidinium bis (trifluoromethylsulfonyl)amide ionic liquid. The self-diffusion rate of the neutral ester is 2.5 times higher than the carboxylate donor, but the activation enthalpies for self-diffusion are both ~30 kJ mol^{-1}. The right graph shows the bimolecular electron-transfer rate derived from reductive quenching data of photoexcited 9,10-dicyanoanthracene by the two donors shown on the left, also in 0.1 M solution of the same ionic liquid; he E_a values are 16 (neutral) and 11 (anionic) kJ mol^{-1}. Higher viscosities in ILs lead to solvent-limited electron-transfer and the short-time limit for the Smoluchowski equation.
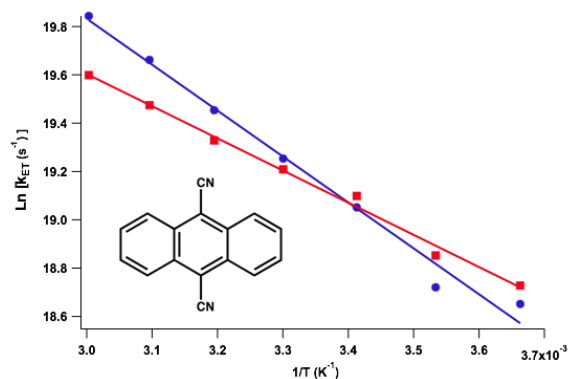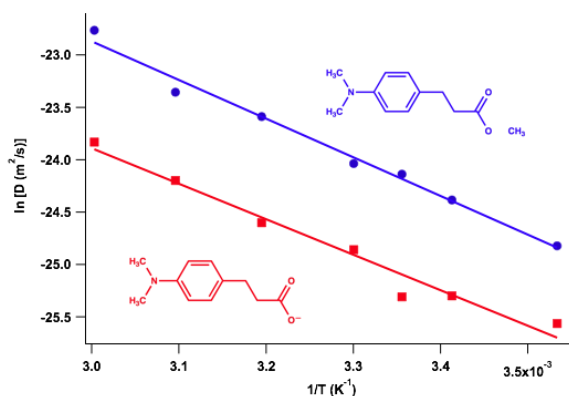
The graph at right shows the structure functions S(q) obtained from high energy x-ray scattering at APS 11-ID-C.   One crucial difference in ionic liquid structures is that the two with octyl chains show a peak at 0.4 Å^{-1} while the isoelectronic ether-substituted cations do not. The ether-substituted cations have viscosities that are three-fold lower than the alkyl homologs. We are now exploring the differences in ion transport and electron-transfer reactivity in these liquids.
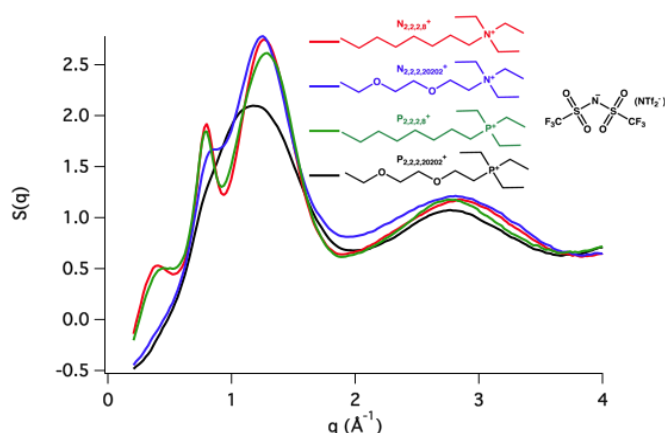
Composition Tuning of Fe- and W-Based Binary and Ternary Oxide Photoanodes for Use in the Photoelectrolysis of Water

Kenneth J. McDonald, James C. Hill, Ryan L. Spray, and Kyoung-Shin Choi
Department of Chemistry
Purdue University
West Lafayette, IN, 47907

Among binary oxides that can utilize the visible portion of the spectrum, α-Fe$_2$O$_3$ (E$_g$ = 2.1 eV) and WO$_3$ (E$_g$ = 2.6 eV) are two of the most intensively studied systems as photoanodes for solar water splitting cells because both are abundant, easy to process, environmentally benign, and not cost-prohibitive for bulk production. However, both semiconductors have a few challenges to overcome to enhance their efficiencies to the desired level. The main concerns for α-Fe$_2$O$_3$ include its poor charge transport properties (short hole diffusion length and poor electrical conductivity) and the presence of significant surface states that prohibit efficient electron-hole separation. As for WO$_3$, its relatively large band gap (2.6 eV), reduced stability in a neutral solution, and photocorrosion by the formation and accumulation of H$_2$O$_2$ species during the photo-oxidation of water are the main issues that need to be addressed.

In this presentation, we report our recent investigations on the composition tuning of nanoporous α-Fe$_2$O$_3$ and WO$_3$ electrodes, which were aimed to address the aforementioned issues. The method we used for surface composition tuning involved a simple solution treatment followed by mild heating and dissolution processes, which can be easily added to various synthesis methods used to make semiconductor electrodes (Figure 1). As this treatment did not significantly alter the native electrode morphology, it enabled us to investigate the effect of incorporating various ions on the performance of host electrodes in a more controlled manner. The effect of incorporating Al, Sn, Zn and Co ions into nanoporous α-Fe$_2$O$_3$ electrodes and the effect of incorporating Cu and Al ions into nanoporous WO$_3$ electrodes were investigated. Some of these treatments resulted in the formation of ternary oxide electrodes (e.g. ZnFe$_2$O$_4$ and CuWO$_4$), which have distinctive advantages over their binary forms for use as photoanodes for the photoelectrolysis of water. The changes caused by each composition tuning in photocurrents, conductivities, surface states, and catalytic properties for O$_2$ evolution will be discussed in detail in this presentation.
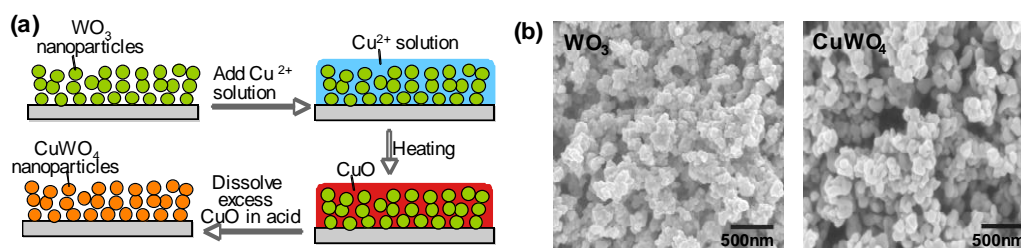

Figure 1. (a) Schematic representation of a method used to tune the compositions of nanoporous α-Fe$_2$O$_3$ and WO$_3$ electrodes. A conversion of WO$_3$ to CuWO$_4$ is shown for example. (b) SEM images of a nanoporous WO$_3$ electrode used in this study and a CuWO$_4$ electrode resulted from the treatment shown in (a).

A Comparison of Hydricities in Water and Acetonitrile Solvents

Yasuo Matsubara and <u>Carol Creutz</u>
Chemistry Department
Brookhaven National Laboratory
Upton, New York 11973-5000

The thermodynamic ability of a transition-metal hydride to serve as a hydride ion (H^-) donor

$$M\text{-}H \rightleftharpoons M^+ + H^- \qquad \Delta G^0_{H^-} \qquad\qquad (1)$$

($\Delta G^0_{H^-}$ hydricity eq 1) has been extensively characterized by DuBois, Angelici, Morris and Bruno groups in organic solvents. Earlier our group determined values for aqueous media (*J. Am. Chem. Soc.* **2009**, *131*, 2794).
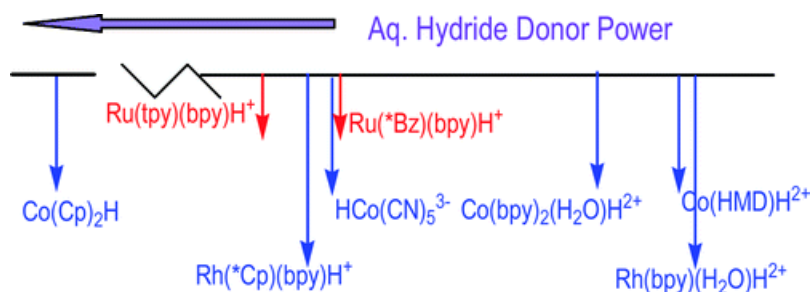
Despite the fundamental importance of hydricity in a range of reactions important in catalysis and solar energy storage, ours are the only values reported for water solvent and there has been no basis for comparison of these with the wider range already determined for acetonitrile solvent, in particular. We have now used a variety of approaches to determine hydricity values in acetonitrile of Ru(II) hydride complexes previously studied in water.

For complex **1**, Ru(tpy)(bpy)H$^+$ we utilized organic hydride ion acceptors (A$^+$) of characterized hydricity derived from imidazolium cations and NAD$^+$ model compounds and determined K_2 by ^{1}H NMR measurements. Equilibration of initially 7 mM solutions in CD$_3$CN was slow—on the timescale of a day or more (eq 2). For complex **2**, Ru(η^6-C$_6$Me$_6$)(bpy)H$^+$, we used an approach based on evaluation of the acidity of **2** (eq 3) pK_a(**2**) = 22.5 and the Ru$^{II/0}$ electrochemical potential (-1.22 V vs. Fc$^+$/Fc) (see eq 4).

$$\text{Ru(tpy)(bpy)H}^+ + \text{A}^+ + \text{CD}_3\text{CN} \rightleftharpoons \text{Ru(tpy)(bpy)(CH}_3\text{CN)}^{2+} + \text{HA} \qquad K_2 \qquad (2)$$

$$\text{Ru}(\eta^6\text{-C}_6\text{Me}_6)(\text{bpy})\text{H}^+ + \text{B} \rightleftharpoons \text{Ru}(\eta^6\text{-C}_6\text{Me}_6)(\text{bpy})^0 + \text{BH}^+ \qquad K_3 \qquad (3)$$

$$\Delta G = 1.37\, \text{p}K_a + 46.1\, E(\text{II/0, vs. Fc/Fc}^+) + 79.6\ [\text{kcal/mol}] \qquad (4)$$

The hydricities of **1** and **2,** respectively, were estimated as 39.2 and 54.2 ± 2.0 kcal/mol in acetonitrile to be compared with the values 22 and 31 kcal/mol found for aqueous media.

Efforts to Understand Kinetic and Thermodynamic Factors Relevant for Controlling Photochemical Transformations with Light

Niels H. Damrauer, Erik M. Grumstrup, Paul A. Montgomery
Department of Chemistry and Biochemistry
University of Colorado at Boulder
Boulder, CO 80309

We have been interested in controlling photophysical and photochemical transformations using shaped laser fields and what such experiments can tell us about dynamics relevant for conversions between electronic states. Because of laser bandwidth within our laboratory and typical time scales for reactivity versus decoherence, we have become increasingly interested in understanding how shaped laser fields can exploit low-frequency coherent nuclear motions within condensed phase systems as a way of altering the electronic coupling and/or reorganization energy between reactant and product states.

One element of this poster will explore recent efforts motivated by our findings published at the end of last year (*PRL* **105**, 257403 (2010)) that singlet fission yields in polycrystalline tetracene can be manipulated when broad-band shaped pulses exploit low-frequency lattice vibrations. These experiments identified optimal laser fields consisting of trains of weak but short pulses with separation times matched to the period of coherent vibrations identified with pump-probe measurements. Here we will describe efforts to determine whether these coherent motions occur on ground state or excited state surfaces and efforts to combine optimal pulse trains with systematic variation (throughout the train) of laser-pulse chirp. Such measurements are a necessary step towards developing theoretical models for the control mechanism. We will also discuss efforts to simulate dynamics induced by pulse trains in simple multistate models and explore pitfalls in trying to understand how laser pulse phase can alter state populations.

A second element of this poster concerns recent efforts (*JPCA* **115**, 3122-3132 (2011)) using computational tools to identify transition metal complexes with favorable thermodynamic properties for heterolytic carbon-halogen bond scission photoreactions. In such systems, low-frequency motions may be expected to facilitate reactivity by increasing electronic coupling between an excited-state MLCT reactant and a photoproduct consisting of an oxidized metal complex radical and the halogen anion (i.e. an electron transfer mediated dissociation reaction). We believe that pulse shaping can exploit such motions

Fig. 1. Key conformational changes important for reducing the reaction energy in two promising Ru(II) systems.

but promising candidates first need to be identified. Here we will discuss findings that promising species such as those shown in *Fig. 1.* store energy in geometrical strain that is released upon electron-transfer mediated halide dissociation.
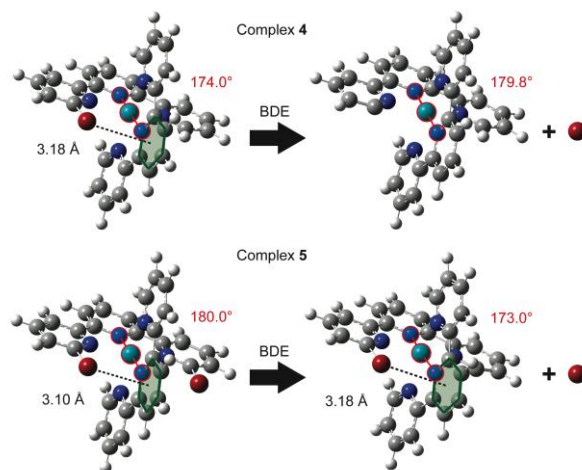
Multi-Step, Photo-Induced Charge Separation in a Cu(I) bis-Phenanthroline Based Donor-Chromophore-Acceptor Triads

C. Michael Elliott
Department of Chemistry, Colorado State University
Ft. Collins, CO 80523

The multi-step formation of a photo-induced charge separated state (CSS) is achievable in $Ru(II)L_3$-based donor-chromophore-acceptor complexes (D-C-A, where L = 2,2'-bipyridine) with excellent quantum yields ($\Phi_{css} \approx 1$) and lifetimes ($\tau_{css} \approx 0.3$ µs) while retaining approximately 70% ^{3}MLCT energy in the CSS.   The large quantum yield in part results from: (1) a ground-state association between the donor moiety and metal-based chromophore and (2) the fact that charge separation initiates from the ^{3}MLCT excited state resulting in a ^{3}CSS. As a consequence of the triplet nature of the CSS, an approximately ten-fold increase in the average lifetime is achieved in a relatively small applied magnetic field (0.5 T).

Bisphenanthrolinecopper(I) complexes have long been recognized to have similar photophysical properties to $Ru(II)L_3$ but with some notable differences. These differences include: (1) ligand lability in the ground state, (2) changes in coordination geometry upon photoexcitation and oxidation and (3) different redox potentials (relative to $Ru(II)L_3^{2+}$) in the ground and excited states. These differences present challenges when designing D-C-A systems based on Cu(I). Despite these challenges we have been able to demonstrate multistep CSS formation in several copper-based triad systems. Like the ruthenium based systems, the CSS exhibits magnetic-field dependent kinetics for the CSS decay but the effect is more dramatic. Fields of a few hundred mT increase the CSS life time by ca. ×100. In contrast to the ruthenium systems, fields <100 mT affect Φ_{css} of Cu(I)-based D-C-As.

To deal with the lability issue our synthesis strategy involves using a combination of steric bulk in the 2- and 9-positions of the phenanthroline and electrostatic interactions to thermodynamically favor heteroleptic complex formation (i.e., Cu^I(L-A)(L-D)).   Several examples of the donor- and acceptor-appended ligands we have successfully synthesized, or are in the process of synthesizing, are shown below:
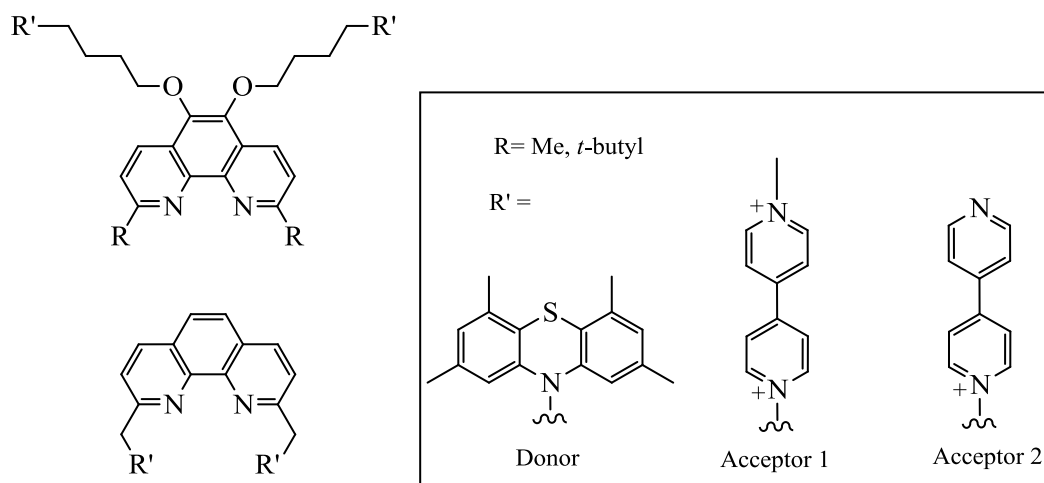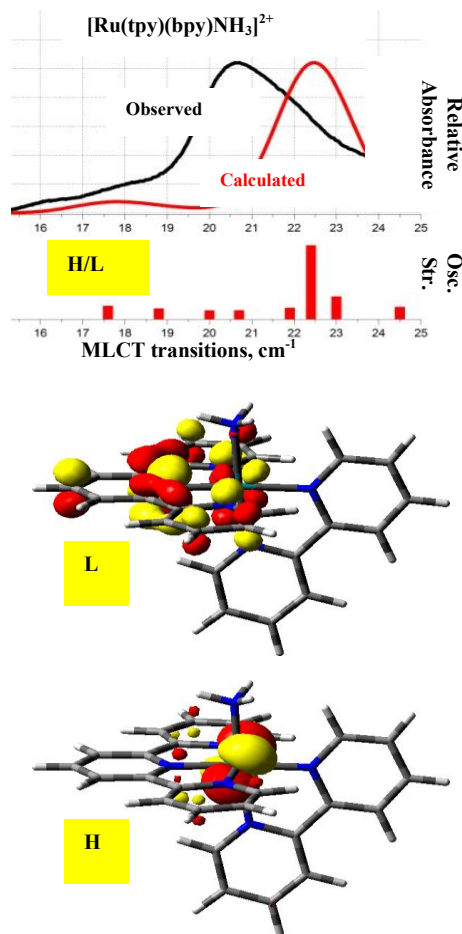
Photoinduced Reactions of Multi-metallic Complexes:
Experimental and Computational Probes of the Lowest Energy Excited States and their Electron-Transfer Reorganizational Energies

Marco M. Allard,[a] Yuan-Jang Chen,[b] Richard L. Lord,[a] H. Bernhard Schlegel,[a] Cláudio N. Verani[a] and John F. Endicott[a]

Departments of Chemistry, Wayne State University, Detroit, Michigan 48202[a] and Fu-Jen Catholic University, New Taipei City 24205, Taiwan, R.O.C.[b]

It is difficult to determine the relationship of excited state physical properties to their lifetimes and reactivities owing to the transient nature of these states. Some sort of spectroscopic probing is the most common way to investigate them. We have been using absorption and emission spectroscopy in combination with TD-DFT computational modeling to investigate the variations in the energies and structures of the lowest energy CT excited states of $[Ru(bpy)_nL_{6-2n}]^{m+}$ (n = 2 or 1), $[Ru(tpy)(bpy)L]^{m+}$ and $[Ru(bpy)_2(PX_n)]^{m+}$ complexes (PX_n = a substituted phenanthroline ligand) and some of their multimetallic analogs.

The dominant low energy absorption features of transition metal polypyridyl complexes are often associated with the HOMO→LUMO (H/L) transitions, but our work with some series of monometallic $[Ru(bpy)_2L_2]^{m+}$ and $[Ru(tpy)(bpy)L]^{m+}$ complexes indicates that this transition is relatively weak and tends to be observed on the low energy side of the lowest energy MLCT absorption envelope ($MLCT_{a/e}$); for the $[Ru(bpy)L_4]^{m+}$ complexes the computed H/L transitions have oscillator strengths so small that they would not be easily detected. For the $[Ru(bpy)_nL_{6-2n}]^{m+}$ complexes the energy maxima of the H/L transitions are 2000-3000 cm^{-1} lower than the maximum of $MLCT_{a/e}$. The H/L transitions of the monometallic $[Ru(tpy)(bpy)L]^{m+}$ complexes often appear as weak bands on the low energy side of the lowest MLCT absorption envelope and are 4000-5000 cm^{-1} lower in energy than the absorption maxima. This pattern of weak H/L transitions is also observed for cyanide-bridged complexes containing 2, 3 or 4 Ru(II) centers. These observations and the observed 77K emission energies imply that the corresponding Ru/polypyridine electron transfer reorganizational energies are relatively small. The CT excited state distortions as manifested in the emission sidebands vary in amplitude and energy with the chromophore and they tend to decrease in amplitude with the excited state energies. In some $[Ru(bpy)_2(PX_2)]^{m+}$ complexes the lowest energy CT excited state appears to involve the substituents (X_2) and result in very different distortions than observed in simpler polypyridyl complexes.

Multimetallic Complexes for Photoinduced Reactions: Efforts toward Species that Merge Antenna/Amphiphile and Antenna/Active Site Functions

Frank D. Lesh, Rajendra Shakya, Rama Shanmugan, Lanka Wickramasinghe, Debashis Basu, Marco M. Allard, Richard Lord, H. Bernhard Schlegel, John F. Endicott, Cláudio N. Verani
Department of Chemistry
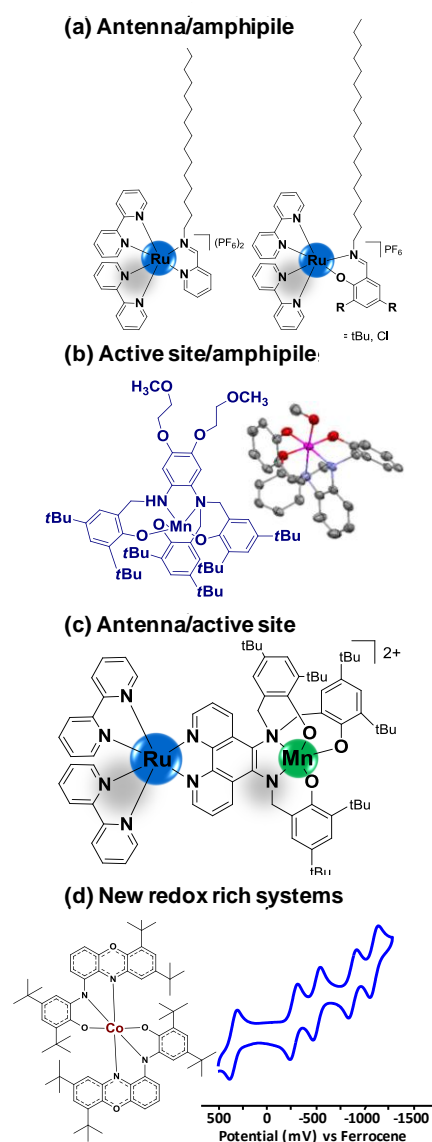Wayne State University
Detroit, MI-48202

A comprehensive effort is under development at Wayne State University aiming at the development of supramolecular multimetallic complexes with integrated acceptor, antenna and active sites. The understanding of how directional electron transfer and charge separation can be controlled in such systems is a necessary step toward effective water oxidation catalysts.

Considerable progress was made in the synthesis and characterization of species that merge a $[Ru^{II}(bipy)_2]$ antenna with amphiphilic pyridine and phenol moieties (**Figure 1a**). The $[(L^{pyridine})Ru^{II}(bpy)_2](PF_6)_2$ species show multiple redox processes attributed to bipyridine reduction and ruthenium oxidation, whereas the $[(L^{phenolate})Ru^{II}(bpy)_2](PF_6)_2$ species present relatively lower reduction potentials and more reversible redox behavior, along with $Ru^{II/III}$ and phenolate/phenoxyl oxidations. The interpretation of the observed redox behavior was supported by DFT calculations. The study of their film formation capabilities at the air/water interface was characterized by compression isotherms and Brewster angle microscopy. These species show moderate to high collapse pressures and are strong candidates for the formation of redox-responsive monolayer films.

We have also developed several new redox-active pentadentate ligands that incorporate amphiphilic properties and we are currently studying the formation of their manganese complexes. Structural information reveals an octahedral environment around the manganese ion with the sixth position being occupied by a solvent molecule such as methanol or water (**Figure 1b**).

Furthermore, synthetic methodology has been developed that allowed us to prepare a series of bimetallic $[(bipy)_2Ru^{II}M^{III}L]^{2+}$ species (**Figure 1c**) where the antenna is directly connected to a metal center that can accommodate substrate binding and redox transformations. Currently we are evaluating the electrochemical and photochemical behavior of such species with cores $[Ru^{II}Ga^{III}]$ $[Ru^{II}Fe^{III}]$ and $[Ru^{II}Mn^{III}]$.

Further details regarding new $[Co^{III}radical]$ species with exceptionally redox-rich phenoxazine ligands will also be presented. (**Figure 1c**)

(a) Antenna/amphipile

(b) Active site/amphipile

(c) Antenna/active site

(d) New redox rich systems

500   0   -500   -1000   -1500
Potential (mV) vs Ferrocene

Photoprotection in Plants and Algae

Graham R. Fleming, Julia Zaks, and Kapil Amarnath
Physical Biosciences Division
Lawrence Berkeley National Laboratory
Berkeley, CA 94720

Photosystem II of plants and algae contains feedback mechanisms, collectively called non-photochemical quenching (NPQ), that turn on dissipative processes that convert excitation to heat under excess light conditions. Figure 1 shows an example of the phenomenon in a green algae. We have built a systems model of PSII using ideas from control theory. In particular, to reject a step change in light intensity, an integrator is necessary in the feedback loop. To reject a ramp (continuous change) in light intensity, a double integral of the error is required in the controller (Figure 2). Photosynthetic organisms use lumen pH as the error signal, and two pH sensitive proteins to control the most important, and rapidly reversible, component of NPQ, called qE. The two proteins are PsbS, and violaxanthin deepoxidase, respectively. The latter converts violaxanthin to zeaxanthin, a key component of qE. The concentration of zeaxanthin (Zea) is roughly proportional to the double integral of the error while PsbS is roughly proportional to the integral of the error. Both PsbS and Zea are required for qE so that the fraction of PSIIs being quenched is proportional to the product of fractions of PsbS and Zea, assuming the concentrations are uncorrelated. This idea explains why qE can be turned off quickly despite the fact that the concentration of Zea does not change quickly when the light level drops: when protonated PsbS drops to zero, the qE turns off, but is poised to turn back on quickly because now Zea is already present.

Our model uses 14 differential equations and can simulate the standard pulse amplitude modulated (PAM) fluorescence traces quite well.
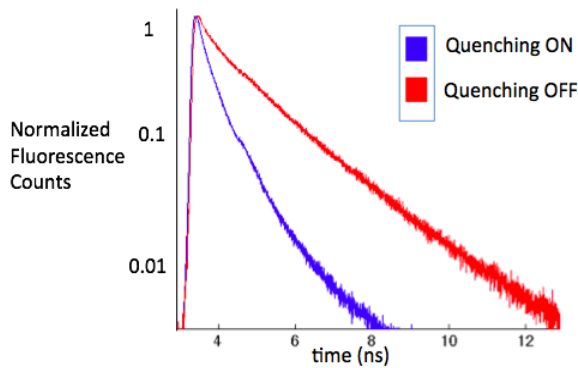

Figure 1.
Fluorescence decays from *Chlamydomonas reinhardtii* with and without quenching
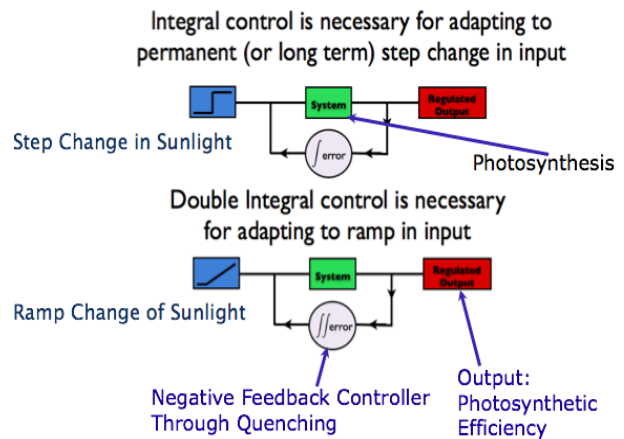

Figure 2.
Control loops for non-photochemical quenching

Nanoscaled Components for Improved Efficiency in a Multipanel Photocatalytic Water-Splitting Device

Marye Anne Fox and James K Whitesell
Department of Chemistry and Biochemistry
University of California, San Diego
La Jolla, CA 92093-0358

We have successfully constructed a multi-cell assembly and demonstrated separated generation of hydrogen and oxygen. However, reproducibility has been an issue with preparation of the metal oxide faces, an area that we are actively exploring as this remains a central and critical issue for tuning other parameters in the assembly.

We have prepared a new series of ruthenium based dye sensitizers T1, T2, & T2) that exhibit broad absorption in the region of the solar spectrum. The preparation of these materials is straight forward and proceeds in good overall yield. The syntheses are readily amendable for the preparation of derivatives in order to fine tune absorption characteristics.
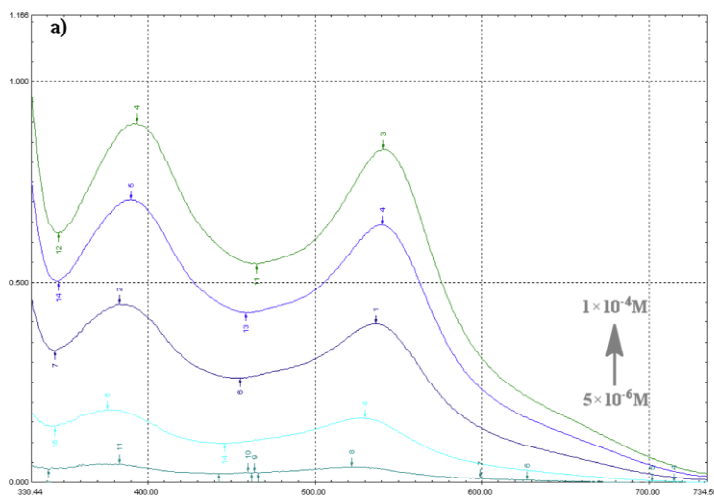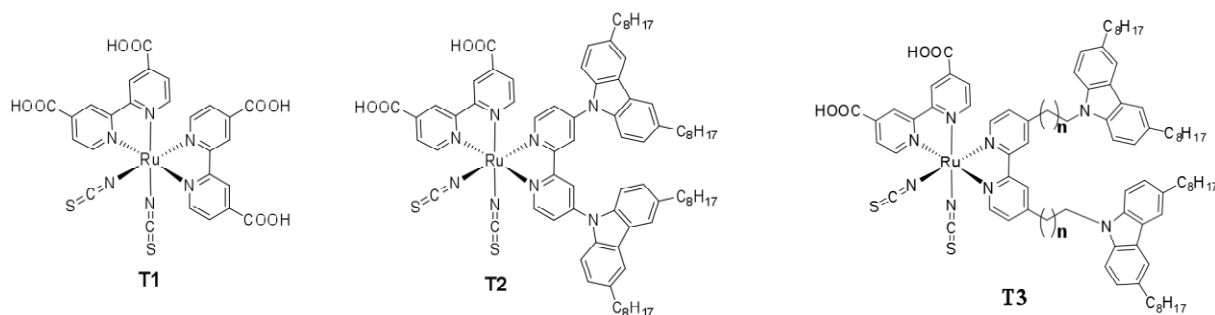
UV/Vis absorption spectra of ruthenium sensitizer T1(a) and T2(b) at different concentration in dichloromethane and methanol (1:1)

We have begun evaluation of these sensitizers but detailed studies of effectiveness and efficiencies must await resolution of the metal oxide fabrication issues.

Electronic Structure Calculations of Nanomaterials: Theory and Applications

Tom Hughes, Jing Zhang, Louis Brus, Mike Steigerwald, and Richard A. Friesner
Department of Chemistry
Columbia University
New York, NY 10027

We have continued to develop our approach to improving the accuracy of DFT calculations, with a particular focus on transition metals. Results demonstrating large improvements in the calculation of spin splittings, and metal-ligand bond energies, will be presented. We have also incorporated dispersion interactions into our model. These results, combined with prior work, will soon enable us to assemble a complete, automated model for carrying out corrected DFT calculations, with near-chemical accuracy for organic systems, and somewhat larger errors for transition metal containing systems (but vastly improved as compared to standard DFT methods, including the most recent currently available functionals).

We have pursued two principal applications over the past year. The first is modeling of ruthenium based catalysts for water splitting developed by Meyer and coworkers. We have modeled the entire catalytic cycle with a particular focus on the rate determining steps of the reaction; we have also computed redox potentials of a large number of related Ru based compounds in solution and compared these results with experiment. Agreement between the theoretical and experimental redox calculations is very good. The water splitting calculations accurately predict the experimental barrier heights at two key points in the catalytic cycle, supporting proposed mechanisms for the reactions and also validating the computational modeling. The calculations are complicated by the necessity of exploring a large number of initial guesses for the transition metal electronic structure in order to make sure that the lowest energy states are found.

The second application we have pursued is modeling of TiO_2 nanostructures in an effort to understand the functioning of the Gratzel cell. We have built large models of TiO_2 nanoparticles passivated by water-derived ligands (OH, H_2O, etc.) and investigated the electronic structures of these models. We have also studied what happens when a Li atom or Li+ cation is introduced at various locations into the model. There are various proposals as to how electrons become trapped in the nanoparticle and how transport of these trapped electrons occurs. One important possibility is that the electrons are stabilized by cations (Li+ or H+, e.g.) and that the diffusion of the electrons is really a coupled electron-proton motion in the nanoparticle lattice. The key quantity is the barrier height as one moves the Li+ from one oxygen location to another. We will soon be able to compute this barrier height using the models we have developed. The continuum solvent has proved to be quite important in understanding properties of the model. We have benchmarked the results by calculating the bandshift with and without Li present and in different solvents. The continuum solvent results agree quite well with experimental data. Finally, we have substantially improved the parallel performance of Jaguar for this problem and are now getting a speedup of 13x on 16 processors.
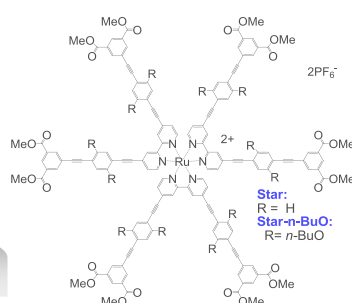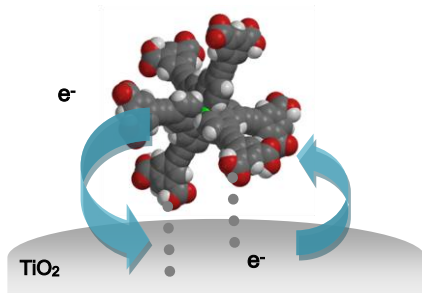
Synthesis and Properties of Star-Shaped Ruthenium Polypyridyl Complexes: Binding Control on Metal Oxide Surfaces

Elena Galoppini, Yongyi Zhang, Patrik G. Johansson, Gerald J. Meyer
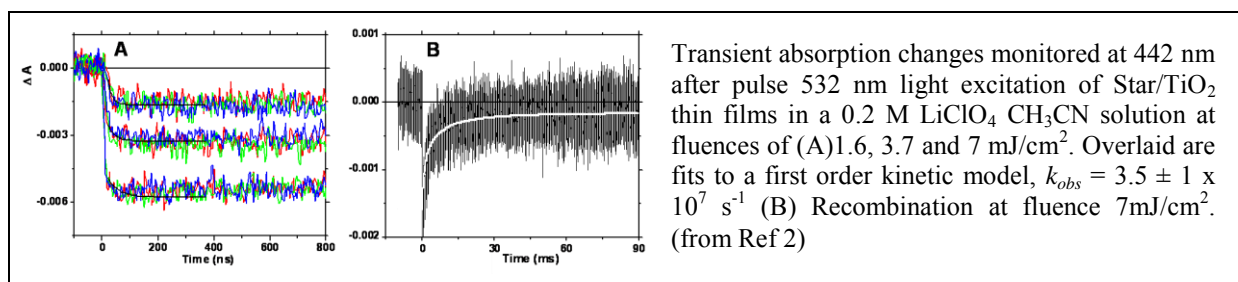Department of Chemistry, Rutgers University, Newark, NJ 07102
Department of Chemistry, John Hopkins University, Baltimore, MD 21218

Control of charge transfer between dye-linker-anchor sensitizers to metal oxide (MO) semiconductor interfaces is important for renewable energy projects involving nanostructured semiconductors. However, it is difficult to control effectively the positioning of a molecule on a MO surface, a prerequisite to engineer and study this complex interface. Uncertainty over the binding mode and orientation, and the heterogeneity of the nanostructured metal oxide films can prevail over the molecular design. A series of novel homoleptic Ru(II) star complexes were synthesized as part of a new surface engineering strategy. In the nano-sized, highly symmetrical star-shaped complexes, the Ru(II) center is coordinated to three identical bipyridine ligands carrying conjugated oligophenylenethynylene rigid linker units with (**Star-n-BuO**) or without (**Star**) solubilizing alkoxy chains, and terminating with carboxylic anchor groups. The chromophoric Ru(bpy) core cannot come in close contact to the semiconductor surface. The UV-Vis spectra of both complexes displayed intense $\pi{\rightarrow}\pi^*$ bands at ~320 nm, a broad MLCT band at ~ 490 nm, and both exhibited a long lived excited state (τ_{PL} ~1.2 µs). **Star-n-BuO** exhibited an additional absorption band near 400 nm assigned to a $n{\rightarrow}\pi^*$ transition from the alkoxy substituents, an enhanced ϕ_{PL}, and an exctinction coefficient that was one order of magnitude larger than that of **Star.** In both cases interfacial electron transfer occurred on unusually slow time scales, and charge recombination was not yet complete in 90 ms. Synthetic modifications, computational studies and binding studies to enhance injection yield are in progress and will be presented in the poster. We will also describe other new surface engineering concepts involving host-guest chemistry that are being developed in our group.
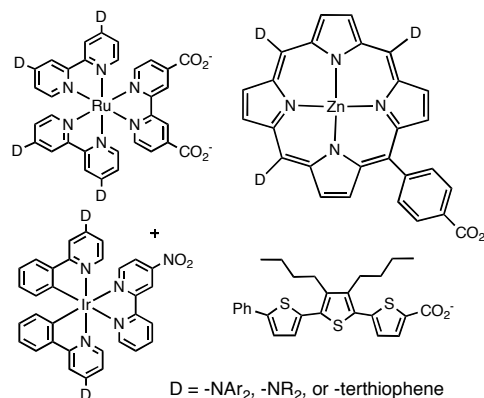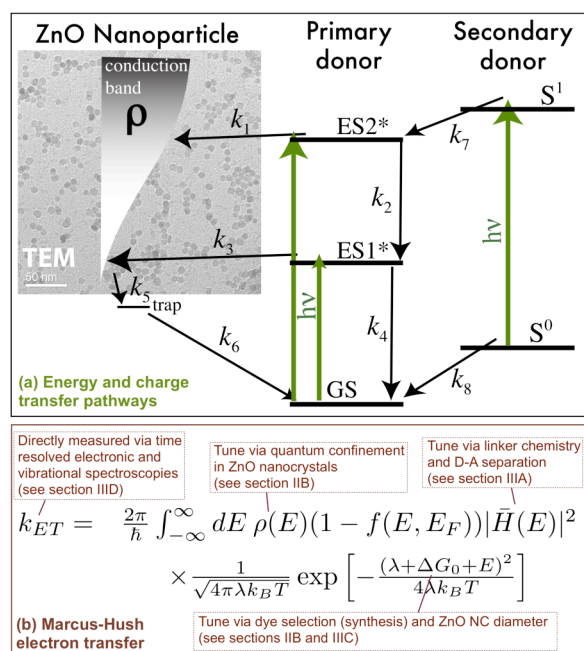

Transient absorption changes monitored at 442 nm after pulse 532 nm light excitation of Star/TiO$_2$ thin films in a 0.2 M LiClO$_4$ CH$_3$CN solution at fluences of (A)1.6, 3.7 and 7 mJ/cm^2. Overlaid are fits to a first order kinetic model, k_{obs} = 3.5 ± 1 x 10^7 s^{-1} (B) Recombination at fluence 7mJ/cm^2. (from Ref 2)

(1) Y. Zhang, E. Galoppini, P.G. Johansson, G.J. Meyer, Pure Appl. Chem., **2011**, 83, 861–868.
(2) P. G. Johansson, Y. Zhang, M. Abrahamsson, G. J. Meyer, E. Galoppini, Chem. Commun., **2011**, in press DOI: 10.1039/c1cc11210d

Excited State Charge Transfer from Dyes to ZnO Nanocrystals

A. S. Huss, A. Bierbaum, R. Hue, J. E. Saunders, R. Chitta, D. J. Ceckanowicz, K. R. Mann, D. A. Blank and W. L. Gladfelter
Department of Chemistry
University of Minnesota
Minneapolis, MN 55455

Well-defined dyads of organic or transition metal complex chromophores and ZnO nanocrystals provide a valuable platform to examine charge transfer events across this important interface (section a of the figure). The overarching goal of this research is to study the relationship between structure, energetics, and dynamics in a set of synthetically controlled donor-acceptor dyads and triads. Monodispersed ZnO NCs in the quantum-confined regime (< 6 nm in diameter), prepared by published methods, are used as a dispersible platform to which a variety of sensitizers (see structures below) are attached for study using ultrafast spectroscopic techniques. Dye binding to the ZnO NCs is measured using static fluorescence measurements. Ultrafast spectroscopy is used to evaluate charge transfer rates from the dye excited state to the ZnO NC. Spectroelectrochemistry of the oxidized dyes provides an invaluable comparison to the pump-probe spectroscopy. The effect of NC size and the energy of the excited state of the dye will be described and is understood using Marcus-Hush theory (section b of the figure). The initial results of dyads using porphyrin- and terthiophene-based dyes have been published.[1-3] This poster will focus on the recent variations involving modified donors.

(a) Energy and charge transfer pathways

Directly measured via time resolved electronic and vibrational spectroscopies (see section IIID)

Tune via quantum confinement in ZnO nanocrystals (see section IIB)

Tune via linker chemistry and D-A separation (see section IIIA)

$$k_{ET} = \frac{2\pi}{\hbar} \int_{-\infty}^{\infty} dE \, \rho(E)(1 - f(E, E_F))|\bar{H}(E)|^2$$
$$\times \frac{1}{\sqrt{4\pi\lambda k_B T}} \exp\left[-\frac{(\lambda + \Delta G_0 + E)^2}{4\lambda k_B T}\right]$$

(b) Marcus-Hush electron transfer

Tune via dye selection (synthesis) and ZnO NC diameter (see sections IIB and IIIC)

D = -NAr$_2$, -NR$_2$, or -terthiophene

References:
1. Huss, A. S.; Rossini, J. E.; Ceckanowicz, D. J.; Bohnsack, J. N.; Mann, K. R.; Gladfelter, W. L.; Blank, D. A. *J. Phys. Chem. C*, **2011**, *115*, 2-10.
2. Rossini, J. E.; Huss, A. S.; Bohnsack, J. N.; Blank, D. A.; Mann, K. R.; Gladfelter, W. L. *J. Phys. Chem. C*, **2011**, *115*, 11-17.
3. Huss, A. S.; Bierbaum, A, Chitta, R.; Ceckanowicz, D. J.; Mann, K. R.; Gladfelter, W. L.; Blank, D. A. *J. Am. Chem. Soc.*, **2010**, *132*, 13963-13965.

Bidirectional Energy Transfer and Excitonic Coupling in Carotenoid Tetrapyrrole Dyads

Smitha Pillai,[1] Miroslav K. Kloz,[2] Gerdenis Kodis,[1] John T. M. Kennis,[2] Rienk van Grondelle,[2] Peter Jomo Walla[3,4], Pen-Nan Liao[3], Devens Gust[1], Thomas A. Moore[1], Ana L. Moore[1]

[1]Department of Chemistry & Biochemistry and Center for Bioenergy and Photosynthesis, Arizona State University, Tempe, AZ, 85287; [2]Department of Biophysics, Division of Physics and Astronomy, Vrije Universiteit, 1081, Amsterdam; [3]Technische Universität Braunschweig, Institute for Physical and Theoretical Chemistry, Department for Biophysical Chemistry, Hans-Sommer-Strasse 10, 38106 Braunschweig, Germany; [4]Max Planck Institute for Biophysical Chemistry, Department of Spectroscopy and Photochemical Kinetics, Am Fassberg 11, 37077 Göttingen, Germany

Understanding the control of energy and mass flux through photosynthesis is key to optimizing its performance and that of artificial photosynthetic systems in order to better meet societal energy needs. In photosynthetic membranes, carotenoid pigments act as both energy quenchers that reduce the yield of photosynthesis and light harvesters that enhancing the collection of the solar spectrum. In order to unravel this apparent paradox, a series of dyads (Car-Pc) featuring a secondary amine group as a bridge between a carotenoid (Car) and a phthalocyanine (Pc) have been prepared. The carotenoid moieties contain 8 to 11 conjugated double bonds in addition to a phenyl group.

The S_1 state of Pc (^{1}Pc) is considerably quenched by the attached Car in both polar and non-polar solvents (1). In toluene quenching increases monotonically with the length of the conjugated
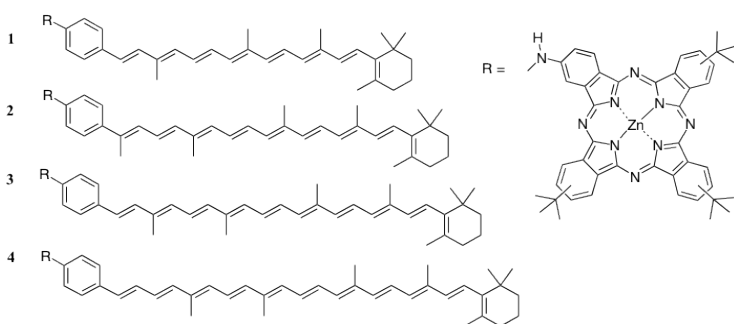
polyene, and is consistent with quenching by singlet energy transfer from ^{1}Pc to the carotenoid. In addition, pump-probe spectroscopy (both Car (488 nm) and Pc (670 nm) excitation) yields evolution associated difference spectra in which a ^{1}Car state signature was present in the transient spectra immediately after Pc excitation. This observation cannot be described with only a sequential Car-^{1}Pc → ^{1}Car-Pc energy transfer scheme. Steady state fluorescence excitation studies using two-photon excitation to populate the dipole-forbidden ^{1}Car state in **1** and **3** revealed efficient energy transfer ^{1}Car-Pc → Car-^{1}Pc (2). Thus, in these molecules, singlet excitation energy flows between the two chromophores in both directions. This phenomenon is explained by the presence of excitonic coupling between the ^{1}Pc and ^{1}Car states, as has been proposed in LHCII. The fluorescence data in polar solvents indicate stronger quenching of ^{1}Pc, and in THF transient absorption experiments on **3** clearly show absorption characteristic of both Car$^{\bullet+}$ and Pc$^{\bullet-}$, indicating photoinduced electron transfer.

(1) M. Kloz, S. Pillai, G. Kodis, D. Gust, T. A. Moore, A. L. Moore, R. van Grondelle, J. T.M. Kennis, *J. Am. Chem. Soc.* **2011**, *ASAP*. (2) P.-N. Liao, S. Pillai, D. Gust, T. A. Moore, A. L. Moore, and P. J. Walla, *J. Phys. Chem. A* **2011**, *ASAP*.
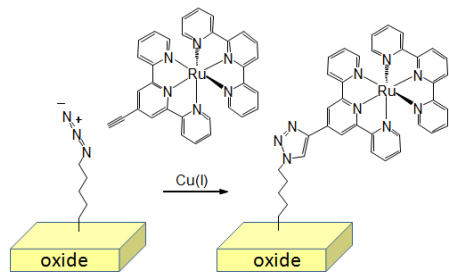
Hybrid Molecule-Surface Architectures and Charge Transfer at Metal Oxide Surfaces

Michelle Benson, Lee Bishop, Jixin Chen, Rose Ruther, James Gerken,
Matthew Rigsby, Shannon Stahl, and <u>Robert J. Hamers</u>
Department of Chemistry
University of Wisconsin-Madison
Madison, WI 53706

Molecular interfaces to metal oxides play a central role in many emerging solar photovoltaic and photocatalytic processes. Our work focuses on developing and implementing new strategies for preparing well defined molecular interfaces to metal oxides, and characterizing the resulting interfacial charge-transfer characteristics relevant to solar photochemistry.

We have recently developed a modular approach to interface metal oxide semiconductors with molecular and/or inorganic sensitizers by making use of the Copper-catalyzed Azide-Alkyne Cycloaddition (CuAAC) Reaction, one form of "click" chemistry. A key advance has been to develop a method to functionalize metal oxides with reactive azide groups that can then be linked to any of a variety of molecules or used to link to other inorganic nanoparticles to form nanoparticle dyads. As model systems we have been investigating covalently linked adducts of $[Ru(tpy)_2]^{2+}$ organometallic complexes (see figure at left), ferrocene (a model redox-active molecule) and simple porphyrins onto surfaces of SnO_2, andn ZnO. We tested the stability of the $[Ru(tpy)_2]^{2+}$ complex and associated molecular scaffolding on carbon surfaces and successfully oxidized and reduced the complex more than one million times to >1.35 V vs. NHE with only minimal degradation, thereby establishing the intrinsically high stability of the $[Ru(tpy)_2]^{2+}$ complex and the associated molecular scaffold. To test electron injection from $[Ru(tpy)_2]^{2+}$ into metal oxides, we used time-resolved surface photovoltage (TR-SPV) measurements as depicted at left. The results show that the modular "click" chemistry developed here leads to molecule-metal oxide interfaces with excellent charge-transfer characteristics. One notable result from these studies is that the use of a few-carbon chain (here, n=4) greatly enhances the range of chemical methodologies available and does not adversely impact charge transfer at the interface.

We have also been investigating alternative methods of forming molecular interfaces to metal oxides by taking advantage of the ubiquitous surface hydroxyl groups. We demonstrate a new simple approach to formation of uniform self-assembled monolayers on ZnO surfaces, with measurements on single crystal ZnO (10-10) surfaces showing highly conformal coatings even over 1-atom high atomic steps. Initial results using this approach to link porphines to metal oxides and the resulting photo charge-transfer properties will be presented.
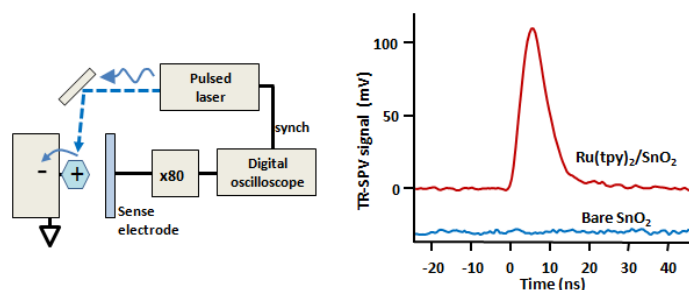
Synthesis and Characterization of TiO$_2$-Photosensitizer-Polyoxometalate Photocatalytic Triadic Systems for H$_2$O Splitting

John Fielden, Zhuangqun Huang, Yurii V. Geletii, William Rodriguez,
Djamaladdin G. Musaev, Tianquan Lian, Craig L. Hill
Department of Chemistry, Emory University, Atlanta, GA 30322

Our efforts to develop and understand new photocatalytic water-splitting systems have continued in the past year with the discovery of a new family of efficient cobalt and ruthenium polyoxometalate (POM) molecular water oxidation catalysts (WOCs). Concurrently, we have developed a new multifunctional polypyridyl ruthenium dye (**Crown2P2**) which simultaneously serves as a photosensitizer and a catalyst immobilizer. **Crown2P2** has been designed to assemble a triadic system by binding to TiO$_2$ through phosphonic acid groups, while using a metallated crown ether to recognize the POM via electrostatic and/or weak coordinative interactions. In this poster, we present the assembly of this triadic photoanode and investigation of its properties by various static and ultrafast spectroscopic techniques and computational methods.
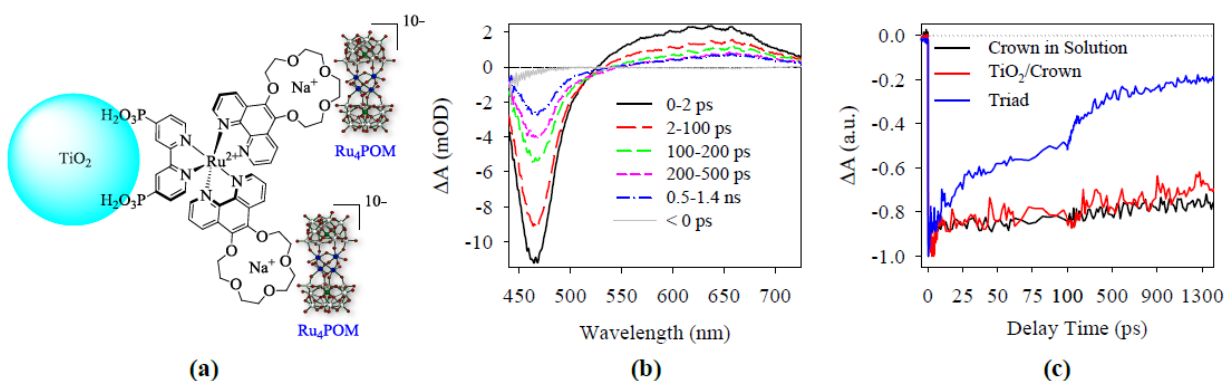
Figure 1. a) Schematic view of the TiO$_2$-**Crown2P2**-Ru$_4$POM photocatalytic system; b) Transient spectra and c) kinetics indicating regeneration of the **Crown2P2** ground state.

Crown2P2 is synthesized from a crown-ether appended phenanthroline and 2,2'-bipyridine-4,4'-diphosphonic acid ligands, using well-established procedures for preparing Ru-polypyridyl complexes. Its electronic and geometrical structures are studied by various computational techniques. Uptake of the dye onto nanoporous titania films is completed within a few hours, and in the presence of Na$^+$, the POM-WOC is adsorbed onto the **Crown2P2** sensitized films within minutes. A typical case is shown in Figure 1, where a Ru-based catalyst, [{Ru$_4$O$_4$(OH)$_2$(H$_2$O)$_4$}(γ-SiW$_{10}$O$_{36}$)$_2$]$^{10-}$ (Ru$_4$POM), is removed from aqueous solution by **Crown2P2** and immobilized on the photoanode surface. Femtosecond/nanosecond transient absorption studies suggest that excited **Crown2P2** is efficiently quenched by ultrafast electron transfer to TiO$_2$, leading to the generation of the oxidized dyes. In the presence of WOCs, the ground state of **Crown2P2** is regenerated within 1 ns by efficiently taking electrons from the attached WOCs. The resulting long-lived charge-separated state (with electrons in TiO$_2$ and oxidized WOCs) is required for efficient water oxidation on a photoanode. Ongoing studies aim to optimize the photoelectrochemical conditions for water splitting, examine how charge recombination competes with the oxidation of water in a working cell, and explore various strategies for improving the chemical and quantum yields.

Interfacial Charge Separation and Recombination Dynamics in Photocatalytic Systems Consisting of α-Fe₂O₃ and Carbon-Free Water Oxidation Catalysts

Zhuangqun Huang, Zhen Luo, William Rodriguez, John Fielden, Yurii V. Geletii, Zheng Liu, Naifei Zhang, James W. Vickers, Warrick S. Macmillan, Kenneth J. McDonald, Kyoung-Shin Choi, Djamaladdin G. Musaev, Craig L. Hill, Tianquan Lian

Department of Chemistry, Emory University, Atlanta, GA 30322; Department of Chemistry Purdue University, West Lafayette, Indiana 47907

We have investigated our recently developed fast, stable and soluble water oxidation catalysts, $[\{Ru_4O_4(OH)_2(H_2O)_4\}(\gamma\text{-}SiW_{10}O_{36})_2]^{10-}$ **(Ru₄POM)** and $[Co_4(H_2O)_2(PW_9O_{34})_2]^{10-}$ (Co₄POM), in photodriven water oxidation systems. We demonstrated that water oxidation takes place under light with polypyridyl ruthenium dyes as photosensitizers and persulfate as a sacrificial electron acceptor.[1-4] As polypyridyl-based dyes are destructively oxidized under catalytic turnover conditions, the use of oxidatively stable fully-inorganic photosensitizers is an attractive approach to developing viable light-driven water splitting systems. From this vantage, nanoporous colored (narrow bandgap) iron oxide (hematite, α-Fe₂O₃) is a promising photosensitizer. Here, we report photocatalytic activity of Ru₄POM and Co₄POM sensitized by iron oxide films.
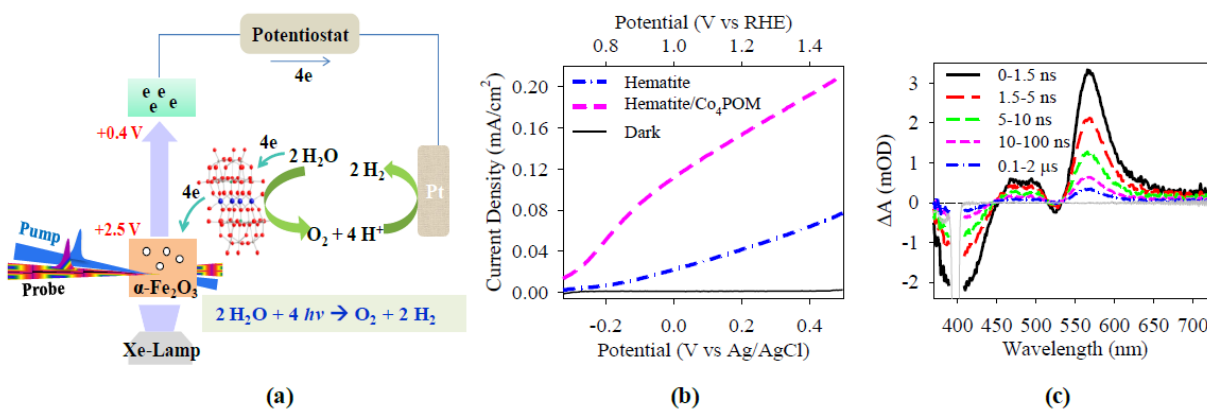
Figure 1. (a) Time-resolved spectro/photo-electrochemical experimental (S/PEC) scheme; (b) PEC behavior of photoanodes; and (c) nanosecond-transient spectra of the photoanode

We have now prepared α-Fe₂O₃/Ru₄POM or α-Fe₂O₃/Co₄POM dyads and characterized them by various static and time-resolved spectroscopic and photoelectrochemical techniques, as well as computational (VASP) approaches. We observed that in the photo-electrochemical cell consisting of these photoanodes and Pt cathodes, O₂ was evolved from water. In the presence of Co₄POM, the photocurrent is enhanced approximately four-fold at an external bias of 1.23 V vs RHE at pH 13.6 (Figure 1). We have also carried out transient absorption studies of interfacial charge separation and recombination dynamics in these dyads. The transient spectra show an absorption peak at 570 nm that can be attributed to trapped electrons in α-Fe₂O₃.[5] The dynamics of hole capture by the catalysts and electron-hole recombination in the Fe₂O₃/Co₄POM or Fe₂O₃/Ru₄POM dyads under the device working conditions are under investigation.

References: (1) Huang, Z. et. al., *J. Am. Chem. Soc.*, **2011**, *133*, 2068, (2) Besson, C. et. al., *Chem. Comm.* **2010**, *46*, 2784; (3) Geletii, Y. V. et. al., *J. Am. Chem. Soc.*, **2009**, *131*(22), 7522, (4) Yin, Q. et. al. *Science*, **2010**, *328*, 342.; (5) Dimitrijevic, N. M. et. al., *J. Phys. Chem.* **1984**, *88* (19), 4278

Artificial Photosynthetic Assemblies Directed Toward Reduction of CO_2

Benjamin M. Lovaasen, Davis Moravec, Daniel C. O'Hanlon, and <u>Michael D. Hopkins</u>
Department of Chemistry
The University of Chicago
Chicago, Illinois 60637

Molecular assemblies that contain luminescent tungsten–alkylidyne (WCR) complexes produce the highly reducing excited states necessary to drive the photochemical conversion of CO_2 to solar fuels, and participate in proton-coupled electron-transfer reactions that offer the possibility of deriving reducing equivalents without conventional sacrificial donors. The porphyrin/tungsten–alkylidyne dyads shown in the figure implement these properties in a platform that combines broad spectral coverage, controllable excited-state energy- and electron-transfer dynamics, and convenient means for catalyst attachment.

In polar solvents, dyads **1**, **1′**, and **2′** have been found to produce the strongly reducing $[Zn(TPP)]^-–[W]^+$ charge-separated state ($E_{1/2}^{0/-} = -1.85$ V vs $FeCp_2^{0/+}$) upon porphyrin excitation. Ultrafast vis–near-IR TA measurements show that the kinetics of charge separation and recombination are controlled by the torsion angle of the meso aryl group and length of the phenylene-ethynylene bridge connecting the subunits (τ_{CR}(THF): **1**, 425 ps; **1′**, 1.3 ns; **2′**, >5 ns). The highly reducing CS state can be harvested by Zn-ligated acceptors; for example, in triad **1′**(PI) the

1: R = H, *n* = 1
1′: R = Me, *n* = 1
2′: R = Me, *n* = 2

initial CS state rapidly decays to $[PI]^-–[Zn(TPP)]–[W^+]$, which is long lived (τ_{CR} 17.5 ns). Triad **1′**(Re), which contains an appended $CO_2{\rightarrow}CO$ reduction catalyst, produces the charge-separated state $[Re]–[Zn(TPP)]–[W]^+$ upon excitation; this state is the immediate precursor to the catalytically active state of the Re catalyst. Initial photochemical CO_2 reduction reactions are underway.
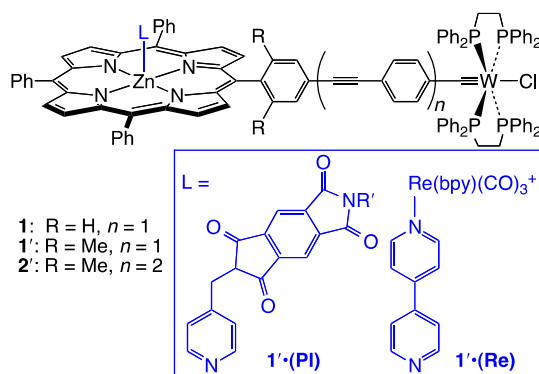
These dyads also exhibit large "lifetime reservoir" effects—an important general mechanism for lengthening the excited-state lifetimes of short-lived chromophores. We reported for **1** that intra-dyad triplet-triplet equilibrium between the emissive WCR $^3[(d_{xy})^1(\pi^*_{WCR})^1]$ state and Zn(TPP) T_1 state lengthens the WCR emission lifetime 19× compared to that of free WCR, and that enhancements of up to 1300× are achieved by tuning the equilibrium via Zn ligation (**1**L, L = pyridyl). The nature of the linkage between the Zn(TPP) and WCR units has now been shown to have a large impact on the magnitude of the lifetime-reservoir effect. Dyads **1′** and **1′**L exhibit much larger enhancements than **1** and **1**L, ranging from 125× for **1′** to ca. 6000× for **1′**L. DFT calculations and spectroscopic measurements have revealed that this improvement arises from the decrease in orbital mixing between Zn(TPP) and WCR units. Ultrafast TA measurements of **1′** indicate that Zn(TPP) $S_1{\rightarrow}T_1$ intersystem crossing is circumvented by decay through a short-lived $[Zn(TPP)]^-–[W]^+$ charge-separated state, even in nonpolar solvent. In contrast, attaching the WCR unit to Zn(TPP) via an axial dative linkage, in $[Zn(TPP)]{\cdot}pyCCC_6H_4CW(dppe)_2Cl$ quenches Zn(TPP) S_1 fluorescence without producing a lifetime reservoir effect.

Fundamental Studies of Light-induced Charge Transfer, Energy Transfer and Energy Conversion with Supramolecular Systems

Joseph T. Hupp
Dept. of Chemistry
Northwestern University
Evanston, IL 60208

This poster will describe some aspects of our current and recent work on redox shuttles that may supplant iodide/tri-iodide in liquid-junction cells that employ supramolecular structures as high-extinction sensitizers. Requiring ca. 600 mV of overpotential in order to regenrate dyes at acceptable rates, the $I^-/I_3^=$ is responsible for a very sizable portion of the power loss encountered in champion dye-sensitized solar cells. Additionally, we have shown that triiodide strongly associates with highly polarizable dyes, leading to anomalously large dark currents and thereby degrading cell photovoltages. Interestingly, chemically similar tribromide does not preferentially associate with highly polarizable dyes, so does not engender the same problems. Effective utilization, however, of bromide/ tribromide as an alternative redox shuttle requires redesign of the light harvester, gross manipulation of the semiconductor band-edge energetics, and effective passivation of sub-band-edge electronic states of the semiconductor. The poster will touch on these issues.
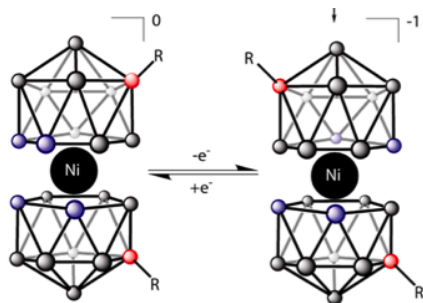
Additionally, the poster will describe the behavior of several members of a new class of redox shuttles based on Ni(IV/III) in a bis-dicarbollide coordination environment. Electron transfer to and from the nickel shuttle is slowed by oxidation-state-dependent changes in bonding between the nickel center and the dicarbollide species. As shown in the figure below, the rate of reaction of the Ni(IV) form of the new shuttle with dye-injected electrons in the semiconducting photoelectrode is about three orders of magnitude slower than the rate of reaction of injected electrons with a the oxidized half of a characteristically fast shuttle like ferrrocenium/ferrocene. At the same, the electron interception rate with Ni(IV) is about two orders of magnitude faster than the same reaction with tri-iodide. Unfortunately, Ni(IV) is still about a factor to of five too fast for the Ni shuttle to yield cell performance similar to, or better than, that of the iodide/tri-iodide couple. Current work is focused, in part, finding the next needed factor of five in back electron transfer reactivity, as this will enable dye cell photovoltages and/or photocurrents to be boosted significantly.
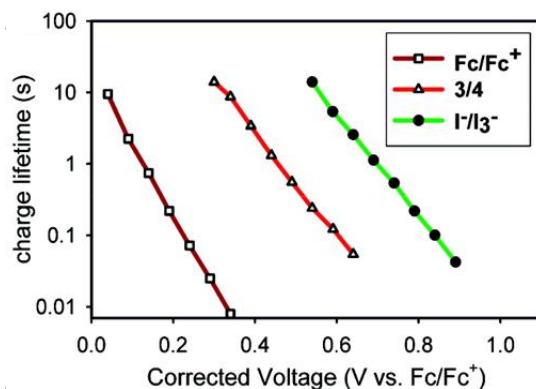
Exciton Delocalization in Cdse/Cds Nanocrystalline Heterostructures Investigated Using Polarized Optical Techniques

Eric Ryan Smith and Justin C. Johnson
National Renewable Energy Laboratory
Golden, CO 80401

Investigation of CdSe nanocrystal-seeded CdS nanorod heterostructures has led to contradicting conclusions about the nature of the excited state and band structure. Is the photogenerated exciton localized on the CdSe seed according to a type I band configuration, or do the carriers dissociate as per a type II configuration, allowing the electron to delocalize along the CdS rod? Intense interest in this topic arises from a desire to both understand fundamental charge carrier dynamics under the influence of quantum confinement and to evaluate the potential of such structures in photoconversion schemes.

The lowest exciton state of CdSe nanocrystals has levels that absorb linear or circularly polarized light depending on the angular momentum state, allowing for detection of exciton dynamics using polarized optical techniques. We investigated CdS rods seeded with 2.1, 3, and 4.4 nm diameter CdSe dots using ultrafast cross-polarized transient grating (CPTG) and polarized time-resolved photoluminescence (PL). The CPTG technique probes spin relaxation between quasi-degenerate fine structure levels, showing shape- and size-dependent exciton wavefunction evolution occurring on timescales from tens of fs to several ps. Comparison of PL lifetimes and polarization anisotropy between the heterostructure and CdSe seeds reveals changes in coupling of fine structure levels to trap states and changes in radiative efficiency of fine structure levels due to encapsulation within the rod. The results of these measurements will be used to construct a model of the exciton wavefunction dynamics.

Coupling of the photogenerated exciton to longitudinal-optical (LO) photon modes can be observed in the transient grating signal. Damping of the CPTG coherent oscillation of a CdSe/CdS sample (Figure 1a) and its evolution from containing strictly CdSe lattice components to entirely CdS lattice components (Figure 1b) helps to characterize the rate and extent of electron delocalization as a function of band offset, quantum confinement, and temperature. The combination of CPTG and polarization anisotropy promises to be a powerful tool for evaluating heterostructures that may exhibit directed charge transfer, energy transfer, or catalytic properties.
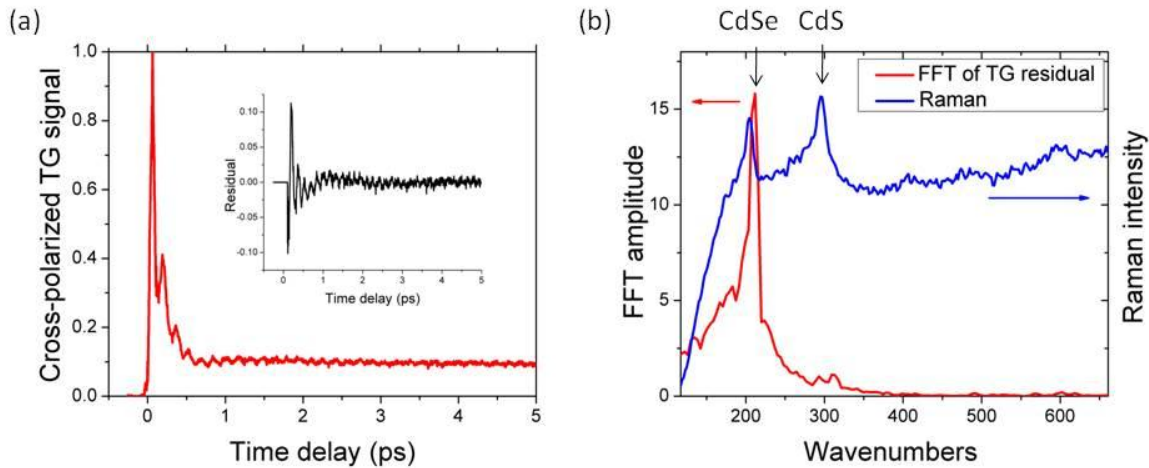
Tuning the Photophysics of Germanium Nanocrystals Through Chemistry

<u>Nathan R. Neale</u>, Daniel A. Ruddy, Justin C. Johnson, and E. Ryan Smith
Chemical and Materials Science Center
National Renewable Energy Laboratory
Golden, CO 80401

Group IV nanocrystals composed of single phase, alloyed, or doped Si, Ge, or Sn could potentially be used to form printable inks for depositing low-cost solar cells, infrared detectors and related devices that would interface well with the existing PV and microelectronics infrastructure. However, only recently have studies been carried out to characterize their optoelectronic properties primarily due to the lack of synthetic protocols for preparing well-defined samples of these quantum-confined materials.

We will present our recent efforts in exploring both the synthesis and photophysical properties of group IV nanocrystals. In particular, a solution-phase mixed-valence precursor method based on the reduction of GeI_4/GeI_2 mixtures afforded Ge nanocrystals with highly tunable sizes and optical properties.[1] The size of the nanocrystals (2.3–11.3 nm) was controlled by adjusting both the Ge(IV)/Ge(II) ratio and the temperature ramp rate following reductant injection. The NIR absorption (1.6–0.70 eV) and corresponding band-edge emission demonstrated the highly tunable quantum confinement effects in Ge nanocrystals prepared using this mixed-valence precursor method (Figure 1). For the first time, it was shown that these nanocrystals have optical properties consistent with the values expected from quantum theory, resolving longstanding issues on the nature of the optical properties of nanoscale germanium. A proposed mechanism for the observed size control, which relies upon the difference in reduction temperatures for Ge(II) versus Ge(IV), will be presented (Figure 2).
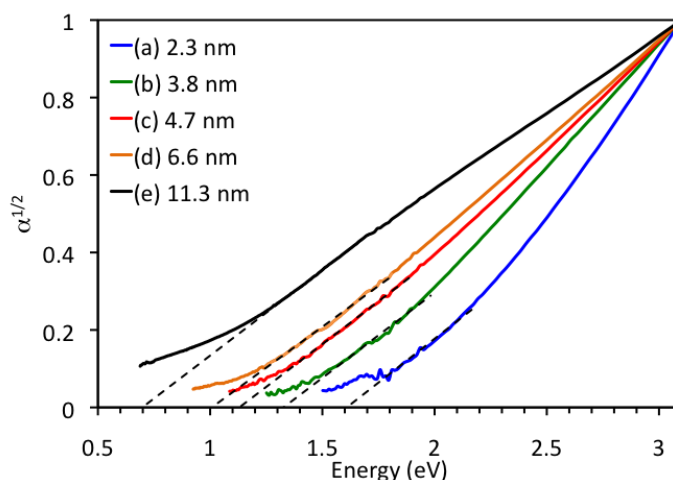
Figure 1. Tauc plot of 2.3–11.3 nm Ge nanocrystals.
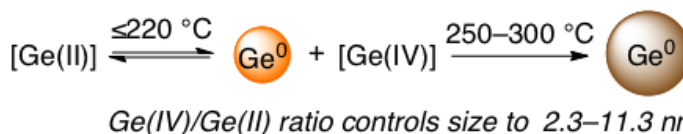
Figure 2. Proposed mechanism for Ge NC size control.

Additionally, recent results have demonstrated that this novel method has facilitated alloying these Ge nanocrystals with Si and Sn as well as doping with elements from groups III and V. We will also describe the opportunities and challenges that remain to be explored in understanding the fundamental properties of group IV nanocrystals.

1. D. A. Ruddy, J. C. Johnson, E. R. Smith and <u>N. R. Neale</u> "Size and Bandgap Control in the Solution-Phase Synthesis of Near-Infrared-Emitting Germanium Nanocrystals," *ACS Nano*, **2010**, *4*, 7459–7466. DOI: 10.1021/nn102728u

Photoinduced Electron Transfer Between CdSe Quantum Dots and Oxide Nanoparticles

Kevin Tvrdy, Ian Lightcap, Jin Ho Bang and Prashant V. Kamat
Radiation Laboratory and Department of Chemistry and Biochemistry
University of Notre Dame, Notre Dame, IN 46556

Quantum dot-metal oxide junctions provide a useful means of inducing charge separation under bandgap excitation. We have successfully employed this approach in investigating photoelectrochemical behavior of quantum dot solar cells. For the first time we have undertaken a comprehensive examination of electron transfer at QD-metal oxide junctions, using a series of CdSe quantum dot donors and metal oxide nanoparticle acceptors. Utilizing ultrafast transient absorption spectroscopy, we measured electron transfer rates from four different sizes of CdSe quantum dots (sizes 2.8, 3.3, 4.0, and 4.2nm) to three unique metal oxide species (SnO_2, TiO_2, and ZnO) (Figure 1). Electron transfer rates ranged from 1.9×10^{10} s^{-1} to 4.6×10^{11} s^{-1} and were dependent on both the QD size and the type of oxide substrate employed.
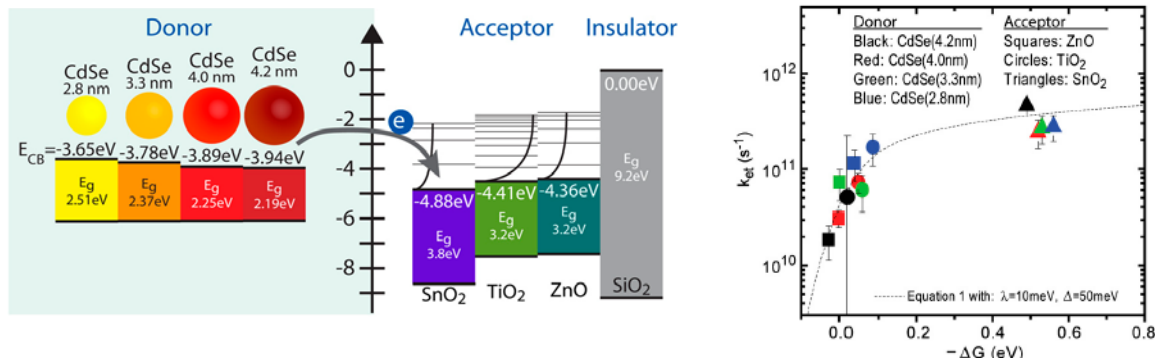
Figure 1. Left. Diagram of the relative electronic energy differences between CdSe donating species and MO accepting species. Right: Global plot of the dependence of electron transfer rate constant on the free energy change for all CdSe (donor) to MO (acceptor)

Such a dependence highlights the accuracy of the many-state Marcus model, in conjunction with our determination of change in free energy for QD to nanoparticulate MO electron transfer, over a range of CdSe QD sizes and MO accepting species. .Apparent electron transfer rate constants showed strong dependence on change in system free energy, exhibiting a sharp rise at small driving forces followed by a modest rise further away from the characteristic reorganization energy. The observed trend mimics the predicted behavior of electron transfer from a single quantum state to a continuum of electron accepting states, such as those present in the conduction band of a metal oxide nanoparticle.

Efforts are also underway to determine the energy gap dependence of electron transfer of CdSe quantum dots using C_{60} and graphene oxide as electron acceptors. The rate constants for the electron injection from excited CdSe QDs to C_{60} varied from 7.9×10^9 (4.5 nm) to 9.0×10^{10} s^{-1} (2.6 nm), respectively. As expected from Marcus theory, the electron transfer rate is dictated by the energy difference between the conduction band of CdSe and LUMO of C_{60}. These findings of electron transfer at the quantum dot-electron acceptor interface will enable to elucidate the key role of excited state interactions of quantum dots in determining overall device efficiency.

Surface Charge and Piezoelectric Fields Control Auger Recombination in Semiconductor Nanocrystals

Zhong-Jie Jiang and David F. Kelley
University of California, Merced
Merced, CA 95343

The dynamics of biexcitons in spherical and rod-shaped CdSe nanoparticles are examined as a function of the magnitudes of internal electric fields. These studies show that the presence of strong internal fields results in rapid Auger recombination. The strengths of the electric fields and hence the Auger recombination rates are controlled in three different ways: first, by varying the dielectric constant of the surrounding solvent; second, by changing the particle surface stoichiometry and hence the magnitude of surface charges; and third, by inducing a piezoelectric field through the deposition of a lattice-mismatched shell material. The dependence on solvent dielectric constant is shown in the figure below.
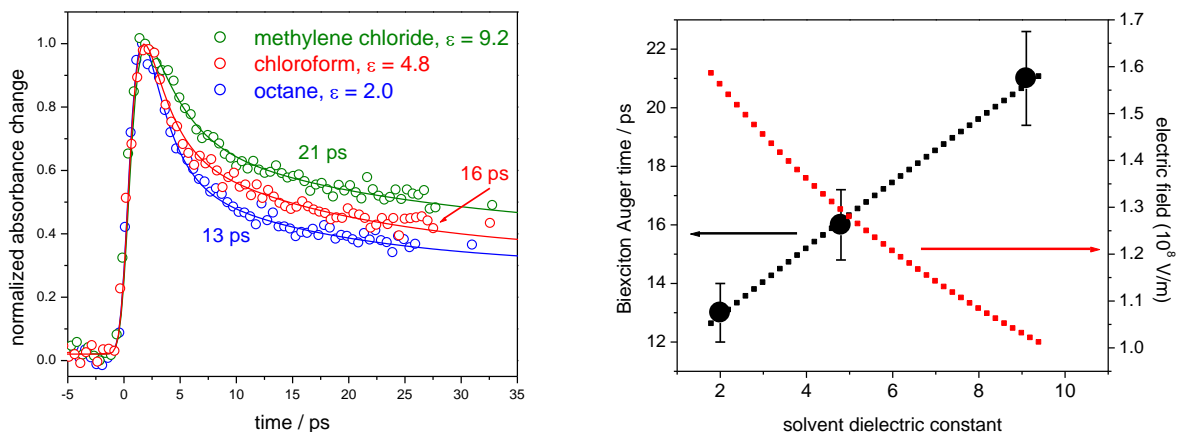
Left panel) Transient bleach kinetics for the lowest energy transition of 3.2 nm wurtzite CdSe nanocrystals in octane, chloroform and methylene chloride. The fast decay component is in all cases about 2 ps and corresponds to nonradiative electron-hole recombination at surface defects. The decay time of the intermediate component is indicated and is assigned to the biexciton AR times. The long components decay very slowly and are assigned to decay of single excitons. Right panel) Calculated internal electric field intensities (red dotted curve) and relative Auger recombination times (black dotted curve) as a function of external dielectric constant. Also shown are the experimentally determined AR times (large black dots).

Auger recombination times depend upon the extent to which the internal electric fields mix conduction band levels, which is easily calculated. Auger recombination is a momentum forbidden process and Fourier transformation shows that higher conduction band states have large momentum components that relax the momentum conservation constraints. The experimental results can therefore be understood in terms of mixing of higher conduction band states with the lowest state, from which recombination occurs.

The Mechanism of Solar Water Oxidation: Pulsed Multi-Frequency Multi-Dimensional EPR Spectroscopy Studies of Photosystem II

R. Chatterjee, S. Milikisiyants, C. Coates and K. V. Lakshmi
Department of Chemistry and Chemical Biology and
The Baruch '60 Center for Biochemical Solar Energy Research
Rensselaer Polytechnic Institute
Troy, NY 12180

The solar water-splitting protein complex, photosystem II (PSII), catalyzes one of the most energetically demanding reactions in Nature by using light energy to drive water oxidation. The four-electron water oxidation reaction occurs at the tetranuclear manganese-calcium-oxo (Mn_4Ca-oxo) cluster that is present in the oxygen-evolving complex of PSII. Proton-coupled electron transfer (PCET) reactions, which are exquisitely tuned by smart protein matrix effects, are central to the water-oxidation chemistry of PSII. However, the details of PCET processes are not yet understood because of the inability of conventional methods to probe these processes. A major challenge is to develop methods to directly investigate the mechanism of PCET reactions. We will describe ongoing efforts in our laboratory to understand the tuning and regulation of the PCET reactions of PSII. We are developing two-dimensional (2D) hyperfine sublevel correlation spectroscopy methods that provide direct 'snapshots' of the photochemical intermediates of the Mn_4Ca-oxo,[1-2] tyrosine and quinone[3-5] cofactors of PSII.

References:

1. S. Milikisiyants, R. Chatterjee, A. Meenaghan, C. Coates and K. V. Lakshmi (2010) *J. Phys. Chem. B*, 114, 10905.

2. S. Milikisiyants, R. Chatterjee and K. V. Lakshmi (2011) *J. Phys. Chem. B*, Manuscript Submitted.

3. R. Chatterjee, S. Milikisiyants, C. Coates and K. V. Lakshmi (2011) *Biochemistry*, 50, 491.

4. N. Srinivasan, R. Chatterjee, S. Milikisiyants, J. H. Golbeck and K. V. Lakshmi (2011) *Biochemistry*, 50, 3495.

5. A. M. Weyers, R. Chatterjee, S. Milikisiyants and K. V. Lakshmi (2009) *J. Phys. Chem. B*, 113, 15409.

Increasing the Speed Limit for Hole Hopping on the DNA π-Way

Frederick D. Lewis
Department of Chemistry
Northwestern University
Evanston, Il 60208

Hole transport over long distances in DNA occurs via an incoherent multi-step hopping mechanism. We recently reported the measurement of distance- and temperature-dependent rate constants for charge separation in capped hairpins in which a stilbene hole acceptor and hole donor are separated by a A_n or A_3G_n diblock polypurine sequence consisting of 3 adenines and 1-19 guanines (Figure 1a).[1] The short A_3 block serves as a rectifier, preventing charge recombination once the hole has entered the G_n block (Figure 1b). The longer diblock systems obey the simplest model for an unbiased random walk, providing a direct measurement of $k_{hop} = 4.3 \times 10^9$ s^{-1} for a single reversible G-to-G hole hopping step. This is somewhat faster than the value of 1.2×10^9 s^{-1} calculated from our data for A-tract hole hopping in A_n systems using a kinetic model.[2] The temperature dependence for hopping in A_3G_{13} provides values of $E_{act} = 2.8$ kcal/mol and $A = 7 \times 10^9$ s^{-1}, consistent with a weakly-activated, conformationally-gated process.

Significantly slower rate constants are observed for hopping in alternating or random base sequences. Thus DNA hole transport via natural base pairs is a slow process, at best. A recent report by Kawai et al. suggests that faster hole transport might be possible using modified bases deazaadenine (^ZA) in place of the natural bases A or G.[3] We are currently investigating the efficiency and dynamics of hole transport in diblock and triblock systems possessing A, G, and ^ZA bases (Figure 2). The results show a significant increase in both the quantum yield for charge separation and the hole transport time for $A_2{}^ZA_n$ vs. A_2G_n systems. Data for longer diblock systems provide a value of $k_{hop} = 4 \times 10^{10}$ s^{-1} for ^ZA hopping, an order of magnitude faster than for G hopping.
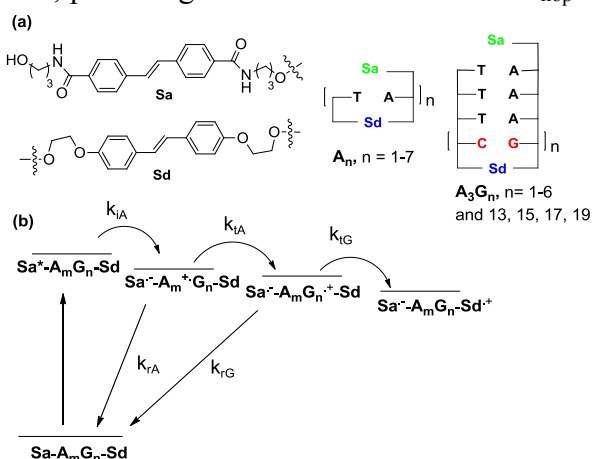
Figure 1. (a) Structures of Sa and Sd chromophores and Sa/Sd capped hairpins having An base sequences and A3Gn diblock sequences. (b) Simplified mechanism for charge separation in AmGn diblock systems.

A$_2{}^Z$A$_2$
$\Phi_{cs} = 0.56$
$\tau = 52$ ps

A$_2$G$_2$
$\Phi_{cs} = 0.38$
$\tau = 220$ ps

A$_2{}^Z$A$_4$
$\Phi_{cs} = 0.41$
$\tau = 150$ ps

A$_2$G$_4$
$\Phi_{cs} = 0.32$
$\tau = 1000$ ps
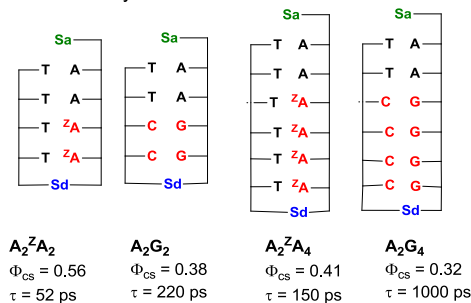
Figure 2. Comparison of charge separation efficiency and dynamics in A$_2{}^Z$A$_n$ vs. A$_2$G$_n$ systems.

(1) (a) Mickley Conron, S. M.; Thazhathveetil, A. K.; Wasielewski, M. R.; Burin, A. L.; Lewis, F. D. *J. Am. Chem. Soc.* **2010**, *132*, 14388; (b) Vura-Weis, J.; Wasielewski, M. R.; Thazhathveetil, A. K.; Lewis, F. D. *J. Am. Chem. Soc.* **2009**, *131*, 9722.

(2) Blaustein, G. S.; Lewis, F. D.; Burin, A. L. *J. Phys. Chem. B* **2010**, *114*, 6732.

(3) Kawai, K.; Kodera, H.; Osakada, Y.; Majima, T. *Nature Chem.* **2009**, *1*, 156.

Solar Energy Conversion Properties of Zn_3P_2 and Cu_2O Absorbers

Gregory M. Kimball, Chengxiang Xiang, Nathan S. Lewis
Department of Chemistry and Chemical Engineering
California Institute of Technology
Pasadena, California 91125

Zinc phosphide (Zn_3P_2) and cuprous oxide (Cu_2O) are promising materials for solar energy conversion and have received renewed interests after early work in 1980s. The performance of these materials in solar energy conversion has been limited by surface defects and reactivity, motivating the need to prepare interfaces that are electrically passive and chemically inert.

We demonstrate a chemical treatment for Zn_3P_2 that shows significant improvement over basic etching procedures (Figure 1). The defective, as-polished surface is etched with Br_2:MeOH to produce a surface for which room temperature steady-state photoluminescence (PL) is observed. The Br-etched surface is free of zinc and phosphorus oxides, but has 2-3 monolayers of residual elemental phosphorus. Treating the surface with dilute $HF:H_2O_2$ (aq) is shown to reduce the residual elemental phosphorus (<1 monolayer) and result in a 3-fold enhancement in steady-state band edge PL intensity. Time-resolved PL decays show that $HF:H_2O_2$ treatment decreases the surface recombination velocity (SRV) of Br-etched Zn_3P_2 samples from 2.8×10^4 to 1.0×10^4 cm/s.

We use semiconductor/liquid junctions to investigate the energy-conversion properties of large-grain Cu_2O photoelectrodes (Figure 2). In contact with the decamethylcobaltocene$^{+/0}$ ($Me_{10}CoCp_2^{+/0}$) redox couple, Cu_2O yields open-circuit voltage, V_{oc}, values of 820 mV and short-circuit current density, J_{sc}, values of 3.1 mA cm^{-2} under simulated air mass 1.5 illumination. X-ray photoelectron spectroscopy and Auger electron spectroscopy indicate that the photoelectrodes have a high-quality cuprous oxide surface and reveal no observable photocorrosion during operation in the nonaqueous electrolyte. The high open-circuit voltages of p-Cu_2O/liquid junctions demonstrate that high efficiency solid-state junctions may be realized with rigorous control of the surface chemistry and surface passivation of p-Cu_2O absorbers.
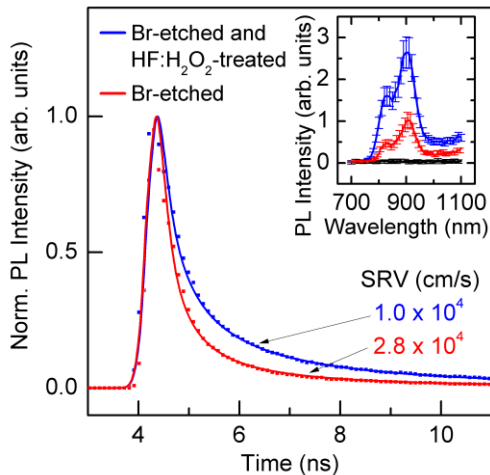
Figure 1. Photoluminescence (PL) data demonstrate the improved quality of chemically-treated Zn_3P_2 surfaces. Time-resolved PL decays show a reduction in surface recombination velocity (SRV) and inset shows enhanced steady-state PL from $HF:H_2O_2$ treatment.
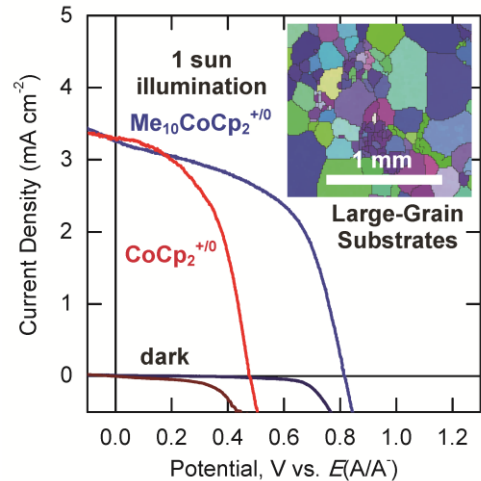
Figure 2. 820 mV open-circuit voltages were observed from Cu_2O photoelectrodes in contact with the decamethylcobaltocene$^{+/0}$ ($Me_{10}CoCp_2^{+/0}$) redox couple. Inset shows an electron diffraction image of the grain structure in Cu_2O substrates.

Photochemical and Photovoltaic Properties of Conjuaged Ionomer Junctions

Thomas J. Mills, Stephen G. Robinson, Ethan M. Walker, Chris Weber and <u>Mark C. Lonergan</u>
Department of Chemistry
University of Oregon
Eugene, OR 97403

The photochemical and photovoltaic properties of two types of systems based on ionically functionalized conjugated polymers (conjugated ionomers or polyelectrolytes) are being studied. Both contain sources of asymmetry that are different from the band offsets conventionally used to generate a photovoltaic effect in organic semiconducting systems. The first involves the junction between undoped (intrinsic) ionomers with differing signs of mobile ions. This asymmetry in ion content can drive the photochemical formation of a p-n junction and in turn a photovoltaic effect. Our recent work in this area has been in quantifying and understanding charge injection, both photoinduced and from electrified interfaces. Extensive analysis of a drift/diffusion/Poisson model (e.g. see Fig. 1) is being used to help quantify levels of charge injection as well as the factors limiting charge transport and ultimately solar energy conversion. Ion exchange is also being used as a tool to probe the dependence of junction properties on factors such as ion mobility, and it has also revealed some very unexpected results relating to the ability of a sulfonate group paired with alkali metal ions to stabilize the polyacetylene-oxygen charge-transfer complex.
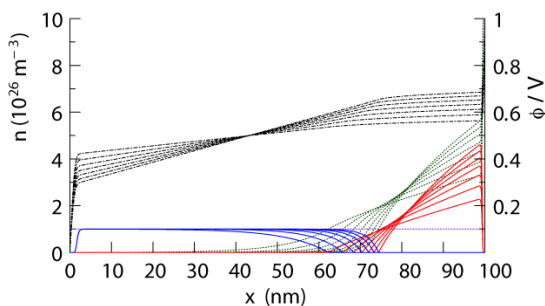
Fig. 1. Profiles of electrons (blue), holes (red), anions (green), cations (purple) and electrostatic potential (black, dashed) calculated for a mixed ionic electronic conductor possessing one type of mobile ion (anions) in the high injection regime.
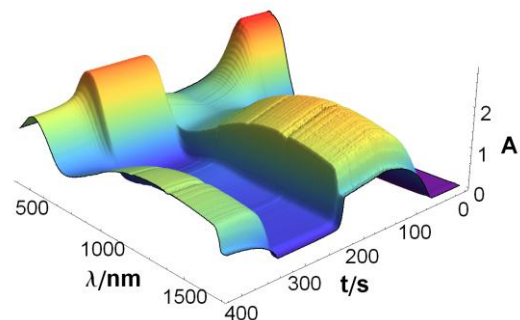
Fig. 2. Spectroelectrochemistry following the formation of a p-n junction using a polyelectrolyte-mediated electrochemical approach. The relative absorbances are used to quantify doping levels.

The second system involves the junction between a p-doped conjugated anionomer and an n-doped conjugated cationomer. We have developed internal compensation, where bound ionic functional groups compensate charge injected into the polymer backbone, as a means of stabilizing these types of junctions. The junctions are synthesized using a polyelectrolyte-mediated electrochemical approach. Our recent work has focused on using this approach to study the dependence of junction properties on doping level (see Fig. 2), primarily as a means of understanding the connection to more conventional p-n junctions. Impedance analysis has demonstrated that ionomer-based p-n junctions do not show the same type of depletion effects as their more conventional counterparts. We have also worked to extend the polyelectrolyte-mediated approach to a wider range of systems, including ionically functionalized C_{60}s.

Photoelectrochemistry, Electronic Structure, and Bandgap Sizes
of Semiconducting Cu(I)-Niobates

Paul A. Maggard
Department of Chemistry
North Carolina State University
Raleigh, NC 27695-8204

Semiconducting metal-oxides have remained of intense research interest owing to their potential for achieving efficient solar-driven photocatalytic reactions in aqueous solutions that occur as a result of their bandgap excitation. The photocatalytic reduction of water or carbon dioxide to generate hydrogen or hydrocarbon fuels, respectively, can be driven on p-type (photocathodic) electrodes with suitable band energies. However, metal-oxide semiconductors are typically difficult to dope as p-type with a high mobility of carriers. Recently, our research has focused on the investigation of new p-type $CuNbO_3$ film electrodes that can be prepared on FTO glass. Photoelectrochemical measurements were carried out using a three electrode system, with $CuNbO_3$ film as the working electrode. Under chopped visible-light irradiation, a strong photon-driven cathodic current is observed that confirms the p-type semiconductor behavior of the $CuNbO_3$ electrode, illustrated in Figure 1. Incident-photon-to-current efficiencies are measured that approach greater than ~5%, with the film exhibiting good resistance to photocorrosion over many hours. Electronic-structure calculations based on density functional theory reveal the visible-light absorption stems from a nearly-direct bandgap transition involving a copper-to-niobium (d^{10} to d^0) charge-transfer excitation, shown in Figure 1, that occurs across a bandgap of ~2.0 eV.

New high-purity flux syntheses of several Cu(I)-niobates and related tantalates have been achieved, and which have enabled their full structural determination, as well as new investigations of their optical and photoelectrochemical properties and electronic structures via density-functional theory

Figure 1. Upper, current-potential curve in an aqueous solution under chopped visible light irradiation for a $CuNbO_3$ electrode. Lower, plot of electron density for the highest valence (blue) and lowest conduction band (red) energy levels from DFT calculations.

calculations. For example, using either a CuCl or Cu_2O molten flux at high temperatures, both $CuNb_3O_8$ and $CuNb_{13}O_{33}$ were prepared in high purity and their structures were characterization by both single-crystal and powder X-ray diffraction techniques. Diffuse reflectance measurements exhibited optical bandgap sizes of ~1.47 eV and ~2.25 eV for $CuNb_3O_8$ and $CuNb_{13}O_{33}$, respectively. Our most recent progress will be presented that has focused on detailed investigations of their electronic structures, as well as their preparation as p-type or n-type doped thin film forms for new photoelectrochemical investigations.

Nanostructured Photocatalytic Water Splitting Systems

Yixin Zhao, Nella M. Vargas-Barbosa, Emil A. Hernandez-Pagan, Seung-Hyun Anna Lee,
John R. Swierk, Deanna R. Lentz, Nina I. Kovtyukhova, and Thomas E. Mallouk
Department of Chemistry,The Pennsylvania State University, University Park, PA 16802

Thomas A. Moore, Ana L. Moore, and Devens Gust
Department of Chemistry and Biochemistry, Arizona State University, Tempe, AZ 85287

The goal of our DOE-supported work is to explore the assembly and electron/proton transfer kinetics of molecular photoanode and photocathodes for visible light-driven water splitting. The photoanodes are high surface area TiO_2 electrodes coupled to ruthenium polypyridyl or porphyrin sensitizers, which are themselves linked to water oxidation catalysts. The photocathodes are donor-acceptor assemblies grown layer-by-layer on high surface area transparent conductor substrates and coupled to hydrogen evolution catalysts. Electrochemical and transient spectroscopic techniques are used to study the kinetics of the individual components and donor-acceptor diads, as well more complex systems assembled from them.

In the photoanode, our focus over the past year has been to understand and control back electron transfer between TiO_2 and the oxidized sensitizer molecule, lateral electron transfer between dye molecules, and proton transport. To study these effects systematically we developed an improved synthesis for ligand-free iridium oxide nanoparticles. Cold acid condensation of $[Ir(OH)_6]^{2-}$ ions yields ligand-free 1-2 nm diameter particles that are stable over a wide range of pH. These particles, which are highly active electrocatalysts for water oxidation, bind strongly to molecules with bidentate carboxylate (malonate or succinate) groups and can be deposited anodically to form catalytically active films on electrodes. When the nanoparticles are incorporated into porous TiO_2 electrodes containing phosphonated $[Ru(bpy)_3]^{2+}$ sensitizers, stable photocurrents are obtained and the current efficiency for oxygen evolution is near unity.

Several groups have now reported similar photoanode structures and have observed initial photocurrent densities corresponding to an internal quantum yield of 10-15%. The photocurrent decays over tens of seconds by ~90%, but can be restored if the cell is disconnected briefly. We observe much higher photocurrent and less electrode polarization when I^- is added as an electron donor. This suggests that the injection yield is high, but that slow electron transfer from IrO_2 to the oxidized dye results in a low initial quantum yield. The slow polarization process is most likely caused by protons generated in the water oxidation reaction, since the driving force for water oxidation is pH-dependent. The first hypothesis was confirmed by flash photolysis experiments with TiO_2 and core-shell ZrO_2/TiO_2 and Nb_2O_5/TiO_2 electrodes. Slower recombination ($e_{(TiO2)} \rightarrow$ oxidized dye) with core-shell electrodes resulted in a twofold increase in the photocurrent. Based on experiments conducted by Frei et al. with silica-supported water oxidation catalysts, we hypothesized that the hydrolysis of alkoxysilanes in the TiO_2 pore network could buffer the system. This effect was indeed observed and led to an additional twofold increase in the steady state photocurrent. We are presently experimenting with one-electron mediators (analogous to the tyrosine-histidine complex in Photosystem II) that bridge between IrO_2 and the dye in order to accelerate the regeneration of the oxidized dye molecule. We are also studying current rectification and light-induced electron transfer in photocathode structures by a transient ATR method developed in collaboration with the Saavedra group.

How is Charge Transport Different in Ionic Liquids and Electrolyte Solution?

Hemant K. Kashyap, Harsha V. R. Annapureddy and Claudio J. Margulis
Department of Chemistry
University of Iowa
Iowa City, IA 52242

Electrolyte solutions and room temperature ionic liquids (RTILs) are similar in that NMR derived conductivities via the Nernst-Einstein approximation are always larger than observed from impedance measurements. This is often attributed to ion pairing. Here we show that this intuitive interpretation is correct in the case of electrolyte solutions but not in the case of molten salts or RTILs.

Since ions are the only components of a RTIL, they are responsible for satisfying momentum conservation laws. Instead in electrolyte solutions the solvent which is often the major component lifts this requirement on the ions; it is the overall system (solvent+ions) that must satisfy momentum conservation. This distinction imposes in the case of molten salts and RTILs strict rules of motion. Here we present analytically derived and computationally verified equations that shed light on these rules for conductivity in RTILs. A key result is that cation-anion cross correlation coefficients (sometimes referred as cross diffusion constants) must be negative definite in RTILs and molten salts. This implies that overall cationic-anionic motion is anticorrelated! This is in contrast to cationic-anionic motion in solutions that is correlated by pairing. This pairing is a major cause for conductivity decrease in electrolyte solutions but not in RTILs. The decrease of conductivity in RTILs with respect to the Nernst Einstein approximation is due instead to anticorrelated motion of ions of the same charge.
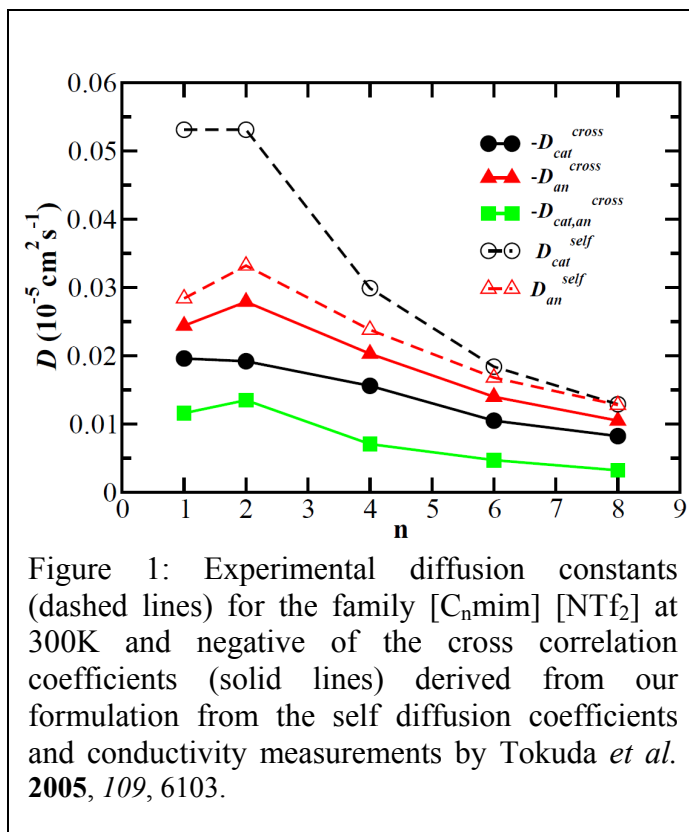
Figure 1: Experimental diffusion constants (dashed lines) for the family [$C_n$mim] [NTf_2] at 300K and negative of the cross correlation coefficients (solid lines) derived from our formulation from the self diffusion coefficients and conductivity measurements by Tokuda *et al.* **2005**, *109*, 6103.

From a practical perspective, we present a set of useful equations for experimentalists to derive the elusive cross correlation couplings between ions for which there is no direct experiment. As an example, Fig.1 shows cross correlation coefficients we derived from diffusion and impedance measurements performed by Tokuda and coworkers on the [$C_n$mim] [NTf_2] family of RTILs. This opens an opportunity for understanding the enigmatic role of shape on ionic motion cross correlation with obvious implications in the design of RTILs for energy applications.

Intra- and Inter-Molecular Electron Transfer in Ionic Liquids

Min Liang, Xiang Li, Minako Kondo, and Mark Maroncelli
Department of Chemistry, The Pennsylvania State University
University Park, PA 16802

We have been studying intra- and inter-molecular electron transfer reactions in ionic liquids in order to determine how such processes might differ in a purely ionic medium compared to the well-studied case of conventional dipolar solvents.

We have recently completed a study of the three excited-state intramolecular electron transfer reactions illustrated in Fig. 1. All three reactions were previously shown to be solvent controlled in conventional dipolar solvents. In the cases of BPAc$^+$ and BA, and with less certainty CVL, the nature of the solvent control appears to be similar in ionic and dipolar solvents. The main distinguishing feature of ionic liquids is simply the fact that their solvation response is ~100-fold slower than in most conventional solvents.

Bimolecular electron transfer has been more widely investigated than intramolecular reactions in ionic liquids. It has often been observed that diffusion-limited reactions proceed at rates greatly exceeding predictions based on viscosity-scaling rates observed in conventional solvents. We have used fluorescence quenching and NMR diffusion measurements to understand the origins of these surprisingly high rates. One system we have studied is the reductive quenching of dCNA by DMA in a series of ionic liquids [Pr$_{n1}$][Tf$_2$N] (Fig. 2). Consistent with previous studies, we find quenching rates much faster than predicted using the bulk viscosities of the ionic liquids and simple bimolecular reaction models. Diffusion measurements show that these faster rates are partly due to diffusion of neutral solutes being 3-10 times faster than Stokes-Einstein predictions in ionic liquids. Detailed modeling of the reaction kinetics shows that under the high-viscosity conditions prevailing in ionic liquids, "transient" effects and long-distance electron transfer are equally important in producing the surprisingly fast rates of bimolecular electron transfer.
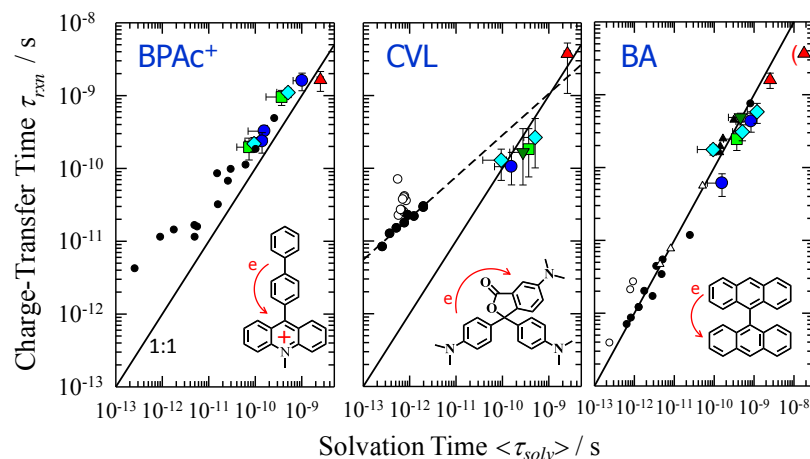
Fig. 1: Comparison of times associated with charge-transfer reaction in three excited state reactions to solvation times measured with the non-reactive probe coumarin 153. Smaller black & white circles denote data in conventional solvents and larger colored symbols denote different ionic liquids.
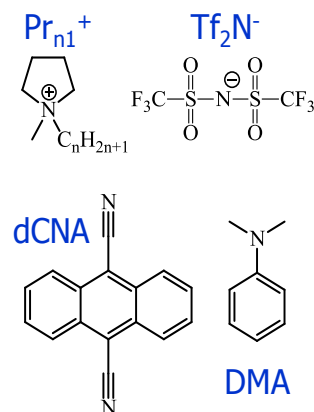
Fig. 2: Ionic liquids and quenching system studied. Liquids [Pr$_{n1}$][Tf$_2$N] n = 3, 4, 5, 6, 8, 10 have been studied.

Iron-based Chromophores for Solar Energy Conversion

Allison M. Brown, Lindsey L. Jamula, Lisa Harlow, Dong Guo, and <u>James K. McCusker</u>
Department of Chemistry
Michigan State University
East Lansing, MI 48824

Our research program is focused on the development of chromophores based on first-row transition metal ions for applications in solar energy conversion strategies; specific interests revolve around their use as sensitizers for semiconductor-based photovoltaics. The overriding motivation for this line of research is based on the earth-abundant nature of iron relative to the second- and third-row charge-transfer complexes more commonly employed in dye-sensitized solar cells (DSSCs). More generally, however, fundamental knowledge concerning the dynamics of transition metal-based excited states on short time scales – ultimately leading to an ability to manipulate these processes to favor reactions of interest for energy conversion (e.g., interfacial electron transfer in DSSCs) – constitutes the conceptual underpinning of the work. This past year has witnessed two important advances in our efforts along these lines.

Synthesis and Characterization of [Fe(bpcp)$_2$]$^{2+}$. We have prepared a new Fe(II) complex that we believe holds promise for useful applications in photo-induced redox chemistry. Using the previously known ligand 2,6-bis(2-pyridylcarboxy)pyridine (bpcp), the bis adduct of Fe(II) – [Fe(bpcp)$_2$]$^{2+}$ – exhibits a near-perfect octahedral geometry (Figure 1); this geometry coupled with the orbital energetics of the ligand itself gives rise to a dramatic change in the electronic structure of this compound relative to all previously reported low-spin Fe(II) compounds. In particular, we note a substantial degree of stabilization of the highest-occupied metal-centered orbitals that leads to an inversion of the lowest-energy excited states of the compound. The electrochemical, optical, and photophysical properties of this compound will be described.

Figure 1. ORTEP drawing of the cation of [Fe(bpcp)$_2$](PF$_6$)$_2$ obtained from single-crystal X-ray structure determination. Atoms are repre-sented as 50% probability thermal ellipsoids. Hydrogen atoms and anions are omitted for clarity. Selected bond lengths (Å) and angles (°): Fe1-N1, 1.985(2); Fe1-N2, 1.974(2); Fe1-N3, 1.989(2); O2-C12, 1.211(2); O1-C6, 1.213(2); N2-Fe1-N1A, 90.48(7); N2-Fe1-N1, 88.79(6); N2-Fe1-N3, 88.87(6); N2-Fe1-N3A, 91.86(6); N1-Fe1-N1A, 90.61(9); N1-Fe1-N3A, 89.07(7); N3-Fe1-N3A, 91.35(9); N1-Fe1-N3, 177.63(6); N2-Fe1-N2A, 178.96(8).

Electron Injection Studies of DSSCs Employing First-row Sensitizers. The recent acquisition of a new laser system with improved temporal resolution (< 40 fs) and broad spectral coverage (240 nm – 2.5 µm) has now enabled us to directly probe dynamics on time scales appropriate for charge-transfer relaxation in first-row metal complexes as well as interfacial electron transfer in DSSCs derived from these chromophores; such measurements are critical to enable us to establish structure-function correlations across series of compounds as an aid to the design of compounds suitable for photovoltaic applications. Results from these experiments on Fe(II)-based solar cells will be presented.

How to Rapidly Inject Holes and Electrons Into Conjugated Polymers

John R Miller, Andrew R. Cook, Matthew Bird and Hung-Cheng Chen
Chemistry Department
Brookhaven National Laboratory
Upton, NY 11973

This poster describes our efforts to create and improve methods to inject holes into molecular materials, particularly conjugated polymers, using ~ 5 ps pulses from an electron accelerator. We target injection of holes into single chains in solution, into aggregates that may simulate conditions in films and into films with high time resolution detection. Electron injection into polymer chains in solution is better understood and has been aided by the recent finding in our laboratory of very rapid, "step" appearance of electrons in polymer chains within the 15 ps time resolution of the optical fiber single shot (OFSS) detection system developed at BNL. Electrons in some molecular liquids have mobilities as large as 100 cm^2/Vs, but this is not true for holes, so it is natural to assume that the very fast "step" capture is exclusive to electrons, which are initially mobile and delocalized after they are produced by ionization. Therefore fast injection into conjugated polymer chains, known for electrons, might not be available for holes. We are excited to find, on the contrary, that fast formation of holes in conjugated polymer chains occurs with efficiencies similar to those for electrons. The figure shows results of current experiments that observe fast formation of polyfluorene radical cations in chloroform, a good solvent for conjugated polymers.

Figure 1 Transient absorption showing fast hole injection into polyfluorene (pF) with an average length of 40 repeat units. In a 1.1 mM solution of pF_{40} molecules in chloroform two thirds of the $pF^{+\bullet}$ cations are formed within the 15 ps time resolution of the OFSS detection system.

The newly-discovered fast injection of holes will create opportunities to investigate their properties and transport at short times. Their natures depend on the still poorly-understood radiation chemistry for hole creation in these solvents. Determinations of transport will require free ions, but a substantial fraction of the holes may be ion-paired with Cl^- counterions. An example will be shown of ion-pairing of $pF^{-\bullet}$ ions in THF, where the pairing to protons appears not to give a spectroscopic signature.

To characterize holes in polymer films it will be valuable to investigate holes in aggregates that have been created in solution and have been found to possess semicrystalline structures. Because they are present only in low concentration we have examined methods to inject holes to very dilute structures. At the same time we are developing methods to directly study holes in solid films. These investigations will benefit from the time resolution of the OFSS detection system.
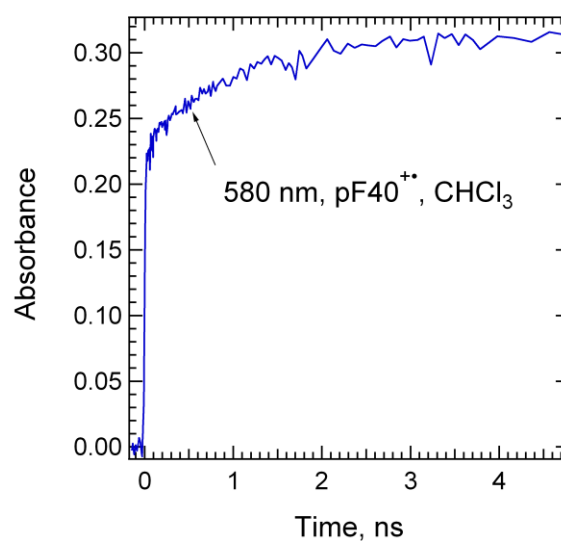
Structure-Function Mapping of Cobaloxime-Based H₂ Photocatalysts

Karen L. Mulfort, Rebecca A. Jensen, David M. Tiede
Division of Chemical Sciences and Engineering
Argonne National Laboratory
Argonne, IL 60439

A significant challenge for effective solar fuels production is the efficient integration of ultrafast, generally one-electron photoexcitation and charge separation with the slower, often multi-electron, processes relevant to catalysis. Our group is focused on the design and discovery of new and novel photocatalyst structural motifs which effectively bridge these disparate temporal and spatial processes. We are specifically targeting supramolecular strategies to couple light-harvesting components with the well-known cobaloxime molecular electrocatalysts for proton reduction.

We have synthesized and investigated several new supramolecular architectures based on axial coordination of pyridyl-functionalized photosensitizers to the Co(II) site of the cobaloxime macrocycle. Solution phase X-ray scattering and ultrafast transient optical spectroscopy analyses were used in tandem to correlate the self-assembled photocatalysts' structural integrity in solution with electron transfer and charge separation between the photosensitizer and catalyst fragments. The results indicate that poor catalytic performance is attributable to configurational dispersion in solution as well as unoptimized electronic coupling.

Follow-up work has been targeted at manipulating the photosensitizer-catalyst orientation to encourage directional photoinduced electron transfer. In this effort, we have synthesized an equatorially-linked cobaloxime photocatalyst in which the photocatalyst is self-assembled by metal-mediated coordination of two glyoxime-functionalized Ru(II)(bpy)₃²⁺-based light-harvesting component (Figure 1A). Notably, preliminary transient optical measurements suggest a charge-separated state which persists for approximately 0.8ns (Figure 1B,C). We are currently exploring related strategies for ligand-based photocatalyst assembly to further extend photoinduced charge separation. We anticipate that the synthesis of new supramolecular photocatalyst structures coupled with targeted high-resolution physical characterization methods will provide fundamental knowledge of the processes which enable artificial photosynthesis and facilitate design strategies for next-generation photocatalyst architectures.
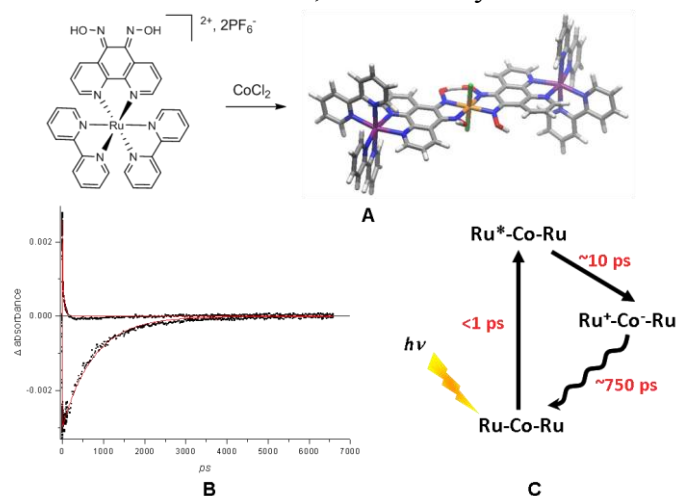
Figure 1. A) Chemical structure and self-assembly of equatorially-coordinated cobaloxime photocatalyst. B) Ultrafast transient optical spectroscopy of equatorial photocatalyst in acetone: 430nm pump; excited state quench monitored at 600nm (top kinetic) with bi-exponential decay of 8ps (61%) and 53ps (39%); ground state monitored at 520nm recovers with τ~750ps. C) Proposed energy level diagram of photocatalyst.

Structural Studies of Photosensitizers and Catalysts Models for Water-Splitting in Solution Using High Energy Synchrotron X-ray Scattering

David M. Tiede, Oleksandr Kokhan, and Karen L. Mulfort
Chemical Sciences and Engineering Department
Argonne National Laboratory

One challenge for achieving efficient solar-driven fuels production lies in gaining control of the structure and dynamics of light-harvesting molecules and catalysts that are designed to drive multiple electron and proton coupled redox reactions linked to water-splitting and fuels production. Our program is developing approaches to follow ground and excited-state inner and outer sphere atomic reorganization in solar energy converting molecular modules and supramolecular assemblies using *in-situ* synchrotron X-ray techniques. High energy (> 60 keV) X-ray scattering measurements are of special interest because they allow pair distribution function (PDF) analyses to be carried out with sufficient resolution (>0.1 Å) to allow atomic resolution of metal coordination structure.

We have begun an investigation of the solution structures for a variety of metal coordination complex photosensitizers and catalysts that function in solar-driven photocatalysis. Detailed *ab initio* methods have been used to model the structures of a variety metal tris bipyridyls and predict that both the ground and excited-state complexes are associated with a responsive hydration layer that potentially contribute to solvent-dependent energies for excited state electron transfer and modulate donor/acceptor interactions. Our measurements of high energy X-ray scattering for a sequence of Fe(II), Ru(II), and Os(II) tris bipyridyl complexes are found to resolve contributions from each of the metal-bipyridyl ligand atom distances and from an associated solvation layer. Sensitivity gains are seen in heavy metal analogues. Comparisons to molecular models show that the scattering data are sensitive to the number, packing density, and disorder of solvation layer molecules, and are consistent with contributions from 14 water molecules wrapped in a partially disordered layer. On-going high energy scattering measurements resolve coordination and longer range structure for both water oxidation and reduction catalysts.
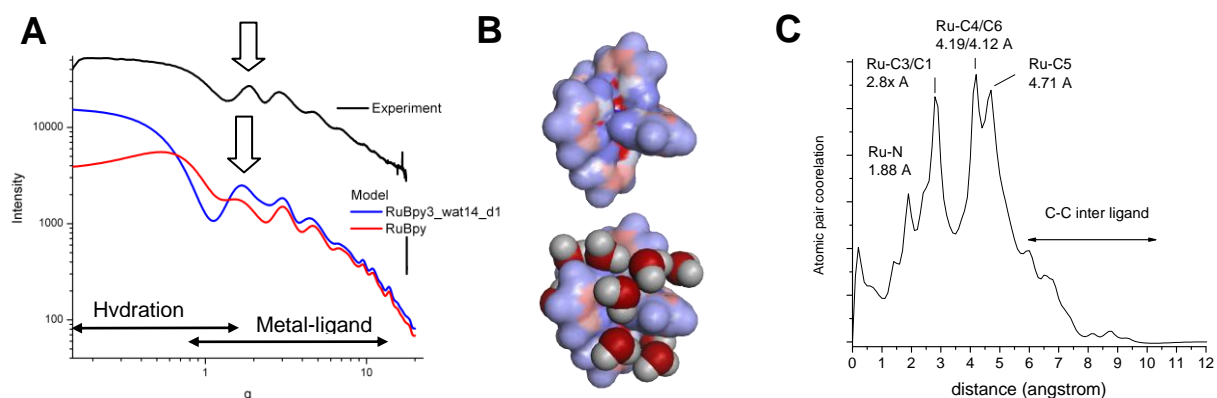
Figure 1. Part A compares experimental high energy x-ray scattering pattern measured for 15 mM $Ru(bpy)_2^{+2}$ in water to scattering patterns calculated for the coordination complex alone and with a hydration layer. Part B shows the van der Waals surface model for $Ru(bpy)_2^{+2}$ in the absence (top) and presence (bottom) of the hydration layer. Part C shows the atomic pair distribution function analysis of the scattering patterns, showing resolution of each of the metal-ligand atom distances.

Nature-driven Photochemistry for Solar Fuels Production:
Photosystem I-Cobaloxime Biohybrid Catalytically Produces Hydrogen

Lisa M. Utschig, Karen L. Mulfort, Oleg G. Poluektov, and David M. Tiede
Chemical Sciences and Engineering Division
Argonne National Laboratory
Argonne, IL 60439

Photosynthetic reaction center (RC) proteins are finely tuned molecular systems optimized for solar energy conversion. The primary reaction in RCs involves rapid, sequential electron transfer that results in stable charge separation. Following efficient charge separation, the energy captured is utilized in a series of reactions that ultimately drive the chemical conversion of CO_2 into carbohydrates. Our group has developed new energy conversion strategies that mimic Nature and couple the photon energy, efficiently captured as a stabilized charge separation across the RC, to the direct synthesis of energy-rich compounds. Specifically we have designed two types of Photosystem I (PSI)-catalyst biohybrid complexes that use Nature's optimized photosynthetic chemistry to drive the catalytic production of the solar fuel hydrogen.

A photocatalytic hydrogen-evolving system based on intermolecular electron transfer between native PSI and electrostatically associated Pt nanoparticles has been developed. Visible-light-induced H_2 production occurs for the PSI/Pt nanoparticle biohybrid at a rate of >21,000 mol H_2 (mol PSI)$^{-1}$ h^{-1}. These results demonstrate that highly efficient photocatalysis of H_2 can be obtained for a self-assembled, noncovalent complex between PSI and Pt nanoparticles; a molecular wire between the terminal acceptor of PSI, the [4Fe-4S] cluster F_B, and the nanoparticle is not required.
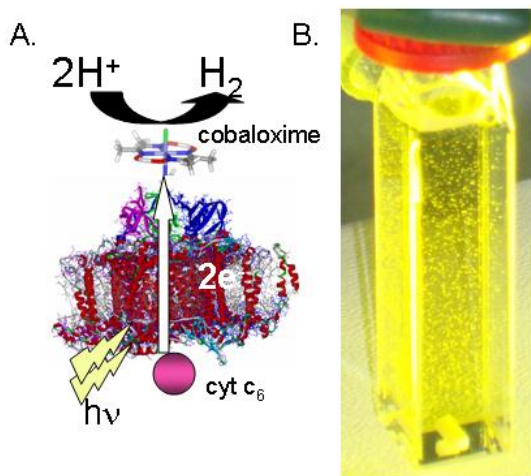
Figure 1 A. Photocatalytic scheme for PSI/cobaloxime H_2 production. B. H_2 bubbles produced upon illumination of a 80 nM solution of PSI/cobaloxime biohybrid.

Although a great catalyst, platinum is a rare and expensive noble metal. For a practical energy future we need chemical catalysts that are made from cheap, earth abundant elements. For this reason, we have initiated studies of biohybrid complexes of PSI with cobaloximes, pseudo-macrocyclic bis(dimethylglyoxamato) cobalt complexes. We have successfully developed the first functional biohybrid PSI-cobaloxime complex that uses light-initiated photosynthetic RC chemistry to drive hydrogen production from a synthetic molecular catalyst. Importantly, this PSI-cobalt biohybrid accomplishes solar photocatalysis using totally cheap, earth abundant elements to make a clean fuel and creates new opportunities for solar fuel production that merges synthetic inorganic and biochemical capabilities.

Rapid Synthesis/Screening and Nano-Structuring of Doped BiVO$_4$ Photocatalysts

Allen J. Bard, C. Buddie Mullins, S. P. Berglund, D. W. Flaherty, N. T. Hahn, and Hyun S. Park
Departments of Chemistry and Chemical Engineering and Center for Electrochemistry
University of Texas at Austin
Austin, TX 78712

We employ a variation of scanning electrochemical microscopy (SECM) for rapid screening of photocatalysts. Multi-component doped metal oxide semiconductor arrays are fabricated with a pattern of ~200 μm sized photoelectrocatalyst spots on FTO. The first component (metal-salt solution) is loaded and dispensed followed sequentially by the other components and then heated in a furnace. Different potentials can be applied to the working electrode (arrays), while the optical fiber tip scans the arrays about 50 μm above the array surface. The photocurrent produced at a given potential during the scan is measured and recorded as a false-color image. Figure 1 displays an example SECM scan for BiVO$_4$ films doped with Mo and W suggesting that 2%W and 6%Mo-doping is optimal.

Figure 1: (a) Photocatalyst spot array with different mol %/Mo and W in BiVO$_4$. (b) SECM scanning at 0.4 V (vs. NHE) in 0.1 M Na2SO3, 0.1 M Na$_2$SO$_4$ with visible light ($\lambda \geq$ 420 nm). Mo concentration increases from 0% to 10% in 2% increments starting at the top and likewise for W from left to right. 2% W and 6% Mo yields the highest photocurrent.

BiVO$_4$ films with dopants, identified through the screening tests described above, are then fabricated into nano-structured thin films using reactive ballistic deposition (RBD), altering both the structure and composition to tune photocatalytic and optical properties. RBD involves the metallic component(s) of the film being evaporated at a glancing angle onto the substrate through an ambient of reactive gas (e.g., oxygen) to create high surface area films (e.g., Figure 2; S. P. Berglund, *et al.*, *J. Phys. Chem. C* **115**, 3794 (2011)) with high internal porosity. BiVO$_4$ films doped with tungsten and molybdenum have been characterized and tested electrochemically (see Figure 3) and are generally consistent with the rapid screening SECM results.

Figure 2: SEM of BiVO$_4$ film deposited by Reactive Ballistic Deposition with an incidence angle of 65° (a) as grown and (b) after annealing in air at 500°C for 2 hours.

Figure 3: PEC water oxidation with W,Mo-doped RBD BiVO$_4$ films.

151

Reduced State Spaces and D/A Coupling: Modeling Electronic Transport Rates

Marshall D. Newton
Chemistry Department, Brookhaven National Laboratory
Upton, New York 11973-5000

A general issue in modeling electronic transport between localized donor and acceptor (D/A) sites is the nature and minimally adequate number of electronic states required to characterize quantitatively the D/A electronic coupling (H_{DA}), balancing the tradeoffs involving accuracy and compactness. At the 2-state level, the desired diabatic states correspond to the initial and final states in the electronic process of interest. Generally, the criterion for defining and computing such states is that the pair should be maximally localized according to some plausible physical criterion, thus defining the localized D and A states. Such localization is, of course, not necessarily the best choice for the prepared initial states in some processes, a topic worthy of further consideration. The term 'localized' here denotes states which are largely localized at D and A sites, but which typically contain crucial small 'tails' extending onto intervening bridges or even the opposite terminal sites, and it is a primary task of theory and computation to evaluate such tails and assess their role in establishing H_{DA} magnitudes.

The above issues, and in particular, the validity of the 2-state approximation (TSA), have been extensively addressed for 1-particle transport (*e.g.* electron or hole transport, denoted here collectively as ET), but have also very recently (Vura-Weis *et al.*; *JPC* C **114**, 20449 (2010)) been raised in connection with singlet electronic excitation transport (EET), an important 2-particle process. We have examined these issues for a wide range of state spaces using as localization criteria the Generalized Mulliken Hush (GMH) model for ET and the Edmiston-Ruedenberg (ER) based model of Subotnik, *et al.* (*JCP* **130**, 234102 (2009)) for EET, with supermolecule electronic states based on Kohn-Sham orbitals or *ab initio* single excitation configuration interaction (CIS) wavefunctions.

The ET results (*in vacuo*) involved some (RupzRu) mixed valence complexes (reported previously), which showed that the 2-state model can be viable if the two states are suitable effective D and A states, dressed with tails extending onto the pz (in contrast to bare states strictly confined to Ru sites), with coupling in some cases moderate enough to permit expression in terms of a perturbative superexchange (se) model. In the case of the Creutz-Taube complex, however, the se model was quantitatively inadequate.

For EET, *in vacuo* calculations were carried out (Vura-Weis *et al.*; *op cit*) for the (HeH$^+$)$_2$ dimer and the perylenemonoimide- perylenediimide (PMI-PDI) dimer. The total H_{DA} values were decomposed into Coulomb (J), exchange (K), and an additional '1-electron' term (O). In both cases the salient feature for the conventional 2-state model (based on the two lowest singlet excited dimer adiabatic states (electronic eigenstates)) is that in the asymptotic region (D/A separations > 10 Å), all three terms displayed algebraic falloff ($1/R^3$), whereas exponential falloff for K and O was expected. The issue was resolved by observing that the exponential behavior of K and O was restored for larger state spaces, revealing that the 2-state results are influenced by small tails (an A component in the D state and *vice versa*). These tails do not noticeably affect the total coupling values, in spite of their marked effect on the individual components.

Two-dimensional Electronic Spectroscopy of the D1-D2 Cyt b559 Reaction Center: Experiments and Modeling

K. L. M. Lewis[1], J. A. Myers[1], F. D. Fuller[1], Y. C. Yocum[2] and J. P. Ogilvie[1]
[1]Department of Physics and Biophysics
[2]Department of Molecular, Cellular and Developmental Biology
University of Michigan
Ann Arbor, MI, 49109

The photosystem II (PSII) reaction center is the heart of oxygenic photosynthesis, taking absorbed light from neighboring antenna complexes and creating a charge separation capable of splitting water. Despite the wealth of spectroscopic studies of the PSII reaction center, the basic energy transfer and charge separation dynamics remain poorly understood. With six chlorophyll a pigments and two pheophytins, the reaction center has a complex electronic structure; similar pigment site energies and varying degrees of electronic coupling combine to create a broad linear absorption spectrum, making spectral assignments particularly difficult. In traditional nonlinear spectroscopy experiments, one must choose between temporal and spectral resolution, complicating the interpretation of these experiments. In addition, the degree of static disorder and electronic coupling in the system is difficult to discern. Two-dimensional electronic spectroscopy (2DES) overcomes many of these challenges, providing a more direct view of electronic coupling and femtosecond energy and charge dynamics. We present low-temperature 2DES data of the D1-D2-Cyt b559 reaction center complex from the femtosecond to the hundred picosecond timescale [1]. We also present the decomposition of 2DES data into two-dimensional decay associated spectra (2D DAS), a method that characterizes the spectral signatures of energy and charge separation. Within this framework, we discuss the ultrafast energy and charge transfer dynamics of the PSII reaction center. A number of competing excitonic models for the PSII reaction have been proposed in the literature. We present simulated 2D spectra based on these models for comparison with our 2DES data, and suggest possible refinements of these models. Finally, we discuss future experiments aimed at better separating signatures of energy and charge transfer.
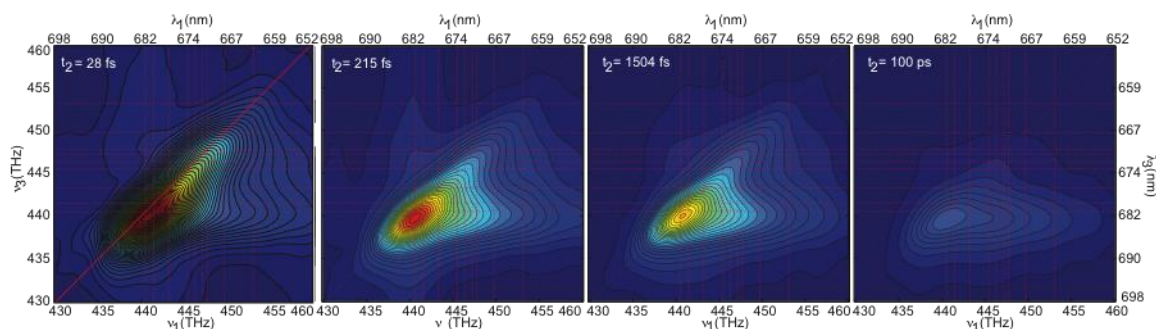
Figure 1: 2DES spectra of the PSII RC at 77K for waiting times t_2 = 28 fs, 215 fs, 1.5 ps and 100 ps. Superimposed as a grid are the excitonic states of a proposed exciton model for the PSII reaction center.

1. J. A. Myers, K. L. M. Lewis, F. D. Fuller, P. F. Tekavec, C. F. Yocum, and J. P. Ogilvie, "Two-dimensional electronic spectroscopy of the D1-D2-cyt b559 photosystem II reaction center complex," Journal of Physical Chemistry Letters **1**, 2774-2780 (2010).

Single-Molecule Spectroelectrochemistry of Interfacial Charge Transfer in Hybrid Organic Solar Cell

Caleb M. Hill[1], Daniel A. Clayton[1], HongWei Geng[1], Dehong Hu[2], Shanlin Pan[1]

1. Department of Chemistry, The University of Alabama, Tuscaloosa, Alabama, 35487
2. Pacific Northwest National Laboratory, Richland, WA 99352

Hybrid organic photovoltaics (OPVs) (**Figure 1 A**) containing a light-absorbing polymer and TiO_2 electron acceptor layer have been studied extensively and promise to be efficient and cheap architecture to convert solar energy in comparison with their inorganic counterparts. Most often, a hybrid OPV possessing a heterojunction (HJ) (e.g., TiO_2/ poly (3-hexylthiophene) (P3HT)) has limited efficiency because of the conflict between the need for a thick donor layer for maximum light absorption and the bottleneck of a short exciton diffusion distance. Poor charge-transport mobility and stability of organic semiconductor are additional factors limiting the device overall performance.

Figure 1. Schematic of TiO_2/polymer hybrid solar cell (A), and ordered TiO2 nanostructure with evenly spaced perpendicular mesochannels on the order of 10 nm supported on ITO for single molecule spectroelectrochemistry study (B).

The central goal of this project is to investigate the interfacial charge transfer dynamics of single fluorescent polymer molecules at a TiO_2 electrode with ordered nanostructure by using combined methods of electrochemistry and single molecule spectroscopy. To achieve this goal, TiO_2 films with evenly spaced perpendicular nanopillars and mesochannels on the order of 10 nm have been prepared on conducting ITO/glass electrodes (**Figure 1 B**). To test the single molecule photoluminescence dynamics on the surface of the above TiO_2 substrate we first use CdSe/ZnS Core/Shell quantum dots (QDs) as a model system to obtain meaningful data from single-molecule/particle measurements (**Figure 2**). We also investigated single poly [2-methoxy, 5-(2-ethylhexoxy)-1, 4-phenylene vinylene], MEH-PPV, on such ordered TiO_2 surface and their dynamic changes in PL intensity. Understanding the interfacial charge transfer dynamics of these fluorescent species and electrochemical activities on such ordered TiO_2 nanoelectrode are in progress.
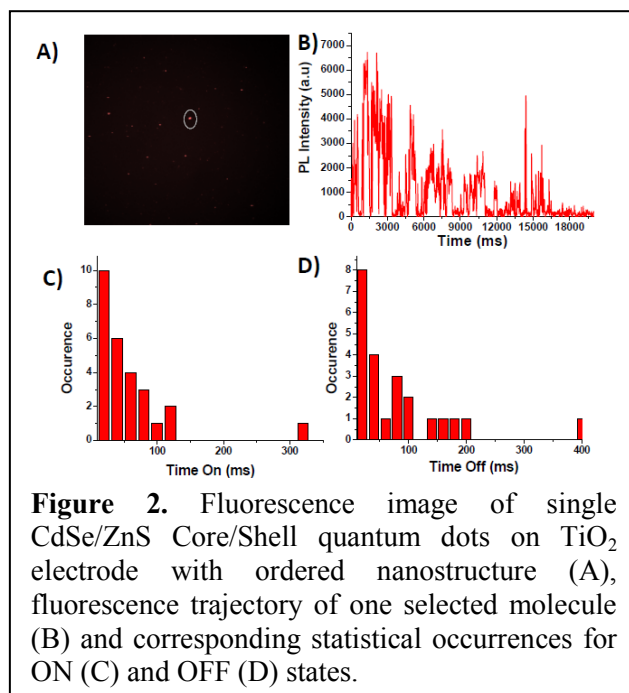
Figure 2. Fluorescence image of single CdSe/ZnS Core/Shell quantum dots on TiO_2 electrode with ordered nanostructure (A), fluorescence trajectory of one selected molecule (B) and corresponding statistical occurrences for ON (C) and OFF (D) states.

Photooxidation of Chloride by Oxide Minerals: Implications for Perchlorate on Mars

Jennifer Schuttlefield[1], Justin B. Sambur[1], Carrick M. Eggleston[2] and B. A. Parkinson[1]

Departments of Chemistry[1] and Geology and Geophysics[2], University of Wyoming
Laramie, WY   82071

Chemical analysis of Martian soil in the North Polar region by the Phoenix Mars Lander unexpectedly detected high concentrations of perchlorate ion (0.4-0.6 weight %) that accounted for ~60% of the anionic charge and exceeded chloride concentrations by factors of 4 to 8. The atmospheric chemical reaction mechanisms proposed for perchlorate formation on Earth (ozone oxidation of chloride aerosols) has been extended to explain perchlorate production on Mars appears implausible. We show that highly oxidizing valence band holes, produced by ultraviolet (UV) illumination of naturally occurring semiconducting minerals, are capable of oxidizing chloride ion to perchlorate in aqueous solutions.
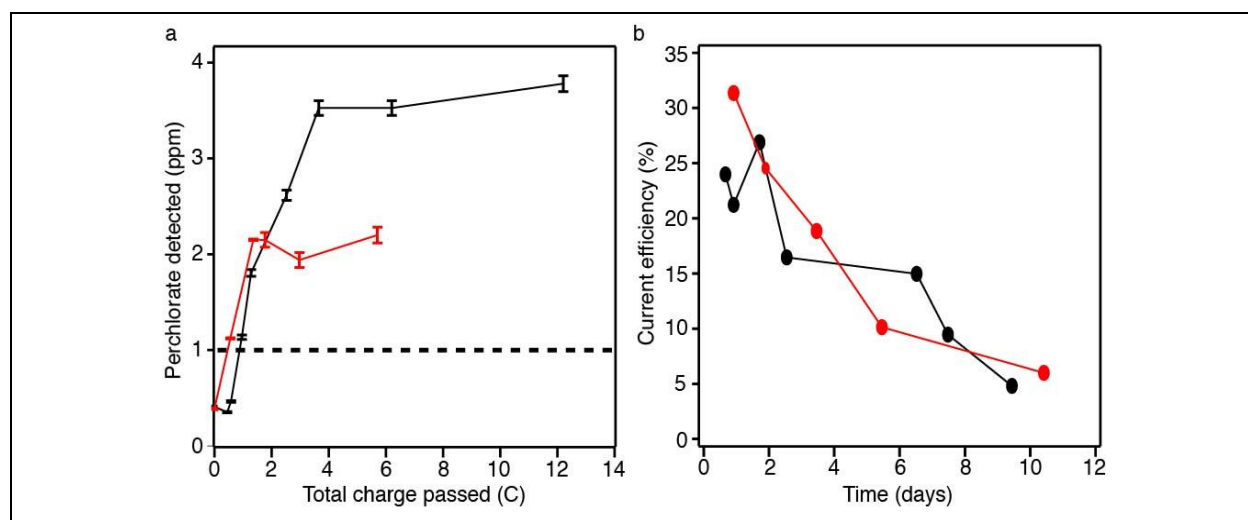
Figure 1 The photoelectrochemical production of perchlorate in chloride solutions. a, The total amount of perchlorate detected as a function of total charged passed during UV illumination of A natural anatase (101) (black) and A synthetic rutile (110) (red) TiO_2 crystals over ~10 days. The dashed line represents the calculated ion selective electrode response from the maximum concentration from interfering ions and error bars represent the standard error in the electrode based on multiple perchlorate measurements. b, The current efficiency of perchlorate production versus time for the anatase (101)(black) and rutile (110) (red) crystals.

Figure 1a shows the photoelectrochemical production of perchlorate as a function of total charged passed during UV illumination of a natural anatase (101) surface (black) and synthetic rutile (110) surface (red) TiO_2 crystals. The initial current efficiency for perchlorate production (Figure 1b) exceeded 20% and also decays with time. We assume that the photooxidation of water to oxygen or chloride to chlorine accounts for the majority of the photocurrent on anatase and rutile photoelectrodes.

Our mechanism predicts that over millennia, even small amounts of semiconducting oxide minerals could eventually convert almost all the chloride to kinetically stable perchlorate, explaining the disparate perchlorate to chloride ratios found on Mars compared to those in naturally occurring perchlorate-containing soils on Earth.

Superatom States of Hollow Molecules and their Origin in Molecular Sheets

Hrvoje Petek
Department of Physics and Astronomy
University of Pittsburgh
Pittsburgh, PA   15260

Electronic and optical properties of molecular materials are traditionally considered from the perspective of the frontier orbitals and their intermolecular interactions. How molecules condense into crystalline solids, however, depends on the polarization interaction. In this poster we show that long-range polarization also introduces a distinctive set of diffuse molecular electronic states, which in quantum structures or solids combine into nearly-free-electron (NFE) bands[1]. These NFE properties, usually associated with good metals, are vividly evident in sp^2 hybridized carbon materials, namely graphene and its derivatives.

The primary manifestation of the polarization interaction is the screening of an external charge by a solid. It is responsible for the universal image potential and the associated unoccupied image potential (IP) states. The molecular electronic properties that we describe stem from the IP states of graphene, which float above and below and undergo free motion parallel to the molecular plane. Rolling or wrapping graphene into a nanotube or a fullerene, transforms the IP states into diffuse atom-like orbitals that are bound to hollow molecular cores, rather than the component atoms; we therefore we named them the superatom molecular orbitals (SAMOs)[2,3]. SAMOs of fullerenes separated by their Van der Waals distance can combine to form diatomic molecule-like orbitals of C_{60} dimers, and for larger aggregates, they form NFE bands of super-atomic quantum structures and solids.

The overlap of SAMO wave functions in molecular solids provides a different paradigm for band formation than the valence or conduction bands derived from HO MO or LUMO states. Therefore, they provide a new paradigm for design of molecular materials with potentially superior properties for electronics.

Fullerenes have been considered as atom-like building blocks of electronic materials. Unlike, metallic gas phase clusters, only in the case of fullerenes, do the superatom properties survive even in the condensed phase. The superatom states and their bands are usually unoccupied, and therefore do not contribute to intermolecular bonding; instead, their significance lies in the electronic properties they confer when electrons are introduced.

We describe the IP states of graphene, and show how these states in turn define the NFE properties of graphite, fullerenes, and nanotubes. Through low-temperature scanning tunneling microscopy we describe the electronic properties of SAMOs, for single C_{60} molecules and their self-assembled quantum structures.

The measured and calculated SAMOs of C_{60}.

1   M. Feng, et al., Acc. Chem. Res., ASAP (2011).
2   M. Feng, J. Zhao, and H. Petek, Science 320, 359 (2008).
3   S. Hu, et al., Nano Lett. 10, 4830 (201

Transition Metal Complexes as Artificial NADH Analogs:
Towards Photochemical Reduction of CO_2

Dmitry E. Polyansky, Diane Cabelli, Etsuko Fujita and James T. Muckerman
Chemistry Department
Brookhaven National Laboratory
Upton, NY 11973-5000

One of the key components of the Photosystem I that is responsible for CO_2 reduction is the NADPH co-enzyme, which serves as a hydride donor (or the donor of two electrons and a proton). $[Ru(bpy)_2(\mathbf{1})]^{2+}$ (bpy = 2, 2'-bipyridine, $\mathbf{1}$ = 2-(pyrid-2'-yl)-1-azaacridine) was shown to act as an electrocatalyst to reduce acetone to isopropanol.[1] We have found that the two-electron-reduced species $[Ru(bpy)_2(\mathbf{1HH})]^{2+}$ can be formed photochemically with 0.21 quantum yield without forming any side products. Our earlier work described the detailed mechanism of photochemical formation of $[Ru(bpy)_2(\mathbf{1HH})]^{2+}$ and its structural isomer $[Ru(bpy)_2(\mathbf{2HH})]^{2+}$ ($\mathbf{2}$ = 3-(pyrid-2'-yl)-4-azaacridine) based on a combination of experimental and theoretical investigations including pulse radiolysis and photochemical techniques in aqueous and non-aqueous media.[2-5] One of the most important features of the mechanism was a bimolecular interaction between one-electron-reduced intermediates allowing the pooling of the energy of two photons into a single molecule to produce a hydride donor species. In addition, structural differences between the ligands $\mathbf{1}$ and $\mathbf{2}$ have a significant effect on the mechanism of formation of $[Ru(bpy)_2(\mathbf{1HH})]^{2+}$ and $[Ru(bpy)_2(\mathbf{2HH})]^{2+}$. We determined that the reactivity at the hydride donor/acceptor cite was governed by steric factors as evidenced by: (a) protonation of $[Ru(bpy)_2(\mathbf{2}^{\bullet-})]^{+}$ in aprotic and even protic media is slow compared to that of $[Ru(bpy)_2(\mathbf{1}^{\bullet-})]^{+}$; (b) the excited state of $[Ru(bpy)_2(\mathbf{1})]^{2+}$ can abstract a hydrogen atom from hydroquinone, but $*[Ru(bpy)_2(\mathbf{2})]^{2+}$ does not show such reactivity; (c) the rate of hydride transfer to Ph_3C^+ is ca. 100 times faster for $[Ru(bpy)_2(\mathbf{2HH})]^{2+}$ compared to $[Ru(bpy)_2(\mathbf{1HH})]^{2+}$.[6] While both isomers $[Ru(bpy)_2(\mathbf{1HH})]^{2+}$ and $[Ru(bpy)_2(\mathbf{2HH})]^{2+}$ are very weak hydride donors and cannot transfer a hydride ion to CO_2 or M–CO, theory indicates that hydride donation ability (or hydricity) can be increased by additional one-electron reduction of these species. $[Ru(bpy)_2(\mathbf{1HH})]^{+}$ can be produced chemically (Na/Hg reduction) or photochemically and shows an increased reactivity compared to $[Ru(bpy)_2(\mathbf{1HH})]^{2+}$.[6]

$[Ru(bpy)_2(\mathbf{1HH})]^{2+}$

$[Ru(bpy)_2(\mathbf{2HH})]^{2+}$

[1]Koizumi, T.; Tanaka, K., *Angew. Chem. Int. Ed.* **2005**, *44*, 5891-5894; [2]Polyansky, D.; Cabelli, D.; Muckerman, J. T.; Fujita, E.; Koizumi, T.; Fukushima, T.; Wada, T.; Tanaka, K., *Angew. Chem. Int. Ed.* **2007**, *46*, 4169-4172; [3]Polyansky, D. E.; Cabelli, D.; Muckerman, J. T.; Koizumi, T.; Fukushima, T.; Tanaka, K.; Fujita, E. *Inorg. Chem.* **2008**, *47*, 3958-3968; [4] Fukushima, T.; Fujita, E.; Muckerman, J. T.; Polyansky, D. E.; Wada, T.; Tanaka, K. *Inorg. Chem.* **2009**, *48*, 11510–11512; [5] Cohen, B. W.; Polyansky, D. E.; Zong, R.; Zhou, H.; Ouk, T.; Cabelli, D. E.; Thummel, R. P.; Fujita, E. *Inorg. Chem.* **2010**, *49*, 8034–8044; [6] Cohen, B. W.; Achord, P.; Cabelli, D.; Fujita, E.; Muckerman, J. T.; Polyansky, D. E.; Tanaka, K.; Thummel, R. P.; Zong, R. *Faraday Discuss.* submitted.

Theoretical Studies of Quantum Dot Chromophores for Solar Energy Harvesting

Oleg V. Prezhdo
Department of Chemistry
University of Rochester
Rochester, NY 14627

Semiconductor quantum dots (QDs) exhibit strong absorption cross sections across a broad energy range, and therefore, can improve solar energy. Multiple exciton generation (MEG) has the potential to increase photovoltaic efficiencies by transforming the excess energy stored in short wavelength photons into additional charge carriers. The solar applications of QDs depend critically on interplay of dynamical processes that follow photoexcitation.
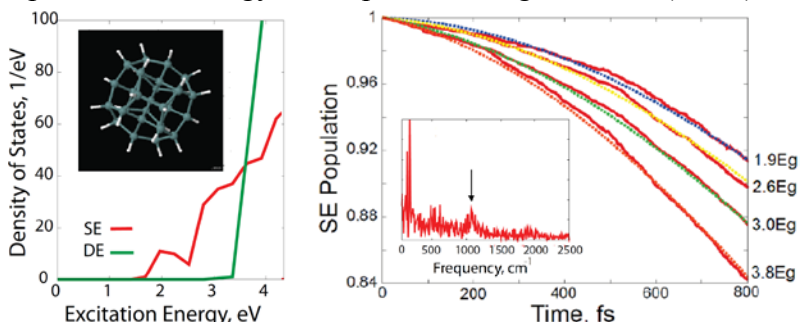
We developed time-domain ab initio simulation of Auger phenomena, including MEG and ME recombination (MER). It is the first theoretical approach describing phonon-assisted processes and early dynamics. MEG starts below electronic threshold, strongly accelerating with energy. Ligands are particularly important to phonon-assisted MEG. Short-time Gaussian component gives 5-10% of MEG, justifying rate theories that assume exponential dynamics. MER is preceded by electron-phonon relaxation to low energies.

Our time-domain ab initio simulations of phonon-induced relaxation in Si and Ge QDs show that in spite of the symmetric density of states (DOS), the electrons decay faster than the holes. The asymmetry arises due to stronger coupling of electrons to surface ligands. Linear relationships between the relaxation rates and DOS are found in agreement with Fermi's golden rule. The difference in the phonon-induced electron and hole decay rates is larger in Ge than Si, indicating that Auger processes are particularly important in Ge QDs.
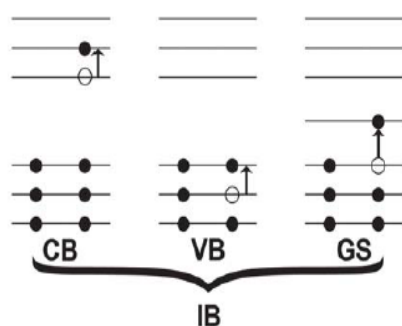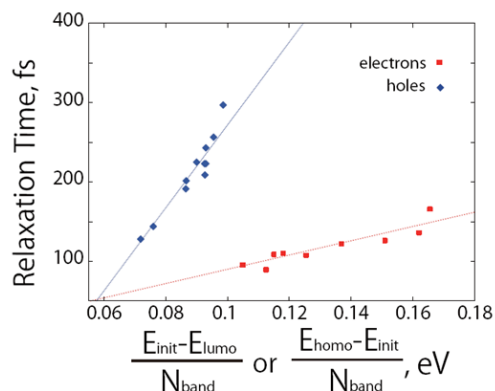
High-level ab initio electronic structure calculations on Si and PbSe QDs indicate that charging, doping, dangling bonds and other defects introduce new intra-band transitions, shift optical absorption spectra and push the normal excitonic and multiexcitonic transitions to higher energies. These defects can dramatically reduce MEG yields. Generally, doping and charging have similar effects on the excited state properties, while introduction of dangling bonds cause less severe changes, since the latter defect can be partially accommodated by reorganization in the local bonding pattern.

Electronic and Atomic Requirements in Catalytic Water Oxidation by Ru Complexes - Insights from EPR and X-Ray Spectroscopy

D. Moonshiram[1], I. Alperovich[1], J. W. Jurss[2], T. J. Meyer[2], Y. Pushkar[1]

[1]Department of Physics, Purdue University, West Lafayette, IN, 47907
[2]Department of Chemistry, University of North Carolina at Chapel Hill, Chapel Hill, NC 27599

Water oxidation is a key half reaction of photosynthesis and it will play an important role in the production of solar fuels by artificial photosynthesis. Coupling the multi-electron nature of this reaction to single photon solar absorption poses a significant mechanistic challenge. This reaction is carried out in the oxygen evolving complex of Photosystem II. Ru complexes such as the Ru "blue dimer" and single site Ru complexes are among the few systems which can oxidize water catalytically. Understanding the critical electronic, energetic and geometric requirements of the water oxidation reaction is necessary for achieving increased efficiency and for the design of new catalysts.

Using Ce(IV) as an oxidant, we generated reactive intermediates of various Ru-based catalysts for water oxidation. Kinetic analysis of the reaction mixtures with the UV-Vis stopped-flow and freeze-quench techniques at millisecond resolution allowed us to determine the times and conditions in which particular reactive intermediates exist and to trap them for further characterization. EPR and X-ray techniques (XANES, EXAFS) were then used to detect the changes in the oxidation state of Ru and in the geometry of the ligand environment in these intermediates.

In the "blue dimer" (pH=1, HNO_3), a highly reactive intermediate with the $Ru^{IV,V}$ oxidation states was generated on the time scale of a few seconds. This intermediate reacts with water to form a $Ru^{III,IV}$ species which is spectroscopically different from the stable $Ru^{III,IV}$ product of one-electron oxidation of "blue dimer". The $Ru^{IV,V}$ and $Ru^{III,IV}$ intermediates have unique EPR signals and their oxidation states were assigned from Ru K-edge and Ru L-edges XANES. EXAFS at the Ru K-edge demonstrated changes in the Ru-ligand distances and the angle of the Ru-O-Ru bridge.

To extract detailed information about the electronic structure of water oxidation intermediates from Ru $L_{2,3}$-edges X-ray absorption (XAS) spectroscopy, we developed a method to simulate such spectra based on a two-component relativistic zeroth-order regular approximation (ZORA) implemented in density functional theory (DFT). This approach allows us to predict Ru $L_{2,3}$-edges XAS starting with a particular molecular geometry and electronic structure of an intermediate. The main advantage of the approach is an accurate inclusion of spin-orbit coupling effects. The obtained theoretical Ru $L_{2,3}$-edge spectra are in good agreement with experiment.

π-Conjugated Donor-Acceptor-Donor Ions for Solar Energy Conversion

Dinesh G. (Dan) Patel, Fude Feng, Yu-ya Ohnishi, Coralie A. Richard, Kahlil A. Abboud,
So Hirata, Kirk S. Schanze, and John R. Reynolds
Department of Chemistry, University of Florida, Gainesville, FL, 32611-7200

π-Conjugated donor-acceptor-donor (D-A-D) oligomers can show light absorption properties extending fully through the visible and into the near infrared region of the spectrum, while simultaneously allowing precise control of the HOMO and LUMO energy levels. While these features make D-A-D oligomers ideal for use in dye-sensitized solar cells, these systems have yet to be modified with bound anions such as carboxylate groups that can be used for binding the systems to metal oxide interfaces.

In our initial effort, we focused on the benzotriazole acceptor (BTz), which posesses both electron withdrawing imine groups but also a central atom that can be alkylated thus allowing for the inclusion of carboxylate groups. Our experiments show that BTz is a poor acceptor, as a D-A-D oligomer containing BTz flanked by thiophene (Th) donors shows minimal visible light absorption and it does not exhibit reduction at potentials above -2.0 V vs. Fc/Fc$^+$. To introduce electron deficiency, we have synthesized a hybrid acceptor that contains the BTz moiety in addition to a benzo-fused thiadiazole acceptor. This BTzTD hybrid acceptor shows both visible light absorption before and after alkylation, along with reversible reductive and oxidative processes with the LUMO level at -3.93 eV, which is close to the conduction band edge of anatase TiO$_2$ at -4.0 eV.
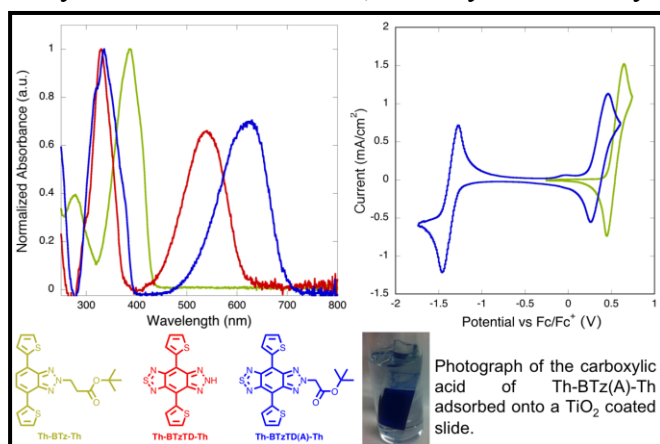
To study charge injection into TiO$_2$, the t-butyl protecting groups were removed from the BTzTD acceptor to give the free carboxylic acid for TiO$_2$ adsorption experiments. We find that
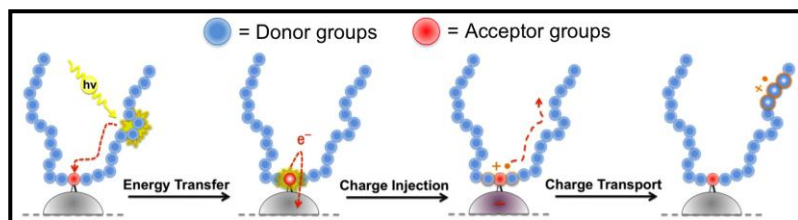
the triethylammonium salt of this D-A-D oligomer carboxylate ion adsorbs well to TiO$_2$ from a DMF solution giving rise to a deep blue colored film (see photograph above). Data will be presented on the photoelectrochemistry of these D-A-D oligomers adsorbed onto nanocrystalline TiO$_2$ films. We will, in systematic fashion, increase the number of donor units per single BTzTD acceptor eventually leading to polymeric systems and probe the electron transfer dynamics and evolution of the radical cation on the donor portion of the oligomers and polymers. Additionally, we have begun work on benzo-fused D-A cores, which have the benefit of ensuring planarity between D-A units and have only recently gained attention for use in energy conversion in polymeric systems.

160

Ultrafast Energy Transfer in Conjugated Polyelectrolyte Dendrimers

Sevnur Kömürlü, Fude Feng, Seoung Ho Lee, Valeria D. Kleiman, John R. Reynolds and Kirk S. Schanze
Department of Chemistry, University of Florida, Gainesville, FL, 32611-7200

Three different families of π-conjugated polyelectrolyte dendrimers (CPE-Ds) have been synthesized and their energy and electron transport properties studied by steady state and ultrafast time-resolved spectroscopy. CPE-Ds feature conjugated cores and a periphery with branched ionic groups providing high solubility, low tendency to aggregate, and the potential to study analogous CPE-Ds in organic (ester form) and polar (ionic form) solvents. Ultrafast fluorescence dynamics were used to study intramolecular energy transfer and intermolecular energy or electron transfer to dye or electron acceptor ions.

The first family of CPE-Ds consists of three generations of meta-linked phenylene ethynylene units. The short conjugation length characteristic of this system results in a relatively high HOMO-LUMO gap. As the conjugation length does not change from generation to generation, there is no energy gradient within these compact dendrimers. To create an energy gradient, two families of extended conjugation CPE-Ds with para-phenylene ethynylene (or 2,5-thienylene) units at their core and meta-phenylene ethynylene units at the periphery were synthesized. The longer conjugation length in the dendrimer core provides a lower HOMO-LUMO gap, producing an energy gradient from the periphery to the core.

Energy transfer dynamics of the extended conjugation CPE-Ds were investigated by ultrafast fluorescence up-conversion. At long times (700 ps – 1.1 ns), the organic-soluble ester form of the CPE-Ds present dynamics independent of excitation or emission λ. In the sub-ps time scale, excitation of the periphery
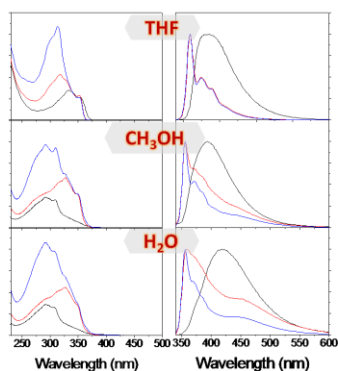
results in wavelength dependent dynamics. At the blue edge of the emission spectrum there is a fast decay component which becomes a rise component at the red edge of the spectrum. This component is attributed to energy transfer from periphery to core. For generation 2, the time component is 0.6 ps while generation 3 shows similar behavior with a slower energy transfer time constant (0.9 ps) as the distance from donor to acceptor units increases. The thiophene containing CPE-Ds exhibit slower energy transfer due to weaker electronic coupling between periphery and core. CPE-Ds in ester form and their water soluble analogs are compared to understand the effects of the ionic groups on the energy transfer. The presence of ionic groups leads to H-aggregate formation for the first generation dendrimers. The 2nd and 3rd generation CPE-Ds show only a small contribution from excimer-like aggregate formation: the observed dynamics become wavelength dependent at long time scale. The sub-ps time scale, associated with periphery to core energy transfer, exhibits a wavelength dependence similar to the organic-soluble analogs. The decay times detected at short wavelength become rise times at long wavelength with similar rates from 2nd and 3rd generation (0.6 ps). Both 2nd and 3rd generation ionic CPE-Ds exhibit faster energy transfer rates compared to their organic-soluble analogs. This effect is believed to arise due to a partial "collapse" of the CPE-D in the aqueous solution due to hydrophobic interactions within the dendrimer structure. The structurally well-defined CPE-Ds provide a platform to study intrachain and intermolecular energy and electron transfer mechanisms in better defined systems compared to the linear conjugated polyelectrolytes which have been the focus of previous work in our labs.
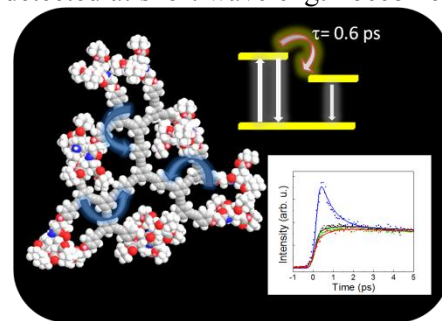
1. S. Kömürlü, S-H Lee, K. S. Schanze, and V. D. Kleiman "Energy Transfer in Thiophene Containing Phenylene Ethynylene Dendrimers", submitted to *J. Phys. Chem. B*.

Trends in (P-P)$_3$m^{n+} D^6 LMCT Photooxidant Systems

Dean M. Roddick, Jeramie J. Adams, and Navamoney Arulsamy
Department of Chemistry, Dept. 3838
University of Wyoming
Laramie, WY 82071

Building upon Sullivan's earlier studies on (dmpe)$_3$Re^{2+} photooxidant systems, our primary findings in the previous two years for this novel class of photoactive compounds were (1) Significantly increased emission lifetime for the more electron-rich (depe)$_3$Re^{2+} (depe = Et$_2$PCH$_2$CH$_2$PEt$_2$) analog relative to (dmpe)$_3$Re^{2+}, (2) Emission quenching for (R$_2$PCH$_2$PR$_2$)$_3$Re^{2+} systems with a single methylene diphosphine chelate bridge and also aryl-linked phosphine systems (dmpb)$_3$Re^{2+}, and (3) An insensitivity of absorption and emission energies for (R$_2$P(CH$_2$)$_n$PR$_2$)$_3$Re^{2+} (n = 1 or 2; R = Me, Et, Ph) despite a 500 mV ground state variation in E$_0$(Re^{2+}/Re$^+$) between +0.16 and +0.6V. The more sterically- demanding and electron-poor chelating phosphines dppe (Ph$_2$PCH$_2$CH$_2$PPh$_2$), dmpc (Me$_2$P(o-C$_2$B$_{10}$H$_{10}$)PMe$_2$), and Ph$_2$P(o-C$_6$H$_4$)PMe$_2$ reacted to give the Re(II) dihalides *trans*-(PP)$_2$ReX$_2$ (X = I or Cl).

The surprising sensitivity of emission to phosphine chelate bridge variation has prompted us to examine the propyl-linked phosphine dmpp (Me$_2$PCH$_2$CH$_2$CH$_2$PMe$_2$) complex (dmpp)$_3$Re^{2+}. (dmpp)$_3$Re^{2+} is highly emissive at 569 nm when excited at the major absorption CT band at 470 nm. When combined with the ground state Re$^{+/2+}$ oxidation potential (0.195 V), the dmpp

emissivity

system gives a EOP slightly less than (dmpe)$_3$Re^{2+} at 2.59 V. Excited state emission properties for (dmpp)$_3$Re^{2+} are being quantified in collaboration with the Schmehl group at Tulane University.
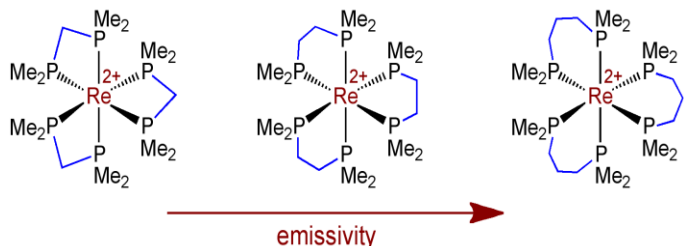
In addition to the remarkable sensitivity of emission efficiency in tris chelate Re(II) systems, we have also been more broadly investigating the anti-symbiotic nature of ground state oxidation potential and emission energies for the isoelectronic octahedral tris-chelate d^6 series (dmpe)$_3$Mo$^+$, (dmpe)$_3$Re^{2+}, and (dmpe)$_3$Ru^{3+}. Transition metal electronegativity and oxidation state trends predict an increase in d^6 ground state oxidation potentials and a decrease in emission energy, E$_{00}$:

The very low oxidation potential of (dmpe)$_3$Mo$^{0/+}$ (-1.21 V) required the weak oxidant C$_7$H$_7$B(C$_6$F$_5$)$_4$ to successfully prepare (dmpe)$_3$Mo$^+$ and prevent over oxidation to (dmpe)$_3$Mo^{2+}. (dmpe)$_3$Mo$^+$ has a strong blue emission at 455 nm and the highest observed E$_{00}$ at 2.85 V and an associated EOP of +1.64 V. Interestingly, the d^4 dicationic species (dmpe)$_3$Mo^{2+} is weakly emissive (E$_{ox}$ = -0.07 V, EOP = +2.4 V). Emission from other d^4 analogs such (dmpe)$_3$Re^{3+}is currently under investigation.

E$_{00}$

E$_{ox}$
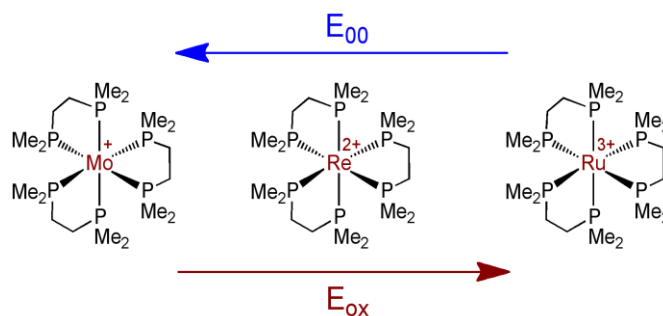
The isoelectronic d^5 ruthenium complex (dmpe)$_3$Ru^{3+} should have the highest ground state potential and the lowest E$_{00}$ value. We have reexamined early reports of irreversible (dmpe)$_3$Ru$^{2+/3+}$ oxidation at ~ 1.80 V and see a quasi-reversible Ru$^{2+/3+}$ couple. Results of spectroelectrochemistry experiments to define the absorption and emission properties of (dmpe)$_3$Ru^{3+} will be presented.

Photophysical Behavior And Photoredox Reactions Of Square Planar Pt(II) Complexes in Solution: One Electron Oxidation Processes

Jeff Draggich, Amelia Neuberger and Russell Schmehl
Department of Chemistry, Tulane University, New Orleans, LA 70118

A variety of square planar Pt(II) complexes have been shown to exhibit luminescence and to sensitize photoinduced electron transfer reactions. The excited states of these chromophores range from those in which the metal serves as a template for electron donating and accepting ligands that exhibit charge transfer absorption to complexes for which electronic transitions have significant metal orbital contributions. Many of these complexes also have electrochemically irreversible oxidation and, as a result, one (or two) electron potentials are not known. In an effort to understand the oxidative chemistry of these complexes in both the ground and excited states, we have investigated excited state quenching with a variety of reversible and sacrificial electron acceptors for two groups of complexes : $[(Xtpy)PtL]^+$ derivatives where L = OH or OMe and X= H, p-tolyl, Cl and $[(N^\wedge C^\wedge N)PtCl]$ complexes where $N^\wedge C^\wedge N$ is one of a group of bis-pyridylbenzene derivatives. Density functional calculations of each of these groups of chromophores reveals that the HOMO has significant Pt $d\pi$ orbital character. One electron oxidation should lead to a species with a significant degree of Pt(III) character that might, under certain circumstances react with Pt(II) species to form Pt(III)-Pt(II) bimetallic complexes with a partial Pt-Pt bond or, alternatively, the Pt(III) species may disproportionate to yield Pt(II) and Pt(IV) species. For light induced electron transfer reactions, these processes will compete with back electron transfer with the reduced electron acceptor to regenerate the starting complex.
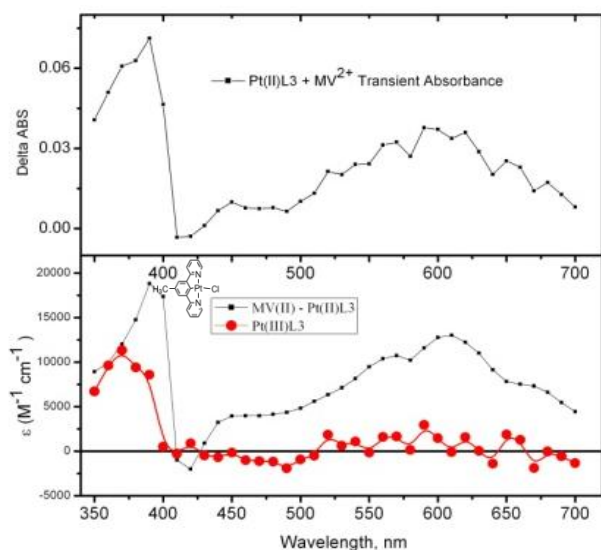
The $[(N^\wedge C^\wedge N)PtCl]$ complexes are strongly luminescent and the emission can be quenched by a broad range of one electron acceptors including pyridinium ions and aryldisulfides. Exploration of the free energy dependence of the quenching process with pyridinium acceptors indicates that the excited complex is a strong reductant ($E^0(Pt(III)/Pt(II)^* < -1.1$ V vs. SCE). In addition, photoinduced electron transfer with acceptors having reversible reduction and well known radical ion spectra allows determination of the uv-vis spectroscopic behavior of the transient Pt(III) species (figure).

The $[(Xtpy)PtOH]$ complexes also exhibit red luminescence in acetonitrile solution at room temperature. In addition excited state electron transfer to electron acceptors is observed and transient uv-vis spectra can be obtained. An interesting possibility with these complexes is that one electron oxidation can be followed by deprotonation of the hydroxo ligand to produce a unique oxo like species.

Novel Approaches for Photoelectrosynthesis

J. Oh, T.G. Deutsch, H-C, Yuan, H. Branz, A.J. Nozik, J.A. Turner
National Renewable Energy Laboratory
Golden, CO 80401

Nanostructured Si eliminates several critical problems with Si photocathodes and dramatically improves the photoelectrochemical (PEC) reaction important to water-splitting. Our nanostructured black Si photocathodes enhance H_2 production by providing (1) near-ideal anti-reflection that enables the absorption of most of the incident light and its conversion to photogenerated electrons and (2) extremely high surface area in direct contact with water that reduces the overpotential needed for the PEC H_2 redox reaction. Finally, the nanostructured Si surface facilitates bubble evolution and reduces the need for surfactants in the electrolyte.
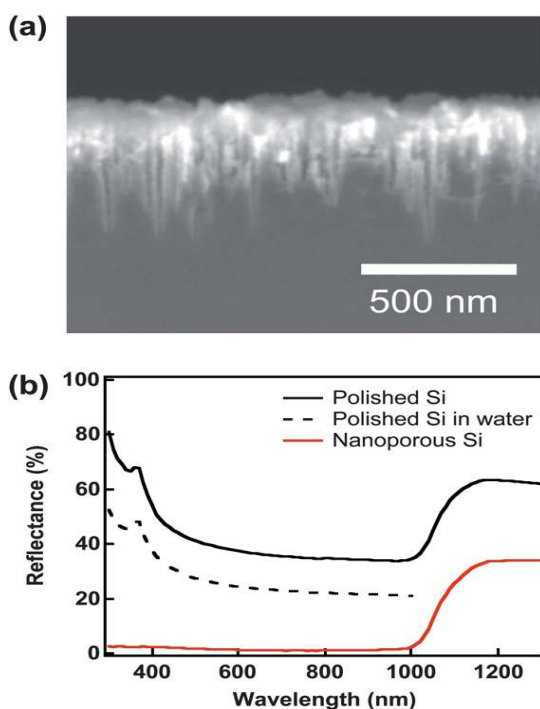
Figure 1. Nanostructure and optical reflectance of Si photocathodes. (a) Cross-sectional scanning electron microscopy (SEM) image of nanoporous Si fabricated by a one-step metal-assisted etching process. Pores have s conical shape with a diameter of about 20nm. Scale bar = 500 nm. (b) measured total hemispherical optical reflectance of polished and nanoporous Si in air, and calculated reflectance of polished Si in water.
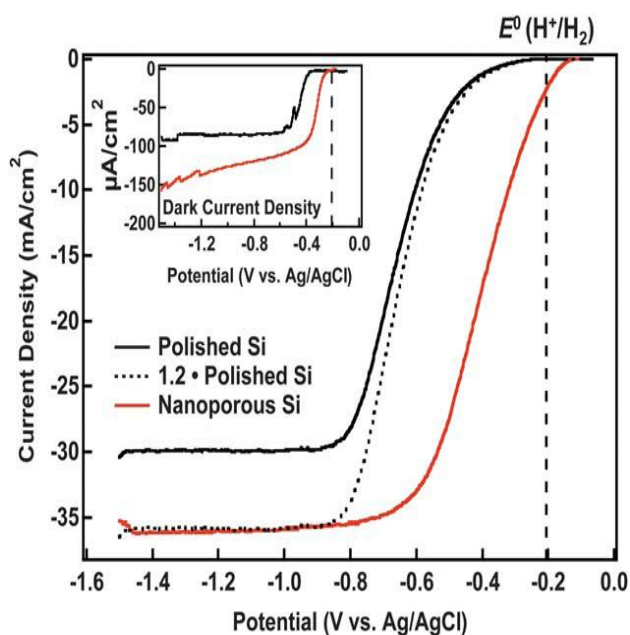
Figure 2. Photoelectrochemical current–voltage curves of Si photocathodes during H_2 production under simulated 1 sun illumination. The black dotted line normalizes the j–V curve of the polished Si to the limiting photocurrent density of the nanoporous Si and indicates that the anodic shift of the nanoporous Si originates from the increased surface area. The inset shows the dark current density of the nanoporous and polished Si electrodes in the same electrolyte.

164

Imaging of Energy and Charge Transport in Nanoscale Systems

Klara Maturova, Manuel Romero, and Jao van de Lagemaat
Chemical and Materials Sciences Center, National Center for Photovoltaics
National Renewable Energy Laboratory
Golden, Colorado, 80004

Extraordinary and sometimes unexpected properties are observed when electrons and excitons are confined to small spaces and nanoscale energy flow in such systems is an important and not always well understood phenomenon. Most current techniques that address nanoscale energy and charge transport phenomena have good energy resolution, good spatial resolution, or good temporal resolution, but not all at the same time. The current project aims to investigate nanoscale energy and charge flow in photochemical conversion systems by expanding a technique based on scanning tunneling luminescence, which has good energy and spatial resolution, to also include temporal information.

In previous work, we have demonstrated that strong coupling occurs between surface plasmons formed between substrate and tip upon current injection and excitons on semiconductor quantum dots. This causes energy transfer from the plasmon to the exciton on the particle which is followed by luminescent decay. We also demonstrated strong plasmon/exciton coupling between conjugated polymers such as poly-3-hexyl thiophene and metal substrates which allowed us to study the exciton diffusion length in those materials when mixed with acceptor molecules.

Currently, we are extending the scanning tunneling luminescence technique to include time resolution by using current injection into the substrate during the "tap" event occurring by oscillating the tip in a tapping-mode AFM experiment. We demonstrate that microsecond time resolution is possible this way. We apply the technique to study charge and exciton

Fig. 1. Schematic of the experiment. Current is injected during a tapping event, followed by light emission.

transport in single quantum dots and quantum rods as well as in clusters and multiple layers of quantum dots. Results show that the initial current injection pulse into a single dot is followed by multiple afterbeats of current contrary to other conductive systems. This beating of the current is possibly related to the well-known blinking of these dots and we are studying the kinetics of this process as well as that of the resulting luminescence in order to study this in more detail. In addition to current injection and light emission, we are also studying photocurrent spectroscopy in single dots and clusters of dots and its relation to blinking and multiple exciton generation.

2010-2011 DOE Solar Photochemistry supported publications

A. J. Morfa, A. M. Nardes, S. E. Shaheen, N. Kopidakis, and J. van de Lagemaat, "Time-of-flight Studies of Electron Collection Kinetics in Polymer:Fullerene Bulk Heterojunction Solar Cells", Advanced Functional Materials, *in press*

Long Range Energy Transfer in Highly Ordered Single Polymer Chains

David Vanden Bout, Matthew C. Traub, Girish Lakhwani, Joshua C. Bolinger, Takuji Adachi
and Paul F. Barbara
Department of Chemistry
The University of Texas at Austin
Austin, TX 78712

It is extremely difficult to probe the complex relationship between structure and energy transfer in thin films of conjugated polymers due to the existence of features far smaller than the diffraction limit of light ($\sim\lambda/2$). To understand these relationships beyond the limitations imposed in thin films, we have probed interchromophoric exciton migration and exciton-to-polaron quenching in single chains of the prototypical conjugated polymer MEH-PPV using sub-diffraction imaging, simulation, and the simultaneous measurement of the excitation and emission anisotropy for single molecules. Increases in average anisotropy from excitation to emission, accompanied by very small average changes in the measured dipole orientation were consistent with efficient energy transfer to a small number of low energy sites in a highly-ordered rod-like confirmation. The results, along with previously reported single molecule emission data, were simulated using an incoherent FRET energy transfer model between chromophores on highly ordered bead-on-a-chain model polymer molecules. These simulations correctly reproduced the observed anisotropy histograms, and suggested that excitons migrate on average ~6 nm, probably a lower limit based on the energy transer model used.

To directly visualize energy transfer, we used the new technique bias-modulated intensity centroid (BIC) spectroscopy. In this technique, hole polarons are reversibly and repeatedly injected into single MEH-PPV molecules, and the resulting fluorescence centroid fit to nm precision, allowing imaging of exciton-to-polaron quenching beyond the diffraction limit. We found that holes repeatedly return to existing low energy trap sites from cycle-to-cycle. Average centroid shifts of more than 13 nm, with many individual molecules displaying shifts of more than 30 nm, imply that in these ordered single chains, energy transfer can occur over distances of greater than 50 nm.
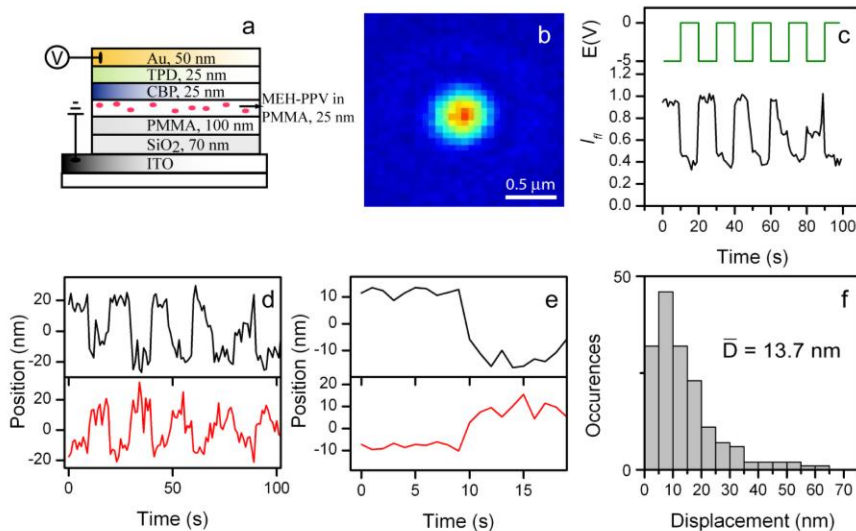
Photodriven Reduction of a Cobaloxime Hydrogen Evolution Catalyst: Avoiding Unproductive Excited State Quenching

Brad S. Veldkamp, Amanda L. Smeigh, Mark A. Ratner, and Michael R. Wasielewski
Department of Chemistry
Northwestern University
Evanston, IL 60208-3113

Economically viable photodriven H_2 production requires the discovery and integration of *abundant, robust materials able to efficiently collect light energy, separate charges, and catalyze fuel forming reactions*. It is important to develop photosensitizers that separate charge more rapidly than their excited states are quenched by electronic interactions with the metal catalysts that do not result in productive charge delivery to the catalysts. We have developed a new organic photosensitizer ligand for the photodriven reduction of cobaloxime hydrogen evolution catalysts. The chromophore-acceptor dyad ligand is prepared by linking perylene (Per) to a 4-(4'-pyridyl)-1,8-naphthalimide (NMI) using a phenyl bridge. Coordination of the pyridyl ligand to the catalyst $[Co^{II}(dmgBF_2)_2(L)_2]$, where $dmgBF_2$ = (difluoroboryl)dimethylglyoximato and L = water or a solvent molecule ($Co^{II}Cat$), yields the Per-NMI- $Co^{II}Cat$ triad assembly. Selective photoexcitation of the uncoordinated Per-NMI ligand in CH_2Cl_2 with 416 nm, 110 fs laser pulses results in rapid electron transfer from $^{1*}Per$ to NMI with $\tau = 9 \pm 2$ ps. Charge recombination occurs with $\tau = 561 \pm 66$ ps. Excitation of the full Per-NMI- $Co^{II}Cat$ triad with 416 nm, 110 fs laser pulses results in electron transfer from $^{1*}Per$ to NMI with $\tau = 4.0 \pm 0.7$ ps followed by electron transfer from $NMI^{\bullet}$ to $Co^{II}Cat$ in $\tau = 208 \pm 20$ ps. The quantum yield of catalyst reduction is ~43%. The process that competes with reduction of $Co^{II}Cat$ is energy transfer from the excited Per to $Co^{II}Cat$. Charge recombination of the fully charge separated state: $Per^{+\bullet}$ -NMI-$Co^{I}Cat$ is slow with $\tau > 1$ µs.

Donor chromophore: perylene (E_{ox} = 1.05 V vs. SCE)
Acceptor: 1,8-naphthalimide (E_{red} = -1.37 V vs. SCE)[4]
Catalyst: $[Co^{II}(dmgBF_2)_2(H_2O)_2]$ (E_{red} = -0.55 V vs. SCE)[1]
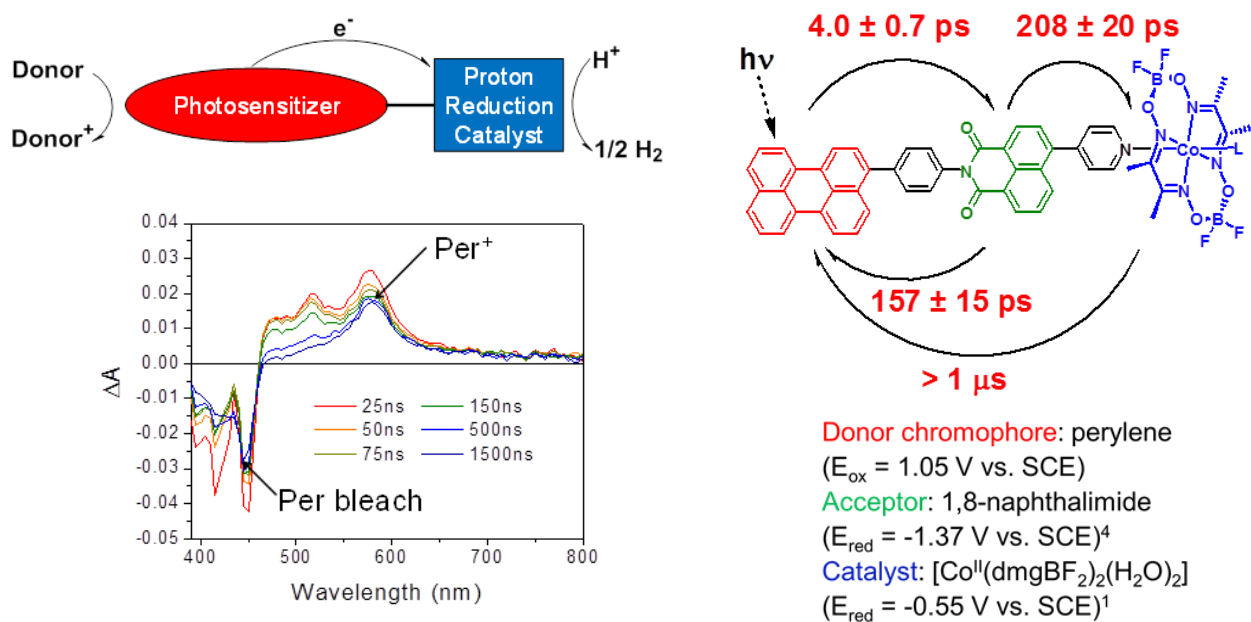
Control of Exciton Delocalization and Splitting at the Quantum Dot-Organic Interface

Matthew T. Frederick, Adam J. Morris-Cohen, Laura C. Cass, and Emily A. Weiss
Department of Chemistry
Northwestern University
Evanston, IL 60208-3113

The objective of this research program is to determine, systematically and quantitatively, the role of organic ligands, coordinated to the surface of semiconductor quantum dots (QDs), in the dynamics of electrons and holes created upon photoexcitation of the QDs. In our first year of this project, we have attacked this problem by asking three major questions: (i) What is the relationship between the structural and chemical parameters at the QD-organic interface, and the rate of heterogeneous charge transfer across that interface? (ii) Can we design ligands to interact not only with local surface states of the QD, but also with the QD core in order to modify the optical properties of QDs? (iii) How can we directly measure the influence of vibrations of ligands and surface states on the dissipation of electronic energy in photoexcited QDs? This poster describes our progress on all three of these fronts.
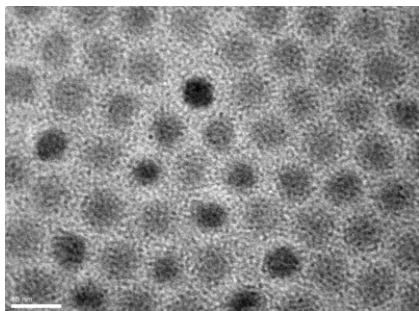
Fig.1 – Transmission electron micrograph of PbSe nanocrystals. The scalebar represents 10 nm.
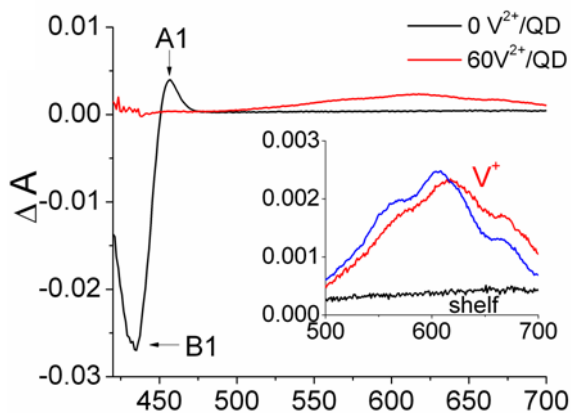
Fig.2 – Charge Transfer Transient absorption spectrum (x-axis is λ in nm) at 100 ps after photoexcitation, of 4.6-nm CdS QDs in DCM without (black) and with (red) 60 V^{2+} added per QD. The signal from V^+ radical cation is maximum at t = 100 ps (spectrum shown in inset and compared with the V^+ spectrum obtained with spectroelectrochemistry).
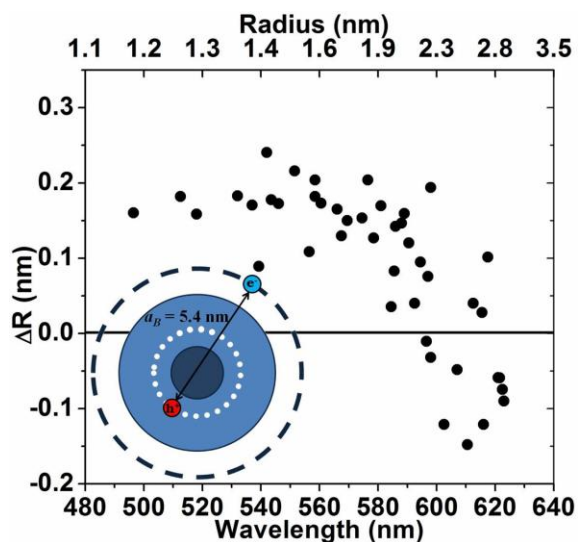
Fig.3 – Exciton Delocalization Change in apparent radius (ΔR) as a function of initial absorption wavelength (bottom axis), and the physical radius of the inorganic core (top axis) for CdSe QDs. Flat region = strong confinement regime, decreasing regions = intermediate confinement. The inset is a picture of the smallest and largest QDs we synthesized. The characteristic delocalization area of the excitonic hole is outlined by a white dotted line, and the delocalization area of the excitonic electron is outlined by a black dotted line. The maximum distance between the two carriers is the Bohr exciton radius of the bulk, and is represented as a black arrow.

168

Charge Type Effects on Bimolecular Electron Transfer Reactions in C$_4$mpyrr NTf$_2$

Masao Gohdo and James Wishart
Chemistry Department
Brookhaven National Laboratory
Upton, NY 11973

Electron transfer reactions underlie many of the important applications of ionic liquids (ILs), including solar cells, fuel cells and batteries. The unusual dynamical properties of ILs, and the fact that they are composed solely of ions, have important mechanistic consequences for reactions involving charge redistribution. Interactions between solutes and IL cations and anions can be affected by changing the charge of the solute. Depending on the reactant charges, preferred solvation environments may change during the course of charge transfer. Furthermore, electrochemical experiments have shown that the diffusion constants of redox-active species may depend on charge type much more strongly in ILs than in conventional solvents.
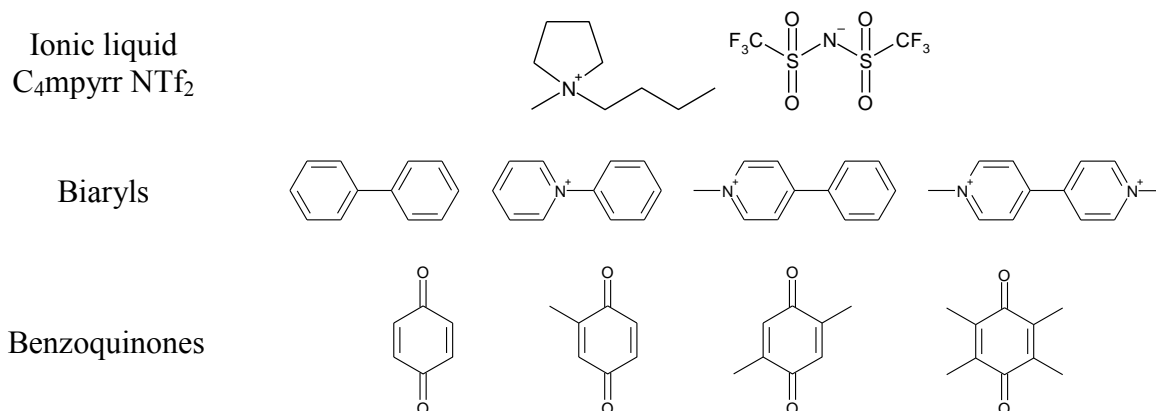
To explore these effects, we are studying intermolecular redox reaction mechanisms in ionic liquids to quantify their dependence on reactant charge types and the physical properties of the ILs. For our preliminary studies we are measuring a series of electron transfer reactions between quasi-isostructural biaryl electron donors (biphenyl anion, phenylpyridinyl radical, methyl viologen monocation, etc.) and substituted *p*-benzoquinones in C$_4$mpyrr NTf$_2$. We use pulse radiolysis to generate solvated electrons in the IL, which react with the biaryl scavengers to produce radical redox intermediates of different charge types that react with the benzoquinones. Compared to electrochemical methods, pulse radiolysis has certain merits: the reduced species are generated homogeneously in solution instead of near a polarized electrode surface; the redox kinetics can be directly observed down to the nanosecond time scale, and it is usually possible to spectroscopically observe both the reductant and oxidant. The effects of different charge types on the diffusion coefficients of the reactants and their electron transfer rates will be discussed, also taking the thermodynamics into account.

Water Oxidation in Natural Photosynthesis Studied Using X-ray Spectroscopy

Jan Kern, Rosalie Tran, Benedikt Lassalle, Ken Sauer, Junko Yano, <u>Vittal K. Yachandra</u>
Physical Biosciences Division
Lawrence Berkeley National Laboratory
Berkeley, CA 94720

The Mn_4Ca catalytic cluster of the oxygen-evolving complex (OEC) in Photosystem II (PS II) cycles through five oxidation states (S_i-states, i=0-4) coupling the one electron photochemistry of the reaction center with the 4 electron redox chemistry of water oxidation.

We have reported detailed X-ray absorption spectroscopy studies from solution and single crystal XANES and EXAFS data from the native S_1 (dark) state and proposed structural models of the Mn_4Ca cluster of PS II within the context of the protein environment. This study used PS II dimer crystals obtained from *T. elongatus*, in which the crystal unit cell contains four PS II dimers. We have also collected polarized spectra of monomer PS II single crystals, which have been recently crystallized. Monomer crystals have a favorable orientation for deriving a structure for the Mn_4Ca cluster. In addition to X-ray spectroscopy, the structure of the Mn_4Ca cluster has been extensively studied by X-ray crystallography between a resolution of 3.8-2.9 Å, with the most recent X-ray crystallography structure being at a resolution of 1.9 Å. This study for the first time gives us a starting point to think about the detailed chemical structure of the Mn_4CaO_5 cluster in the dark state (S_1) and also the consequence of specific radiation damage to the redox-active Mn site. We will discuss the structural parameters including the geometry derived from X-ray spectroscopy in relation to the crystallography structure at 1.9 Å resolution.

Fig. 1. A structural model of the Mn_4Ca cluster from X-ray spectroscopy. Mn_A-Mn_B, Mn_B-Mn_C, and Mn_C-Mn_D are ~ 2.7, 2.7 and 2.8 Å, Mn_D-Mn_B is ~ 3.3 Å. Ca-$Mn_{B,C,D}$ distances are ~3.4 Å, while Ca-Mn_A is 3.9-4.0 Å.

We have extended the study to the higher S-states by illuminating the S_1 state solution and single crystals either by continuous illumination or by laser flashes to create intermediate S-states (S_2 and S_3). The solution state spectra show changes in the structure of the catalytic cluster as it advances through the intermediate states. Polarized XANES and EXAFS spectra from these crystals show unique orientation dependence and provide additional information about the structural changes taking place in these intermediate states.

We have used X-ray emission spectroscopy to directly study the involvement of the oxo-bridges in the Mn_4Ca cluster in all the S-states. The relevance of the geometric and electronic structural changes derived from the X-ray absorption and emission spectroscopy studies to the mechanism of water oxidation will be discussed. Future plans for the use of the LCLS X-ray laser facility for simultaneous crystallography and spectroscopy studies will be presented.

We have also used X-ray absorption and emission spectroscopy to study artificial water oxidation Co and Ni oxide electrocatalysts (with the Nocera group, MIT) using *in situ* spectroelectrochemistry. These studies have been able to describe the structure of Co/Ni oxide catalyst on the electrode surface and have provided information about the mechanism.

List of Participants

Participants List – 33rd DOE Solar Photochemistry Research Meeting

Neal Armstrong
University of Arizona
Department of Chemistry
Tucson, AZ 85721
520-621-8242
nra@email.arizona.edu

Allen Bard
University of Texas
1 University Station A5300
Austin, TX 78712-0165
512-471-3761
ajbard@mail.utexas.edu

Victor Batista
Yale University
225 Prospect Street
New Haven, CT 06520
203-432-6672
victor.batista@yale.edu

Matthew Beard
National Renewable Energy Laboratory
1617 Cole Blvd
Golden, CO 80401
303-384-6781
matt.beard@nrel.gov

Jason Benedict
University at Buffalo
726 Natural Sciences Complex
Buffalo, NY 14216
715-645-4276
jbb6@buffalo.edu

Carol Bessel
U.S. Department of Energy
19901 Germantown Road
Germantown, MD 20874
301-903-1873
carol.bessel@science.doe.gov

Jeffrey Blackburn
National Renewable Energy Laboratory
16253 Denver West Parkway
Golden, CO 80401
303-384-6649
jeffrey.blackburn@nrel.gov

David Blank
University of Minnesota
207 Pleasant St SE
Minneapolis, MN 55455
612-624-0571
blank@umn.edu

David Bocian
University of California
Department of Chemistry
Riverside, CA 92521
951-827-3660
David.Bocian@ucr.edu

Kara Bren
University of Rochester
120 Trustee Rd.
Rochester, NY 14627
585-275-4335
bren@chem.rochester.edu

Karen Brewer
Virginia Tech
Department of Chemistry
Blacksburg, VA 24061-0212
540-231-6579
kbrewer@vt.edu

Gary Brudvig
Yale University
Department of Chemistry
New Haven, CT 06520-8107
203-432-5202
gary.brudvig@yale.edu

Louis Brus
Columbia University
3000 Broadway
New York, NY 10027
212-854-4041
leb26@columbia.edu

Emilio Bunel
Argonne National Laboratory
9700 S. Cass Ave., Bldg. 200
Argonne, IL 60439
630-252-4383
ebunel@anl.gov

Ian Carmichael
Notre Dame Radiation Laboratory
University of Notre Dame
Notre Dame, IN 46556
574-631-4502
carmichael.1@nd.edu

Edward W. Castner, Jr.
Rutgers University
610 Taylor Road
Piscataway, NJ 08854-8066
732-445-2564
ed.castner@rutgers.edu

Lin Chen
Northwestern University
9700 S. Cass Ave.
Argonne, IL 60439
630-252-3533
lchen@anl.gov

Kyoung-Shin Choi
Purdue University
Department of Chemistry
West Lafayette, IN 47907
765-494-0054
kchoi1@purdue.edu

Philip Coppens
University at Buffalo
732 NSc Complex
Buffalo, NY 14260-3000
716-645-4273
coppens@buffalo.edu

Robert Crabtree
Brookhaven National Laboratory
225 Prospect St.
New Haven, CT 06520-8107
203-432-3925
robert.Crabtree@yale.edu

Carol Creutz
Brookhaven National Laboratory
Bldg. 555
Upton, NY 11973-5000
631-344-4359
ccreutz@bnl.gov

Niels Damrauer
University of Colorado at Boulder
Dept. Chemistry and Biochemistry
Boulder, CO 80309
303-735-1280
niels.damrauer@colorado.edu

C. Michael Elliott
Colorado State University
Ft. Collins, CO 80523
970-491-5204
elliott@lamar.colostate.edu

John Endicott
Wayne State University
Department of Chemistry
Detroit, MI 48202
313-577-2607
jfe@chem.wayne.edu

Participants List – 33rd DOE Solar Photochemistry Research Meeting

Gregory Fiechtner
U.S. Department of Energy
19901 Germantown Rd, SC-22.11
Germantown, MD 20874-1920
301-903-5809
gregory.fiechtner@science.doe.gov

Graham Fleming
Lawrence Berkeley National Lab
Berkeley, CA 94720
510-643-2735
grfleming@lbl.gov

Marye Anne Fox
University of California
5926 Sagebrush Rd
La Jolla, CA 92037
858-349-3182
mafox@ucsd.edu

Arthur Frank
National Renewable Energy Laboratory
1617 Cole Boulevard
Golden, CO 80401
303-384-6262
afrank@nrel.gov

Heinz Frei
Lawrence Berkeley National Laboratory
1 Cyclotron Road
Berkeley, CA 94720
510-486-4325
HMFrei@lbl.gov

Richard Friesner
Columbia University
3000 Broadway, MC 3110
New York, NY 10027
212-854-7606
ec31@columbia.edu

Etsuko Fujita
Brookhaven National Laboratory
Chemistry Department
Upton, NY 11973-5000
631-344-4356
fujita@bnl.gov

Elena Galoppini
Rutgers University
73 Warren Street
Newark, NJ 07102
973-353-5317
galoppin@rutgers.edu

Wayne Gladfelter
University of Minnesota
Department of Chemistry
Minneapolis, MN 55455
612-624-4391
wlg@umn.edu

Richard Greene
U.S. Department of Energy
19901 Germantown Road
Germantown, MD 20874
301-903-6190
Richard.Greene@science.doe.gov

Brian Gregg
National Renewable Energy Laboratory
1617 Cole Blvd.
Golden, CO 80401
303-384-6635
brian.gregg@nrel.gov

David Grills
Brookhaven National Laboratory
Chemistry Department
Upton, NY 11973-5000
631-344-4332
dcgrills@bnl.gov

Devens Gust
Arizona State University
Tempe, AZ 85287-1604
480-965-4547
gust@asu.edu

Robert Hamers
University of Wisconsin
1101 University Avenue
Madison, WI 53706
608-262-6371
rjhamers@wisc.edu

Alexander Harris
Brookhaven National Laboratory
Chemistry, Bldg 555, PO 5000
Upton, NY 11973
631-344-4301
alexh@bnl.gov

Michael Henderson
Pacific Northwest National Laboratory
PO Box 999, MS K8-87
Richland, WA 99352
509-371-6527
ma.henderson@pnl.gov

Craig Hill
Emory University
1515 Dickey Dr, NE
Atlanta, GA 30322
404-727-6611
lchauvi@emory.edu

Patrick Holland
University of Rochester
Dept of Chemistry, U Rochester
Rochester, NY 14627
585-273-3092
holland@chem.rochester.edu

Dewey Holten
Washington University
One Brookings Drive
St. Louis, MO 63130
314-935-6502
holten@wustl.edu

Michael Hopkins
University of Chicago
Department of Chemistry
Chicago, IL 60637
773-702-6490
mhopkins@uchicago.edu

Libai Huang
Notre Dame Radiation Laboratory
223A Radiation Lab
Notre Dame, IN 46556
574-631-2657
lhuang2@nd.edu

Joseph Hupp
Northwestern University
Dept. of Chemistry
Evanston, IL 60208
847-491-3504
j-hupp@northwestern.edu

James Hurst
Washington State University
Chemistry Department
Pullman, WA 99164
509-432-3194
hurst@wsu.edu

Justin Johnson
National Renewable Energy Laboratory
1617 Cole Blvd
Golden, CO 80401
303-384-6190
justin.johnson@nrel.gov

Participants List – 33rd DOE Solar Photochemistry Research Meeting

David Jonas
University of Colorado
215 UCB
Boulder, CO 80309-0215
303-492-3818
david.jonas@colorado.edu

Prashant Kamat
University of Notre Dame
Radiation Laboratory
Notre Dame, IN 46556
574-631-5411
pkamat@nd.edu

David Kelley
University of California
5200 N. Lake Road
Merced, CA 95343
209-228-4354
dfkelley@ucmerced.edu

Christine Kirmaier
Washington University
Dept. of Chemistry, Box 1134
St. Louis, MO 63130
314-935-6480
kirmaier@wustl.edu

Lowell Kispert
University of Alabama
Box 870336, 250 Hackberry Lane
Tuscaloosa, AL 35487-0336
205-348-7134
lkispert@bama.ua.edu

Valeria Kleiman
University of Florida
PO Box 117200
Gainesville, FL 32611-7200
352-392-4656
kleiman@ufl.edu

Todd Krauss
University of Rochester
120 Trustee Road
Rochester, NY 14627-0216
585-275-5093
krauss@chem.rochester.edu

K. V. Lakshmi
Rensselaer Polytechnic Institute
Dept of Chemistry, 110 8th St.
Troy, NY 12180
518-698-7976
lakshk@rpi.edu

Nathan Lewis
California Institute of Technology
1200 E California Blvd 127-72
Pasadena, CA 91125
626-395-6470
nslewis@caltech.edu

Frederick Lewis
Northwestern University
2145 Sheridan Road
Evanston, IL 60208
847-491-3441
fdl@northwestern.edu

Tianquan Lian
Emory University
1515 Dickey Dr. NE
Atlanta, GA 30322
404-727-6649
tlian@emory.edu

Jonathan Lindsey
North Carolina State University
Campus Box 8204
Raleigh, NC 27695-8204
919-515-6406
jlindsey@ncsu.edu

Mark Lonergan
University of Oregon
1253 Department of Chemistry
Eugene, OR 97403
541-346-4748
lonergan@uoregon.edu

Mark Maroncelli
Penn State
104 Chemistry Building
University Park, PA 16802
814-865-0898
maroncelli@psu.edu

Paul Maggard
North Carolina State University
532 Cayman Avenue
Holly Springs, NC 27540
919-557-4814
paul_maggard@ncsu.edu

James McCusker
Michigan State University
Department of Chemistry
East Lansing, MI 48824
517-355-9715
jkm@chemistry.msu.edu

Tom Mallouk
Penn State University
104 Chemistry Building
University Park, PA 16802
814-863-9637
tom.mallouk@gmail.com

Gail McLean
U.S. Department of Energy
1000 Independence Ave SW
Washington, DC 20585
301-903-7807
Gail.McLean@science.doe.gov

Kent Mann
University of Minnesota
Chemistry Department
Minneapolis, MN 55455
612-625-3563
krmann@umn.edu

Tom Meyer
University of North Carolina
Department of Chemistry
Chapel Hill, NC 27599-3290
919-843-8312
tjmeyer@unc.edu

Diane Marceau
U.S. Department of Energy
19901 Germantown Road
Germantown, MD 20874
301-903-0235
diane.marceau@science.doe.gov

Gerald Meyer
Johns Hopkins University
3400 N. Charles St.
Baltimore, MD 21218
410-516-7319
meyer@jhu.edu

Claudio Margulis
University of Iowa
118 IATL, U. of Iowa
Iowa City, IA 52242
319-335-0615
claudio-margulis@uiowa.edu

John Miller
Brookhaven National Laboratory
Chemistry 555
Upton, NY 11973
631-344-4354
jrmiller@bnl.gov

Participants List – 33rd DOE Solar Photochemistry Research Meeting

Thomas Moore
Arizona State University
Dept of Chemistry and Biochemistry
Tempe, AZ 85287-1604
480-965-3308
tmoore@asu.edu

Ana Moore
Arizona State University
Dept of Chemistry and Biochemistry
Tempe, AZ 85287-1604
480-965-2953
amoore@asu.edu

James Muckerman
Brookhaven National Laboratory
Chemistry Department
Upton, NY 11973-5000
631-344-4368
muckerma@bnl.gov

Karen Mulfort
Argonne National Laboratory
9700 South Cass Ave
Argonne, IL 60439
630-252-3545
mulfort@anl.gov

Charles Mullins
University of Texas
1 University Station C0400
Austin, TX 78712
512-471-5817
mullins@che.utexas.edu

Djamaladdin Musaev
Emory University
1515 Dickey Dr
Atlanta, GA 30322
404-727-2382
dmusaev@emory.edu

Nathan Neale
National Renewable Energy Laboratory
MS 3216, 1617 Cole Blvd.
Golden, CO 80401
303-384-6165
nathan.neale@nrel.gov

Marshall Newton
Brookhaven National Laboratory
Chemistry Department
Upton, NY 11973
631-344-4366
newton@bnl.gov

Arthur Nozik
National Renewable Energy Laboratory
1617 Cole Blvd
Golden, CO 80401
303-384-6603
anozik@nrel.gov

Jennifer Ogilvie
University of Michigan
450 Church St
Ann Arbor, MI 48109
734-615-0485
jogilvie@umich.edu

Donald Ort
University of Illinois
1406 IGB, 1206 W. Gregory Dr
Urbana, IL 61822
217-333-2093
d-ort@uiuc.edu

Shanlin Pan
University of Alabama
Department of Chemistry
Tuscaloosa, AL 35406
205-348-6381
span1@bama.ua.edu

Participants List – 33ʀᴅ DOE Solar Photochemistry Research Meeting

John Papanikolas
University of North Carolina
Department of Chemistry
Chapel Hill, NC 27599
919-962-1619
john_papanikolas@unc.edu

Bruce Parkinson
University of Wyoming
Department of Chemistry
Laramie, WY 82071
307-766-9891
bparkin1@uwyo.edu

Hrvoje Petek
University of Pittsburgh
3941 O'Hara Street, G01 Allen
Pittsburgh, PA 15260
412-624-3599
petek@pitt.edu

Piotr Piotrowiak
Rutgers University
3 Warren Street
Newark, NJ 07102
973-353-5318
piotr@andromeda.rutgers.edu

Oleg Poluektov
Argonne National Laboratory
9700 S. Cass Ave.
Argonne, IL 60439
630-252-3546
Oleg@anl.gov

Dmitry Polyansky
Brookhaven National Laboratory
Chemistry Department
Upton, NY 11973
631-344-4315
dep@bnl.gov

Oleg Prezhdo
University of Rochester
Department of Chemistry
Rochester, NY 14618
585-276-5664
oleg.prezhdo@rochester.edu

Yulia Pushkar
Purdue University
525 Northwestern Ave
West Lafayette, IN 47907
765-496-3279
YPushkar@purdue.edu

Jeffrey Pyun
University of Arizona
1306 E University Blvd
Tucson, AZ 85721
520-626-1834
jpyun@email.arizona.edu

John Reynolds
University of Florida
PO Box 117200
Gainesville, FL 32611
352-392-9151
reynolds@chem.ufl.edu

Dean Roddick
University of Wyoming
Chemistry, Dept. 3838, 1000 E.
University Ave.
Laramie, WY 82071
307-766-2535
dmr@uwyo.edu

Garry Rumbles
National Renewable Energy Laboratory
1617 Cole Boulevard
Golden, CO 80401-3393
1-303-885-3581
garry.rumbles@nrel.gov

Participants List – 33rd DOE Solar Photochemistry Research Meeting

Amy Ryan
U.S. Department of Energy
19901 Germantown Rd, SC22-13
Germantown, MD 20874
301-903-5805
margaret.ryan@science.doe.gov

S. Scott Saavedra
University of Arizona
1306 E University
Tucson, AZ 85721
520-621-9761
saavedra@email.arizona.edu

Kirk Schanze
University of Florida
PO Box 117200
Gainesville, FL 32611-7200
352-392-9133
kschanze@chem.ufl.edu

Russell Schmehl
Tulane University
Department of Chemistry
New Orleans, LA 70118
504 862-3566
russ@tulane.edu

Charles Schmuttenmaer
Yale University
225 Prospect St.
New Haven, CT 06520-8107
203-432-5049
charles.schmuttenmaer@yale.edu

Mark Spitler
U.S. Department of Energy
1000 Independence Ave, SW
Washington, DC 20585
301-903-4568
mark.spitler@science.doe.gov

Robert Stack
U.S. Department of Energy
19901 Germantown Rd
Germantown, MD 20874
301-903-5652
robert.stack@science.doe.gov

Michael Therien
Duke University
124 Science Dr
Durham, NC 27707
919-684-0785
michael.therien@duke.edu

Randolph Thummel
University of Houston
136 Fleming Bldg., U of H
Houston, TX 77204-5003
713-743-2734
thummel@uh.edu

David Tiede
Argonne National Laboratory
9700 South Cass Ave
Argonne, IL 60439
630-252-3539
tiede@anl.gov

William Tumas
National Renewable Energy Laboratory
1617 Cole Blvd MS3221
Golden, CO 80401
303-384-6406
bill.tumas@nrel.gov

John Turner
National Renewable Energy Laboratory
1617 Cole Blvd
Golden, CO 80401
303-275-4270
jturner@nrel.gov

Participants List – 33rd DOE Solar Photochemistry Research Meeting

Lisa Utschig
Argonne National Laboratory
9700 S. Cass Ave.
Argonne, IL 60439
630-252-3544
utschig@anl.gov

Jao van de Lagemaat
National Renewable Energy Laboratory
1617 Cole Blvd
Golden, CO 80004
303-384-6143
jao.vandelagemaat@nrel.gov

David Vanden Bout
University of Texas
1 University Station, A5300
Austin, TX 78731
512-232-2824
davandenbout@mail.utexas.edu

Claudio Verani
Wayne State University
5101 Cass Ave.
Detroit, MI 48310
313-577-1076
cnverani@chem.wayne.edu

Michael Wasielewski
Northwestern University
Department of Chemistry
Evanston, IL 60208
847-467-1423
m-wasielewski@northwestern.edu

Emily Weiss
Northwestern University
2145 Sheridan Rd
Evanston, IL 60208-3113
847-491-3095
e-weiss@northwestern.edu

James Whitesell
University of California
5926 Sagebrush Rd
La Jolla, CA 92037
858-349-3182
jkwhitesell@mac.com

Mary Elizabeth Williams
Penn State
104 Chemistry Building
University Park, PA 16802
814-865-8859
mbw@chem.psu.edu

James Wishart
Brookhaven National Laboratory
Chemistry Dept.
Upton, NY 11973
631-344-4327
wishart@bnl.gov

Vittal Yachandra
Lawrence Berkeley National Laboratory
1, Cyclotron Road, MS: 66R0200
Berkeley, CA 94720
510-486-4963
vkyachandra@lbl.gov

Author Index